ESCUELA DE DOCTORADO
INTERNACIONAL DE LA USC

Nadia Gabriela
Pérez Fuentes

Tesis doctoral

ESTUDIO DEL MECANISMO DE ACCIÓN DE MICOTOXINAS REGULADAS Y EMERGENTES

Lugo, 2024

Programa de doctorado en Medicina y Sanidad Veterinaria

ESCOLA DE DOUTORAMENTO
INTERNACIONAL DA USC

TESIS DOCTORAL

ESTUDIO DEL MECANISMO DE ACCIÓN DE MICOTOXINAS REGULADAS Y EMERGENTES

Autor

Nadia Gabriela Pérez Fuentes

Directores: Luis Miguel Botana López y Rebeca Alvariño Romero

Tutor: Luis Miguel Botana López

PROGRAMA DE DOCTORADO EN MEDICINA E SANIDADE VETERINARIA

LUGO, 2024

USC
UNIVERSIDADE
DE SANTIAGO
DE COMPOSTELA

Yo **Nadia Gabriela Pérez Fuentes**, declaro que esta tesis doctoral no presenta conflictos de interés.

Lugo a 26 de julio de 2024

USC
UNIVERSIDADE DE SANTIAGO DE COMPOSTELA

USC
UNIVERSIDADE
DE SANTIAGO
DE COMPOSTELA

A mis abuelas Carmen y Dosinda, eternas luchadoras

USC
UNIVERSIDADE
DE SANTIAGO
DE COMPOSTELA

USC
UNIVERSIDADE
DE SANTIAGO
DE COMPOSTELA

AGRADECIMIENTOS

Gracias a Luis, por haberme dado la oportunidad de realizar la presente tesis en el grupo de investigación y poder aprender tanto.

A Rebeca, por haber sido la mejor directora que se puede tener, haberme enseñado, guiado y aconsejado en este largo proceso, y sobre todo por haber sido una gran amiga. Un millón de gracias.

A Amparo, mi guía espiritual y gran apoyo a lo largo de todo este proceso, por las enseñanzas, la paciencia y por haberme puesto los pies en la tierra cuando lo necesitaba.

A todos mis compañeros (Noelia, Sandra R., Alex, Luis, Inés) a los que ya no están (Celia, Andrea) y a los que han ido llegando (Klara) por hacerme ameno el proceso. En especial a Sandra G. por haberme aconsejado y brindado apoyo y por ser una gran amiga y a Jesús, por ser un 9.9 de persona y hacerme reír.

A mis amigos de toda la vida (Carballo rules) y a los que han llegado más tarde para quedarse. En especial a Laura Pena, Laura Balboa y Laura Souto, por llevar años siendo incondicionales y haberme sufrido durante este largo proceso.

A mi padre y a mi madre y a mi hermana por ser los mejores y preocuparse siempre por mi bienestar, apoyarme en todas mis aventuras y siempre estar ahí.

A mi cuñado, por haberme enseñado todas las caras de la carrera y aconsejarme siempre que lo necesité.

A Nico y Greta por ser la alegría y felicidad personificada y sacarme la mayor sonrisa siempre.

A Marcos, por haber sobrevivido a este largo proceso y seguir ahí, por aguantarme día a día y ayudarme siempre y a toda su familia por haberme integrado como una más y preocuparse siempre por mí.

Y a Rita, Astrid y Timón, por ser mi mayor soporte emocional.

USC
UNIVERSIDADE DE SANTIAGO DE COMPOSTELA

USC
UNIVERSIDADE
DE SANTIAGO
DE COMPOSTELA

ABREVIATURAS Y ACRÓNIMOS

AFs: aflatoxinas
ANT: traslocador de nucleótidos de adenina, del inglés *adenine nucleotide translocator*
API: apicidina
ATCC: American Type Culture Colletion
BEA: beauvericina
BHE: barrera hematoencefálica
CPA: ácido ciclopiazónico
CsA: ciclosporina A
Cyp: ciclofilina
CTN: Citrina
ΔΨm: potencial de membrana mitocondrial
DCFH-DA: 7′,2′-dichlorofluorescein diacetato
DEST B: Destruxina B
DISC: complejo de señalización inductor de muerte, del inglés *death-inducing signaling complex*
DMEM: del inglés *Dulbecco's Modified Eagle's Medium*
DON: deoxinivalenol
EAs: Alcaloides del Ergot o alcaloides del cornezuelo de centeno, del inglés *ergot alkaloids*
EFSA: Autoridad Europea de Seguridad Alimentaria, del inglés *European Food Safe Authority*
ELEM: leucoencefalomalacia equina, del inglés *equine leukoencephalomalacia*
ELISA: ensayo por inmunoabsorción ligado a enzimas, del inglés *enzyme-linked immuno sorbent assay*
ENN A: eniatina A
ENN A1: eniatina A1
ENN B: eniatina B
ENN B1: eniatina B1
ENNs: eniatinas
FAO: Organización de las Naciones Unidas para la Agricultura y la Alimentación, del inglés *Food and Agriculture Organization of the United Nations*
FBs: fumonisinas de tipo B
FB1: fumonisina B1
FB2: fumonisina B2
FB3: fumonisina B3
GRP75: chaperona regulada por glucosa 75 kDa, del inglés *75 kDa glucose-regulated protein*
IARC: Agencia Internacional de Investigación sobre el Cáncer, del ingés *International Agency for Research on Cancer*
IL: interleucina
IMM: membrana interna mitocondrial, del inglés *inner mitochondrial membrane*
IP3Rs: receptores de inositol 1,4,5-trifosfato
LDH: lactato deshidrogenasa
LETM1: antiportador de protons/calcio "Leucine Zipper And EF-Hand Containing Transmembrane Protein 1"
LPS: lipopolisacárido
MCU: el uniportador de calcio mitocondrial, del inglés *mitochondrial calcium uniporter*
MON: moniliformina

USC UNIVERSIDADE DE SANTIAGO DE COMPOSTELA

mPTP: poro de transición de permeabilidad mitocondrial, del inglés *mitochondrial permeability transition pore*
MTT: bromuro de 3-(4,5-dimetiltiazol-2-il)-2,5-difeniltetrazolio
NCLX: intercambiador $Na^+/Ca^{2+}/Li^+$, del inglés *$Na^+/Ca^{2+}/Li^+$ exchanger*
OMM: membrana mitocondrial externa, del inglés *outer mitochondrial membrane*
OMS: Organización Mundial de la Salud
OTA: ocratoxina A
PAT: patulina
PBS: solución salina tamponada con fosfato, del inglés *phophate buffered saline*
PI: yoduro de propidio, del inglés *propidium iodide*
PMCA: Ca^{2+}-ATPasa de la membrana plasmática, del inglés *plasma membrane calcium ATPase*
PPE: Síndrome de edema pulmonar en cerdos, del inglés *pig pulmonary edema*
RE: retículo endoplasmático
ROS: especies reactivas de oxígeno, del inglés *reactive oxigen species*
ROQC: roquefortina C
Rot: Rotenona
RPMI: del inglés *Roswell Park Memorial Institute Medium*
RyR: receptores de rianodina
SDS: Sodio-dodecil-sulfato
SERCA: bomba ATPasa de calcio del retículo sarcoplásmico, del inglés *sarcoendoplasmic recticulum calcium ATPase*
SOC: canales de calcio dependientes de reservorio, del inglés *store-operated calcium channels.*
SPCA1: vía secretora de la ATPasa1de Ca^{2+}, del inglés *secretory pathway Ca^{2+} ATPase1*
STIM1: moléculas de interacción estromal 1, del inglés *stromal interaction molecule 1*
Tg: tapsigargina
TMRM: Tetrametilrodamina metil éster
TPCs: canales de dos poros, del inglés *two pore channels*
TRPs: canales de potencial receptor transitorio, del inglés *transient receptor potential channels*
TRPMLs: subfamilia mucolínica de canales de potencial receptor transitorio, del inglés *transient receptor potential mucolipin channels*
UE: Unión Europea
VDACs: canales aniónicos dependientes del voltaje, del inglés *voltage-dependent anion channels*
transient receptor potential
VGCCs: canales de calcio dependientes de voltaje, del inglés *voltage-gated calcium channels*
ZEA: Zearalenona

USC
UNIVERSIDADE DE SANTIAGO DE COMPOSTELA

ÍNDICE

RESUMEN 1
1 INTRODUCCIÓN 3
1.1 Micotoxinas en la alimentación: Historia, Panorama Global y Regulación 3
1.2 Clasificación de las micotoxinas y efectos toxicológicos 8
1.2.1 Micotoxinas reguladas 8
1.2.1.1 Alcaloides del centeno 8
1.2.1.3 Ocratoxinas 10
1.2.1.4 Patulinas 11
1.2.1.5 Tricotecenos 12
1.2.1.5.1 Deoxinivalenol 14
1.2.1.6 Fumonisinas 15
1.2.1.6.1 Fumunosina B1 16
1.2.1.7 Zearalenona 16
1.2.2 Micotoxinas emergentes 17
1.2.2.1 Beauvericina 18
1.2.2.2 Eniatinas 18
1.2.2.3 Apicidina 20
1.2.2.4 Destruxina B 20
1.2.2.5 Ácido ciclopiazónico 21
1.2.2.6 Roquefortina 22
1.3 Co-ocurrencia de micotoxinas reguladas y emergentes 22
1.4 Vías de señalización celular 23
1.4.1 Calcio 24
1.4.2 Muerte celular 28
2 HIPÓTESIS Y OBJETIVOS 31
3 MATERIAL Y MÉTODOS 33
4 PUBLICACIONES 45
SECCIÓN I: ARTÍCULOS PUBLICADOS 47
1. Single and combined effects of regulated and emerging mycotoxins on viability and mitochondrial function of SH-SY5Y cells 47
2. Enniatins A1 and B1 alter calcium homeostasis of neuronal cells leading to apoptotic death 67
3. The Mode of Action of Enniatins A and B is Mediated by Interaction with SOC Reservoirs (A) and Mitochondrial Permeability Transition Pore (B) 79
4. Enniatins A1 and B1 Modulate Calcium Flux through Alternative Pathways beyond Mitochondria 93
5. In Vitro Testing of Lung Carcinogenicity for an In Silico-Identified Cluster of Mycotoxins 105
SECCIÓN II: ARTÍCULO EN REVISIÓN 123
6. In vitro assessment of emerging mycotoxins co-occurring in cheese: A potential health hazard 123
5 DISCUSIÓN 149
6 CONCLUSIONES 161
7 REFERENCIAS 163

USC
UNIVERSIDADE DE SANTIAGO DE COMPOSTELA

USC
UNIVERSIDADE
DE SANTIAGO
DE COMPOSTELA

RESUMEN

La contaminación de cereales y productos derivados por micotoxinas es un problema global y representa un riesgo para la salud. Estos compuestos pueden provocar daños a humanos y animales tanto mediante ingestión como por inhalación, siendo la primera la principal vía de exposición. Aunque la presencia de ciertas micotoxinas está regulada, la mayoría no se analiza de forma rutinaria debido a la falta de requisitos legales. Esta situación permite que muchos compuestos lleguen al consumidor sin ser controlados, presentando un riesgo desconocido y potencialmente creciente, debido al calentamiento global. Además, el mecanismo subyacente a su toxicidad se desconoce en la mayoría de los casos, y varias micotoxinas suelen contaminar conjuntamente los alimentos, añadiendo complejidad a la hora de entender sus efectos.

En la presente tesis doctoral se utilizaron la línea celular de neuroblastoma humano SH-SY5Y y la de cáncer de pulmón NCI-H226 para evaluar los efectos producidos por micotoxinas reguladas y emergentes, individualmente y en combinación, con el fin de profundizar en el estudio de su mecanismo de acción. Se seleccionaron las micotoxinas más frecuentemente encontradas en piensos y leche del noroeste europeo, incluyendo el deoxinivalenol (DON), la fumonisina B1 (FB1) y la zearalenona (ZEA), entre las reguladas, y las eniatinas (ENNs) A, A1, B y B1, junto con la beauvericina (BEA), entre las emergentes, así como las micotoxinas más frecuentes en quesos, la roquefortina C (ROQC) y el ácido ciclopiazónico (CPA).

En cuanto al efecto individual de las micotoxinas sobre la viabilidad celular de las células de neuroblastoma, la ENN B fue la molécula más dañina, seguida por el DON, la BEA, la ENN A1, la ENN A, la ENN B1, el CPA, la ZEA, la ROQ C y la FB1, que no afectó a las células. Además de presentar una mayor toxicidad las micotoxinas emergentes produjeron apoptosis. Por otro lado, al evaluar los efectos de combinaciones binarias de micotoxinas reguladas y emergentes frecuentemente encontradas en piensos, se observaron efectos antagónicos. Sin embargo, en la mayoría de los casos las mezclas de micotoxinas emergentes resultaron en una potenciación de los efectos individuales de cada toxina. Además, se probaron extractos contaminados de pienso, leche y queso, observándose un mayor efecto tóxico del esperado.

Debido a que las ENNs aparecen frecuentemente en distintos alimentos, se profundizó en el estudio de su mecanismo de acción. Para ello, se evaluaron sus efectos sobre la homeostasis del calcio y función mitocondrial. Estas toxinas han sido consideradas como ionóforos durante muchos años, sin embargo, en la presente tesis doctoral se describe que ninguno de los análogos evaluados presenta un comportamiento ionofórico para el Ca^{2+}. Aunque todos estos compuestos producen daño mitocondrial, parecen presentar un distinto mecanismo de acción, ya que los efectos sobre los flujos de Ca^{2+} difieren entre análogos. Mientras que las ENNs A y A1 activan la entrada del ion a través de los canales de calcio dependientes de reservorio (SOC), la ENN B no afecta a la entrada de Ca^{2+} y parece actuar exclusivamente a través de la mitocondria. Por otro lado, la ENN B1 actúa en la mitocondria y aumenta la entrada de Ca^{2+} por un canal no SOC.

Por último, se estudiaron los efectos de micotoxinas emergentes (apicidina, dextrusina B, ENN A, ENN B y BEA) sobre la línea NCI-H226 y se observó que la ENN A, la BEA y la apicidina disminuyeron la viabilidad, produciendo muerte por apoptosis.

Por tanto, los resultados de la presente tesis doctoral sugieren que la co-ocurrencia de micotoxinas emergentes y reguladas en matrices naturales puede representar un riesgo para la salud y describe por primera vez el efecto de las ENNs sobre los flujos de Ca^{2+}, descartando que actúen como ionóforos de este ion.

USC
DE SANTIAGO
DE COMPOSTELA

USC
UNIVERSIDADE
DE SANTIAGO
DE COMPOSTELA

1 INTRODUCCIÓN

Las micotoxinas son un grupo diverso de toxinas producidas principalmente por hongos filamentosos de los géneros *Aspergillus*, *Penicillium* y *Fusarium*. Estos hongos contaminan alimentos, como cereales, nueces, frutas e incluso leche y pescado, y son responsables de la producción de más de 300 compuestos (1, 2). Las micotoxinas se clasifican en reguladas o emergentes, incluyéndose en el primer grupo aquellas para las que existen límites máximos establecidos y considerándose emergentes todas aquellas para las que no existe regulación ni se analizan de forma rutinaria (3, 4). La presencia de micotoxinas en alimentos y piensos supone una amenaza para la salud humana y animal. Esto se debe a que la exposición a las mismas, así como su ingestión pueden dar lugar a intoxicaciones agudas o incluso a patologías de carácter crónico, como inmunodeficiencias o cáncer (5, 6). A pesar de la gravedad de estos efectos, todavía se desconocen la mayoría de los mecanismos exactos que causan la toxicidad de las micotoxinas, sobre todo en lo que respeta a micotoxinas emergentes. Debido a que son químicamente estables y resistentes al procesamiento de alimentos, su prevención y eliminación supone un desafío importante. Teniendo en cuenta estos aspectos, existe una clara necesidad de ampliar la investigación sobre estos abundantes compuestos, especialmente en lo que respecta a sus mecanismos toxicológicos, abriendo así la puerta a estrategias más efectivas de prevención y mitigación de los mismos (7-9).

1.1 MICOTOXINAS EN LA ALIMENTACIÓN: HISTORIA, PANORAMA GLOBAL Y REGULACIÓN

La presencia de micotoxinas en alimentos se ha notificado a lo largo de la historia. En la antigua China, textos datados hace más de dos mil años mencionan casos de enfermedades vinculadas al consumo de granos mohosos, mientras que, en Europa durante la Edad Media, se registraron dolencias provocadas por el consumo de pan de centeno infectado con el hongo *Claviceps purpurea*, causante del ergotismo. Esta enfermedad afectaba a comunidades enteras, y presentaba una sintomatología que incluía convulsiones, alucinaciones, gangrena e incluso muerte. En aquel entonces se desconocía qué causaba esta afección, sin embargo, hoy se sabe que se produce al ingerir alimentos contaminados por alcaloides producidos por el hongo (10, 11).

El interés general en las micotoxinas aumentó en 1960 cuando una micotoxicosis causada por aflatoxinas (AFs), denominada enfermedad "X" del pavo, provocó la muerte de 100.000 animales en granjas de Inglaterra. Tras esta crisis veterinaria, se descubrió que las AFs son hepatocarcinógenas en animales y humanos, y esto incrementó la investigación sobre otros metabolitos producidos por hongos (12).

Los hongos productores de micotoxinas son patógenos muy comunes y frecuentes en todas las regiones agrícolas del mundo. Crecen en una amplia variedad de alimentos, incluyendo cereales, frutos secos, especias, frutas y granos de café, a menudo en condiciones cálidas y húmedas. Todos estos alimentos pueden estar contaminados con micotoxinas, pero también se han hallado estos compuestos en leche, carne y pescado (13-15). Los principales hongos productores de micotoxinas pertenecen a los géneros *Aspergillus*, *Penicillium*, *Fusarium*, o *Alternaria*. Estos pueden invadir un variado número de cultivos y son capaces de producir micotoxinas en un conjunto diverso de condiciones (16, 17).

Existen numerosos factores que afectan al desarrollo de los hongos y la producción de micotoxinas. La contaminación por estas sustancias puede producirse en distintas etapas de la cadena alimentaria (Figura 1), comenzando en el campo y pudiendo aumentar durante la

USC DE COMPOSTELA

recolección, el secado y el almacenamiento, lo cual facilita su llegada al ser humano (16). Además, las micotoxinas pueden bioacumularse en músculo, hígado e incluso aparecer en leche (18). Sin embargo, la presencia de hongos no garantiza la contaminación con micotoxinas, ya que su síntesis depende de condiciones específicas. Por otro lado, la eliminación de un hongo productor de micotoxinas no asegura la eliminación de las micotoxinas una vez que han sido generadas, debido a su gran estabilidad química y termodinámica (16, 19).

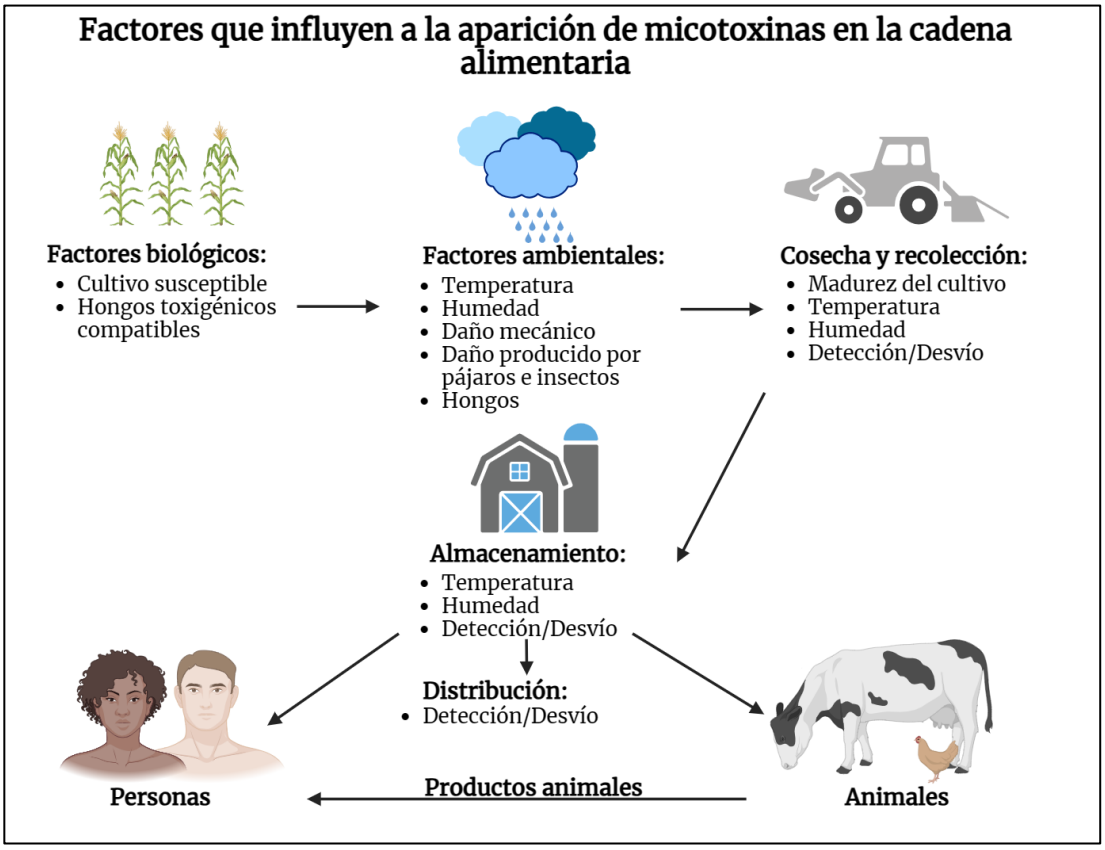


Figura 1. Factores que influyen en la aparición de micotoxinas en la cadena alimentaria. Imagen creada con biorender.com

El crecimiento de hongos se divide en dos etapas: primaria y secundaria. Durante el crecimiento primario, los hongos necesitan compuestos orgánicos para sintetizar biomasa y obtener la energía necesaria para impulsar reacciones químicas y producir metabolitos esenciales. Por otro lado, el crecimiento secundario tiene lugar después de un período de crecimiento sostenido y puede conducir a la formación de esporas y a la producción de metabolitos secundarios, como micotoxinas, que no afectan al crecimiento, pero pueden acumularse debido a un exceso de precursores de metabolitos primarios (16, 20).

Dado que los hongos que producen micotoxinas y sus hospedadores son muy diversos, no se puede definir de manera sencilla un único conjunto de condiciones que contribuyan a la contaminación por micotoxinas (16, 19). En general, los principales factores que afectan a la producción de micotoxinas pueden resumirse en:

- Cepa fúngica: Las distintas especies de hongos presentan variaciones en cuanto a su toxicidad, y la generación de micotoxinas a menudo se limita a ciertos tipos de hongos, e incluso puede restringirse a cepas específicas dentro de una misma especie (2, 21).

- Sustrato: Los hongos micotoxigénicos pueden crecer en una variedad de sustratos, pero se desconoce por qué predominan en un alimento específico. Los nutrientes necesarios para su crecimiento, como el carbono y el nitrógeno, son comunes en los alimentos ricos en carbohidratos, lo que permite que los hongos estén presentes en casi cualquier tipo de alimento (22). Sin embargo, los factores que promueven el crecimiento fúngico no siempre resultan en la producción de micotoxinas, ya que las condiciones específicas necesarias para esto suelen ser más limitadas. La generación de micotoxinas se ve influenciada por factores como el pH, la temperatura y la composición del sustrato, especialmente la presencia de monosacáridos (16). La presión osmótica en el sustrato también incide en el crecimiento fúngico y la producción de micotoxinas. Los hongos pueden adaptar su fisiología al estrés osmótico, y en presencia de monosacáridos fácilmente digeribles, el crecimiento fúngico se acelera (23).
- Temperatura, humedad relativa y actividad de agua: Cada hongo tiene un rango óptimo de temperatura y actividad de agua para su crecimiento, germinación y producción de toxinas, y debido a las diferencias en las condiciones ambientales, se observan variaciones en el desarrollo de hongos y la producción de toxinas entre las distintas regiones geográficas (24). La invasión fúngica puede ocurrir en distintas etapas, ya sea en el campo, durante el secado o almacenamiento. Cuando las condiciones de humedad y temperatura son propicias, pueden darse cambios en la fase inicial del crecimiento fúngico (19). Durante el almacenamiento, el incremento en la actividad del agua se relaciona con la susceptibilidad al crecimiento fúngico y la producción de micotoxinas. La mayoría de las especies fúngicas son mesófilas y se desarrollan mejor en un rango de 5 a 35 ℃, pero condiciones fuera de este intervalo pueden detener su crecimiento. Aunque las condiciones que promueven el crecimiento fúngico no siempre conducen a la producción de micotoxinas, se considera óptimo un rango de temperatura entre 25 y 30 ℃, una actividad de agua superior a 0.78 y una humedad relativa entre 88% y 95% (16, 24).
- pH: El entorno y el pH que rodean a los hongos desempeñan un papel fundamental en su desarrollo y en la producción de micotoxinas. El pH tiene un impacto directo en el crecimiento de los hongos y la disponibilidad de nutrientes, y estos pueden modificar el pH mediante la secreción de ácidos o bases, lo que les otorga una ventaja para sobrevivir en el huésped. Además, el pH influencia la interacción entre la actividad del agua y la temperatura, lo que afecta procesos metabólicos como la formación de esporas y la morfogénesis (25, 26). Asimismo, el valor de pH incide en la expresión génica de la biosíntesis de micotoxinas (27). En términos generales, las condiciones ácidas favorecen la germinación y producción de micotoxinas, como en el caso de la AF que requiere un pH ácido, y la ocratoxina A (OTA), cuya prevalencia es superior a pH bajo. La fumonisina B1 (FB1) no mantiene su estabilidad en un entorno alcalino y requiere un pH específico para su síntesis, al igual que la producción de tricotecenos, la cual se induce en condiciones ácidas (20, 27, 28).

Dado que el crecimiento fúngico, la germinación y la producción de micotoxinas están regulados por factores ambientales y prevalecen bajo un conjunto de condiciones óptimas, las oscilaciones de temperatura y humedad debidas al **cambio climático** pueden tener efectos variados en la producción de estos compuestos (29). Por ejemplo, micotoxinas que normalmente se dan a bajas temperaturas podrían no ser producidas a medida que estas aumenten, mientras que otras que son dominantes en áreas subtropicales y tropicales, como las AF, podrían comenzar a producirse en regiones generalmente templadas debido al aumento esperado de la temperatura en esas áreas. Esto ya se evidenció en Italia en los años 2003 y 2004, donde una serie de episodios calurosos y secos provocaron un grave aumento de *Aspergillus flavus* y la consecuente producción de AF (30, 31). Por lo tanto, cada micotoxina se verá

USC SANTIAGO DE COMPOSTELA

afectada de diferentes maneras según la prevalencia de sus condiciones óptimas de producción. El cambio climático también puede afectar indirectamente a la contaminación global de micotoxinas mediante el aumento de poblaciones de plagas de insectos y su propagación, la maduración temprana de los cultivos o la disminución de la resistencia de las plantas. No obstante, dado que los hongos tienden a adaptarse a los cambios, es complejo establecer una relación clara (16).

La Organización de las Naciones Unidas para la Agricultura y la Alimentación (FAO) estima que casi el 25% de las cosechas a escala mundial se ve afectado anualmente por hongos toxigénicos, lo que provoca pérdidas anuales del orden de un millón de toneladas. Sin embargo, estudios recientes han demostrado que la presencia de micotoxinas por encima de los niveles detectables puede alcanzar el 60-80%, lo que indica una subestimación significativa del problema (32, 33). Un estudio mundial a gran escala sobre la contaminación por micotoxinas en piensos entre 2008 y 2017 reveló que el 88 % de las muestras estaban contaminadas con al menos una micotoxina (34).

Las micotoxinas tienen un impacto significativo en la salud humana, la productividad animal y el comercio nacional e internacional (35). Cuando se ingieren, pueden provocar desde intoxicaciones agudas hasta efectos a largo plazo como inmunodeficiencias o cáncer (35, 36). La Agencia Internacional de Investigación sobre el Cáncer (IARC) ha clasificado varias micotoxinas como posibles carcinógenos humanos basándose en datos epidemiológicos y estudios en animales de experimentación. Las AF (B1, B2, G1, G2 y M1), las fumonisinas (B1 y B2) y la OTA son algunas de las micotoxinas cuyo riesgo cancerígeno se ha evaluado (37). Por otro lado, la naturaleza lipofílica de estos compuestos les facilita atravesar la barrera hematoencefálica (BHE), permitiéndoles causar daños en el sistema nervioso central. Hay estudios que dilucidan el efecto neurotóxico de algunas micotoxinas como el deoxinivalenol (DON) o las fumonisinas (FBs) (38-41). En lo que respecta a productividad animal y comercio, las micotoxinas pueden provocar pérdidas en la producción ganadera, dificultades en la gestión de los animales y llevar a que los productos agrícolas no sean aceptables en el mercado nacional o internacional. Su presencia disminuye tanto la cantidad como la calidad de los cultivos y la producción ganadera, lo que se traduce en considerables pérdidas económicas (42, 43).

La conciencia sobre los residuos químicos y los contaminantes naturales en los alimentos ha aumentado junto con la preocupación de los consumidores por la seguridad alimentaria. Esto ha dado lugar a una imposición más estricta de nuevos límites legislativos, a nivel nacional e internacional, para una variedad de micotoxinas que pueden contaminar las materias primas y entrar en la cadena alimentaria (1, 17).

La Organización Mundial de la Salud (OMS), en colaboración con la FAO, se encarga de evaluar los riesgos que estas micotoxinas representan para los seres humanos a través de la contaminación alimentaria. Estos organismos establecen un conjunto de normas, directrices y códigos de prácticas que se recogen en el Codex Alimentarius. Estas normas tienen como objetivo proteger la salud de los consumidores y garantizar prácticas comerciales justas en el comercio internacional de alimentos (6, 7). En la Unión Europea (UE), el Reglamento 2023/915 de la Comisión de 25 de abril de 2023, establece niveles máximos para AFs, OTA, patulina (PAT), DON, zearalenona (ZEA), FB1, FB2 y citrinina (CTN). Además, existen niveles máximos de esclerocio del cornezuelo del centeno (*Claviceps purpurea*) para los cereales no transformados, así como para alcaloides del cornezuelo de centeno o alcaloides del Ergot (EAs) (3). Por otro lado, existe una Recomendaciones de la Comisión 2013/165 que establece niveles indicativos para las toxinas T-2 y HT-2 (44). La legislación sobre alimentación animal incluye niveles máximos de aflatoxina B1 (AFB1) y esclerocios de cornezuelo de centeno, así como

USC UNIVERSIDADE DE SANTIAGO DE COMPOSTELA

valores orientativos para DON, ZEA, OTA, FB y toxinas T-2 y HT-2. En la tabla 1 se resumen los contenidos máximos de micotoxinas en la UE (45-47).

Tabla 1. Principales micotoxinas, alimentos que contaminan y rango de límites máximos establecidos en la UE. Aflatoxinas (AFs), aflatoxina M1 (AFM1), ocratoxina A (OTA), patulina (PAT), deoxinivalenol (DON), zearalenona (ZEA), fumonisina B1 (FB1), Fumonisina B2 (FB2), citrina (CTN), alcaloides del cornezuelo (EAs) (3, 44, 47, 48)

Micotoxina	Grupo de alimentos	Límites en alimento (µg / Kg)	Límites en alimentación animal (µg / Kg)
AFs	Frutas desecadas, higos, cacahuete, frutos de cáscara, almendras pistachos y huesos de albaricoque, avellanas y nueces, cereales y derivados, especias, jengibre, alimentos infantiles y de uso médico para lactantes	0,1 – 12 (AFB1) 4 – 15 (Suma de AFs)	5- 20 (AFB1) *
AFM1	Leche, productos lácteos, alimentos infantiles y de uso médico para lactantes	0,025 – 0,05	-
OTA	Uvas pasas, otras frutas desecadas, jarabe de dátil, pistachos, hierbas secas, jengibre, raíces secas, semillas de: girasol, calabaza, melón, sandía cáñamo y soja, granos de cereal y productos derivados, productos de panadería, productos que contienen y no contienen semillas oleaginosas, bebidas no alcohólicas a base de malta, derivados de uva, gluten de trigo, café y derivados, cacao, especias, regaliz y derivados, *Capsicum* spp., vino, alimentos infantiles y de uso médico para lactantes.	0,5 – 15	10 – 250
PAT	Zumos de frutas y derivados, bebidas espirituosas fermentadas con manzana, productos sólidos de manzana, alimentos infantiles	10 – 50	-
DON	Granos de cereales, granos de trigo, granos de maíz, cereales comercializados, pasta alimenticia, pan, pasteles, galletas y aperitivos de cereales, harina de maíz, otros productos de la molienda y alimentos infantiles a base de cereales	200 – 1750	900 - 12000
ZEA	Granos de cereales, granos de maíz, cereales comercializados, pasta alimenticia, pan, pasteles, galletas y aperitivos de cereales, maíz comercializado, productos de la molienda del maíz, aceite de maíz y alimentos infantiles a base de cereales	20 – 350	100 - 3000
FB1 y FB2	Granos de maíz y derivados (harina, cereales de desayuno…), alimentos infantiles que contengan maíz	200 – 4000	5000 – 60.000
CTN	Complementos alimenticios a base de arroz fermentado	100	-
Esclerocios del cornezuelo	Granos de cereales y centeno	0,2 (desde el 1 de julio de 2024)	-
EAs	Productos de la molienda de cebada, trigo, espelta y avena, centeno y subproductos, gluten de trigo, alimentos elaborados a base de cereales para lactantes	20 – 400	-
T-2 y HT-2	Cebada, avena, trigo, centeno y subproductos	15 – 1000	250 – 2000

****En alimentación animal, solo hay límites máximos establecidos para la AFB1, el resto son recomendaciones.***

Además, la Autoridad Europea de Seguridad Alimentaria (EFSA) se establece como autoridad independiente para proporcionar asesoramiento científico en todos los campos relacionados con la seguridad de los alimentos y piensos (49). Esta entidad proporciona procedimientos de evaluación de riesgos basados en estudios científicos con estimaciones cuantitativas de la probabilidad de efectos adversos para la salud asociados con la exposición a agentes tóxicos (50).

1.2 CLASIFICACIÓN DE LAS MICOTOXINAS Y EFECTOS TOXICOLÓGICOS

Las micotoxinas pueden clasificarse en reguladas o emergentes, según la gravedad de sus efectos. En el primer grupo se encuentran las micotoxinas para las que existen límites máximos establecidos (ver tabla 1), mientras que se denominan emergentes todas aquellas que no están reguladas (4).

1.2.1 Micotoxinas reguladas

En el actual apartado se definen las micotoxinas reguladas a nivel europeo y sus principales efectos tóxicos, haciendo especial hincapié en el DON, FB1 y ZEA, objeto de estudio en la presente tesis doctoral.

1.2.1.1 Alcaloides del centeno

Los EAs son micotoxinas producidas principalmente por hongos del género *Claviceps*, siendo *C. purpurea* la especie más conocida (51). Este hongo infecta cereales como el centeno, el trigo o la cebada, sustituyendo las semillas del huésped por sus esclerocios, conocidos como cornezuelo o ergot. Posteriormente se producen EAs que se acumulan dentro de los esclerocios (51, 52).

El descubrimiento de los EAs se remonta a la Edad Media en Europa, cuando el consumo de alimentos contaminados con esclerocios del cornezuelo provocó numerosos brotes de intoxicación humana conocidos como fuego de San Antonio, enfermedad actualmente denominada como ergotismo. Estos brotes se caracterizaban por síntomas graves que incluían alucinaciones, convulsiones, gangrena e incluso la muerte (11). En aquel entonces se desconocía qué causaba esta afección, sin embargo, en el siglo XIX se estableció la conexión entre el ergotismo y el hongo *Claviceps purpurea*. El aislamiento y la identificación de alcaloides específicos del cornezuelo, como la ergotamina, comenzó a principios del siglo XX, lo que condujo a un conocimiento más profundo de su estructura química y sus efectos (53, 54). Aunque actualmente los brotes graves de ergotismo son poco frecuentes gracias a la mejora de las prácticas agrícolas y las técnicas de procesado de alimentos, la eliminación completa de los EAs de los cereales sigue siendo un reto (55-57). La presencia de EAs residuales en la cadena alimentaria sigue suscitando preocupación en materia de seguridad alimentaria (57).

Se han identificado más de 80 EAs diferentes, los cuales comúnmente se clasifican en tres grupos: clavinas (derivados hidroxilados y deshidroxilados de la 6,8-dimetilergolina), aminas simples del ácido lisérgico y ergopeptinas, que constituyen el grupo más grande y diverso de EAs (56). Estructuralmente, todos los EAs se caracterizan por la presencia de un sistema tetracíclico de anillos de ergolina. Algunos de los análogos más importantes son, entre otros, la ergotamina, o la amida del ácido lisérgico, ergometrina (Figura 2)(56, 58).

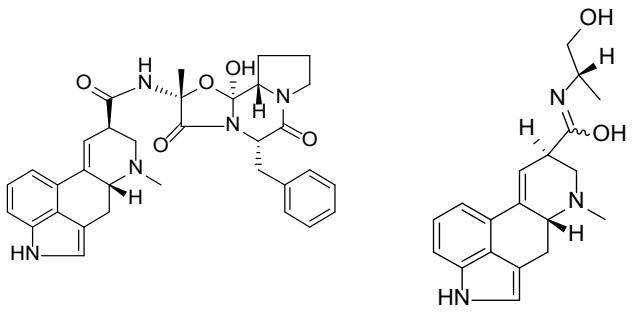


Figura 2. Estructura de algunos alcaloides del cornezuelo

Los efectos de los EAs son diversos y dependen del compuesto específico y de la dosis (57). En pequeñas cantidades, algunos EAs, como la ergotamina y la ergometrina, tienen usos terapéuticos, sobre todo en el tratamiento de las migrañas y en la prevención de la hemorragia uterina postparto (59, 60). Sin embargo, en grandes cantidades, estos compuestos pueden causar toxicidad grave, dando lugar a síntomas de ergotismo (54). Su núcleo ergolínico es estructuralmente similar a las aminas biógenas, dopamina, serotonina y adrenalina, por lo que los EAs pueden actuar sobre los receptores dopaminérgicos, serotoninérgicos y adrenérgicos, modulando la liberación de neurotransmisores y el tono vascular (56, 61). Los ergopéptidos, por ejemplo, producen vasoconstricción (61). En este sentido, la ergotamina se une a los receptores de serotonina del cerebro, ayudando a aliviar los síntomas de la migraña al contraer los vasos sanguíneos dilatados (59). Sin embargo, esta misma propiedad vasoconstrictora puede provocar isquemia periférica grave y gangrena en casos de sobredosis o exposición crónica (síntomas de ergotismo)(54, 56).

La UE establece límites en alimentos tanto para esclerocios del cornezuelo (0,2 µg / kg) como para los EAs (20 – 400 µg / kg) (3).

1.2.1.2 Aflatoxinas

Las AFs son un grupo de 20 micotoxinas producidas por distintas especies de *Aspergillus*, entre las que destacan *Aspergillus flavus* y por *A. parasiticus (9, 62)*. Estas toxinas se aislaron por primera vez en la década de 1960 tras el brote de la ya mencionada enfermedad "X" del pavo, que causó muertes y lesiones hepáticas graves en pavos, pollos y patos alimentados con harina de cacahuete contaminada (63).

A.flavus contamina principalmente las partes aéreas de las plantas y cultivos oleaginosos, como frutos secos, algodón, cacahuete o maíz, mientras que *A. parasiticus* se detecta con mayor frecuencia en suelos(64). Estos hongos prosperan en condiciones cálidas (15-40ºC) y de humedad elevada, por lo que su presencia se asocia a regiones tropicales y subtropicales(65). Sin embargo, están presentes en todo el mundo y su prevalencia está aumentando debido a los efectos del cambio climático (66, 67).

Entre los principales análogos de AFs se encuentran las AFB1, aflatoxina B2 (AFB2), aflatoxina G1 (AFG1) y la aflatoxina G2 (AFG2), presentes en nueces, especias, cereales, aceites, frutas, verduras o carne, a nivel mundial. También destaca la AFM1, metabolito hidroxilado de la AFB1, que se puede encontrar en leche de animales que han ingerido pienso contaminado con AFB1. Son compuestos heterocíclicos altamente oxigenados caracterizados por la fusión de enlaces dihidrodifurano con una cumarina sustituida. Se clasifican en 2 grupos según su estructura química. Un grupo difurocumarociclopentenona que comprende, entre otros, la AFB1, la AFB2 y la AFM1, y un grupo difurocumarolactona, que incluye la AFG1 y la AFG2 (Figura 3).

USC UNIVERSIDADE DE SANTIAGO DE COMPOSTELA

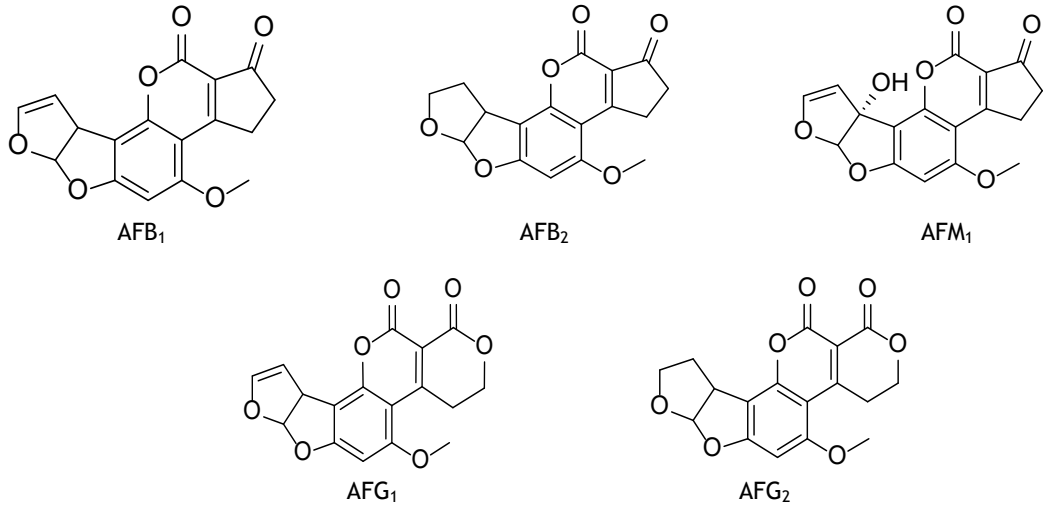


Figura 3. Estructura de las principales Afs

La exposición de los seres humanos y los animales a las AFs se produce principalmente por la ingestión de alimentos y piensos contaminados (68). Estos compuestos lipofílicos son absorbidos desde el tracto gastrointestinal al torrente sanguíneo y distribuidos a diversos órganos, especialmente el hígado, donde sufren una biotransformación catalizada por las enzimas del citocromo P450. Este proceso implica hidroxilación, desmetilación y epoxidación, lo que conduce a la formación de metabolitos como el AF-8,9-epóxido. Este metabolito puede unirse a las proteínas, causando toxicidad aguda (aflatoxicosis) o daños en el ADN, induciendo potencialmente cáncer. La AFB1 es la aflatoxina más tóxica debido a su alto grado de epoxidación(67, 69).

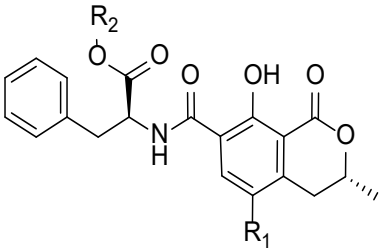
La UE establece límites en alimentos para la AFB1 (0,1 - 12 µg / kg), así como para la suma de AFs (4 - 15 µg / Kg)(3).

1.2.1.3 Ocratoxinas

Las ocratoxinas son micotoxinas producidas por varias especies de *Aspergillus* y *Penicillium*, principalmente *A. carbonarius* y *P. verrucosum* (70). *A. carbonarius,* es la principal fuente de contaminación por OTA en uvas y vinos en Europa (71). Sin embargo, *P. verrucosum* también es productora de OTA y constituye una de las principales preocupaciones en lo que respeta a contaminación de cereales en regiones más frías, como el norte de Europa (72, 73).

La OTA se considera una de las micotoxinas más importantes y es la ocratoxina más relevante en términos de presencia y toxicidad. Se aisló por primera vez en los Balcanes en 1965 a partir de cultivos de cereales que habían causado la muerte de animales (71, 73). Esta ocratoxina se compone de una fracción de dihidrocumarina unida a una molécula de L-β-fenilalanina por un enlace amida. Otras ocratoxinas, como la ocratoxina B (OTB), un derivado declorado de la OTA, y la ocratoxina C (OTC), un éster etílico de la OTA, también suelen encontrarse en productos contaminados (Figura. 4)(74).

USC UNIVERSIDADE DE SANTIAGO DE COMPOSTELA



Compuesto	R_1	R_2
OTA	Cl	H
OTB	H	H
OTC	Cl	C_2H_5

Figura 4. Estructura de las ocratoxinas

La OTA se absorbe rápidamente a través del tracto gastrointestinal y en el torrente sanguíneo se une a la albúmina y a otras proteínas plasmáticas, lo que le confiere una larga vida media en suero (de 35 días en humanos). Es metabolizada en el hígado, principalmente por hidroxilación y se excreta a través de los riñones (75). La OTA y la OTB tienen una actividad *in vitro* similar, sin embargo, la OTA es más nociva debido a su menor acumulación en plasma y tejidos (76).

La OTA produce su toxicidad a través de varios mecanismos que conducen a efectos adversos para la salud humana y animal. Inhibe la síntesis de proteínas, induce la peroxidación lipídica, altera la función mitocondrial, interfiere en la homeostasis del calcio y genera especies reactivas del oxígeno (ROS, del inglés *reactive oxigen species*)(77, 78). Estas acciones contribuyen al estrés oxidativo, al daño celular y a la alteración de funciones celulares. La capacidad de la OTA para inhibir la síntesis de proteínas e inducir la peroxidación lipídica puede provocar una disminución de la producción de proteínas esenciales y dañar las membranas celulares. Además, su impacto sobre la respiración mitocondrial y la homeostasis del calcio puede conducir al agotamiento energético y a la disfunción celular(78). Los efectos tóxicos generales de la OTA abarcan nefrotoxicidad, hepatotoxicidad, inmunotoxicidad, neurotoxicidad y posibles efectos genotóxicos, lo que pone de relieve la amplia gama de riesgos para la salud asociados a la exposición a la OTA. Además, se ha descrito que esta toxina puede atravesar la placenta, resultando en embriotoxicidad y teratogénesis (74).

La IARC ha clasificado a la OTA como posible carcinógeno humano (Grupo 2B), enfatizando su papel potencial en el desarrollo de cáncer. Se cree que los efectos genotóxicos de la OTA se relacionan con el metabolismo oxidativo, el cual desempeña un importante papel en su acción carcinogénica (79).

Los límites máximos en alimentación humana para esta toxina oscilan entre 0,5 - 15 µg / kg (3).

1.2.1.4 Patulinas

Las PAT son lactonas heterocíclicas insaturadas producidas por varias especies de *Penicillium, Aspergillus* y *Byssochlamys,* siendo *P. expansum*, su principal productor (Figura. 5). La contaminación con PAT se asocia a manzanas y sus subproductos. Sin embargo, también se ha identificado en otras frutas como peras, higos o tomates (80). Se aisló en 1943 como un antibiótico efectivo frente a bacterias gram-positivas y gram-negativas, pero estudios posteriores demostraron su toxicidad en humanos y animales (81).

USC UNIVERSIDADE DE SANTIAGO DE COMPOSTELA

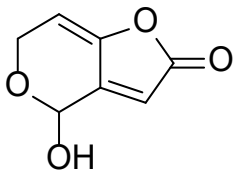


Figura 5. Estructura de la PAT

Existen pocos datos acerca de su metabolismo y absorción, sin embargo, se sabe que se acumula principalmente en eritrocitos y que se excreta unas 24 h después de su exposición (58). Se trata de un compuesto con gran afinidad por moléculas que contienen sulfhidrilo como la cisteína o el glutatión. Gracias a esta afinidad, inhibe numerosas enzimas, entre las que destacan ATPasas, enzimas lisosomales y la ARN polimerasas. También suprime la actividad catalasa, lo cual produce un aumento de ROS que lleva a estrés oxidativo dentro de las células y afecta la replicación del ADN (82).

Entre los efectos tóxicos de la PAT destacan alteraciones agudas en el tracto gastrointestinal. Esta toxina, altera la permeabilidad de las células intestinales y el transporte de iones al tiempo que destruye las uniones estrechas del epitelio celular, causando ulceración e inflamación de las mucosas, gástrica e intestinal (58, 82).

Por otro lado, la exposición crónica a la PAT modifica la composición de la flora gastrointestinal, y puede conducir a neurotoxicidad y efectos inmunosupresores. Además, altera la expresión genética relacionada con la apoptosis y la proliferación celular, provocando potencialmente cambios cancerígenos con una exposición prolongada (83).

En alimentos, se establecen límites ente 10 y 50 µg/ kg (3).

1.2.1.5 Tricotecenos

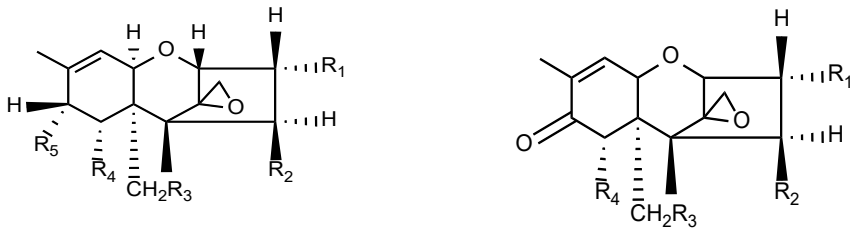
Los tricotecenos son micotoxinas producidas principalmente por hongos del género *Fusarium,* que contaminan distintos tipos de cereales como maíz o trigo y que presentan una elevada prevalencia a nivel mundial (84, 85). Otros géneros de hongos como *Stachybotrys*, *Trichoderma*, *Trichothecium*, *Cephalosporium* y *Cylindrocarpon,* también son productores de tricotecenos (86).

Estas micotoxinas fueron descubiertas en la década de 1940 durante una búsqueda de agentes antifúngicos. Sin embargo, no fue hasta 1980 cuando se estableció la conexión entre los tricotecenos y determinadas enfermedades. En particular, se encontró que los tricotecenos estaban vinculados con la aleucosis alimentaria (ATA) en la Unión Soviética y la enfermedad del moho rojo en Japón (85, 87). La ATA fue una afección particularmente grave que durante la Segunda Guerra Mundial causó la muerte de miles de personas en Rusia, y que se asoció al consumo de cereales contaminados con hongos del género *Fusarium*. Esta enfermedad se caracterizaba por síntomas como fiebre, hemorragia, necrosis y supresión del sistema inmunológico (36). Por otro lado, la enfermedad del moho rojo se reportó por primera vez el Japón rural en 1800 y se relacionó con un aumento en la producción de trigo. Posteriormente, también se asoció al consumo de cereales como cebada o avena, infectados por distintas especies de *Fusarium.* Esta afección se caracterizaba por cuadros de gastroenteritis en humanos (88, 89). Años después se descubrió que la micotoxina T-2, uno de los tricotecenos más tóxicos, estaba implicada en la ATA y que el DON, tricoteceno más abundante, era el responsable de la enfermedad del moho rojo (88, 90).

Los tricotecenos son un grupo de sesquiterpenos que incluyen más de 200 análogos, todos ellos conteniendo un grupo epóxido (Figura 6). Las características estructurales de los tricotecenos están estrechamente relacionadas con sus actividades biológicas y su toxicidad.

Estos compuestos comparten un núcleo tricíclico, conocido como 12,13-epoxitricotec-9-eno (EPT) o tricoteceno, que contiene un grupo espiro-epóxido en C-12 y C-13 y un doble enlace entre C-9 y C-10, esenciales para su toxicidad, ya que su eliminación provoca una pérdida total de esta. Según el patrón de sustitución del EPT, se clasifican en cuatro grupos (Tipos A, B, C y D). Los tipos A, B y C se pueden diferenciar en función de la sustitución en la posición C-8. Así, los tricotecenos de tipo A tienen una cadena lateral de tipo éster o hidrógeno en la posición C-8. Los tricotecenos de tipo B tienen un grupo cetónico en esta posición y los tricotecenos de tipo C tienen un segundo grupo epóxido en C-7/C-8. En lo que respecta a los tricotecenos de tipo D, menos comunes, incluyen compuestos macrocíclicos con anillos adicionales (84, 91).

Tipo A **Tipo B**



Tricotecenos de TIPO A

Toxina	R_1	R_2	R_3	R_4	R_5
T-2	OH	$OCOCH_3$	$OCOCH_3$	H	$OCOCH_2CH(CH_3)_2$
HT-2	OH	OH	$OCOCH_3$	H	$OCOCH_2CH(CH_3)_2$

Tricotecenos de TIPO B

Toxina	R_1	R_2	R_3	R_4
DON	OH	H	OH	OH
3-AcDON	$OCOCH_3$	H	OH	OH
15-AcDON	OH	H	$OCOCH_3$	OH
Nivalenol	OH	$OCOCH_3$	$OCOCH_3$	H

Figura 6. Estructura de los tricotecenos de Tipo A y Tipo B

Los tricotecenos producidos por especies de *Fusarium*, y por tanto los más frecuentes, pertenecen a los tipos A y B(58).En el primer grupo se incluyen toxinas como el diacetoxiscirpenol (DAS), la toxina T-2 y la toxina HT-2, conocidos por ser altamente tóxicas, mientras que en el tipo B destacan el nivalenol y el DON (92).

En lo que respeta a los tricotecenos de tipo A, la mayor parte de los datos toxicocinéticos se refieren a la toxina T-2, tricoteceno más tóxico y principal responsable de la ATA. Esta toxina puede transmitirse por ingestión de alimentos o agua contaminados, inhalación o vía dérmica y su absorción, distribución y eliminación se producen rápidamente. Se metabolizan en el hígado y en diversos tejidos a través de procesos como la hidroxilación, la desepoxidación, la acetilación y la conjugación (58, 90). Sus efectos toxicológicos dependen de la dosis y vía de exposición (oral, dérmica o aerosol), e incluyen, entre otros, vómitos, diarrea hemorrágica, enteritis, necrosis estomacal, dermatitis, leucopenia, agranulocitosis y agotamiento de la médula ósea (90). La HT-2 surge como un compuesto significativo entre los productos del metabolismo de la T-2. Tanto la T-2 como sus metabolitos se expulsan a través de la orina y las

USC DE COMPOSTELA

heces (93). La principal toxicidad de estos tricotecenos deriva de su interacción con la subunidad 60S de los ribosomas, lo que provoca la inhibición de la síntesis de proteínas y la subsiguiente alteración de la síntesis de ADN y ARN. En consecuencia, los tricotecenos de tipo A impiden la hematopoyesis e interfieren en la diferenciación de los monocitos en macrófagos y células dendríticas (58, 94). Además, la intoxicación con estas toxinas produce estrés oxidativo, que se asocia a efectos deletéreos como el aumento de la peroxidación lipídica, daños en el ADN nuclear y mitocondrial, alteraciones en la señalización celular y alteraciones en vías inflamatorias. Por otro lado, se ha descrito que afectan al ciclo celular e inducen apoptosis (90, 95).

Como ya se mencionó anteriormente, la exposición aguda a tricotecenos de tipo A, principalmente a la toxina T-2, conduce al desarrollo de ATA. Mientras que la exposición crónica a los mismos se asocia con anorexia, reducción de la ganancia de peso corporal y lesiones en el tracto digestivo superior (96).

Los datos disponibles sobre tricotecenos de tipo B se centran en el DON, sobre todo, en animales de producción.

1.2.1.5.1 Deoxinivalenol

El DON es la micotoxina con mayor importancia y más amplia distribución de todas las toxinas producidas por *Fusarium* (97). Fue asilada por primera vez en la década de 1970 en Japón por Morooka et al, a partir de cebada contaminada con hongos del género *Fusarium* (98). Inicialmente se identificó como “toxina Rd” y se relacionó con la enfermedad del moho rojo, previamente descrita. Posteriormente, se denominó como “vomitoxina”, dado que se asoció con cuadros agudos de vómitos. Actualmente, ambos términos están en desuso (88, 99).

El maíz, la cebada, la avena y el trigo son los granos más afectados por el DON, así como por sus derivados de acetilo y conjugados de glucósido, que predomina en regiones templadas y frías, aunque su prevalencia es mundial (100, 101).

La exposición al DON se produce por ingestión, ya sea de alimentos contaminados como granos de cereales, o indirectamente a través de alimentos derivados de animales que han consumido piensos contaminados. En este sentido, se ha encontrado DON en huevos y carne, así como su metabolito de-epoxi-deoxinivalenol (DOM-1) en leche (102, 103). El consumo de alimentos contaminados con esta toxina puede dar lugar a intoxicaciones agudas o crónicas, en función de la cantidad ingerida. La intoxicación aguda con DON resulta en fiebre, mareos, dolores de cabeza, diarrea, vómitos, náuseas y dolor abdominal, mientras que la exposición crónica a esta toxina produce, entre otros, citotoxicidad, neurotoxicidad e inmunotoxicidad (97, 104). Numerosos estudios relacionan los efectos agudos del DON con alteraciones en el sistema nervioso central. Además, la exposición a esta toxina altera el equilibrio de la microbiota intestinal, afectando así al eje intestino-cerebro y provocando síntomas como náuseas y vómitos (40, 104, 105).

A nivel orgánico, el DON produce principalmente toxicidad intestinal, hepatotoxicidad, nefrotoxicidad y toxicidad reproductiva (100). La toxicidad del DON comprende numerosas vías de señalización celular. Esta toxina se une a una parte específica del ARN ribosomal 28S desencadenando un proceso llamado "síndrome de estrés ribotóxico", que conlleva la inhibición de la síntesis de proteínas. Esta unión puede provocar la activación de proteínas quinasas activadas por mitógenos (MAPK) y la disminución de la expresión de proteínas de unión estrecha, lo que resulta en la pérdida de la función de barrera intestinal(106). También afecta a otras vías de señalización como la proteína quinasa R activada por ARN (PKR) o la quinasa de células hematopoyéticas (Hck)(107). Por otro lado, sabe que el DON altera la función

USC UNIVERSIDADE DE SANTIAGO DE COMPOSTELA

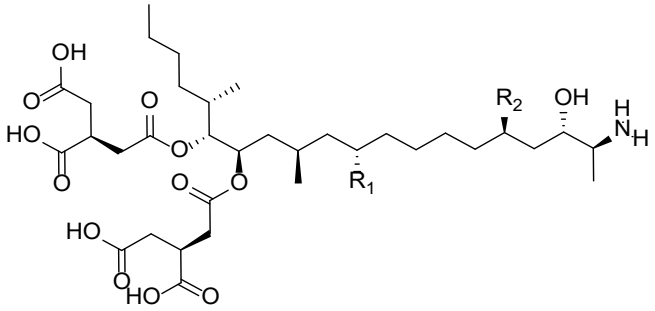
mitocondrial, lo que conduce a estrés oxidativo y apoptosis en diversas líneas celulares (108-110).

La especie más susceptible al DON son los cerdos, lo cual puede deberse a que poseen una tasa de absorción gastrointestinal mayor a la de otras especies como ratones, aves de corral o rumiantes. En este sentido, hasta un 82% de DON administrado por vía oral llega a circulación sistémica (91, 111). Por este motivo, la legislación europea establece límites máximos en alimentos para esta toxina (200- 1750 µg/ kg de alimento)(3).

1.2.1.6 Fumonisinas

Las FBs son micotoxinas producidas por diferentes especies de *Fusarium*, entre las que destacan *F. verticillioides* (previamente denominado *F. moniliforme*) y *F. proliferatum* (112). Se aislaron por primera vez en 1988 en Sudáfrica, a partir de cultivos de *F. verticillioides* provenientes de piensos a base de maíz, cuyo consumo se había relacionado con un brote de leucoencefalomalacia equina (ELEM)(113, 114). Estas toxinas contaminan principalmente maíz y derivados, aunque también afectan a trigo y otros cereales, a lo largo del todo el mundo (112).

Las FBs poseen una estructura que recuerda a la de la esfingosina. Consiste en una cadena alifática de 20 átomos de carbono con dos grupos metilo, una amina, de uno a cuatro hidroxilos, y dos cadenas laterales de ácido tricarboxílico esterificado (115). Según sus grupos sustituyentes, se clasifican en series A, B, C y P, siendo únicamente las FBs tipo B relevantes en términos de toxicidad y ocurrencia (112, 116). De este último grupo, la FB1 es la más tóxica, y suele aparecer conjuntamente con otros análogos como las FB2 y B3 (FB3), que se diferencian en la posición de sus grupos hidroxilo (Figura. 7)(117). La suma de FB1, FB2 y FB3 supone más del 90% del contenido total de FB presentes en muestras contaminadas (118).



Toxina	R_1	R_2
FB_1	OH	OH
FB_2	H	OH
FB_3	OH	H

Figura 7. Estructura de las FBs

Estos compuestos son solubles en disolventes polares, pero se absorben mal. Menos del 5% de las FBs ingeridas llegan al torrente sanguíneo (119, 120). Las fracciones absorbidas se distribuyen rápidamente, principalmente al hígado y los riñones, causando daños en los mismos y se eliminan tanto en heces como en orina (112). Pese a su baja absorción, son citotóxicas y carcinogénicas. Causan daños como necrosis licuefactiva de la materia blanca del cerebro en caballos o edema pulmonar en cerdos. En humanos se han relacionado con defectos en la formación embrionaria de estructuras nerviosas o cáncer de esófago (112, 121-123).

USC UNIVERSIDADE DE SANTIAGO DE COMPOSTELA

Sus efectos tóxicos se deben a la inhibición de la ceramida sintasa, enzima clave en la biosíntesis de esfingolípidos, importantes constituyentes de la membrana celular (120, 124). Esta inhibición produce la disrupción del metabolismo de esfingolípidos, conduciendo a una acumulación de bases esfingoides libres, que son citotóxicas y pueden alterar los procesos celulares. Además, reduce la producción de esfingolípidos complejos, que son cruciales para el mantenimiento de las funciones de membrana (112, 121, 125). Esta interrupción en el metabolismo de esfingolípidos es aceptada generalmente como el mecanismo de acción de las FBs, sin embargo, solo se ha determinado definitivamente su fisiopatología en cerdos (112).

1.2.1.6.1 Fumunosina B1

La FB1, mayoritariamente producida por *F. verticillioides,* es la fumonisina de mayor prevalencia y por lo tanto la más estudiada. Contamina mayoritariamente maíz en numerosas partes del mundo y su exposición se produce mayoritariamente mediante ingestión (126, 127). Es nefrotóxica, hepatotóxica, neurotóxica y ha sido clasificada como posible carcinógeno para los humanos (Grupo 2B) por la IARC (127, 128). Además, se ha demostrado que produce estrés oxidativo, cambios en el metabolismo mitocondrial y alteración de la homeostasis del calcio en distintas líneas celulares (124, 129, 130). Asimismo, perjudica la formación y deposición de mielina en células de glia (131).

Esta toxina causa diversas enfermedades en animales, como síndrome de edema pulmonar en cerdos (PPE), ELEM, y cáncer de hígado en ratas (132, 133). Sin embargo, solo se conoce el mecanismo fisiopatológico exacto en el caso del PPE. En este sentido, la inhibición de la ceramida sintasa por parte de la FB1, conduce a un aumento de esfingosina, segundo mensajero que inhibe los canales de calcio tipo L, presentes en el miocardio. Esta inhibición da como resultado, una disminución de la salida de calcio del retículo sarcoplasmático, reduciendo así la contractilidad cardiaca. Consecuentemente, se produce fallo agudo del ventriculo izquierdo y edema pulmonar (126, 134). En lo que respeta a la ELEM, una enfermedad fatal que se caracteriza por necrosis licuefactiva del material blanco cerebral, se cree que su mecanismo se debe al efecto directo de la FB1 sobre el aumento de esfingosina. Sin embargo, esta hipótesis no se ha confirmado todavía (112, 134).

En humanos, la exposición a la FB1 se ha asociado con un mayor riesgo de ciertos cánceres, en particular cáncer de esófago y de hígado, en poblaciones que consumen dietas basadas en maíz altamente contaminadas (121, 135). Además, se cree que la FB1 está implicada en la aparición de defectos del tubo neural en niños. En estudios realizados con embriones de ratón, se vio que estos desarrollaban defectos en el tubo neural al ser tratados con FB1 y, en un estudio control realizado en Texas, se observó que el consumo de alimentos contaminados con FB1 se relacionaba con una mayor incidencia de dichas malformaciones en recien nacidos (124).

En Europa, se establecen límites máximos en alimentos para esta toxina y su análogo FB2 (200 – 4000 µg/ kg) (3).

1.2.1.7 Zearalenona

La ZEA, anteriormente denominada toxina F-2, es una micotoxina producida por diferentes especies de hongos del género *Fusarium*, como *F. graminearum, F. culmorum* o *F. cereales*, que contaminan cereales como el maíz, trigo, cebada, avena y centeno (58, 136). Esta micotoxina, conocida por sus efectos estrogénicos, fue aislada en 1962 a partir de una cepa de *F. graminearum* obtenida del pienso de cerdos que presentaban hinchazón vulvar y mamaria (137, 138).

USC UNIVERSIDADE DE SANTIAGO DE COMPOSTELA

Geográficamente, la contaminación por ZEA está muy extendida, pero tiende a ser más frecuente en las regiones templadas, donde las condiciones climáticas favorecen el crecimiento de las especies de *Fusarium* (139).

La estructura química de esta micotoxina recuerda a estrógenos naturales y comprende una fracción de resorcinol unida a un anillo de lactona macrocíclica de 14 miembros, que incluye un doble enlace trans, una cetona y un metilo (140) (Figura 8). La reducción del grupo cetona a un grupo hidroxilo alcohólico da lugar a los estereoisómeros α-ZEA y β-ZEA, que son metabolizados por el hígado y el intestino a α-zearalanol y β-zearalanol. Estos metabolitos se conjugan con ácido glucurónico y se excretan en la orina y la bilis, siento esta última la mayor ruta de excreción de la toxina (141-143).

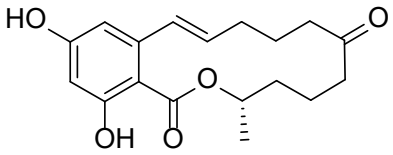


Figura 8. Estructura de la ZEA

Entre los principales efectos tóxicos de la ZEA destacan efectos estrogénicos, hepatotoxicidad, inmunotoxicidad, genotoxicidad y carcinogénesis (139). Estos efectos tóxicos están mediados por la unión de la ZEA y sus metabolitos a receptores de estradiol, activando la expresión génica y la síntesis de nuevas proteínas (140, 143). La toxicidad reproductiva es la más importante, ya que puede causar problemas como infertilidad, reducción del tamaño de las camadas y otros trastornos asociados a la actividad estrogénica, siendo los cerdos la especie más susceptible (143). En los tejidos reproductivos, se ha demostrado que esta toxina induce estrés oxidativo mediante un aumentó en la producción de ROS, apoptosis, disfunción celular y altera el equilibrio hormonal, entre otros daños (139, 144). En cuanto a efectos carcinogénicos, la ZEA ha sido clasificada por la IARC como carcinógeno de grupo 3, ya que produce formación de aductos y fragmentación de ADN, aberraciones cromosómicas, formación de micronúcleos y apoptosis (143). Por otro lado, se ha descubierto que la ZEA presenta efectos inmunosupresores, ya que reduce la producción de citoquinas antiinflamatorias, como la interleucina (IL) - 10 y aumenta la producción de citocinas proinflamatorias (IL-6 e IL-1β) (145). Además, la ZEA y sus metabolitos pueden provocar cambios histopatológicos en el hígado, como congestión sinusoidal, vacuolización citoplasmática, necrosis hepatocelular e infiltración de neutrófilos. También se ha observado que la toxina aumenta la actividad de la alanina transaminasa, la aspartato transaminasa y los peróxidos lipídicos, al tiempo que disminuye la actividad del glutatión tisular y el citocromo P450 (143, 146).

En humanos la exposición a ZEA se ha relacionado con un desarrollo sexual precoz, infertilidad, malformaciones y cáncer de mama. La UE recoge límites máximos (20 -350 µg/ kg) para esta toxina en alimentos (3, 147).

1.2.2 Micotoxinas emergentes

El término "micotoxinas emergentes" no está claramente definido. En un primer lugar, se utilizó para referirse a los metabolitos de *Fusarium* (beauvericina (BEA), eniatinas (ENNs), y moniliformina (MON)). Sin embargo, estudios recientes incluyen en este grupo a todas las micotoxinas que no son analizadas de manera rutinaria ni están reguladas legalmente, pero cuya ocurrencia está aumentando rápidamente (148).

USC DE SANTIAGO DE COMPOSTELA

En la presente tesis doctoral se estudiarán los efectos de la BEA y ENNs, así como de otras toxinas como la apicidina (API), la destruxina B (DEST B), el ácido ciclopiazónico (CPA) y la roquefortina C (ROQC).

1.2.2.1 Beauvericina

La BEA es una micotoxina producida por varias especies de *Fusarium,* entre las que se incluyen *F. proliferatum, F. semitectum, and F. subglutinans* (149). Fue aislada e identificada por primera vez en 1969 a partir del hongo *Beauveria bassiana*, capaz de parasitar insectos y, desde entonces, se ha detectado su presencia en numerosos alimentos, entre los que se incluyen cereales (maíz, arroz, trigo), piensos, frutas, verduras o incluso productos lácteos (14, 150, 151). Esta toxina se produce en condiciones húmedas y frescas, sin embargo, su presencia se extiende por todo el mundo (149, 152).

La BEA es un hexadepsipéptido cíclico que contiene tres residuos D-hidroxiisovaleril y tres residuos N-metilfenilalanil en una secuencia alterna (Figura.9)(153).

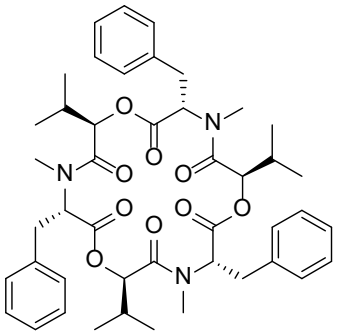


Figura 9. Estructura de la BEA

Los principales efectos de la BEA incluyen citotoxicidad, genotoxicidad, e inmunotoxicidad (153-155). A nivel celular, se ha demostrado que induce estrés oxidativo, altera la función mitocondrial e interfiere con las vías de señalización celular, lo que provoca apoptosis y necrosis en las células (156-158). Además, presenta efectos genotóxicos al provocar daños en el ADN, aberraciones cromosómicas y formación de micronúcleos, lo que puede contribuir a su potencial cancerígeno (159).

Los mecanismos toxicológicos subyacentes a la toxicidad de la BEA implican sus interacciones con membranas celulares y canales iónicos dentro de las células. Esta toxina forma canales selectivos de iones con varios cationes metálicos (entre los que se incluyen Ca^{2+}, Na^{+} y K^{+}), provocando así un aumento en la permeabilidad de la célula, lo cual puede conducir a su muerte (160, 161). Además, se ha demostrado que la BEA inhibe varias enzimas implicadas en el metabolismo celular y las vías de señalización, lo que exacerba aún más sus efectos tóxicos (162).

A pesar de la elevada citotoxicidad de esta toxina, las autoridades pertinentes no han llevado a cabo ninguna evaluación de riesgos debido a la falta de datos sobre la misma, por lo que la investigación sobre el impacto toxicológico del BEA aún está en curso.

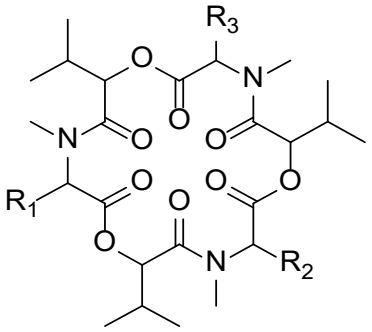
1.2.2.2 Eniatinas

Las ENNs son un grupo de micotoxinas producidas principalmente por hongos del género *Fusarium,* que fueron aisladas por primera vez en 1947, a partir de *Fusarium oxysporum* (163). Estas micotoxinas se han encontrado en diversos alimentos y piensos, incluyendo cereales y

USC DE SANTIAGO DE COMPOSTELA

productos a base de cereales, leche y otros derivados, lo cual contribuye a la exposición humana y animal (14, 164-167).

Estructuralmente, las ENNs son ciclohexadepsipéptidos compuestos por residuos alternos de tres aminoácidos N-metilados, normalmente valina, leucina e isoleucina, y tres hidroxiácidos, principalmente ácido hidroxiisovalérico (Figura 10)(58). Hasta la fecha se han descrito 29 análogos de ENNs, siendo las ENN A, A1, B y B1, los encontrados con mayor frecuencia en alimentos (14, 168, 169).



Toxina	R_1	R_2	R_3
ENNA	$CH(CH_3)CH_2CH_3$	$CH(CH_3)CH_2CH_3$	$CH(CH_3)CH_2CH_3$
$ENNA_1$	$CH(CH_3)CH_2CH_3$	$CH(CH_3)CH_2CH_3$	$CH(CH_3)_2$
ENNB	$CH(CH_3)_2$	$CH(CH_3)_2$	$CH(CH_3)_2$
$ENNB_1$	$CH(CH_3)_2$	$CH(CH_3)_2$	$CH(CH_3)CH_2CH_3$

Figura 10. Estructura de las principales eniatinas

Los principales efectos de las ENNs en los sistemas biológicos incluyen citotoxicidad y alteración de las funciones celulares (170). Varios estudios han demostrado que estas toxinas inducen apoptosis y alteran la función mitocondrial en diferentes líneas celulares (171, 172). Además, pueden aumentar la producción de ROS, lo que provoca estrés oxidativo y daño a lípidos, proteínas y ADN (173, 174). A concentraciones elevadas, estas toxinas también pueden causar necrosis celular (173).Además, las ENNs pueden atravesar la BHE, por lo que podrían causar daños a nivel central (41).

En lo que respecta a toxicidad crónica, los datos existentes son limitados. Sin embargo, estudios *in vivo* llevados a cabo con estos compuestos revelan efectos adversos, como reducción de peso del animal, y bioacumulación de ENNs en tejidos (175).

Debido a las similitudes estructurales entre ENNs y BEA, tradicionalmente sus mecanismos biológicos se han relacionado, considerando estas toxinas como ionóforas (158, 176). En 1973, se propuso que la ENN B formaba complejos en membranas biológicas, permitiendo el paso de iones (177). Sin embargo, los datos sobre el comportamiento ionofórico de las ENNs son escasos y se centran en la ENN B (158, 178). La comprensión de las propiedades ionofóricas de las ENNs y sus efectos toxicológicos aún está evolucionando y los estudios en estas áreas son limitados. La creciente prevalencia de la contaminación por ENNs en Europa, así como su potencial bioacumulación hacen de estas toxinas un peligro inherente para la salud (15, 166, 179, 180).

USC UNIVERSIDADE DE SANTIAGO DE COMPOSTELA

1.2.2.3 Apicidina

La API es una micotoxina mayoritariamente producida por hongos del género *Fusarium*, que se aisló por primera vez en 1996 como un agente antiprozoario (181, 182). Es un tetrapéptido cíclico, compuesto por cuatro residuos de aminoácidos: N-dimetil-L-valina, L-2-amino-8-oxo-9,10-epóxido-decanoico, N-metil-L-valina y L-4-metilprolina (Figura. 11). Esta estructura química le confiere actividades biológicas específicas, como capacidad para inhibir las desacetilasas de histonas (183). La inhibición de estas enzimas provoca alteraciones en la expresión genética y el ciclo celular, así como apoptosis en diversos tipos celulares (184, 185). Por otro lado, la API también produce efectos citotóxicos y autofagia en distintas líneas de carcinoma e inhibe la proliferación de otras líneas tumorales (185-187).

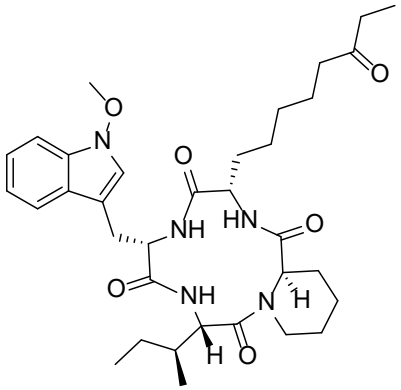


Figura 11. Estructura de la Apicidina

1.2.2.4 Destruxina B

La DEST B es una micotoxina producido por varios hongos, entre los que destaca *Metarhizium anisopliae*, un hongo patógeno de insectos (188). La toxina fue aislada por primera vez de este *Metarhizium* en 1961 y desde entonces, se han descubierto 39 destruxinas diferentes (189, 190).

Estructuralmente, esta toxina es un hexadepsipéptido cíclico (Figura. 12) con una amplia gama de actividades biológicas, incluyendo efectos insecticidas, antitumorales, antivirales, citotóxicos e inmunosupresores (190, 191). Se ha demostrado que suprime la expresión del gen del antígeno de superficie del virus de la hepatitis B en células de hepatoma humano e inhibe la expresión genética y la replicación de este, tanto *in vitro* como *in vivo* (192, 193). Por otro lado, la DEST B induce apoptosis a través de la vía del receptor de muerte y altera el potencial de la membrana mitocondrial en células de linfoma no Hodgkin humano (194).

Aunque se ha descrito como un inhibidor específico y reversible de la ATPasa translocadora de H^+ de tipo vacuolar, el mecanismo de acción subyacente a los efectos de la DEST B aún no se ha dilucidado por completo (195).

USC
UNIVERSIDADE DE SANTIAGO DE COMPOSTELA

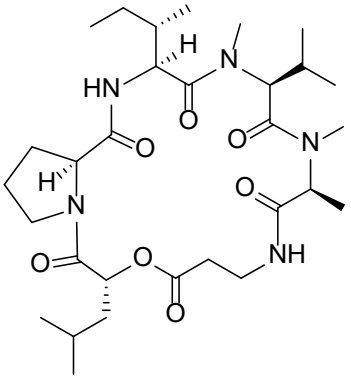


Figura 12. Estructura de la destruxina B

1.2.2.5 Ácido ciclopiazónico

El CPA es una micotoxina producida por varias especies de *Aspergillus* y *Penicillium,* entre las que destaca *P. roqueforti*, usado en el proceso de maduración de algunos quesos (196). Esta toxina contamina diversos tipos de alimentos en todo el mundo, incluyendo cereales, leche y frutos secos, además del queso (197-199). Se aisló por primera vez en 1968 de un cultivo líquido de P. *cyclopium Westling,* y se identificó como el principal componente tóxico de este hongo (196, 200, 201).

Químicamente, esta micotoxina está relacionada con los alcaloides ergolínicos y su estructura constituye un ácido indólico tetramérico (Figura 13), la cual contribuye a su actividad biológica y toxicidad (202, 203).

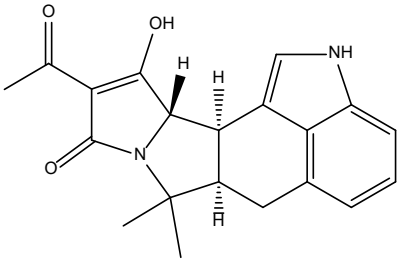


Figura 13. Estructura del CPA

En modelos animales, la exposición al CPA se ha relacionado con toxicidad aguda, incluyendo neurotoxicidad, trastornos gastrointestinales y hepatotoxicidad (204).Además, se han descrito efectos citotóxicos para este compuesto en varias líneas celulares (205, 206). Esta toxina inhibe la bomba ATPasa de calcio del retículo sarcoplásmico (SERCA, del inglés *sarcoendoplasmic recticulum calcium ATPase*), provocando alteraciones en procesos celulares como la liberación de neurotransmisores, la contracción muscular y la actividad enzimática (207, 208). Se ha demostrado que la inhibición de la SERCA por el CPA acorta la hiperpolarización dependiente del Ca^{2+} en neuronas simpáticas de rata, lo que indica un impacto directo en la función celular (209). Por otro lado, esta toxina aumenta las concentraciones cerebrales de dopamina y serotonina en pollos, lo que contribuye a sus efectos neurotóxicos (210).

La elevada prevalencia de CPA en alimentos y su co-ocurrencia con otras micotoxinas como las AFs, hace que esta toxina haya sido reconocida por la EFSA como una sustancia de preocupación toxicológica (211).

USC UNIVERSIDADE DE SANTIAGO DE COMPOSTELA

1.2.2.6 Roquefortina

La ROQC es una micotoxina producida principalmente por hongos del génenro *Penicillium* (212). Se aisló a partir de cepas de *Penicillium roqueforti*, un hongo filamentoso comúnmente utilizado en la producción de queso azul (como el Roquefort o el Gorgonzola) y posteriormente se detectó en otros alimentos como cerveza, cebollas o vino (212-214).

Estructuralmente, la ROQC (Figura 14) es un alcaloide indólico prenilado de dicetopiperazina (212). En cantidades altas, esta toxina es neurotóxica en ratones y su presencia se ha asociado a intoxicaciones en perros y ganado, con síntomas que incluían temblores, convulsiones y malestar gastrointestinal (215-217). Sin embargo, a concentraciones comúnmente encontradas en quesos se considera segura para el consumidor (214). Es importante tener en cuenta que la incidencia de la ROQC en quesos está aumentado, en conjunto con la de otras micotoxinas (164, 166, 218). Además, no hay suficientes datos sobre su toxicidad, y su mecanismo de acción sigue sin estar claro. Se cree que ejerce sus efectos tóxicos a través de interacciones con el citocromo p450 (219). Por lo tanto, nuevas investigaciones pueden aportar datos adicionales sobre la toxicidad de este compuesto.

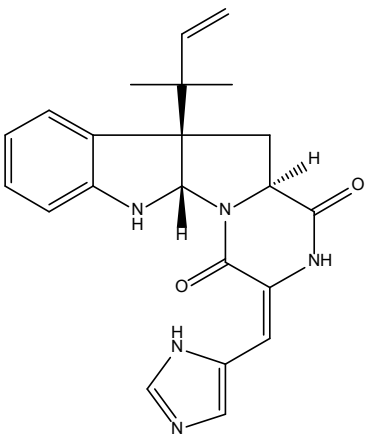


Figura 14. Estructura de la ROQC

1.3 CO-OCURRENCIA DE MICOTOXINAS REGULADAS Y EMERGENTES

Los alimentos no están contaminados por un único tipo de micotoxina. Un cereal como el maíz puede estar infestado simultáneamente por varias especies de *Fusarium, Aspergillus* o *Penicillium*, que producen diferentes tipos de estos compuestos (220). Sin ir más lejos, se ha detectado la co-ocurrencia de micotoxinas reguladas y emergentes en muestras de pienso de Galicia y el noroeste europeo, destacando entre las primeras la presencia de DON, FB1 y ZEA, y entre las emergentes las ENNs y la BEA (167, 221). Estas dos últimas micotoxinas también han sido detectadas en quesos y leche (14, 164, 166).

La mayoría de datos existentes sobre cereales y piensos co-contaminados con micotoxinas corresponden a Europa, aunque existen datos a nivel mundial y los estudios revelan una ocurrencia y una contaminación conjunta generalizadas (34, 148). En un estudio global de 2013, se detectó que el 72 % de las muestras analizadas contenían cantidades detectables de al menos una micotoxina, mientras que el 38 % estaban afectadas por dos o más (222). Datos más recientes muestran una co-contaminación mayor, con un 64 % de las muestras conteniendo dos o más micotoxinas (34). Gran parte de estas combinaciones incluyen las micotoxinas reguladas DON, ZEA y FBs, así como AFs, en menor medida (34, 222). Entre las micotoxinas emergentes

USC UNIVERSIDADE DE SANTIAGO DE COMPOSTELA

detectadas, las ENNs y BEA son los principales contaminantes a nivel mundial, presentando una elevada prevalencia e incluso apareciendo a concentraciones realmente elevadas (148).

En lo que respeta a productos lácteos, los hongos del género *Penicillium* seguidos de *Aspergillus*, son los contaminantes más comunes (197). Algunas especies de *Penicillium*, como *P. roqueforti* o *P. camemberti*, se utilizan en la elaboración de quesos y son productoras de micotoxinas emergentes. Entre estas se incluyen la ROQC, el CPA o incluso micotoxinas reguladas como la PAT (164, 223). Estudios recientes detectaron la presencia de varias micotoxinas no reguladas en quesos comerciales, destacando la presencia de CPA y ROQC en combinación con BEA y ENNs (166).

La coexistencia de múltiples micotoxinas en alimentos y piensos es una preocupación importante, ya que estas toxinas pueden tener efectos sinérgicos o aditivos, lo que lleva a una mayor toxicidad y posibles riesgos para la salud. Sin embargo, apenas hay estudios sobre la toxicidad conjunta de estas sustancias, cuyas concentraciones varían enormemente entre muestras (224-226). Actualmente, la legislación recoge límites máximos para determinados tipos de micotoxinas, de forma individual. Sin embargo, no contempla límites para combinaciones de micotoxinas, exceptuando las AFs, y los datos sobre toxicidad conjunta de estos compuestos, son escasos (3). Hasta la fecha, se han probado diversas combinaciones de micotoxinas en diferentes tipos celulares, describiendose efectos sinérgicos o aditivos en numerosas mezclas que incluyen micotoxinas emergentes (227, 228). Por ejemplo, la co-exposición a CPA y AFB1 altera el metabolismo de los aminoácidos y la homeostasis redox, causando efectos tóxicos sinérgicos en esferoides de hepatocitos (227). Por otro lado, la combinación de ENNs con tricotecenos tiene efectos aditivos sobre el riñón (228). También se han observado efectos aditivos y sinérgicos para combinaciones binarias de ENNs, en distintas líneas celulares. En este sentido, la mezcla de ENN A y ENN A1 produce adición y/o sinergia en células humanas de cancer de colon Caco-2 y en células ováricas de ratón (228, 229). Asimismo, se describieron efectos sinérgicos para mezclas de BEA y DON y de BEA y FB1 en celulas Caco-2 y células epiteliales de riñón porcino, respectivamente (230, 231).

Debido a la creciente incidencia de micotoxinas emergentes y a la escasez de datos sobre su toxicidad conjunta, se requieren más investigaciones para comprender completamente su perfil toxicológico y sus efectos combinados. Esto permitirá establecer límites regulatorios para garantizar la seguridad de alimentos y piensos. Por lo tanto, en la presente tesis doctoral se profundizará en el estudio del efecto conjunto de estas toxinas, haciendo hincapié en el posible mecanismo subyacente de su toxicidad. Además, se evaluarán distintos extractos de alimentos naturalmente contaminados con micotoxinas, incluyendo pienso, leche y quesos, para comparar sus efectos con los producidos por mezclas de estándares de micotoxinas comerciales.

1.4 VÍAS DE SEÑALIZACIÓN CELULAR

Las micotoxinas actúan modulando distintas vías de señalización celular. Estas, son redes complejas de eventos moleculares que permiten a las células comunicarse y responder a su entorno (232, 233). Este proceso implica la recepción, entrega y procesado de señales eléctricas y químicas, siendo estas últimas la base principal de comunicación dentro del organismo (234). Las moléculas de señalización química, endógenas (liberadas por la célula) o exógenas (fármacos, agentes citotóxicos), actúan como una molécula señal (o primer mensajero), que se une a un receptor proteico provocando su activación. A su vez, este receptor activa una o más señales intracelulares (segundos mensajeros) que alteran las proteínas diana para dar lugar a respuestas específicas (233, 235).

USC DE COMPOSTELA

Existen numerosos tipos de receptores proteicos que pueden encontrarse sobre la membrana celular, núcleo o citosol. Las moléculas lipofóbicas, incapaces de difundir

pasivamente a través de la membrana celular, se unen a proteínas receptoras de esta, entre las que se encuentran los canales iónicos dependientes de ligando, receptores acoplados a proteína G, receptores de enzimas y receptores integrinas (233). En el primer grupo se incluyen los receptores de iones de calcio (236). Los iones de calcio constituyen una señal intracelular importante ya que se unen a proteínas efectoras, lo cual le permite modular la apertura de canales iónicos, alterar el potencial de membrana e influir en la actividad enzimática, incluida la de las proteínas quinasas y fosfatasas (237, 238).

Esta regulación de las actividades celulares y las respuestas a diversos estímulos debe funcionar de manera controlada y transitoria para asegurar una correcta función celular. Cualquier alteración en las vías de señalización puede conducir a una respuesta patológica y desencadenar una cascada de procesos que terminen en la muerte celular (233).

En la presente tesis doctoral se estudiarán los efectos de micotoxinas emergentes en factores relacionados con la señalización celular, como el calcio, así como su en el proceso de muerte celular.

1.4.1 Calcio

El Ca^{2+} es el segundo mensajero celular más versátil. Todas las células utilizan señales de Ca^{2+} para regular su actividad en respuesta a estímulos extrínsecos o intrínsecos y cualquier cambio en la señalización y/o homeostasis de este ion puede alterar los procesos fisiológicos (239). Un principio clave en la señalización del Ca^{2+} es que toda variación en su concentración intracelular induce una respuesta. En condiciones de reposo, la concentración citosólica de este ion es baja, sobre 100 nM. Sin embargo, la activación de las células por diversos estímulos (hormonas, factores de crecimiento, pH, temperatura, etc.) puede aumentar significativamente la concentración de Ca^{2+} citosólico a valores de 1µM, volviendo a la concentración de reposo al terminar la estimulación (239, 240).

La célula regula la señalización del calcio, logrando el control espacial y temporal de los flujos de este ion, mediante el uso de orgánulos para liberar y almacenar el mismo (241). Por lo tanto, las células tienen acceso al calcio mediante dos vías principales: Su entrada desde el espacio extracelular y su liberación de reservorios intracelulares. Entre estos últimos se encuentran el núcleo, la mitocondria, el retículo endoplasmático (RE), el aparato de Golgi y los lisosomas. La liberación de Ca^{2+} de los reservorios intracelulares ocurre a través de canales que se encuentran en las membranas de los orgánulos siendo los receptores de inositol 1,4,5-trifosfato (IP3Rs), receptores de rianodina (RyR), canales de dos poros (TPCs, del inglés *two pore channels*) y la subfamilia mucolínica de canales de potencial receptor transitorio (TRPMLs, del inglés *transient receptor potential mucolipin channels*) los de mayor importancia (237, 239). En este sentido, los IP3R constituyen una familia de canales de Ca^{2+} compuestos por tres isoformas, que están presentes mayoritariamente en el RE, pero que también pueden encontrarse en el aparato de Golgi y membrana plasmática. La salida de calcio de estos canales regula numerosas funciones celulares, incluyendo la transcripción de genes o la proliferación celular (242). Los RyR se localizan en la membrana del RE y son responsables de la liberación de Ca^{2+} de las reservas intracelulares durante el acoplamiento excitación-contracción tanto en el músculo cardíaco como en el esquelético (243). En lo que respeta a los TPCs y los TRPMLs, estos constituyen los principales mecanismos de salida de calcio de los lisosomas (239).

A continuación, se presenta un resumen de los principales reservorios de calcio, así como de los canales iónicos involucrados en la movilización del ion, ya sea entre el espacio extracelular y el citosol, o entre el citosol y los orgánulos (Figura 15).

USC UNIVERSIDADE DE SANTIAGO DE COMPOSTELA

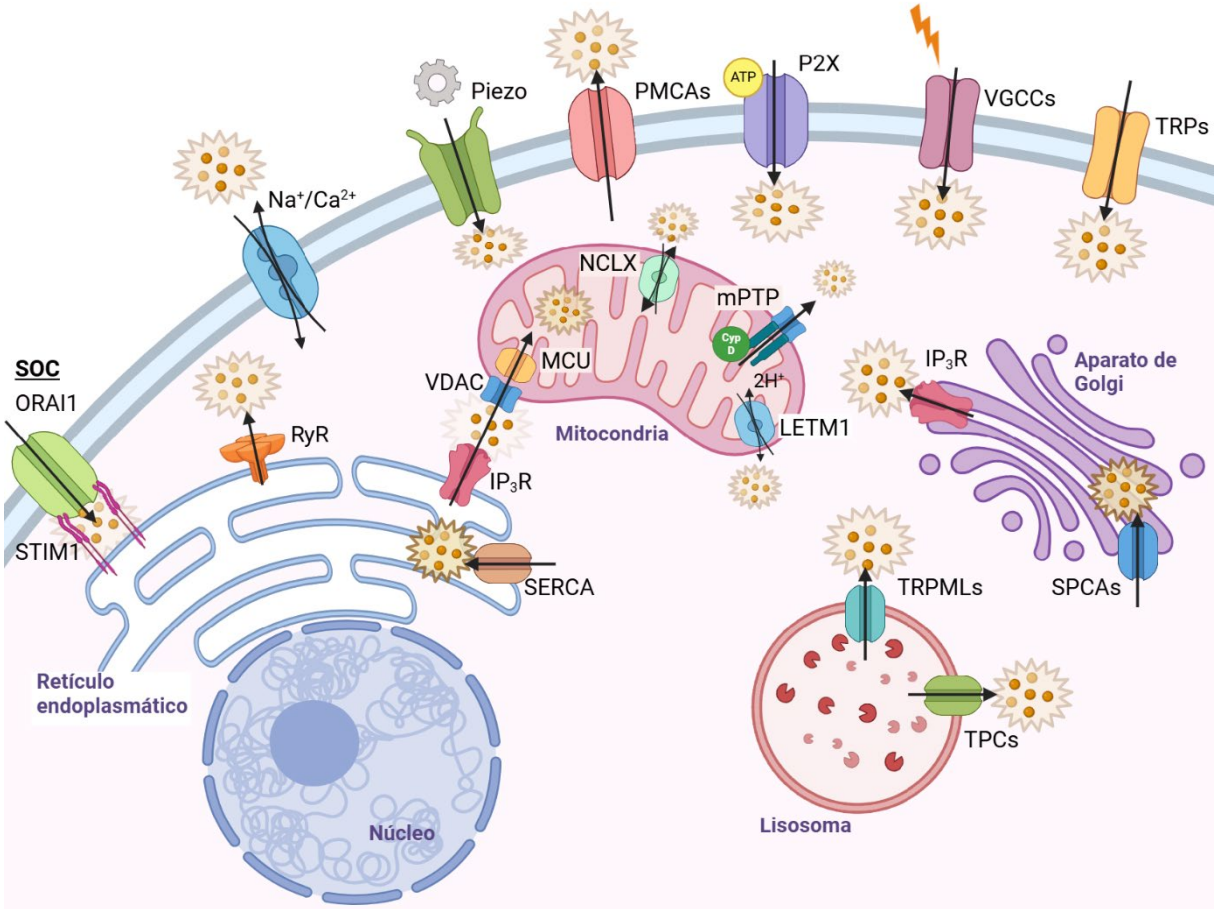


Figura 15. Esquema de los principales canales de calcio de la célula. En la membrana celular moviendo Ca^{2+} desde el citosol hacia el espacio extracelular destaca el PMCA. Introduciendo Ca^{2+} desde el espacio extracelular hacia el citoplasma hay canales "Piezo", receptores ionotrópicos P2X activados por ligando, VGCCs, TRPs y SOC. Dentro de estos últimos se incluye ORAI1, que interacciona con las moléculas STIM1 RE, cuando este se vacía de Ca^{2+}. En el RE el calcio está regulado por la SERCA, que introduce el ion en el orgánulo, y por los RyR y los IP3Rs, mecanismos de salida del ion. Los IP3R interaccionan con los VDAC de la mitocondria, permitiendo la entrada de Ca^{2+} al orgánulo a través del MCU. El ion puede salir de la mitocondria a través del mPTP, mediante el NCLX y el antiportador LETM1. El aparato de Golgi capta calcio a través de la SPCA y presenta IP3R como mecanismo de salida. Los lisosomas liberan calcio al citosol a través de TPCs y TRPMLs. Adaptación de Ahumada-Castro et. al (242). Imagen creada con biorender.com

El **RE** es el mayor reservorio de calcio intracelular, ya que alberga niveles del ion de entre 200 y 2000 µM. Sus altos niveles de Ca^{2+} se mantienen gracias a una familia de transportadores denominados SERCA, encargados de bombear el ion desde el citosol al ER. En lo que respeta a los mecanismos de salida del ion de este orgánulo, destacan los ya mencionados IP3R y RyR (241, 244). La salida de Ca^{2+} del ER a través de estos canales, activa la entrada del ion desde el medio extracelular a través de canales operados por reservorio (SOC, del inglés *store-operated calcium channels.*). En este sentido, las moléculas de interacción estromal 1 (STIM1, del inglés *stromal interaction molecule 1*), proteínas transmembrana del RE que actúan como sensores de Ca^{2+}, se unen al ion y cuando se vacía el reservorio, cambian de conformación uniéndose al canal de membrana plasmática Orai1, (que pertenece a los SOC), causando el influjo de calcio del medio extracelular al citosol. El RE también presenta un papel fundamental en la regulación del estrés celular, mediante la movilización de proteínas de señalización transmembrana del RE, las cuales se pueden dividir en dos grupos, en función de su afinidad para unirse al Ca^{2+}. En el primer grupo se incluyen aquellas con baja afinidad y alta capacidad,

USC UNIVERSIDADE DE SANTIAGO DE COMPOSTELA

mientras que en segundo se incluyen las proteínas con alta afinidad, pero baja capacidad (241, 244).

Las **mitocondrias** desempeñan un papel importante en la regulación de los niveles de Ca^{2+} citosólico, al amortiguar rápidamente sus fluctuaciones mediante la absorción y liberación de este ion según lo requieren los procesos celulares (239). Los niveles de Ca^{2+} en reposo de este orgánulo son similares a los niveles citosólicos (sobre 100 nM), pudiendo elevarse hasta 10 veces bajo estimulación. La entrada del ion a la mitocondria está regulada por proteínas de la membrana como canales aniónicos dependientes del voltaje (VDACs, del inglés *voltage-dependent anion channels*), en la membrana externa (OMM, del inglés *outer mitochondrial membrane*) y por el uniportador de calcio mitocondrial (MCU), presente en la membrana interna mitocondrial (IMM, del inglés *inner mitochondrial membrane*) (241, 245). Los VDACs, presentes en los sitios de contacto entre mitocondria y ER, interaccionan con los IP3R, formando un complejo con estos y la chaperona regulada por glucosa 75 (GRP75). Esta unión permite al calcio que se libera del ER, entrar en la mitocondria de forma directa (242, 246). Si los niveles del ion son demasiado altos, puede provocarse la apertura del poro de transición de permeabilidad mitocondrial (mPTP, del *inglés mitochondrial permeability transition pore*), y consecuentemente la muerte celular (246). El mPTP es una entidad supramolecular ensamblada a la interfaz de las membranas interna y externa de la mitocondria y constituye uno de los mecanismos de salida del ion del orgánulo (247). Existen varios candidatos moleculares para el mPTP, sin embargo, su naturaleza sigue siendo polémica. Recientemente se hipotetizó que está compuesto por la ATP sintasa, un transportador de fosfato y un translocador de nucleótidos de adenina (ANT, del inglés *adenine nucleotide translocator*), el cual se halla en estrecho contacto con la cadena respiratoria. La unión de Cyp D a la ATP sintasa provocaría un cambio en su conformación, provocando la apertura del mPTP. La masiva apertura del mPTP da lugar a una disipación del potencial de membrana mitocondrial, a la pérdida de la producción de ATP y posteriormente, a la muerte celular (248, 249). El Ca^{2+} también puede salir de la mitocondria mediante el intercambiador $Na^{+}/Ca^{2+}/Li^{+}$ (NCLX) y el antiportador LETM1 ("Leucine Zipper And EF-Hand Containing Transmembrane Protein 1"), que intercambia protones por el ion (242, 245).

En lo que respeta a los **lisosomas**, estos se consideran reservorios de Ca^{2+} ácidos (ya que presentan un pH alrededor de 4.6) o "pequeños", a pesar de tener la capacidad de albergar niveles del ion hasta 5000 veces superiores a los niveles citosólicos (~ 500 µM). Al igual que otros reservorios de Ca^{2+}, los lisosomas liberan y captan el ion en respuesta a distintos estímulos celulares. No obstante, los mecanismos mediante los que estos reservorios regulan el Ca^{2+} están poco estudiados hasta la fecha. Anteriormente, los lisosomas se conocían por ser la principal unidad de eliminación de residuos y centro de reciclaje de la célula, pero durante los últimos veinte años, se ha profundizado en el estudio de su papel como reservorio de Ca^{2+}. En este sentido se han descubierto distintos canales iónicos lisosomales capaces de movilizar el ion, entre los que destacan los TPCs, y TRPMLs. El Ca^{2+} lisosomal constituye un importante mensajero. Su liberación desencadena la fusión de los lisosomas con otros orgánulos, como la mitocondria (mediante interacción con los VDAC), y, su capacidad de tamponar el Ca^{2+} citosólico se ha relacionado con efectos neuroprotectores en algunas patologías. Sin embargo, se desconoce cómo estos orgánulos vuelven a captar el ion para mantener sus niveles luminales (241, 250, 251).

El **aparato de Golgi** es fundamental para la modificación, clasificación y empaquetamiento de macromoléculas que se originan el en ER, para el transporte vesicular de lípidos, proteínas y carbohidratos y para la biogénesis de los lisosomas (241, 252). Este orgánulo representa hasta el 5% del almacenamiento total de Ca^{2+} intracelular, pudiendo

albergar entre 100 y 300 μM del ion. Estos niveles se mantienen gracias a la entrada de Ca^{2+} a través de la vía secretora de la ATPasa1 de Ca^{2+} (SPCA1) y SERCA, y a su salida a través de los IP3R (239, 244). En este caso, el Ca^{2+} liberado por los IP3R de la membrana del aparato de Golgi es funcionalmente distinto del que se genera en las reservas de Ca^{2+} del ER. La pérdida de la homeostasis del Ca^{2+} en el aparato de Golgi puede afectar a la secreción y la polaridad neuronal, provocar trastornos cutáneos y causar enfermedades neurodegenerativas (241).

El **núcleo** también puede almacenar Ca^{2+}. El ion entra en el orgánulo a través de los poros nucleares, manteniéndose así una concentración similar a la citoplasmática. El Ca^{2+} nuclear es de particular interés en las neuronas, ya que está implicado en la regulación de la expresión génica. La pérdida de la dinámica nuclear del Ca^{2+} es perjudicial y se relaciona con trastornos neurodegenerativos (241).

El calcio de los orgánulos es finito, por lo tanto, la célula también capta el ion del espacio extracelular para mantener sus niveles citoplasmáticos (239). Para esto existen distintos tipos de canales, bombas e intercambiadores a lo largo de la membrana citoplasmática (253). Los SOC, canales de calcio dependientes de voltaje (VGCCs, del inglés *voltage-gated calcium channels*), canales iónicos de potencial receptor transitorio (TRPs, del inglés *transient receptor potential channels*), los canales de Ca^{2+} dependientes de ligando (como los P2X) y los canales "Piezo", están implicados en la movilización de Ca^{2+} desde el medio extracelular al citoplasma (253).

Los ya mencionados SOC son canales ampliamente estudiados, presentes tanto en células excitables como no excitables, que se activan por el agotamiento de Ca^{2+} de las reservas del RE. La salida de calcio del RE hace que las proteínas STIM se acumulen en las uniones entre RE y membrana plasmática, donde activan los canales Orai, y consecuentemente la entrada del ion. La depleción prolongada de las reservas de Ca^{2+} del RE puede provocar la entrada del ion a través de los SOC durante minutos u horas, resultando en una amplia variedad de procesos biológicos básicos como la secreción, la transcripción génica y la modulación de la actividad enzimática. Debido a que no son dependientes del voltaje, los SOC pueden introducir Ca^{2+} en la célula a potenciales de membrana negativos donde los canales sensibles a la despolarización están inactivos, permitiendo una función complementaria con estos (254, 255). En lo que respeta a los VGCCs, son un grupo de canales presentes en la membrana plasmática de células excitables como músculo y neuronas. Estos canales son permeables al Ca^{2+} y se activan mediante despolarización de la membrana celular, permitiendo a la célula regular varios procesos intracelulares como la transmisión sináptica o la contracción (256). Los TRP son un grupo de 28 canales catiónicos no selectivos (entre los que se incluyen los TRPML), que permiten el paso de iones Na^+, K^+ y Ca^{2+} (257). Se activan por una amplia gama de estímulos, como la temperatura, el pH, las fuerzas mecánicas y diversos mensajeros intracelulares (como el Ca^{2+} per se) (258). Tras su activación, los canales TRP permiten que el Ca^{2+} y otros cationes, fluyan por su gradiente electroquímico hacia el interior de la célula, provocando la despolarización de la membrana. Esto puede influir en la actividad de los VGCC, provocando una entrada adicional de Ca^{2+} (259). La actividad de la mayoría de los canales TRP está modulada por los niveles intracelulares de Ca^{2+}, que puede unirse directamente a estos canales, o activar vías de señalización dependientes del ion (257). Por lo tanto, el vaciamiento de Ca^{2+} de reservorios intracelulares puede activar los TRP, igual que ocurre con los SOC. Sin embargo, debido al gran número de canales pertenecientes al grupo TRP y a sus numerosos activadores, las funciones de estos canales siguen siendo controvertidas (260).

Por otro lado, los receptores ionotrópicos P2X activados por ligando, son una clase de receptores que regulan el paso de Ca^{2+} al interior de la célula en respuesta a ATP. Estos

USC UNIVERSIDADE DE SANTIAGO DE COMPOSTELA

receptores participan en diversos procesos fisiológicos, como la neurotransmisión, la inflamación y la percepción del dolor (253, 261).

Finalmente, los canales "Piezo" son canales mecanosensibles estimulados por fuerzas mecánicas, como presión, estiramiento o esfuerzo cortante. Están involucrados en el sentido del tacto, la propiocepción y el flujo sanguíneo (253, 262).

En cuanto a los mecanismos de salida de calcio de la célula destacan la Ca^{2+}-ATPasa de la membrana plasmática (PMCA, del inglés *plasma membrane calcium ATPase*) y el intercambiador Na^{+}/Ca^{2+} (253). La PMCA es una bomba de calcio que transporta activamente Ca^{2+} fuera de la célula en contra de su gradiente de concentración, utilizando energía procedente de la hidrólisis de ATP, mientras que el intercambiador Na^{+}/Ca^{2+} es un antiportador que utiliza el gradiente electroquímico de sodio para extraer calcio de la célula (263).

En caso de daño celular, las concentraciones de Ca^{2+} citosólico pueden alcanzar niveles mucho más elevados, debido a su entrada masiva desde el medio extracelular y/o al vaciamiento de reservorios. Si estos niveles se sostienen en el tiempo, terminan por dañar la célula e incluso pueden provocar la muerte (239).

1.4.2 Muerte celular

La muerte celular constituye un importante mecanismo para mantener la homeostasis del organismo. Comunmente se emplea el término apoptosis para hacer referencia a la muerte celular programada y necrosis para designar una muerte pobremente controlada, con derrame de contenido celular a los tejidos adyacentes (264).

El Ca^{2+} desempeña un papel importante en la apoptosis ya que desencadena eventos clave en este proceso (265). Como ya se mencionó previamente, el Ca^{2+} regula la función mitocondrial. Éste atraviesa fácilmente los grandes poros de la OMM, pero necesita canales iónicos y transportadores para cruzar la IMM (como el MCU). El gradiente eléctrico del citoplasma a la mitocondria se crea mediante el transporte activo de protones a través de la membrana interna, en la conocida cadena de transporte de electrones (ETC) lo que, en condiciones fisiológicas, aumenta la producción de ATP y da lugar a la formación de superóxidos. Estos superóxidos, junto con otras moléculas reactivas, se conocen como ROS. La producción controlada de ROS es crucial para la señalización celular normal, pero en exceso puede causar estrés oxidativo, dañando los lípidos, las proteínas y el ADN (238). La acumulación de Ca^{2+} en la mitocondria reduce la producción de ATP y, en casos de Ca^{2+} excesivo, también lo consume, ya que el orgánulo intenta restaurar su homeostasis. Además, provoca la apertura del mPTP, lo cual conduce a la liberación de componentes proapoptóticos (245, 266). Otros factores como el estrés oxidativo o un aumento de fosfatos también pueden dar lugar a la apertura de este canal. Esto desencadena un drástico incremento en la permeabilidad de la membrana mitocondrial, causando un rápido colapso de su potencial ($\Delta\Psi m$), despolarización y agotamiento de ATP. Al desacoplamiento inicial le sigue una reducción de la actividad respiratoria debido a la pérdida de nucleótidos de piridina y citocromo C. La consecuente inhibición del flujo electrónico conlleva a un aumento en la producción de ROS, dado que la transferencia incompleta de electrones y la fuga de estos a través de los complejos I, III y IV de la ETC, genera superóxidos (O_2-), también capaces de abrir el mPTP, y consecuentemente causar apoptosis (Figura 16) (245, 267).

USC UNIVERSIDADE DE SANTIAGO DE COMPOSTELA

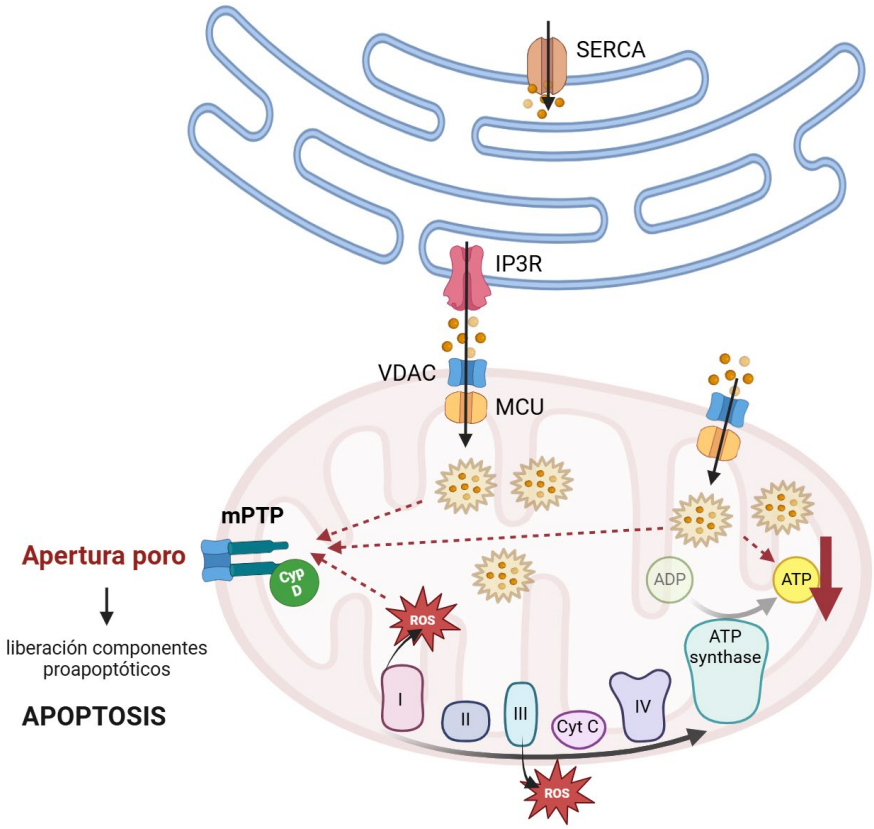


Figura 16. Efectos del exceso de Ca^{2+} mitocondrial. Adaptación de De Nicolo et. al (245). Imagen creada con biorender.com

La apoptosis es un proceso altamente regulado que elimina células dañadas, no deseadas o potencialmente dañinas en los organismos multicelulares. Existen dos vías principales de apoptosis: la vía intrínseca y la vía extrínseca (Figura 17) (264). La vía intrínseca, también denominada vía mitocondria, se desencadena por diversas señales intracelulares, como daños en el ADN, estrés oxidativo o un colapso en el $\Delta\Psi m$. Estos estímulos provocan la formación del mPTP, y la consecuente liberación de proteínas proapoptóticas de las mitocondrias, como el ya mencionado citocromo C, lo que conduce a la activación de las caspasas, una familia de proteasas que ejecutan el proceso apoptótico. Dentro de las caspasas existen caspasas iniciadoras y ejecutoras. Ante un daño, las iniciadoras se activan a partir de pro-caspasas, dando lugar a una cascada de eventos que finaliza en la muerte celular. La caspasa iniciadora de la vía intrinseca es la caspasa-9 (264, 268). La vía extrínseca se inicia por señales extracelulares, como la unión de ligandos de muerte a receptores de muerte de la superficie celular. Esto conduce a la formación del complejo de señalización inductor de muerte (DISC, del inglés *death-inducing signaling complex*), que activa a la caspasas iniciadoras 8 y 10. A continuación, las caspasas iniciadoras activadas escinden y activan las caspasas ejecutoras, que llevan a cabo las etapas finales de la apoptosis (268, 269). Tanto la vía intrínseca como la extrínseca convergen en la activación de las caspasas ejecutoras, como las caspasas 3 y 7. Estas caspasas escinden diversas proteínas celulares dando lugar a los cambios morfológicos característicos asociados a la apoptosis, como la condensación de la cromatina, la fragmentación nuclear y la formación de cuerpos apoptóticos.

USC UNIVERSIDADE DE SANTIAGO DE COMPOSTELA

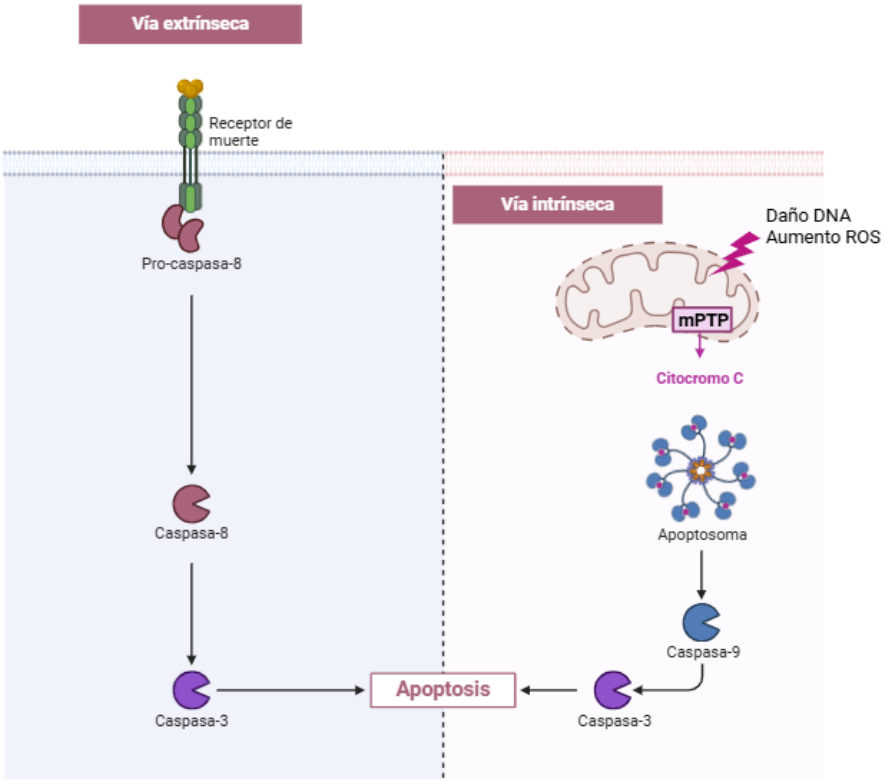


Figura 17. Vías extrínseca e intrínseca de apoptosis. Imagen creada con biorender.com

La apoptosis desempeña un papel crucial en el desarrollo, la homeostasis de los tejidos y la función del sistema inmunitario. Este proceso mantiene un equilibrio entre la proliferación y la muerte celular, garantizando la eliminación de las células dañadas o innecesarias (264). La desregulación de este proceso puede dar lugar a diversas patologías. Un exceso de apoptosis puede provocar daños en los tejidos y disfunciones orgánicas, como ocurre en las enfermedades neurodegenerativas, las lesiones isquémicas y los trastornos autoinmunes. Por el contrario, una apoptosis insuficiente puede provocar una proliferación celular descontrolada y cáncer (268).

La necrosis es un proceso de muerte celular descontrolado, inducida por una lesión externa, como hipoxia, radiación o un daño mecánico, que da lugar a la ruptura de la célula y al derrame del contenido celular, que posteriormente daña los tejidos adyacentes. La necrosis se caracteriza por disfunción mitocondrial, pérdida de ATP y cambios morfológicos distintivos, como degeneración hidrópica (o hinchazón celular). Además, es un proceso independiente del consumo de energía (264).

USC UNIVERSIDADE DE SANTIAGO DE COMPOSTELA

2 HIPÓTESIS Y OBJETIVOS

Las micotoxinas suponen un riesgo reconocido para la salud. Su presencia está regulada para algunos compuestos, pero la mayoría no se analiza debido a la ausencia de requerimientos legales. Esta situación permite que lleguen al consumidor muchos compuestos que suponen un riesgo desconocido, no contralado y posiblemente creciente ya que el calentamiento global está identificado como un riesgo en la expansión geográfica de varias especies de hongos. A esta situación se suma que el mecanismo de acción de muchas micotoxinas no ha sido estudiado y sus riesgos toxicológicos son desconocidos. Además, su presencia simultánea en los alimentos añade una complejidad farmacológica, o mecanística, que necesita ser entendida, ya que las interacciones que causan se desconocen. En este contexto el objetivo de la presente tesis doctoral es:

-Estudiar el mecanismo de acción y el efecto tóxico individual y combinado de las micotoxinas que se detectan con mayor frecuencia en alimentos

USC
UNIVERSIDADE DE SANTIAGO DE COMPOSTELA

USC
UNIVERSIDADE
DE SANTIAGO
DE COMPOSTELA

3 MATERIAL Y MÉTODOS

3.1 MATERIALES Y REACTIVOS

Las células SH-SY5Y de neuroblastoma humano, número CRL2266 y las células NCI-H226 de cáncer de pulmón humano no pequeño, número CRL5826, fueron adquiridas en la American Type Culture Colletion (ATCC).
Los reactivos se adquirieron en las siguientes casas comerciales:

- Thermo Fisher Scientific (Madrid, España): medio de cultivo RPMI (del inglés *Roswell Park Memorial Institute Medium*), medio de cultivo DMEM (del inglés *Dulbecco's Modified Eagle's Medium*), nutriente Mix F-12, suero fetal bovino, glutamax, penicilina-estreptomicina (10000 U/mL), Tripsina/EDTA al 0.05%, SuperSignal west pico, SuperSignal west femto, diacetato 6-carboxi-2',7'-diclorodihidrofluorofluoresceína (carboxy-H_2DCFDA), kit de detección de la Caspasa-3 EnzCheck, tetrametilrodamina metil éster (TMRM) y el anticuerpo monoclonal anti-Actina, ensayo de citotoxicidad de lactato deshidrogenasa (LDH) CyQUANT™, ensayo del poro de transición mitocondrial Mitoprobe™ (M34153) .
- Merk Life Science (Madrid, España): 1-[β-(3-(4-metoxifenil)propoxi)-4-metoxifenetil]-1H-imidazol-HCl (SKF96365), cianuro de carbonilo 4-(trifluorometoxi) fenilhidrazona (FCCP) bromuro de 3-(4,5-dimetiltiazol-2-il)-2,5-difeniltetrazolio (MTT), el anticuerpo anti-rabbit IgG, el anticuerpo anti-mouse IgG (cat. #GENA931), , Sodio-dodecil-sulfato (SDS), filtros durapore (0,22 µM), ZEA, ENN A, ENN A1, ENN B, ENN B1, BEA, CPA y ROQC (pureza >95%) saponina (SAP), estaurosporina (STS).
- Abcam: ciclosporina A (pureza ≥ 98.5 %), el anticuerpo Anti-Caspasa 9 (cat. #ab202068)
- Bio-Rad (Barcelona, España): los geles de poliacrilamida y el marcador de peso molecular Precision Plus Protein Standards Kaleidoscope.
- Romers Labs (Getzersdorf, Austria): DON y FB1 (pureza > 98%)
- Enzo Life Sciences (Lausen, Suíza): Tapsigargina (Tg), API (pureza > 99%)
- Cell Signalling Technology (Massachusetts, EEUU): el anticuerpo anti-caspasa 8
- Immunostep (Salamanca, España): Kit de detección de apoptosis Annexin V-FITC.
- Cayman Chemical (Michigan, EEUU): DEST B (pureza > 96%)

3.2 COMPOSICIÓN MEDIOS DE CULTIVO Y DISOLUCIONES

- Medio de cultivo para las células neuronales SH-SY5Y: medio DMEM/F-12 suplementado con un 10% de suero fetal bovino, glutamax, 100 U/mL de penicilina y 100 µg/mL de estreptomicina
- Medio de cultivo para las células NCI-H226 de cáncer de pulmón humano no pequeño: medio RPMI suplementado con suero fetal bovino al 10%, 100 U/ml de penicilina y 100 µg/mL de estreptomicina
- Solución de Locke's: 154 mM de NaCl, 3,6 mM de $NaHCO_3$, 1,3 mM de $CaCl_2$, 5,6 mM de KCl, 1 mM de $MgCl_2$, 10 mM de HEPES y 5 mM de glucosa, pH 7.2-7.4
- Solución de Umbreit: 119 mM de NaCl, 22,85 mM de $NaHCO_3$, 5,94 mM de KCl, 1,2 mM de $MgSO_4$, 1,2 mM de NaH_2PO_4, 1 g/L de glucosa y 1 mM de $CaCl_2$, pH 7,2-7,4. Para algunos experimentos se utiliza esta solución sin suplementar con 1 mM de $CaCl_2$
- SDS al 5% en Locke's
- Solución salina tamponada con fosfato (PBS, del inglés *phophate buffered saline*): 137 mM de NaCl, 8,2 mM de Na2HPO4, 1,5 mM de KH2PO4 y 3,2 mM de KCl, pH 7,2-7,4

USC DE COMPOSTELA

- PBS-T: PBS + 0,1 % de Tween-20
- PBS-EDTA: PBS + 2 mM de EDTA, pH 7,2-7,4
- Tampón de lisis hipotónico de extracción de proteínas scitosólicas para western blot: 20 mM de Tris-HCl, 10 mM de NaCl y 3 mM de $MgCl_2$, pH 7,2-7,4. En el momento de uso se añade el coctel de inhibición de proteasas (Clorhidrato de fluoruro de 4- (2-aminoetil) bencenosulfonilo, aprotinina, bestatina, E-64, leupeptina y pepstatina A) y fosfatasas (fluoruro de sodio, ortovanadato de sodio, pirofosfato de sodio y beta-glicerofosfato).
- Tampón de carga de proteínas para western blot: 125 mM de Tris-HCl (pH 6,8), 20% de glicerol, 4% de SDS, 10% de β-mercaptoetanol y 0,004% de azul de bromofenol.
- Solución de electroforesis: 25 mM de trizma base, 192 mM de glicina y 0.1 % de SDS.Solución de transferencia: 25 mM de trizma base, 192 mM de glicina, 0,1 % de SDS y 20% de metanol.

3.3 CULTIVOS CELULARES Y TRATAMIENTOS

3.3.1 Cultivos celulares

En la presente tesis doctoral se han utilizado la línea celular NCI-H226 de cáncer de pulmón humano y la línea celular de neuroblastoma humano SH-SY5Y. Ambas se han mantenido a 37ºC en una atmósfera modificada con 95% de aire y 5% de CO_2 en un incubador (Memmert). Para el mantenimiento del cultivo ambas líneas se disocian una vez por semana utilizando tripsina al 0,05 %.

La línea celular SH-SY5Y de neuroblastoma se mantuvo en medio DMEM/F-12 suplementado. Un día antes de los ensayos, las células se siembran en placas de 384, 96 o 12 pocillos, dependiendo del ensayo, a una densidad de 25.000, 50.000 o 1 x 10^6 células/pocillo, respectivamente.

La línea celular de cáncer de pulmón NCI-H226 se mantuvo en medio RPMI suplementado. Un día antes de los ensayos, las células se siembran en placas de 96 pocillos a una densidad de 1.5 x 10^4 células/ pocillo o en placas de 12 a una densidad de 5 x 10^5 células/pocillo.

3.3.2 Tratamientos

Los estándares de micotoxinas se disolvieron en DMSO y se realizaron diluciones seriadas en medio de cultivo. En todos los casos, los niveles de DMSO en las células se mantuvieron por debajo del 0,9 %. Para los ensayos individuales con micotoxinas, las células se trataron con concentraciones que oscilaban entre 0,01 y 100 µM.

En el caso de combinaciones binarias, la proporción entre micotoxinas reguladas y no reguladas se seleccionó en base a las proporciones más frecuentes encontradas en muestras contaminadas del noroeste de la Península Ibérica y muestras comerciales (166, 167). Las células fueron tratadas durante 24 h con las siguientes mezclas:

- DON y FB1 se combinaron en proporción 5:1 con ENN A, ENN B y BEA, mientras que la ZEA se combinó con las mencionadas micotoxinas no reguladas en proporción 2:1.
- Las ENN (A, A1, B y B1) se mezclaron en una proporción de 1:1.
- CPA y ROQC se combinaron en proporción 10:1 con ENN A, ENN A1, ENN B o ENN B1.

A continuación, se evaluaron los efectos de una mezcla 1:1:1:1 de ENN A, A1, B y B1, y una combinación de las cuatro ENNs con BEA (1:1:1:1:1).

Por último, se combinaron las toxinas ROQC y CPA con las ENNs A, A1, B y B1 en proporción 10:1:1:1:1, y con las cuatro ENNs y BEA en proporción 10:1:1:1:1:1.

USC UNIVERSIDADE DE SANTIAGO DE COMPOSTELA

Los intervalos de concentración combinados se seleccionaron basándose en los resultados obtenidos con las micotoxinas individuales para incluir sus valores de concentración inhibitoria 50 (IC_{50}) en el intervalo de concentración analizado.

Para los distintos extractos testados (pienso, leche y queso), se eligieron concentraciones similares a las encontradas en la naturaleza. En el siguiente apartado se explica el proceso de extracción y concentración de las muestras, así como las concentraciones empleadas.

3.4 EXTRACTOS PIENSO, LECHE Y QUESO

3.4.1 Extractos y análisis de piensos y leche de vaca

Se analizó una muestra de pienso de vaca según un método previamente validado para la multidetección de 22 micotoxinas en esta matriz (167). Para los ensayos celulares, se filtró una alícuota de 9 mL del extracto (0,22 µm), se secó en un evaporador centrífugo y se reconstituyó en 0,45 mL de DMSO, obteniéndose una muestra 20 veces concentrada.

Por otro lado, se analizaron dos muestras de leche comercial según un método previamente validado para la multidetección de 40 micotoxinas en estas matrices (14). Para los ensayos celulares, se filtró 1 mL de cada extracto (0,22 µm), se secó en un evaporador centrífugo y se reconstituyó en 0,05 mL de DMSO, obteniéndose una muestra 20 veces concentrada.

Después, se trataron las células con diluciones 1:500, 1:1000, 1:5000 y 1:10000, de cada muestra concentrada 20 veces, para simular las concentraciones que podrían llegar a ingerirse por animales o personas. En ambos casos, se utilizó un blanco (matriz no contaminada) como control.

3.4.2 Extractos y análisis de queso

Se analizaron tres muestras de queso comercial (camembert, emmental y queso azul) utilizando un método previamente validado para la detección simultánea de 32 micotoxinas en esta matriz (166). Brevemente, las muestras se homogeneizaron y 1 g de cada queso se sometió a extracción utilizando un protocolo QuEChERS (rápido, fácil, económico, eficaz, resistente y seguro). Inicialmente, se agregaron 4 ml de solución de ácido acético al 2 %, seguidos de 4 ml de acetonitrilo, y se mezclaron vigorosamente después de cada adición de disolvente utilizando un mezclador vórtex. La separación de fases se logró con 1,6 g de MgSO4 y 0,4 g de NaCl. Posteriormente, la fase orgánica se diluyó 1:2 con ácido acético al 2% y se filtró a través de filtros centrífugos de 0,22 µm. Luego, los extractos resultantes se analizaron utilizando un protocolo de cromatografía líquida ultraalta-espectrometría de masas en tándem (UHPLC-MS/MS). Los extractos de queso (500 µl) se sometieron adicionalmente a secado en un evaporador centrífugo, seguido de reconstitución en 500 µl de DMSO.

Después, las células se trataron con diluciones 1:200, 1:300, 1:400, 1:500 y 1:1000 de cada estracto de queso. La muestra de queso menos contaminada (correspondiente al queso camembert) se utilizó como control, ya que no se encontró ninguna matriz libre de micotoxinas.

3.5 ENSAYO DE VIABILIDAD CELULAR

Para evaluar los efectos de micotoxinas, sus combinaciones y extractos naturales contaminados con micotoxinas sobre la viabilidad celular, se utilizó el ensayo MTT. El MTT es una sal de tetrazolio soluble en agua, de color amarillo. Cuando esta sal es reducida por las deshidrogenasas mitocondrias, da lugar a un formazán de color azul insoluble en agua (Figura 18). Los cristales de formazán obtenidos después de la reducción del MTT se disuelven en disolventes orgánicos y se cuantifica su señal midiendo su absorbancia, a una longitud de onda de entre 570 y 595 nanómetros (nm). La cantidad de células vivas es proporcional a la cantidad

USC UNIVERSIDADE DE SANTIAGO DE COMPOSTELA

de formazán producido, por lo tanto, a mayor absorbancia, mayor número de células vivas (270).

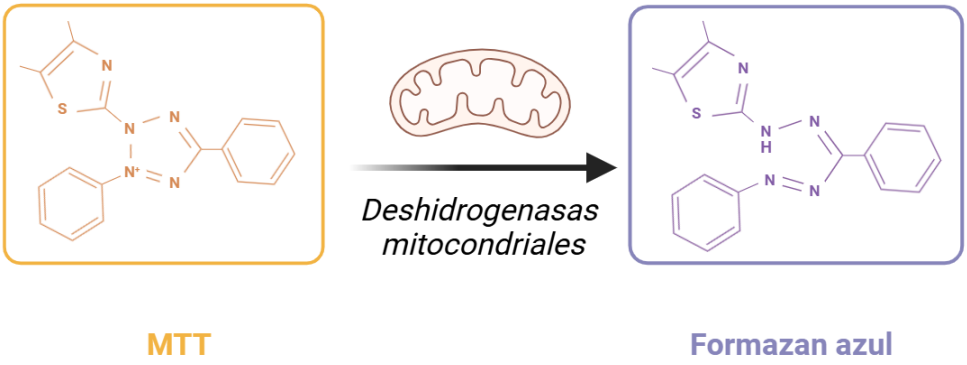


Figura 18. Transformación de la sal de tetrazolio (MTT) a una sal de formazán azul, por parte de las enzimas deshidrogenasas mitocondriales. Imagen creada con biorender.com

Para el ensayo MTT, las células se trataron durante 48, 24 o 6 h con distintas concentraciones de micotoxinas. En vista a los resultados obtenidos, se seleccionó el tiempo de 24 h para evaluar las distintas combinaciones así como los efectos de los extractos de pienso, leche y queso utilizados. Después del tratamiento, las células se lavaron tres veces con solución de Locke's y se añadieron 200 µl de MTT (500 µg/ml) por pocillo. La placa se incubó durante 1 h a 37 ºC y 300 rpm en un agitador de placas. Luego, se aspiró el MTT y se añadió SDS al 5% para disolver los cristales de formazán y poder cuantificar su absorbancia. La absorbancia de los cristales formados se midió a 595 nm en un espectrofotómetro lector de placas. Como control de muerte se utilizó SAP de corteza de Quillaja a 1 mg/mL.

3.5.1 Evaluación de la implicación de las caspasas en la muerte celular

Para evaluar la implicación de las caspasas en la muerte celular, las células SH-SY5Y fueron pretratadas con el inhibidor de caspasa Z-VAD-FMK a una concentración 40 µM durante 24 h. Luego, se agregaron las micotoxinas durante 24 h y se realizó el ensayo MTT.

3.6 Ensayo de actividad de la caspasa-3

Los niveles de caspasa 3 se midieron utilizando el el kit de Ensayo EnzCheck® Caspase 3 siguiendo las instrucciones del fabricante. La base de este ensayo es el sustrato Z-DEVD-AMC derivado de la aminometilcumarina, un compuesto poco fluorescente en el rango UV, que produce un producto azul fluorescente brillante (excitación/emisión máxima de 342/441 nm) tras la escisión proteolítica por parte de la caspasa 3. El kit se puede utilizar para medir de forma continua la actividad de la caspasa-3 y de proteasas estrechamente relacionadas en extractos celulares.

En resumen, tras 24 h de tratamiento, se añadieron 150 µl de tampón de lisis (10 mM Tris, 100 mM NaCl, 1 mM EDTA, 0,01% Triton X-100) a cada pocillo y las muestras se incubaron en hielo durante 30 min. A continuación, los lisados celulares se centrifugaron a 5000 rpm y 4 °C durante 5 mins, y se recogió el sobrenadante para el análisis de la actividad de la caspasa-3 y la concentración de proteínas. Luego, 50 µl de cada muestra se mezclaron con un volumen igual de sustrato Z-DEVD-AMC y se incubaron durante 30 min a temperatura ambiente. Posteriormente, se midió la fluorescencia a 342 nm de excitación y 441 nm de emisión en un lector de microplacas (Synergy 4, BioTek Instruments). Los datos de actividad de la caspasa-3

se corrigieron con los valores de concentración de proteínas, los cuales se determinaron mediante el método de Bradford. Se utilizó STS a 0,05 µM como control positivo y los ensayos se realizaron por duplicado en tres ocasiones independientes.

3.7 Ensayo de citotoxicidad

Para analizar la citotoxicidad celular se empleó el kit de citotoxicidad CyQUANT™ LDH, que mide la actividad de la enzima LDH en el medio extracelular (270). La LDH es una enzima que de forma normal se encuentra en el citosol y que es liberada al medio cuando se produce un daño celular que conlleva la ruptura de la membrana plasmática. La LDH extracelular se puede cuantificar mediante una reacción enzimática acoplada en la que la enzima cataliza la conversión de lactato a piruvato mediante la reducción de NAD^+ a NADH. La oxidación del NADH conduce a la reducción de una sal de tetrazolio a un producto de formazán rojo que se puede medir espectrofotométricamente a 490 nm (Figura 19). En este caso, la cantidad de células muertas es proporcional a la cantidad de formazán producido, por lo tanto, a mayor absorbancia, mayor muerte.

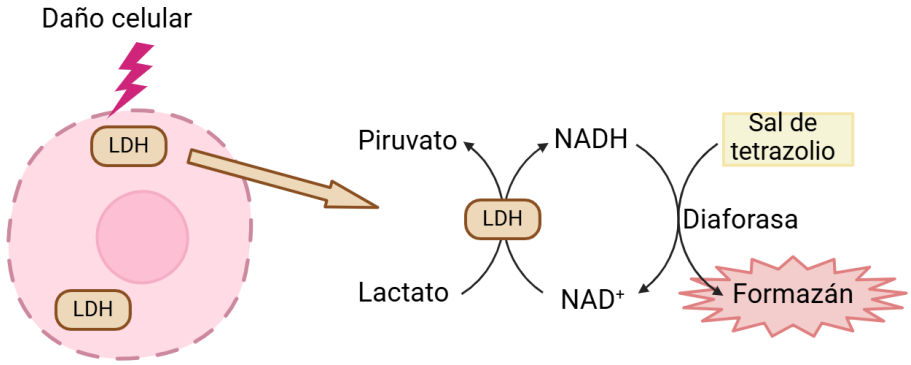


Figura 19. Esquema del mecanismo del ensayo de citotoxicidad de LDH. Imagen creada con biorender.com

Para llevar a cabo este ensayo, las células se sembraron en placas de 96 pocillos y se trataron durante 6 y 24 h en el caso de las micotoxinas solas y durante 24 h en el caso de las mezclas y extractos. Como control de muerte celular se utilizó SAP (1 mg/mL). Después del tratamiento, se transfirieron 50 µl de medio a una placa de fondo plano y se añadió la mezcla de reacción del kit. Después de 30 min, se detuvo la reacción con la solución de "STOP" y se midió la absorbancia a 490 y 680 nm en un lector de placas. Después, el valor de absorbancia de 680 nm (señal de fondo) se substrajo al valor de de 490 nm para determinar la actividad de LDH.

3.8 Medición de variaciones en el potencial de membrana mitocondrial

Las variaciones del $\Delta\Psi m$ se determinaron mediante el uso de TMRM, colorante fluorescente cargado positivamente que penetra con facilidad en las células. Este compuesto es secuestrado por las mitocondrias activas y se acumula en su matriz mitocondrial de forma inversamente proporcional al $\Delta\Psi m$. Cuanto más polarizada esté la mitocondria, mayor será su $\Delta\Psi m$ (más cargas negativas) y más fluoróforo acumulará, emitiendo una fluorescencia superior. En mitocondrias inactivas o despolarizadas (más cargas positivas), la mitocondria no puede retener el colorante dando como resultado una menor señal de fluorescencia (Figura 20) (271).

USC UNIVERSIDADE DE SANTIAGO DE COMPOSTELA

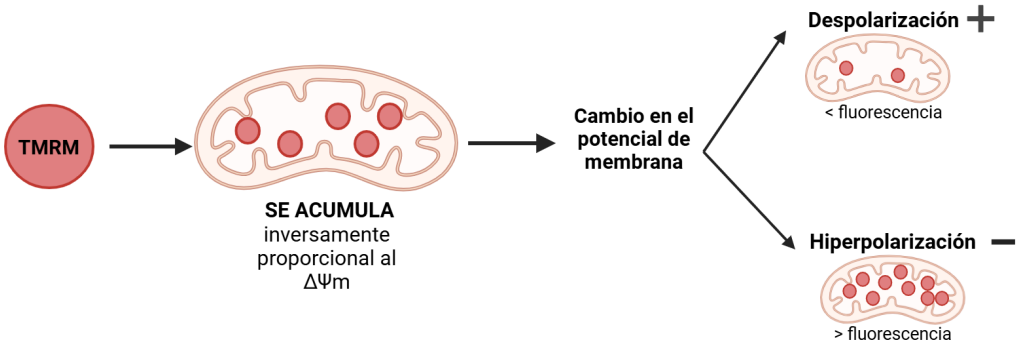


Figura 20. Esquema del mecanismo de acumulación de TMRM en la mitocondria. Imagen creada con biorender.com

Para este ensayo, las células se sembraron en placas blancas de fondo transparente y se trataron con micotoxinas individuales durante 6 y 24 h, y con combinaciones binarias durante 24 h. Luego, las células se lavaron dos veces con solución de Locke's y se añadieron 200 µl de TMRM a una concentración de 20 µM por pocillo. La placa se incubó durante 30 min a 37 ºC y 300 rpm y las células se solubilizaron con H_2O y DMSO (1:1). La fluorescencia se leyó a 535 nm de excitación y 590 nm de emisión en el lector de placas. Como control positivo, de despolarización, se usó rotenona (Rot) a 1 µM.

3.9 Medición de niveles de especies reactivas de oxígeno intracelular

Los niveles intracelulares de ROS se midieron usando una forma reducide de fluoresceína, el carboxi-H_2DCFDA. Como se muestra en la figura 21, este compuesto entra en las células y es desacetilado en el citosol por esterasas intracelulares a H_2DCF, no fluorescente. Posteriormente, este producto es oxidado por las ROS a diclorofluoresceína (DCF), altamente fluorescente (495 nm de excitación y 527 nm de emisión). Por lo tanto, la cantidad de ROS intracelular es proporcional a la fluorescencia del DCF.

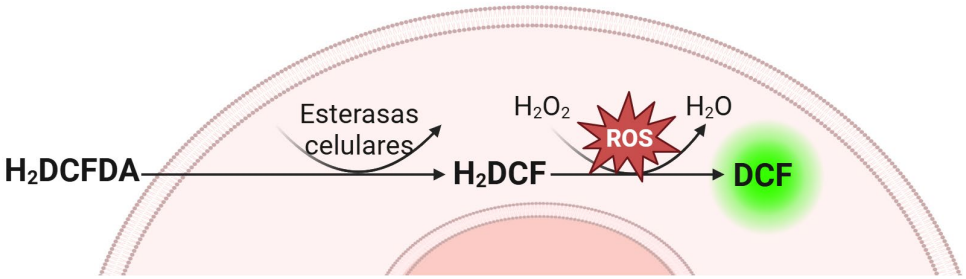


Figura 21. Esquema de la desacetilación y oxidación de la molécula carboxi-H_2DCFDA. Imagen creada con biorender.com

Para este experimento, las células fueron tratadas durante 24 o 6 horas en placas blancas de fondo transparente. Transcurrido el tiempo de incubación, las células se lavaron dos veces con medio sin suero. En ese momento, se añadió carboxi-H_2DCFDA a 20 µM diluido en medio libre de suero y las células se incubaron en un agitador orbital durante 1 h a 300 rpm y 37 ºC. Después, se añadió PBS a cada pocillo y la placa se incubó durante 30 min a 300 rpm y 37 ºC. Finalmente, se leyó la fluorescencia en un lector de placas. Se utilizó H_2O_2 a una concentración de 150 µM como control positivo.

USC UNIVERSIDADE DE SANTIAGO DE COMPOSTELA

3.10 Citometría de flujo

3.10.1 Análisis del tipo de muerte celular

Para determinar el tipo de muerte celular producida por las micotoxinas, se utilizó el kit de detección de apoptosis Anexina V-FITC, siguiendo las instrucciones del fabricante. Este kit está compuesto por anexina conjugada con fluoresceína y yoduro de propidio (PI, del inglés *propidium iodide*). La anexina es una proteína que se une a los residuos de fosfatidilserina en presencia de calcio. En condiciones normales, la fosfatidilserina se encuentra en la cara interna de la membrana celular y se transloca a la cara externa al inicio de la apoptosis. Esto le permite unirse a la anexina conjugada con fluoresceína, dando como resultado una señal fluorescente (488 nm excitación/520 nm emisión). El PI (535 nm excitación/ 617 nm emisión) tiñe el ADN de las células cuya membrana se ha visto totalmente comprometida (Figura 22) (272, 273). Las células negativas (sin fluorescencia) tanto a PI como a anexina V-FITC se consideran sanas, las células anexina V-FITC positivas corresponden a células en apoptosis y las células anexina V-FITC negativas y PI positivas son células necróticas.

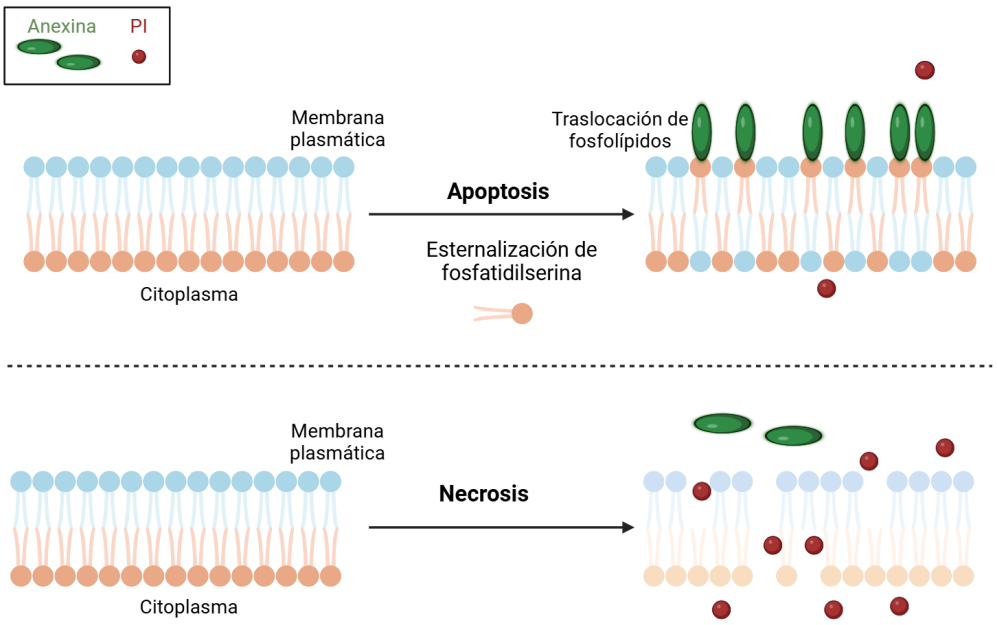


Figura 22. Representación de la traslocación de fosfatidilserina en la apoptosis y su unión a anexina (arriba) y tinción del ADN por parte del PI (abajo), cuando la membrana se ve comprometida. Imagen creada con biorender.com

Para este ensayo, las células SH-SY5Y se sembraron en placas de 12 pocillos a 5×10^5 células por pocillo. Luego, se incubaron con las micotoxinas durante 24 h. Se utilizó STS a 0.1 µM como control de apoptosis (274). Tras el tratamiento, las células se lavaron con PBS y se resuspendieron en una solución tampón que contenía anexina V-FITC y PI. A continuación, las células se incubaron a temperatura ambiente durante 15 min, se resuspendieron en PBS comercial (Thermo Fisher Scientific), se filtraron y se mantuvieron en hielo. La fluorescencia se midió mediante citometría de flujo utilizando el instrumento ImageStreamMKII (Amnis Corporation, Luminex Corp, Austin, TX, EE.UU.). Se adquirió y analizó la fluorescencia de 10.000 eventos con el software IDEAS Application 6.0 (Amnis Corporation, Luminex Corp).

USC UNIVERSIDADE DE SANTIAGO DE COMPOSTELA

3.10.2 Análisis de la apertura del poro de transición mitocondrial

Los efectos de las toxinas sobre el mPTP se evaluaron utilizando el kit de ensayo de poro de transición MitoProbe (Thermo Fisher Scientific). Este kit contiene calceína-AM y cloruro de cobalto ($CoCl_2$). El grupo acetoximetil éster (AM) unido a la calceína incrementa la hidrofobicidad del colorante, permitiendo su difusión pasiva en las células vivas. Posteriormente, la calceína-AM es hidrolizada por esterasas intracelulares para formar calceína altamente fluorescente. Cuando las células se incuban con calceína y $CoCl_2$, ambos penetran en el citoplasma; sin embargo, el $CoCl_2$ no entra en la mitocondria. La calceína que se acumula en las mitocondrias mantiene su fluorescencia, mientras que la que permanece en el citoplasma es quelada por el $CoCl_2$. En condiciones fisiológicas, el mPTP se abre transitoriamente, permitiendo la medición de la fluorescencia mitocondrial. En estados patológicos, el mPTP puede permanecer continuamente abierto y el $CoCl_2$ del citoplasma puede entrar en las mitocondrias y quelar la calceína, resultando en una disminución gradual de la intensidad de fluorescencia (Figura 23) (275, 276).

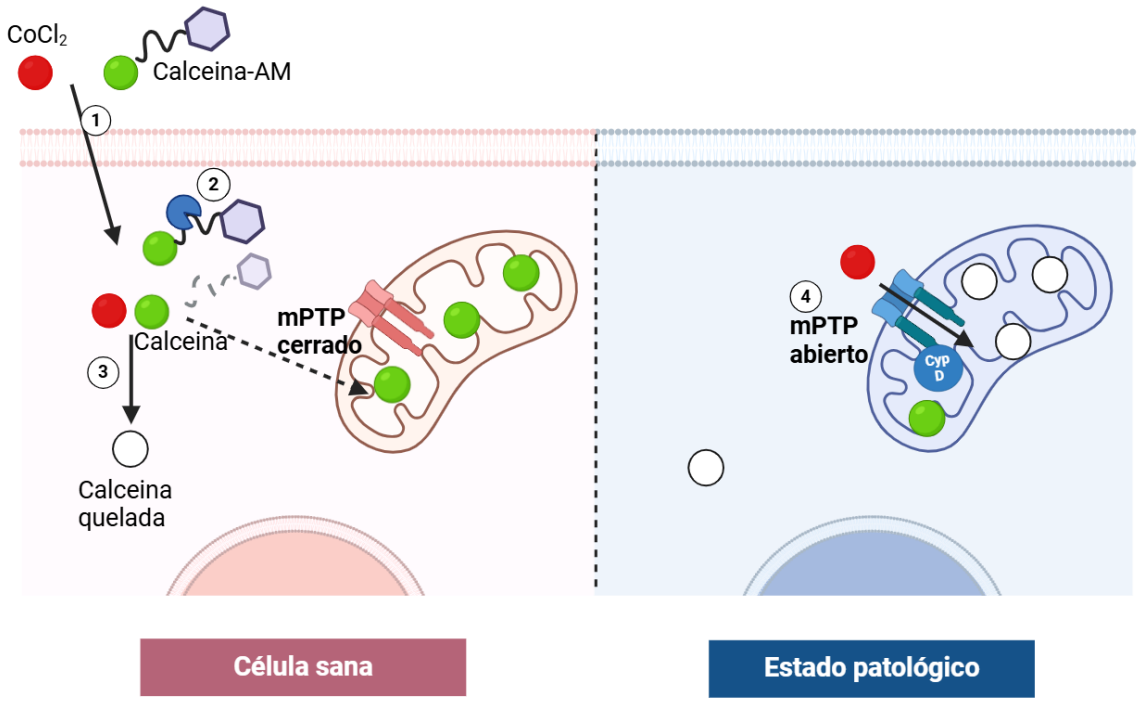


Figura 23. Mecanismo de funcionamiento del ensayo de calceína-AM: (1) el $CoCl_2$ y la calceína-AM y entran en la célula, (2) las esterasas intracelulares metabolizan la calceína-AM a calceina, (3) el $CoCl_2$ quela la fluorescencia de la calceína citosólica, mientras que se mantiene la mitocondrial. Cuando el mPTP se abre, (4) el $CoCl_2$ entra en la mitocondria y quela a la calceína. Imagen creada con biorender.com

Para este experimento, las células se sembraron en placas de 12 pocillos a una densidad de 1×10^6 células por pocillo y se dejaron crecer durante 24 h. A continuación, las células SH-SY5Y se resuspendieron en solución de Umbreit, se cargaron con 0,01 µM de calceína-AM y $CoCl_2$ a 0,4 mM, como quelante de la fluorescencia, y se trataron con CsA a 0,2 µM para evitar la apertura de mPTP. Tras 15 min de incubación a 37 °C, las células se trataron con los compuestos durante 10 min a la misma temperatura. A continuación, se resuspendieron en PBS comercial (pH 7,2) (Thermo Fisher Scientific), se filtraron y se mantuvieron en hielo. Se utilizó FCCP a 10 µM como control positivo para inducir la apertura del mPTP. La intensidad de fluorescencia

de la calceína se evaluó mediante citometría de flujo a longitudes de onda de excitación y emisión de 488 y 517 nm, respectivamente, utilizando el equipo ImageStreamMKII y el software ISX MKII (Amnis Corporation, Luminex Corp, Austin, TX, EE.UU.). La fluorescencia de 10.000 eventos se cuantificó utilizando el software IDEAS Application 6.0 (Amnis Corporation, Luminex Corp).

3.10.3 Análisis del ciclo celular

El perfil del ciclo celular de una muestra se puede determinar tiñendo el ADN con un colorante fluorescente y midiendo su intensidad. Este colorante tiñe el ADN estequiométricamente, lo que permite la diferenciación de células en G0/G1, fase S y G2/M (Figura 24). El método más sencillo para el análisis del ciclo celular consiste en fijar las células con etanol, tratarlas con RNasa y teñirlas con PI. El PI tiñe el ARN además del ADN, por lo que las células deben tratarse con RNasa para analizar el ciclo celular con precisión (277).

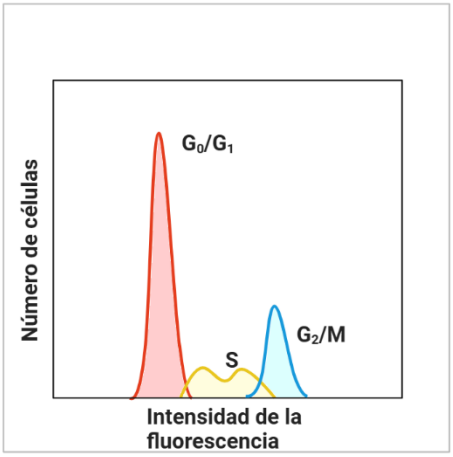


Figura 24. Representación de la distribución de las células según la fase del ciclo celular en la que estén, por citometría de flujo. Imagen creada con biorender.com

Tras 24 h de tratamiento, las células se lavaron con PBS frío y se fijaron con etanol al 70% durante 1 h a 4 °C. Posteriormente, se lavaron y se resuspendieron en PBS que contenía 2.5 µg/ml de PI, y 0.1 mg/ml de ARNasa durante 30 min a temperatura ambiente. Luego, se centrifugaron a 2500 rpm durante 10 min a 4 °C y se mantuvieron en hielo. La fluorescencia se analizó mediante citometría de flujo utilizando el instrumento ImageStreamMKII (Amnis Corporation, Luminex Corp, Austin, EE.UU.). Se midieron 10.000 eventos con el software IDEAS Application 6.0 (Amnis Corporation, Luminex Corp, Austin, EE.UU.). Como control positivo en este ensayo se utilizó STS a 0,01 µM.

3.11 Medición del calcio citosólico libre

Para evaluar las variaciones en el calcio citosólico se empleó el indicador fluorescene selectivo de calcio fura-2AM. Este compuesto permeable difunde fácilmente al citosol, donde es metabolizado por las esterasas intracelulares a un colorante altamente fluorescente, el fura-2, que se une al calcio citosólico debido a su alta afinidad (Figura 25). Por lo tanto, si los niveles de calcio aumentan el el citosol, también lo hará la fluorescencia y viceversa. Las longitudes de onda de excitación típicas utilizadas son 340 nm y 380 nm para fura-2 AM unida a Ca^{2+} y fura-2 AM, respectivamente. En ambos casos, el máximo de emisión es de aproximadamente 510 nm (278).

USC DE SANTIAGO DE COMPOSTELA

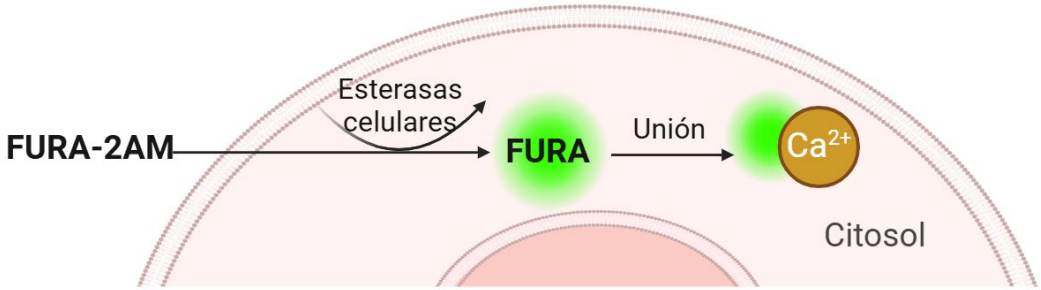


Figura 25. Esquema de la desacetilación de la molécula fura-2 AM a un compuesto fluorescente altamente afín al calcio. Imagen creada con biorender.com

Las células se colocaron en cubreobjetos de 18 mm a una densidad de 5×10^5 células por pocillo y se dejaron crecer durante 24 h. Para evaluar los niveles de $Ca^{2+,}$ las células SH-SY5Y se lavaron dos veces con solución Umbreit enriquecida con 0,1% de BSA. Posteriormente, se cargaron con tinción fluorescente FURA-2 AM a una concentración de 0,5 µM durante 6,5 min a 37 °C y 300 rpm. A continuación, las células se lavaron dos veces con solución Umbreit, y los cubreobjetos se colocaron en una cámara con temperatura controlada (Life Sciences Resources, Reino Unido). Las células fluorescentes se observación utilizando un microscopio invertido Nikon Diaphot 200 equipado con óptica de epifluorescencia (Nikon 40×, objetivo de fluorescencia UV de inmersión). Las diluciones de los compuestos se prepararon en una solución de Umbreit carente de Ca^{2+} y se añadieron directamente a la cámara de incubación. A lo largo de los experimentos, el pH se mantuvo entre 7,2 y 7,4. La proporción de calcio citosólico se determinó a partir de imágenes captadas por un sistema de fluorescencia compuesto por un conmutador de longitud de onda de ultra alta velocidad (Lambda-DG4) para la excitación y un intercambiador de filtro óptico (Lambda 10-2) para la emisión (Sutter Instruments Co., EE.UU.). Como fuente de luz se empleó una lámpara de arco de xenón y se seleccionaron longitudes de onda específicas mediante filtros. Las células se excitaron alternativamente a 340 y 380 nm, y la emisión se recogió a 505 nm. Cada experimento se realizó tres veces independientes por duplicado, con una media de 40 células por campo visual.

3.12 WESTERN BLOTTING

El western blot es una técnica analítica empleada para detectar moléculas proteicas específicas entre una mezcla de proteínas. Esta mezcla puede incluir todas las proteínas asociadas a un determinado tejido o tipo celular (279).

3.12.1 Lisado y cuantificación de proteinas

En un primer lugar se separó la fracción citosólica y se cuantificó la cantidad de proteína presente en esta. Para esto, las células se sembraron en una placa de 12 pocillos a 5×10^5 células por pocillo y se dejaron adherir durante 24 h. Transcurrido este tiempo, se trataron con los compuestos (CPA y ROQC) durante 24 h. A continuación, las células SH-SY5Y se lavaron dos veces con PBS frío, se rasparon y se añadieron 100 µl del tampón de lisis hipotónico frío con cócteles de inhibidores de proteasas y fosfatasas. Las muestras se sonicaron durante 1 min y se centrifugaron durante 20 min a 4 °C y 12000 rpm. A continuación, se recogió el sobrenadante como fracción citosólica. Después, la cantidad de proteinas citosólicas se cuantificó mediante el Direct Detect (Millipore) y se guardaron las muestras a -20ºC hasta su uso.

USC
UNIVERSIDADE DE SANTIAGO DE COMPOSTELA

3.12.2 Electroforesis, transferencia y western blot

Para detectar las proteinas de interés se siguieron los pasos esquematizados en la figura 26.

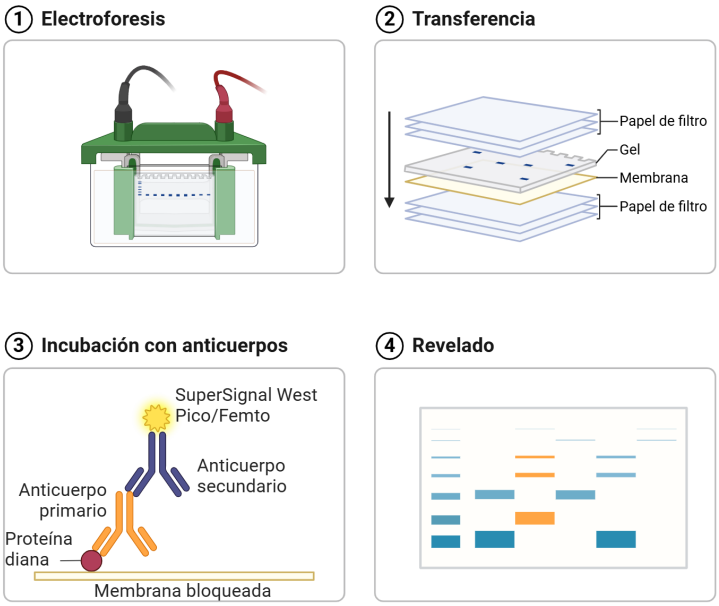


Figura 26. Esquema d los cuatro pasos principapes en el método Western Blot. Imagen creada con biorender.com

Para la electroforesis se utilizaron geles de poliacrilamida con dodecil sulfato sódico al 4-20%. Estos geles se cargaron con 15 µg de proteína citosólica, proveniente de los lisados celulalares, a los que se le añadió el buffer de carga (sección 3.2). Para determinar el tamaño de las proteínas se utilizó el marcador de peso molecular Precision Plus Protein Standards Kaleidoscope. La electroforesis se realizó en la solución de electroforesis (sección 3.2) aplicando un voltaje constante de 200 voltios durante 40 min. De esta forma, las proteínas se separaron según su peso molecular. Luego se transfirieron a una membrana de PVDF (fluoruro de polivinilideno) utilizando el tampón de transferencia (sección 3.2), aplicando un voltaje constante de 10 voltios durante 30 min (280).

A continuación, las membranas se bloquearon con (albúmina de suero bovino) BSA al 0,5% y se realizó la incubación con los anticuerpos, primarios y secundarios (Tabla 2), utilizando el sistema de detección de proteínas SNAP i.d. Después de la incubación con los anticuerpos primarios, las membranas se lavaron con PBS-T, se incubaron con los anticuerpos secundarios y se lavaron de nuevo con PBS-T. La señal se normalizó con la β-actina con el anticuerpo anti-β-actina. Las bandas inmunorreactivas se detectaron utilizando el sistema de emisión de quimioluminiscencia Supersignal West Pico o Supersignal West Femto y el software Diversity GeneSnap (Syngene). Los experimentos se realizaron tres veces independientes por duplicado (280).

Tabla 2. Anticuerpos, hospedador, peso molecular y diluciones empleadas para realizar los western blot

	Proteína diana	*Hospedador*	*Peso molecular (kDa)*	*Dilución*
Anticuerpos primarios	Caspasa-8	Ratón	18/43/57	1:1000
	Caspasa-9 (escindida)	Conejo	35/37	1:2000
	ß-actina	Ratón	42	1:5000
Anticuerpos secundarios	Ratón	Cabra	-	1:10000
	Conejo	Cabra	-	1:10000

3.13 ANÁLISIS ESTADÍSTICO

Los datos se presentan como media ± SEM de al menos tres experimentos independientes. Las diferencias se evaluaron mediante la prueba t de Student o ANOVA unidireccional seguido de pruebas de comparación múltiple de Dunnett o Tukey. La significación estadística se estableció en *p < 0,05, **p < 0,01 y ***p < 0,001. Se utilizó el programa GraphPad Prism 8 para calcular la IC_{50} y la concentración efectiva 50 (EC_{50}) utilizando un ajuste de log(inhibidor) frente a respuesta o un ajuste de log(agonista) frente a respuesta, respectivamente.

El índice de combinación se calculó con la ecuación de Chou y Talalay (281):

$$\text{Índice de combinación} = \frac{D1}{D(X)1} + \frac{D2}{D(X)2}$$

donde (DX)1 y (DX)2 son los valores IC_{50} de cada micotoxina sola, y D1 y D2 son los valores IC_{50} de cada micotoxina en combinación. Si los resultados de la ecuación son <1, =1 y >1, el método de Chou & Talalay considera sinergismo, aditividad o antagonismo, respectivamente.

3.14 IMÁGENES

En la presente tesis doctoral se ha empleado el software Chemdraw 20.0 para la elaboración de las estructuras químicas de las micotoxinas y el programa Biorender para crear las figuras.

USC UNIVERSIDADE DE SANTIAGO DE COMPOSTELA

4 PUBLICACIONES

En este apartado se muestran los resultados obtenidos durante la presente Tesis Doctoral, que incluye cinco artículos publicados en revistas internacionales y uno enviado (incluido como subcapítulo). Estos resultados incluyen la metodología empleada en cada caso, explican la novedad de la investigación y su importancia, así como las conclusiones obtenidas en cada caso.

SECCIÓN I: ARTÍCULOS PUBLICADOS

1. Single and combined effects of regulated and emerging mycotoxins on viability and mitochondrial function of SH-SY5Y cells
2. Enniatins A1 and B1 alter calcium homeostasis of neuronal cells leading to apoptotic death
3. The Mode of Action of Enniatins A and B is Mediated by Interaction with SOC Reservoirs (A) and Mitochondrial Permeability Transition Pore (B)
4. Enniatins A1 and B1 Modulate Calcium Flux through Alternative Pathways beyond Mitochondria
5. In Vitro Testing of Lung Carcinogenicity for an In Silico-Identified Cluster of Mycotoxins

SECCIÓN II: ARTÍCULO EN REVISIÓN

6. In vitro assessment of emerging mycotoxins co-occurring in cheese: A potential health hazard

A continuación, se presentan los resúmenes en castellano de cada artículo, así como la información relativa a las revistas en las que se publicaron y una copia de cada artículo en su versión publicada.

En lo que respecta al artículo en revisión, se presenta una copia del mismo en inglés y su resumen traducido al castellano.

USC
UNIVERSIDADE DE SANTIAGO DE COMPOSTELA

USC
UNIVERSIDADE
DE SANTIAGO
DE COMPOSTELA

SECCIÓN I: ARTÍCULOS PUBLICADOS

1. Single and combined effects of regulated and emerging mycotoxins on viability and mitochondrial function of SH-SY5Y cells

Resumen:

La co-ocurrencia de micotoxinas emergentes y reguladas en muestras contaminadas ha sido ampliamente documentada, pero los estudios sobre su toxicidad combinada son escasos. En este artículo, se probaron las micotoxinas reguladas deoxinivalenol, fumonisina B1 y zearalenona, y las emergentes eniatina A, eniatina B y beauvericina en células de neuroblastoma humano SH-SY5Y. Se evaluaron sus efectos individuales y en combinación binaria sobre la viabilidad celular y la función mitocondrial. Los resultados con micotoxinas individuales revelaron que el deoxinivalenol y las micotoxinas emergentes fueron las más dañinas para las células neuronales, presentando valores de IC_{50} entre 0.35 y 2.4 μM. Curiosamente, las micotoxinas no reguladas desencadenaron apoptosis al afectar el potencial de membrana mitocondrial. Sin embargo, cuando se combinaron de forma binaria con micotoxinas reguladas y no reguladas, se produjeron efectos antagónicos en todos los casos. Finalmente, se analizaron extractos de pienso de vaca y leche mediante UHPLC-MS/MS, y se detectó la presencia de varias micotoxinas incluidas en este estudio. Estos extractos se probaron en células de neuroblastoma y produjeron efectos dañinos sobre la viabilidad celular. Aunque las combinaciones binarias de micotoxinas causaron efectos antagónicos, su mezcla en matrices naturales indujo efectos mayores de lo esperado. Por lo tanto, sería interesante explorar la influencia de la matriz en la toxicidad de las micotoxinas y continuar estudiando el mecanismo de acción neurotóxico de las micotoxinas emergentes, ya que podrían representar un riesgo para la salud.

USC
UNIVERSIDADE DE SANTIAGO DE COMPOSTELA

Información revista:

Single and combined effects of regulated and emerging mycotoxins on viability and mitochondrial function of SH-SY5Y cells

Nadia Pérez-Fuentes[a], Rebeca Alvariño[a], Amparo Alfonso[a], Jesús González-Jartín[a], Sandra Gegunde[a], Mercedes R. Vieytes[b], Luis M. Botana[a]

[a] Departamento de Farmacología, Facultad de Veterinaria, Universidad de Santiago de Compostela, Lugo, 27002, Spain
[b] Departamento de Fisiología, Facultad de Veterinaria, Universidad de Santiago de Compostela, Lugo, 27002, Spain

Revista: Food and Chemical Toxicology
Fecha de publicación: 29 de mayo de 2021
Enlace: https://doi.org/10.1016/j.fct.2021.112308
Editorial: PERGAMON-ELSEVIER SCIENCE LTD, THE BOULEVARD, LANGFORD LANE, KIDLINGTON, OXFORD, ENGLAND, OX5 1GB
ISSN: 0278-6915

Índices de calidad de la revista:
Factor de impacto (2021): 5.572
Factor de impacto 5 años (2021): 5.692
Categoría (2021): "Ciencia y tecnología de los alimentos" Q1 (34/144), "Toxicología" Q1 (15/94)

Contribución doctorando:
N. P-F. llevó a cabo la realización de experimentos, análisis de datos, preparación de figuras, redacción del borrador original, revisión y edición.

Autorización revista:
Contenido reproducido con permiso:



Single and combined effects of regulated and emerging mycotoxins on viability and mitochondrial function of SH-SY5Y cells

Author:
Nadia Pérez-Fuentes,Rebeca Alvariño,Amparo Alfonso,Jesús González-Jartín,Sandra Gegunde,Mercedes R. Vieytes,Luis M. Botana

Publication: Food and Chemical Toxicology

Publisher: Elsevier

Date: August 2021

© 2021 The Author(s). Published by Elsevier Ltd.

Food and Chemical Toxicology 154 (2021) 112308

Contents lists available at ScienceDirect

Food and Chemical Toxicology

journal homepage: www.elsevier.com/locate/foodchemtox

Single and combined effects of regulated and emerging mycotoxins on viability and mitochondrial function of SH-SY5Y cells

Nadia Pérez-Fuentes [a], Rebeca Alvariño [a,*], Amparo Alfonso [a,**], Jesús González-Jartín [a], Sandra Gegunde [a], Mercedes R. Vieytes [b], Luis M. Botana [a]

[a] Departamento de Farmacología, Facultad de Veterinaria, Universidad de Santiago de Compostela, Lugo, 27002, Spain
[b] Departamento de Fisiología, Facultad de Veterinaria, Universidad de Santiago de Compostela, Lugo, 27002, Spain

ARTICLE INFO

Handling Editor: Dr. Bryan Delaney

Keywords:
Mycotoxin
Emerging
Cytotoxicity
Antagonistic
Apoptosis

ABSTRACT

Co-occurrence of emerging and regulated mycotoxins in contaminated samples has been widely documented, but studies about their combined toxicity are scarce. In this report, the regulated mycotoxins deoxynivalenol, fumonisin B1 and zearalenone, and the emerging ones enniatin A, enniatin B and beauvericin were tested in SH-SY5Y human neuroblastoma cells. Their individual and binary combined effects on cell viability and mitochondrial function were evaluated. The results with individual mycotoxins revealed that deoxynivalenol and emerging mycotoxins were the most damaging to neuronal cells, presenting IC_{50} values between 0.35 and 2.4 μM. Interestingly, non-regulated mycotoxins triggered apoptosis by affecting to mitochondrial membrane potential. However, when regulated and non-regulated mycotoxins were binary mixed, antagonistic effects were found in all cases. Finally, cow feed and milk extracts were analysed by UHPLC-MS/MS, detecting the presence of several mycotoxins included in this study. These extracts were tested in neuroblastoma cells, and damaging effects on cell viability were found. Although binary combinations of mycotoxins produced antagonistic effects, their mixture in natural matrixes induces greater effects than expected. Therefore, it would be interesting to explore the matrix influence on mycotoxin toxicity, and to continue studying the neurotoxic mechanism of action of emerging mycotoxins, as they could be a health hazard.

1. Introduction

Mycotoxins are secondary metabolites from different fungi species, highlighting those belonging to the genera *Aspergillus*, *Fusarium* and *Penicillium*. Mycotoxins are usually present in cereals such as corn or rye, as well as in other types of food such as milk or even fish. They are physically and thermodynamically stable substances, which resist the processes of milling and drying, as well as cooking and baking, and their ingestion causes mycotoxicosis in animals and people (Bertero et al., 2020; Sainz et al., 2018).

According to the European Food Safety Authority (EFSA), mycotoxins can be divided into two large groups in relation to the severity of their effects: regulated mycotoxins and unregulated or emerging mycotoxins. Regulated mycotoxins comprise those which are a public health problem due to their high toxicity at known concentrations and, therefore, maximum limits in food have been established (Commission Regulation (EC) No 1881/2006). This group includes fumonisins, zearalenone (ZEA), aflatoxins, ochratoxin A, patulin and trichothecenes. The latter is subdivided into two sub-groups: type A, where the highly toxic T2 toxin is found, and type B, where deoxynivalenol (DON) stands out. Unregulated mycotoxins are those which are not considered a problem for public health. Currently, there are not much data about these toxins, so it cannot be stated if they are safe for animals and humans (EFSA, 2012, 2013, 2014). These mycotoxins include enniatins (ENNs),

Abbreviations: ATCC, American Type Culture Collection; BBB, blood brain barrier; BEA, beauvericin; CI, confidence interval; ΔΨm, mitochondrial membrane potential; DON, deoxynivalenol; EFSA, European Food Safety Authority; ENN, enniatin; FB1, fumonisin: B1; LDH, lactate dehydrogenase; MTT, 3-(4,5-dimethyl thiazol-2-yl)-2,5-diphenyl tetrazolium bromide; NA, not applicable; PBS, phosphate buffered saline; PI, propidium iodide; ROS, reactive oxygen species; Rot, rotenone; STS, staurosporine; TMRM, tetramethylrhodamine methyl ester; UHPLC-MS/MS, ultra-high liquid chromatography tandem mass spectrometry; ZEA, zearalenone.

* Corresponding author.
** Corresponding author.
E-mail addresses: rebeca.alvarino@usc.es (R. Alvariño), amparo.alfonso@usc.es (A. Alfonso).

https://doi.org/10.1016/j.fct.2021.112308
Received 1 March 2021; Received in revised form 19 May 2021; Accepted 25 May 2021
Available online 29 May 2021
0278-6915/© 2021 The Author(s). Published by Elsevier Ltd. This is an open access article under the CC BY-NC-ND license (http://creativecommons.org/licenses/by-nc-nd/4.0/).

beauvericin (BEA), sterigmatocystine, phomopsins and *Alternaria* toxins.

Normally, food is not contaminated by a single type of mycotoxin (Arroyo-Manzanares et al., 2019). A cereal such as maize can be infested by several species of *Fusarium*, *Aspergillus* or *Penicillium* at the same time, which produce different types of mycotoxins that jointly contaminate the cereal. Studies about joint toxicity of these compounds, whose concentrations vary greatly between samples, are scarce (Agahi et al., 2020a; Jia et al., 2020; Juan-García et al., 2020). Co-occurrence of regulated and emerging mycotoxins has been previously detected in studies carried out on samples from NW Iberian Peninsula by our group and other authors (Dagnac et al., 2016; González-Jartín et al., 2020). In these works, it was outstanding the presence of the regulated mycotoxins DON, fumonisin B1 (FB1) and ZEA, while ENN A, ENN B and BEA were the prevalent emerging mycotoxins.

DON is a type B trichothecene, commonly known as vomitoxin, and produced by *Fusarium* spp. which causes a picture of vomiting, anorexia and fever whose origin can be central or peripheral. Oral ingestion of DON activates POMC neurons and the release of nesphatin-1, which are closely related to the reduction of food intake. In addition, it has cytotoxic effects on fast-growing cells such as those of the intestinal epithelium. This cytotoxicity has been associated with the ability of DON to produce ROS and lipid peroxidation (Bonnet et al., 2012; Zhang et al., 2020). FB1 causes equine leukoencephalomalacia and to be involved in the development of neural tube defects in children. To date, the pathway by which this toxin produces neurotoxicity is mostly undisclosed, but it is known that FB1 blocks a key enzyme in the metabolism of sphingolipids, altering the membrane functions (Domijan, 2012; Khan et al., 2018). Regarding ZEA, it is produced by the *Fusarium* genus and has a great oestrogenic activity due to its structure. Its toxicity is not only due to oestrogenic effects, other mechanisms such as oxidative stress are also involved (Tatay et al., 2017).

With respect to emerging mycotoxins, ENN B is the most frequent in processed and unprocessed grains in Europe and, therefore, it is the most studied one. It has antibacterial, insecticidal, and antifungal properties. At cellular level, ENN B produces mitochondrial toxicity due to its ionophoric properties, as the rest of the toxins of the enniatin family (Prosperini et al., 2017). BEA is structurally related to the enniatin family. It also acts as an ionophore, causing mitochondrial dysfunction, and has antimicrobial, entomopathogenic and antitumor activities (Bertero et al., 2020).

Although the mechanism of action of these toxins is not fully understood, they can cross the blood brain barrier (BBB) and cause neurotoxic effects (Bonnet et al., 2012; Osuchowski et al., 2005b; Taevernier et al., 2016). Their neurotoxicity could be related to their effects on mitochondria, as many of them are known to cause mitochondrial dysfunction by producing oxidative stress and inducing the formation of reactive oxygen species (ROS). Neurons are very susceptible to oxidative stress, as they consume large amounts of oxygen through oxidative phosphorylation. On the other hand, there are previous studies which conclude that both regulated and emerging mycotoxins induce apoptotic cell death (Bensassi et al., 2012; Prosperini et al., 2013). ROS can activate apoptotic cell death through the intrinsic pathway, also named mitochondrial pathway because the initiating signals of this mechanism are triggered by mitochondria (Walia et al., 2021). Therefore, mitochondrial dysfunction could be closely related with the cell death produced by mycotoxins. In fact, some studies suggest that DON can induce apoptosis through the opening of the mitochondrial transition pore (Bensassi et al., 2012).

In this study, the effects originated by the regulated and emerging mycotoxins most frequently found in contaminated samples of the NW Iberian Peninsula were analysed in SH-SY5Y human neuroblastoma cells. DON, FB1, ZEA, ENN A, ENN B and BEA were tested individually and in binary combinations to elucidate their cytotoxicity and the effects on mitochondrial function, as well as their type of interaction.

2. Materials and methods

2.1. Chemicals and solutions

Tetramethylrhodamine methyl ester (TMRM), CyQUANT™ lactate dehydrogenase (LDH) Cytotoxicity Assay Kit, Dulbecco's Modified Eagle Medium: F-12 nutrient Mix (DMEM/F-12), trypsin/EDTA (0.05%), glutamax and penicillin-streptomycin (10,000 U/mL) were bought in Thermo Fisher Scientific (Madrid, Spain). Durapore membrane centrifugal filters (0.22 μm pore size) were purchased from Merck Millipore (Billerica, USA). DON and FB1 (purity >98%) were obtained from Romer Labs (Getzersdorf, Austria). ZEA, ENN A, ENN B and BEA (purity >96%), 3-(4,5-dimethyl thiazol-2-yl)-2,5-diphenyl tetrazolium bromide (MTT), saponin (SAP), staurosporine (STS), Annexin V-FITC Apoptosis Detection Kit, and another chemical reagent grade were purchased from Sigma-Aldrich (Madrid, Spain).

The composition of Locke's buffer was: 154 mM NaCl, 5.6 mM KCl, 3.6 mM $NaHCO_3$, 1 mM $MgCl_2$ 1.3 mM $CaCl_2$, 5 mM glucose and 10 mM HEPES. Stock solutions of mycotoxins were prepared in dimethylsulfoxide (DMSO).

2.2. Cow feed and milk extracts and analysis

A cow feed sample was analysed according to a method previously validated for the multidetection of 22 mycotoxins in this matrix (González-Jartín et al., 2020).

For cellular assays, an aliquot of 9 mL of the extract was filtered (0.22 μm), dried in a centrifugal evaporator, and reconstituted in 0.45 mL of DMSO, obtaining a 20 times concentrated sample.

Two commercial milk samples were analysed according to a method previously validated for the multidetection of 40 mycotoxins in these matrixes (González-Jartín et al., 2021).

For cellular assays, an aliquot of 1 mL of each extract was filtered (0.22 μm), dried in a centrifugal evaporator, and reconstituted in 0.05 mL of DMSO, obtaining a 20 times concentrated sample.

2.3. Cell culture and treatment

SH-SY5Y human neuroblastoma cell line was purchased from American Type Culture Collection (ATCC), number CRL2266. Cells were cultured in DMEM/F-12 enriched with 10% fetal bovine serum, 1% glutamax and 10,000 U/mL penicillin-streptomycin. Cells were maintained at 37 °C in a humidified atmosphere of 95% air and 5% CO_2 and dissociated once a week using 0.05% trypsin/EDTA.

SH-SY5Y cells were cultured in 96-well plates at concentration of 5×10^4 cells/well for all the assays performed, except for flow cytometry analysis.

Mycotoxin standards were dissolved in DMSO and serial dilutions were performed in culture medium. In all cases, DMSO levels in cells were kept below 0.5%. For individual mycotoxin assays, cells were treated at concentrations ranging from 0.1 to 30 μM. In the case of binary combinations, the ratio among regulated and unregulated mycotoxins was selected based on the most frequent proportions found in contaminated samples of the NW Iberian Peninsula (González-Jartín et al., 2020). Cells were treated for 24 h with the following mixtures: DON and FB1 were combined at 5:1 ratio with ENN A, ENN B and BEA, whilst ZEA was combined with unregulated mycotoxins at 2:1 ratio. Combined concentration gradients were selected based on the results obtained with single mycotoxins, in order to include half maximal inhibitory concentration (IC_{50}) values in the concentration range analysed.

With regard to the concentrated cow feed and milk extracts, SH-SY5Y cells were treated with 1:500, 1:1000, 1:5000 and 1:10000 dilutions for 24 h. In both cases, a blank sample (uncontaminated matrix) was used as control.

To compare the cow feed extract effects with commercial

USC UNIVERSIDADE DE SANTIAGO DE COMPOSTELA

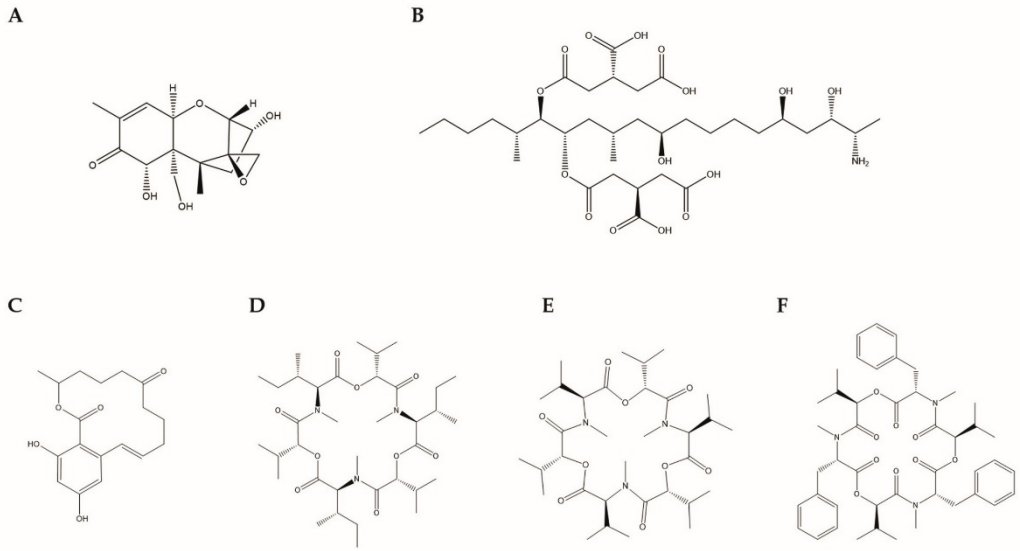


Fig. 1. Chemical structures of regulated and emerging mycotoxins. (A) DON, (B) FB1, (C) ZEA, (D) ENN A, (E) ENN B, (F) BEA.

mycotoxins, a commercial mycotoxin mixture was also added to the cells for 24 h. The concentrations selected for this combination were based on the results obtained from the contaminated extract analysis.

All the experiments were performed in triplicate, at least three independent times.

2.4. Cell viability assay

The effect of single mycotoxins, binary combinations and the concentrated extract on cell viability was analysed with MTT assay as previously described (Alvariño et al., 2017). SAP from *Quillaja bark* at 1 mg/mL was used as cell death control. Cells were treated with individual mycotoxins for 6, 24 and 48 h, whilst binary combinations and extract treatments were performed for 24 h. After treatment, cells were washed three times with Locke's solution and 200 μL of MTT (500 μg/mL) were added to each well. The plate was incubated for 1 h at 37 °C and 300 rpm in an orbital shaker. Then, MTT was removed, and 5% sodium dodecyl sulphate was added to originate cell lysis. The absorbance produced by the tetrazolium salt was read at 595 nm in a spectrophotometer plate reader.

2.5. Cytotoxicity assay

CyQUANT™ LDH Cytotoxicity Assay Kit test was used to analyse cell cytotoxicity, following manufacturer's instructions. Cells were cultured in 96-well plates and treated as previously described. Individual mycotoxins were added for 6 and 24 h, whereas binary mixtures and extract treatments were carried out for 24 h. SAP from *Quillaja bark* (1 mg/mL) was used as cell death control. After treatment, 50 μL of medium were transferred to a 96-well flat-bottom plate and LDH release was evaluated. Absorbance was read at 490 and 680 nm in a plate reader and the 680 nm absorbance value (background signal) was subtracted from the 490 nm absorbance value to determine LDH activity.

2.6. Mitochondrial membrane potential measurement

Mitochondrial membrane potential ($\Delta\Psi_m$) was analysed with TMRM dye, which is a fluorescent lipophilic cationic probe that accumulates within mitochondria in inverse proportion to $\Delta\Psi_m$. For this assay, cells were treated with single mycotoxins for 6 and 24 h, and with binary combinations for 24 h. Then, cells were washed twice with Locke's solution and 200 μL of 20 μM TMRM were added to each well. The plate was incubated for 30 min at 37 °C and 300 rpm and cells were solubilised with H_2O and DMSO (1:1). Fluorescence was read at 535 nm excitation and 590 nm emission in a plate reader (Bornancin et al., 2019). Rotenone (Rot) at 1 μM was used as positive control.

2.7. Flow cytometry analysis

Annexin V-FITC Apoptosis Detection Kit was used to determine the type of cell death produced by mycotoxins, following manufacturer's instructions. SH-SY5Y cells were seeded in 12-well plates at 5×10^5 cells per well and allowed to grow for 24 h. Then, cells were incubated with individual mycotoxins for 24 h. STS at 0.1 μM was used as positive control (Alvariño et al., 2020). After treatment, cells were washed with phosphate buffered saline (PBS) and resuspended in Annexin-binding buffer containing Annexin V-FITC and Propidium Iodide (PI). Next, cells were incubated at room temperature for 15 min, resuspended in commercial PBS (Thermo Fisher Scientific), filtered and maintained on ice. The fluorescence was determined by flow cytometry using the ImageStreamMKII instrument (Amnis Corporation, Luminex Corp, Austin, TX, USA). The fluorescence of 10,000 events was acquired and analysed with IDEAS Application 6.0 software (Amnis Corporation, Luminex Corp).

2.8. Statistical analysis

Data are expressed as mean ± SEM of three independent experiments. Statistical differences were evaluated by Student's t-test. p values ≤ 0.05 were considered statistically significant. IC_{50} and half maximal effective concentration (EC_{50}) values were determined by fitting the data with a log (inhibitor) *vs* response model or a log (agonist) *vs* response model, respectively, with GraphPad Prism 8 software.

The combination index was calculated with Chou & Talalay equation

USC UNIVERSIDADE DE SANTIAGO DE COMPOSTELA

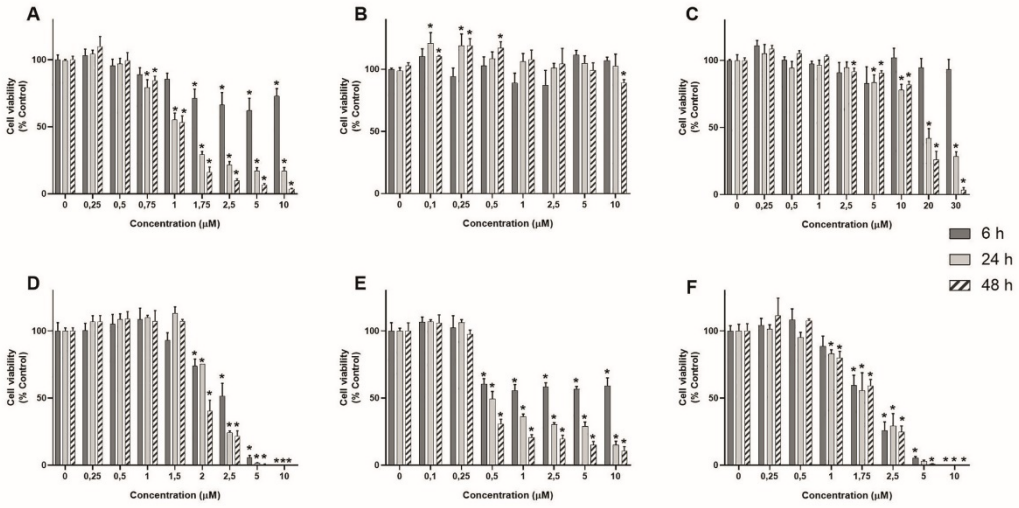


Fig. 2. Effect of selected mycotoxins on cell viability of SH-SY5Y cells. Cells were incubated with mycotoxins for 6, 24 and 48 h and their effect on cell viability was assessed by MTT test. (A) DON, (B) FB1, (C) ZEA, (D) ENN A, (E) ENN B, (F) BEA. Data are mean ± SEM of three independent replicates expressed as percentage of untreated control cells. Statistical differences determined by Student's *t*-test. *p ≤ 0.05, significantly different from the control.

(Chou, 2010):

$$COMBINATION\ INDEX = \frac{D1}{(DX)1} + \frac{D2}{(DX)2}$$

where (DX)1 and (DX)2 are the IC_{50} values of each mycotoxin alone, and D1 and D2 are the IC_{50} values of each mycotoxin in binary combination. According to Chou & Talalay method, synergism, additivity, and antagonism were considered when the combination index was <1, =1 and >1, respectively.

3. Results

3.1. Evaluation of single mycotoxin effects on cell viability and cytotoxicity

At first, MTT assay was used to analyse the effect of regulated and emerging toxins on cell viability of human neuroblastoma SH-SY5Y cells. Cells were treated with DON, FB1, ZEA, ENN A, ENN B and BEA (Fig. 1) at concentrations ranging from 0.1 to 30 μM for 6, 24 and 48 h to compare the effect produced at different incubation times.

DON did not totally produce cell death after 6 h of treatment, it only produced a slight decrease on cell viability (about 30%) at concentrations between 1.75 and 10 μM. This mycotoxin had a similar effect after 24 and 48 h of incubation, producing a significant reduction on cell viability, in a dose-dependent manner, at concentrations over 0.75 μM (Fig. 2 A). FB1 only reduced cell viability at the highest concentration after 48 h of incubation and it seemed to stimulate cell proliferation at the lowest doses used after 24 and 48 h (Fig. 2 B). The last of the regulated mycotoxins tested, ZEA, did not produce any cell damage at 6 h of incubation, but it decreased cell viability at concentrations over 20 μM at 24 and 48 h, producing a reduction of more than 50% compared to control cells (Fig. 2 C). With regard to emerging mycotoxins, treatment with ENN A for 6 h produced a reduction in cell viability of 41.0 ± 8.5% and 94.3 ± 1.6% at 2.5 μM and 5 μM, respectively, and a complete inhibition at 10 μM. At 24 and 48 h of incubation, the decrease on cell viability at 2.5 and 5 μM was higher than 74.5%, and a total reduction was found again at the highest dose tested (Fig. 2 D). In the case of ENN B, the effects observed at 6, 24 and 48 h were more pronounced than for ENN A, resulting in significant cell damage at concentrations over 0.5 μM, but the mycotoxin did not produce a total inhibition of cell viability at the highest dose (Fig. 2 E). Finally, BEA showed similar effects that ENN A, decreasing cell viability more than a 50% at concentrations above 1.75 μM at all the incubation times (Fig. 2 F).

Table 1
IC_{50} values of mycotoxins in MTT assay. DON: deoxynivalenol, FB1: fumonisin B1, ZEA: zearalenone, ENN A: enniatin A, ENN B: enniatin B; BEA: beauvericin, CI: 95% confidence interval, NA: Not applicable.

TOXIN	IC_{50} (μM)		
	6 h	24 h	48 h
DON	NA	0.94 (CI:0.84–1.0) R^2: 0.96	0.97 (CI: 0.88–1.1) R^2: 0.97
FB1	NA	NA	NA
ZEA	NA	17.4 (CI: 15.1–19.8) R^2: 0.94	16.5(CI: 14.3–21.2) R^2: 0.93
ENN A	2.4 (CI: 2.2–2.8) R^2: 0.93	2.25 (CI: 2.2–2.3) R^2: 0.98	2.0 (CI: 1.8–2.1) R^2: 0.96
ENN B	NA	0.43 (CI: 0.37–0.48) R^2: 0.95	0.35 (CI: 0.31–0.41) R^2: 0.96
BEA	1.9 (CI: 1.6–2.3) R^2: 0.96	1.7 (CI: 1.3–2.1) R^2: 0.95	1.5 (CI: 1.3–1.8) R^2: 0.96

With the data obtained, IC_{50} values were calculated for each toxin by fitting the data with a log (inhibitor) *vs* response model (Table 1, Figure S1). At 6 h, only ENN A and BEA produced a complete reduction of cell viability, so IC_{50} values were calculated for these emerging toxins. Both presented similar values, 2.4 μM (CI: 2.2–2.8 μM) and 1.9 μM (CI: 1.6–2.3 μM), respectively. Regarding longer incubation times (24 and 48 h), IC_{50} values were calculated for all the mycotoxins tested, with the exception of FB1, which did not alter the cell function in this cell line. At 24 h, DON and ENN B turned to be the most damaging toxins, with IC_{50} of 0.94 and 0.43 μM, respectively. Otherwise, ZEA presented the highest IC_{50} (17.4 μM). The same trend was observed at 48 h, with DON and emerging mycotoxins presenting IC_{50} values in the low micromolar range, whilst ZEA was again the least harmful toxin. In general,

USC UNIVERSIDADE DE SANTIAGO DE COMPOSTELA

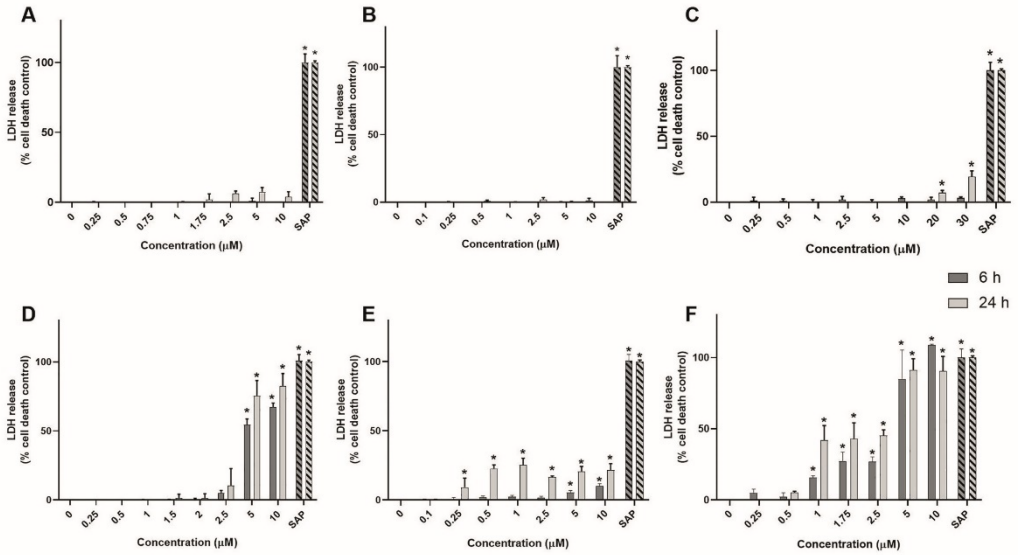


Fig. 3. Cytotoxic effects of regulated and non-regulated mycotoxins on SH-SY5Y cells. Neuroblastoma cells were treated with mycotoxins for 6 and 24 h and cytotoxicity was determined by LDH assay. (A) DON, (B) FB1, (C) ZEA, (D) ENN A, (E) ENN B, (F) BEA. SAP (saponin) was used as cell death control. Data are mean ± SEM of three independent replicates. Data expressed in percentage of cell death control cells. Statistical differences determined by Student's *t*-test. *p ≤ 0.05 compared to control cells.

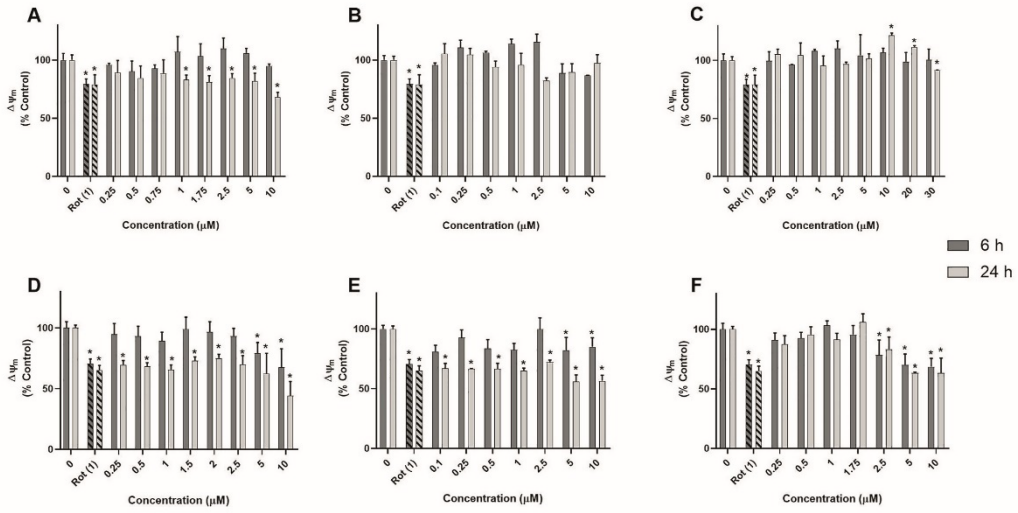


Fig. 4. Mitochondrial membrane potential of human neuroblastoma cells after treatment with regulated and emerging mycotoxins. (A) DON, (B) FB1, (C) ZEA, (D) ENN A, (E) ENN B, (F) BEA. Cells were treated for 6 and 24 h and $\Delta\Psi_m$ was determined by TMRM assay. Data are the mean ± SEM of three independent replicates, expressed as percentage of control cells and compared to untreated control cells by Student's *t*-test. *p ≤ 0.05.

emerging toxins produced a greater cell damage than the regulated ones, with the exception of DON.

Next, cytotoxicity of mycotoxins was determined in the human neuroblastoma cell line with LDH assay. LDH release to the culture medium provides information about the degree of cell membrane damage. SAP at 1 mg/mL was used as membrane rupture control. Cells were treated with mycotoxins at the same concentrations used in MTT assay. Due to the similar results obtained in MTT assay at 24 and 48 h of incubation, LDH experiment was performed at 6 and 24 h. No cytotoxic effects were observed after treatment with the regulated mycotoxins

USC UNIVERSIDADE DE SANTIAGO DE COMPOSTELA

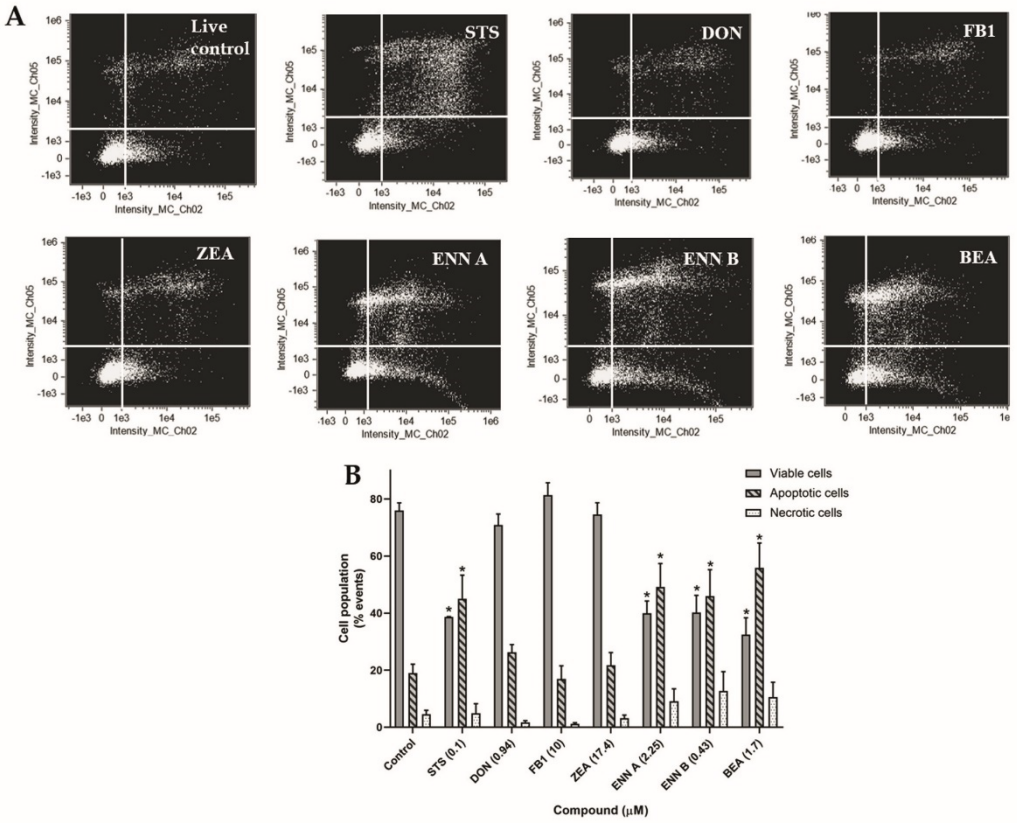


Fig. 5. Analysis of cell death type induced by regulated and emerging mycotoxins in SH-SY5Y cell line. Cells were treated with mycotoxins for 24 h and co-stained with Annexin V-FITC and PI. STS was used as positive control and fluorescence was analysed by flow cytometry. (A) Representative scatter plot of each treatment. X-axis represents PI fluorescence, y-axis represents Annexin V-FITC fluorescence. Data are expressed as percentage of total events analysed. Percentages of viable cells (Annexin V-FITC -/PI -), apoptotic cells including early apoptosis (Annexin V-FITC + /PI –) and late apoptosis (Annexin V-FITC + /PI +), and necrotic cells (Annexin V-FITC –/PI+) were calculated. (B) Bar graph of the type of cell death induced by mycotoxins. Data are mean ± SEM of three independent experiments, compared to control cells by Student's *t*-test. *$p \leq 0.05$.

DON and FB1 (Fig. 3A and B). In the case of ZEA, a slight increase in LDH leakage was found at 20 and 30 μM (9.1 ± 8.9% and 19.5 ± 4.3%, respectively) after 24 h (Fig. 3 C). On the other hand, ENN A significantly increased LDH release of SH-SY5Y cells at 5 and 10 μM at both incubation times, presenting EC_{50} values of 3.9 μM (CI: 3.6–4.2 μM) and 3.5 μM (CI: 2.8–4.4 μM) at 6 and 24 h, respectively (Fig. 3 D, Figure S2). ENN B only showed significant effects on LDH release after 24 h of treatment, producing an increase about 20% at concentrations above 0.25 μM (Fig. 3 E). Finally, the cytotoxic effect produced by BEA was greater than the originated by the other mycotoxins used in this study, inducing LDH leakage at concentrations over 1 μM (Fig. 3 F). EC_{50} was calculated after 6 and 24 h of exposure, and this mycotoxin presented values of 2.9 μM (CI: 1.9–4.6 μM) and 2.0 μM (CI: 1.4–2.9 μM), respectively (Figure S2).

In view of the differences observed in MTT and LDH assay, the study was followed by assessing the effect of the selected mycotoxins on $\Delta\Psi_m$. SH-SY5Y cells were treated at the same concentrations used in the previous assays for 6 and 24 h, and TMRM assay was performed. The assay was validated by using the inhibitor of the electronic transport chain Rot at 1 μM (Zhou et al., 2018).

The regulated mycotoxin DON did not produce any effect at 6 h, but it reduced $\Delta\Psi_m$ between 16.9 and 34.0% at concentrations higher than 1 μM after 24 h of treatment (Fig. 4 A). On the other hand, treatment with FB1 did not generate significant changes in $\Delta\Psi_m$ of SH-SY5Y cells at both incubation times. Finally, ZEA produced a slight decrease at 30 μM after 24 h of incubation (Fig. 4B and C). Regarding emerging mycotoxins, ENN A produced significant differences compared to control cells at 5 and 10 μM after 6 h of incubation (79.0 ± 8.9% and 67.7 ± 14.5%, respectively) (Fig. 4 D). At 24 h, this emerging toxin affected to $\Delta\Psi_m$ at all the concentrations tested. The same was observed with ENN B treatment, which altered $\Delta\Psi_m$ at the highest doses employed (5 and 10 μM) after 6 h of incubation and caused significant differences with respect to the control at all the concentrations assayed at 24 h (Fig. 4 E). Regarding BEA, it depolarized the mitochondrial membrane at concentrations ranging 2.5–10 μM at both incubation times (Fig. 4 F). In all the experiments, Rot produced a depolarization of the mitochondria, resulting in percentages about 75% of control cells.

Finally, the type of death caused by single mycotoxins in SH-SY5Y cells was evaluated. In view of the previous results, cells were treated with mycotoxins at IC_{50} concentrations obtained with MTT test for 24 h.

USC UNIVERSIDADE DE SANTIAGO DE COMPOSTELA

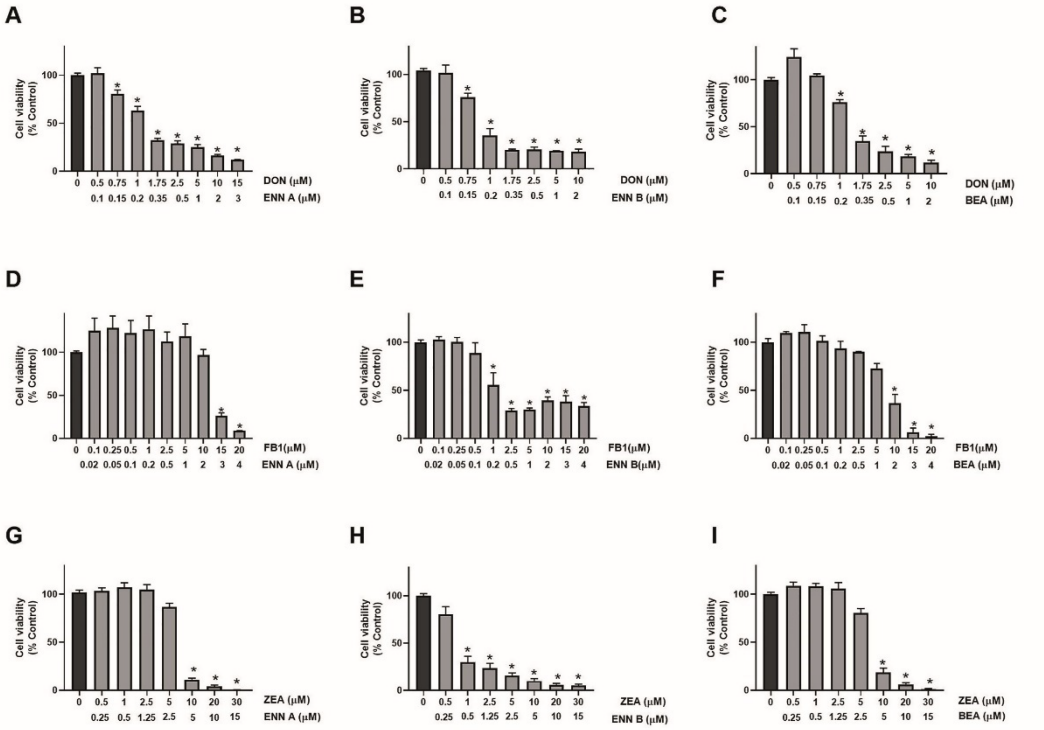


Fig. 6. Effect of regulated and emerging mycotoxin binary combinations in cell viability. SH-SY5Y cells were treated with binary mixtures of regulated and non-regulated mycotoxins for 24 h and MTT assay was carried out. (A) DON + ENN A (5:1), (B) DON and ENN B (5:1), (C) DON + BEA (5:1), (D) FB1+ ENN A (5:1), (E) FB1 + ENN B (5:1), (F) FB1+ BEA (5:1), (G) ZEA + ENN A (2:1), (H) ZEA + ENN B (2:1), (I) ZEA + BEA (2:1). Mean ± SEM of three independent replicates performed by triplicate. Data are expressed as percentage of control cells and compared to untreated control cells by Student's *t*-test. *p ≤ 0.05.

In the case of FB1, cells were treated at the highest dose used in the previous assays, 10 μM. For validating this assay, the known apoptotic inductor STS at 0.1 μM was used as positive control. Then, co-staining with Annexin V- FITC and PI was performed, and the fluorescence was analysed by flow cytometry (Fig. 5). The percentages of apoptotic cells, including early apoptotic cells (Annexin V-FITC positive and PI negative) and late apoptotic cells (Annexin V-FITC positive and PI positive), as well as necrotic cells (Annexin V-FITC negative and PI positive) were calculated.

As expected, 0.1 μM STS produced an increase in apoptotic cell death, reaching a percentage of 45.1 ± 5.5%. The regulated mycotoxins DON, FB1 and ZEA did not produce a significant increase in cell death at the concentrations tested (Fig. 5A and B). On the other hand, ENN A, ENN B and BEA significantly reduced the percentage of viable cells, producing an increase in apoptotic cell death of 49.2 ± 8.2%, 46.0 ± 9.3% and 55.9 ± 8.6%, respectively (Fig. 5 B).

3.2. Evaluation of binary mycotoxin combinations on viability and mitochondrial function of SH-SY5Y cells

In order to mimic the co-occurrence of mycotoxins in food, regulated and emerging mycotoxins were binary combined. Concentration ratios were selected based on the mycotoxin proportions frequently found in local contaminated samples (González-Jartín et al., 2020). DON and FB1 were combined with emerging mycotoxins (ENN A, ENN B and BEA) at 5:1 ratio, whilst ZEA was combined at 2:1 ratio. In view of the effects obtained in the previous experiments, 24 h was chosen as incubation time for mycotoxin combinations.

Firstly, the effect of binary mixtures on cell viability was determined. The results obtained with DON + ENN A combination were similar to the effect produced by DON alone, causing cell damage at concentrations higher than 0.75 μM + 0.15 μM (Fig. 6 A). Regarding DON + ENN B and DON + BEA, the results were quite similar to the combination of DON + ENN A. An acute decrease was observed after treatment with DON + ENN B at 1 μM + 0.2 μM, followed by a stabilized effect at the highest concentrations used (Fig. 6 B). In the case of DON + BEA, a dose-response effect was observed, with significant results from 1 μM + 0.2 μM (Fig. 6 C).

FB1 combinations with ENN A, ENN B and BEA showed a decrease in cell viability in all cases (Fig. 6D–F). FB1 mixture with ENN A presented significant results at concentrations above 15 μM FB1 + 3 μM ENN A (Fig. 6 D). Regarding FB1+ ENN B, this combination seemed to be more harmful, producing cell damage at concentrations over 1 μM + 0.2 μM (Fig. 6 E). Finally, FB1+BEA produced significant effects at the three highest concentrations tested (Fig. 6 F).

In the case of ZEA, its combination with ENN A reduced cell viability a percentage of 89.6 ± 2.5% at concentrations over 10 μM + 5 μM (Fig. 6 G). The combination with ENN B produced an inhibition of cell viability between 69.8 and 94.6% at concentrations over 1 μM ZEA and 0.5 μM ENN B (Fig. 6 H). At last, ZEA + BEA combination had a similar effect than ZEA + ENN A, inducing cell damage at concentrations from 10 μM + 2 μM (Fig. 6 I).

USC UNIVERSIDADE DE SANTIAGO DE COMPOSTELA

Table 2
IC_{50} values and combination index of binary mixtures of regulated and non-regulated mycotoxins. IC_{50} values were used for combination index determination. DON: deoxynivalenol, FB1: fumonisin B1, ZEA: zearalenone, ENN A: enniatin A, ENN B: enniatin B; BEA: beauvericin, CI: 95% confidence interval.

Binary combination	IC_{50} (μM)		Combination index
DON + ENN A (5:1)	**DON** 1.6 (CI: 1.4–1.9) R^2: 0.86	**ENN A** 0.32 (CI: 0.27–0.38)	1.9
DON + ENN B (5:1)	**DON** 0.83 (CI: 0.74–0.89) R^2: 0.95	**ENN B** 0.16 (CI: 0.15–0.18)	1.3
DON + BEA (5:1)	**DON** 1.0 (CI: 0.76–1.2) R^2: 0.97	**BEA** 0.20 (CI: 0.15–0.24)	1.2
FB1 + ENN A (5:1)	**FB1** NA R^2: 0.89	**ENN A** 2.3 (CI: 2.0–2.6)	NA
FB1 + ENN B (5:1)	**FB1** NA R^2: 0.89	**ENN B** 0.15 (CI: 0.12–0.20)	NA
FB1 + BEA (5:1)	**FB1** NA R^2: 0.95	**BEA** 1.4 (CI: 1.2–1.6)	NA
ZEA + ENN A (2:1)	**ZEA** 6.6 (CI: 6.1–7.2) R^2: 0.99	**ENN A** 3.3(CI: 3.0–3.6)	1.9
ZEA + ENN B (2:1)	**ZEA** 1.0 (CI: 0.8–1.2) R^2: 0.86	**ENN B** 0.5 (CI: 0.4–0.6)	1.2
ZEA + BEA (2:1)	**ZEA** 6.5 (CI: 5.8–7.2) R^2: 0.86	**BEA** 3.3 (CI: 2.9–3.7)	2.1

With the results obtained, IC_{50} values for each toxin in binary combination were determined (Table 2, Figure S3). Next, combination index was calculated following Chou & Talalay method (Chou, 2010). If combination index value is higher than 1, it indicates antagonism, if it is equal to 1, it indicates additivity, and if the value is lower than 1, it indicates synergistic effect. For DON mixture with emerging toxins, the combination index obtained was higher than 1, indicating antagonism. With regard to FB1, the combination index could not be calculated due to its lack of effect in MTT assay. In the case of ZEA, its IC_{50} values were lower in combination (among 1–6.6 μM) than the obtained with ZEA alone (17.4 μM). However, emerging toxins in binary mixture with ZEA presented higher IC_{50} values than the toxins alone, so combination index calculation, with values above 1, revealed an antagonistic effect.

Then, the cytotoxicity of binary mycotoxin combinations was determined with LHD assay. In the case of DON, concentrations above 5 μM of this toxin in mixture with ENN A and BEA showed significant differences with the control, with LDH levels between 8.4 and 48.2% in the case of ENN A, and levels between 16.9 and 25.5% for DON + BEA mixtures. Regarding DON + ENN B mixture, only the highest concentration used (10 μM + 2 μM) induced LDH leakage (13.4 ± 3.9%) (Fig. 7A–C). FB1 combinations had a similar effect on LDH release than the reduction observed in cell viability, showing LDH leakage in all cases. FB1+ENN A reduced cell survival at the highest concentrations, starting at 10 μM + 2 μM (Fig. 7 D). In this assay, FB1 presented an EC_{50} of 12.0 μM (CI: 10.8–14.8 μM), whilst ENN A EC_{50} was 2.4 μM (CI: 2.1–2.9 μM) (Figure S4 A). FB1+ ENN B induced a slight and sustained cytotoxicity at concentrations higher than 1 μM + 0.2 μM (Fig. 7 E), whilst FB1+ BEA produced a dose-dependent effect at concentrations higher than 5 μM + 1 μM (Fig. 7 F). For the latter mixture, FB1 presented an EC_{50} of 8.1 μM (CI: 5.3–12.2 μM) and BEA showed a value of 1.6 μM (CI: 1.1–2.4 μM) (Figure S4 B). ZEA combinations also induced an increase on LDH release comparable to the results obtained in MTT assay, without producing total membrane rupture in any case (Fig. 7G–I).

Then, TMRM assay was carried out with mycotoxin combinations to determine their effect on $\Delta\Psi_m$ (Fig. 8). DON + ENN A mixture significantly affected $\Delta\Psi_m$ at the highest concentration tested (15 μM + 3 μM), producing a decrease of 30.3 ± 5.9% (Fig. 8 A). Otherwise, DON + ENN B altered $\Delta\Psi_m$ from 0.75 μM + 0.15 μM to the highest concentrations used (Fig. 8 B). In the case of DON + BEA mixture, the mitochondrial membrane was depolarized at all the concentrations tested, with percentages between 69.8 and 81.0% with respect to control cells (Fig. 8 C). Regarding FB1 combinations, only the mixture with ENN A and ENN B had effects on $\Delta\Psi_m$ at the highest doses used (Fig. 8 D, E). Finally, ZEA + ENN A decreased $\Delta\Psi_m$ at concentrations over 5 μM ZEA and 2.5 μM ENN A (Fig. 8 G). When ZEA was mixed with ENN B and BEA, $\Delta\Psi_m$ was affected at the highest concentrations assayed, reaching levels of 60.6 ± 8.8% and 64.7 ± 9.8% at 30 μM + 15 μM (Fig. 8 H, I). As previously described in individual mycotoxin treatments, 1 μM Rot was used to validate the assay. At this concentration, Rot depolarized mitochondrial membrane, with percentages between 72.0 and 84.7% with respect to control cells.

3.3. Analysis of mycotoxin content and cytotoxicity of a contaminated cow feed sample and two milk extracts

Since mycotoxin co-occurrence is frequent in animal-derived products, two different matrixes were tested in order to analyse the toxicity of real concentrations. A cow feed contaminated extract, as well as two contaminated commercial milk extracts were analysed in SH-SY5Y cells. Firstly, mycotoxin content was determined. In brief, the samples were extracted by using a QuEChERS (quick, easy, cheap, effective, rugged and safe) extraction procedure and analysed by ultra-high liquid chromatography tandem mass spectrometry (UHPLC-MS/MS). In the cow feed extract, it was found the presence of several mycotoxins (Fig. 9), which were quantified using linear 1/X calibration curves, results were corrected for the recovery and the matrix effect. In this sense, the sample contained 118.3 μg/kg of DON, 145.7 μg/kg of FB1, 103.2 μg/kg of FB2, 72.8 μg/kg of ZEA, 17.0 μg/kg of ENN A, 25.0 μg/kg of ENN A1, 134.1 μg/kg of ENN B, 74.1 μg/kg of ENN B1 and 76.3 μg/kg of BEA.

On the other hand, several mycotoxins were also found in milk samples (Fig. 10). They were quantified using linear 1/X calibration curves too. The milk extract **1** contained 0.37 μg/kg of ENN A, 0.42 μg/kg of ENN A1, 0.15 μg/kg of ENN B and 0.94 μg/kg of BEA, while the milk extract **2** contained 0.36 μg/kg of ENN A, 0.40 μg/kg of ENN A1, 0.14 μg/kg of ENN B, 0.30 μg/kg of ENN B1 and 0.52 μg/kg of BEA.

Then, cow feed and milk extracts were tested in human neuroblastoma cells. The cow feed extract was concentrated 20 times and its effects on cell viability and cytotoxicity were determined with MTT and LDH, respectively. Cells were treated with the concentrated extract at dilutions between 1:500 and 1:10000 for 24 h. In MTT assay, the highest concentrations used (1:500 and 1:1000) induced a significant cell damage, with levels of 39.1 ± 3.9% and 81.1 ± 1.9% with respect to control cells (Fig. 11 A). LDH release was increased in more than a 50% at the highest concentration used (Fig. 11 B), which agrees with the results obtained in MTT test.

Then, to validate if the results obtained with the extract could be compared to commercial mycotoxin standard mixture, the highest concentration of the extract (1:500) was chosen to calculate mycotoxin concentrations. SH-SY5Y human neuroblastoma cells were treated with the combination of 4.0 nM DON, 2.0 nM FB1, 2.3 nM ZEA, 0.25 nM ENN A, 2.0 nM ENN B and 0.97 nM BEA for 24 h. Also, single mycotoxin treatments at the calculated concentrations were added as control. No significant differences were observed in both MTT and LDH assays (Fig. 11C and D). Mycotoxins were also tested at higher concentrations, in order to assess their combined effect at doses included in the range of our previous assays. Therefore, the concentrations found in the extract

USC UNIVERSIDADE DE SANTIAGO DE COMPOSTELA

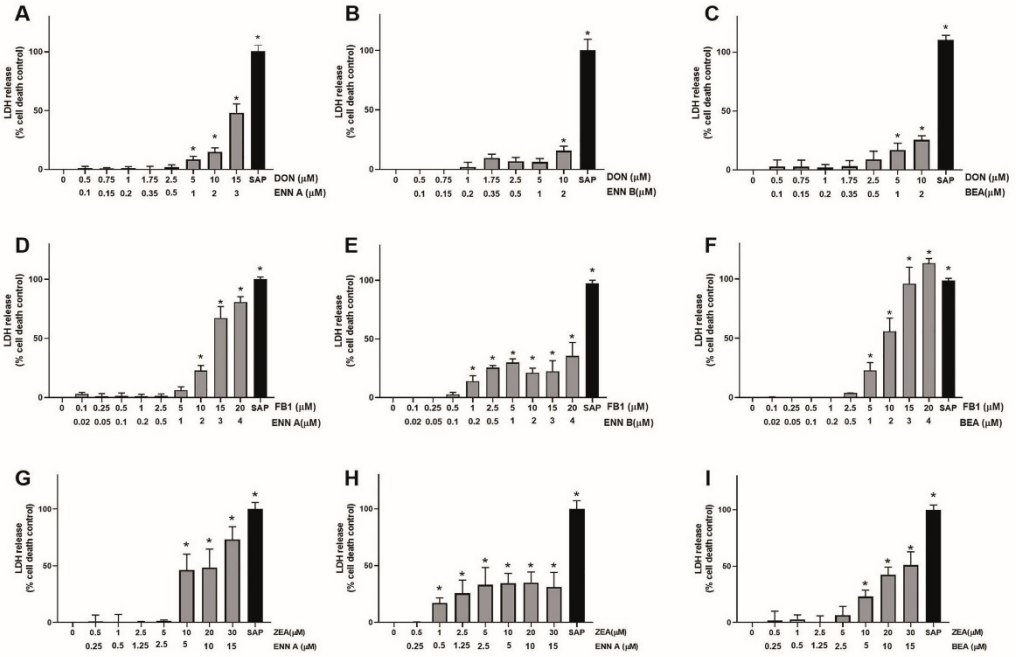


Fig. 7. Effect of regulated and emerging mycotoxin combinations in SH-SY5Y cells. Cells were treated with binary mycotoxin combinations. (A) DON + ENN A (5:1), (B) DON + ENN B (5:1), (C) DON + BEA (5:1), (D) FB1 + ENN A (5:1), (E) FB1 + ENN B (5:1), (F) FB1 + BEA (5:1), (G) ZEA + ENN A (2:1), (H) ZEA + ENN B (2:1), (I) ZEA + BEA (2:1). SAP (saponin) was used as cell death control. Data are mean ± SEM of three independent experiments, expressed as percentage of cell death control cells. Statistical differences determined by Student's *t*-test. *p ≤ 0.05.

were increased 1000 times, keeping the mycotoxin ratio present in the contaminated sample (Fig. 11E and F). In this case, 4.0 μM DON and 2.0 μM ENN B presented the most remarkable effects, decreasing cell viability by 81.9 ± 0.89% and 67.8 ± 6.0%, respectively. BEA at 0.97 μM also produced a slight decrease on the cell activity (11.9 ± 4.9%). Finally, when the mixture of all mycotoxins was added, cell viability was reduced to a percentage of 11.1 ± 1.5% of control cells (Fig. 11 E). However, when LDH assay was performed, the mix of all mycotoxins only increased LDH release by 13.7 ± 0.5%, a rise that seems to be mediated by the effect of DON, ENN B and BEA, which elevated LDH leakage by 11.3 ± 3.7%, 32.5 ± 2.6% and 22.2 ± 10.0%, respectively (Fig. 11 F).

Finally, the milk natural contaminated extracts were tested, in the same way as was done with the cow feed sample. Milk samples were chosen because they did not content regulated mycotoxins and had lower concentrations of ENNs and BEA than those present in the cow feed sample. The extracts were concentrated 20 times and its effects on cell viability and cytotoxicity were determined with MTT and LDH, respectively (Fig. 12A and B). Cells were treated with the concentrated extract at dilutions between 1:500 and 1:10000 for 24 h. With milk extract **1**, no differences were observed with respect to control cells neither on MTT nor LDH assays. However, with milk extract **2**, a reduction on cell viability of 14.0 ± 6.8% was observed at the highest concentration used (1:500), although no significant differences in LDH release were detected. It should be notes that the main difference between these two samples is the presence of ENN B1 in the extract **2**.

4. Discussion

Mycotoxin contamination is a global problem, the Food and Agriculture Organization of the United Nations estimates that approximately 25% of the cereals produced in the world are contaminated by mycotoxins (Janik et al., 2020). Contaminated food consumption supposes an important risk to human health, as mycotoxins are known to produce illnesses such as cancer, kidney pathologies and neurological diseases (Marin et al., 2013). In this sense, several *in vitro* and *in vivo* studies have demonstrated that mycotoxins can cross the BBB due to their physical properties, targeting the brain (Bonnet et al., 2012; Osuchowski et al., 2005b; Taevernier et al., 2016). In this study, a human neuroblastoma cell line, SH-SY5Y cells, was chosen in an attempt to understand how mycotoxin neurotoxicity occurs, with an especial focus on emerging mycotoxins because data about their neurotoxic effect are scarce. In fact, there are not established maximum legal limits for these toxins in food and feed due to the lack of information about their toxicity (EFSA, 2014).

Firstly, the individual effects of regulated and emerging toxins on cell survival and mitochondrial function were analysed. Regarding regulated mycotoxins, DON produced the greatest cell damage, with an IC_{50} of 0.94 μM. ZEA presented an IC_{50} value almost 20-fold greater (17.4 μM), whilst FB1 did not display toxic effects in this cell line up to 10 μM. However, when membrane leakage and cell death type were analysed, DON and ZEA did not show harmful effects on human neuroblastoma cells. Considering that MTT is metabolised by mitochondria and is a more sensitive assay than LDH (Fotakis and Timbrell, 2006), these results could indicate that mitochondria is being affected by DON and ZEA, but plasmatic membrane integrity is not compromised at the

USC UNIVERSIDADE DE SANTIAGO DE COMPOSTELA

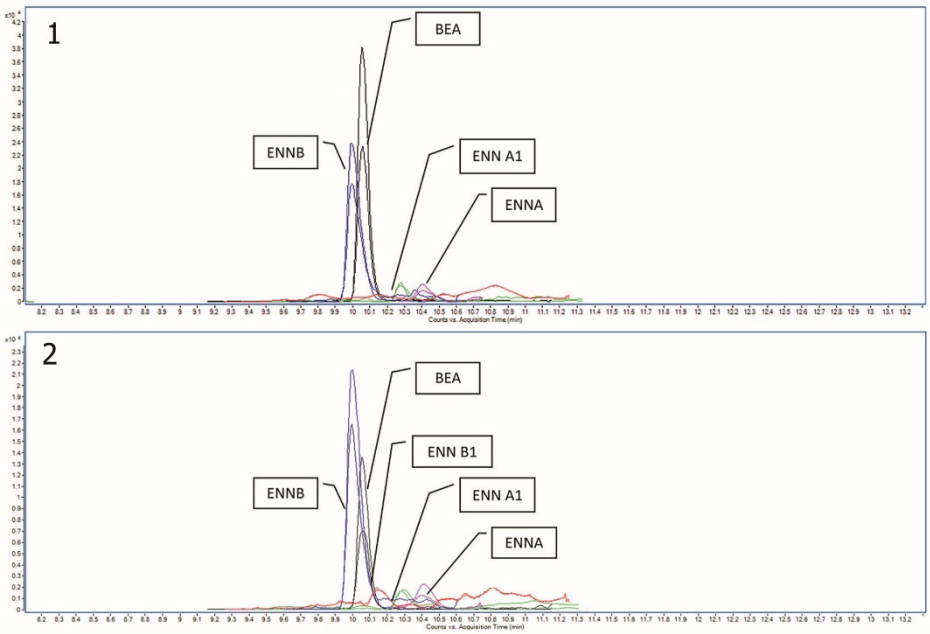


Fig. 10. UHPLC-MS/MS chromatogram of the milk extracts. Compounds were identified by using the *m/z* of the parent compound and two product ions.

permeability transition pore opening in human carcinoma cells (Bensassi et al., 2012). However, apoptosis cannot be confirmed in our report, because a lower dose (0.94 μM) and a different cell type were used in flow cytometry assay. Nevertheless, a decrease in $\Delta\Psi_m$ was observed at concentrations between 1 and 10 μM after 24 h of incubation, indicating that mitochondria were being affected by this toxin. This effect could be related to the mitochondrial permeability transition pore, whose opening can be reversible. Only if this opening is massive and sustained, it leads to apoptotic cell death (Panel et al., 2018), so the effect observed with DON in TMRM assay could be related to a transient mitochondrial permeability transition pore opening, which is not leading to apoptosis.

In the case of FB1, our results indicate that this toxin does not affect to cell viability and mitochondrial function of SH-SY5Y cells, agreeing with previous works (Osuchowski and Sharma, 2005). FB1 is considered neurotoxic due to their involvement in equine leukoencephalomalacia because it induces demyelination and sphinganine elevation. However, there is no evidence of FB1 cytotoxicity in neuronal lines, which could be related to the absence of myelin in cultured cells (Osuchowski and Sharma, 2005). Moreover, it has been hypothesized that its neurotoxic effect could be due to its ability to activate glial cells (Osuchowski et al., 2005a). Regarding ZEA, our results are similar to the data presented by Venkataramana et al. (2014) in SH-SY5Y cells, which reported that this toxin diminished cell viability at concentrations lower than 25 μM. Moreover, the results presented in our work confirm that ZEA cytotoxicity is mediated by mitochondrial dysfunction, since mitochondrial membrane is depolarized at the highest concentrations.

Emerging mycotoxins caused a significant alteration in mitochondrial function, depolarizing the mitochondrial membrane, and being cytotoxic to SH-SY5Y cells through the induction of apoptotic cell death. ENN A, ENN B and BEA presented IC_{50} values of 2.2, 0.43 and 1.7 μM in cell viability, respectively. It is noteworthy the effect produced by ENN B at 6 h, because the mycotoxin induced a sudden decrease in cell viability at 0.5 μM that was sustained until 10 μM, without observing a dose-dependent effect. This response has been previously reported in Caco-2 cells and murine macrophages treated with ENN B (Gammelsrud et al., 2012; Ivanova et al., 2012). In fact, although ENN B presented the lowest IC_{50} in MTT assay, when membrane leakage was assessed by LDH assay, only ENN A and BEA showed a dose-dependent response. ENN B produced again an almost constant response, with an increase on LDH release about 30%. This sustained effect could be related to the binding of ENN B to a specific receptor, which would show a high sensitivity and specificity for the toxin at low concentrations. There are not studies about potential receptors of ENN B in mammalian cells, although it is known that the toxin inhibits the yeast multidrug resistance pump Pdr5p (Hashizume and Nishimura, 2008).

Non-regulated mycotoxins also produced mitochondrial depolarization, which could be related to their ionophoric properties. ENNs and BEA are cyclic peptides which affect biological membranes by forming complexes with metals like K^+, Na^+ and Ca^{+2}, allowing ion transport through the membranes. Thus, mitochondrial membrane is an important target of these emerging mycotoxins (Bertero et al., 2020; Tonshin et al., 2010). In this sense, neuronal cells are very susceptible to mitochondrial malfunction due to their great energy consumption, so a slight decrease on mitochondrial potential could have a great impact on neuronal function (Yin et al., 2014). It should be noted the total inhibition of cell viability produced by ENN A and BEA at the highest doses tested, which could be associated to their effects over mitochondria, as was confirmed when $\Delta\Psi_m$ was analysed. In this assay, the effect produced by ENNs and BEA differs. ENNs affected to $\Delta\Psi_m$ at all the concentrations tested, while BEA depolarized the mitochondria in a dose-dependent manner. These dissimilarities could be due to their differences in ionophoric properties because ENNs mainly modify K^+ channels, while BEA mostly affects to Ca^{+2}channels (Tonshin et al., 2010). Finally, when the type of cell death was analysed, it was found that ENN A, ENN B and BEA were producing apoptotic cell death in SH-SY5Y human neuroblastoma cells. These

USC UNIVERSIDADE DE SANTIAGO DE COMPOSTELA

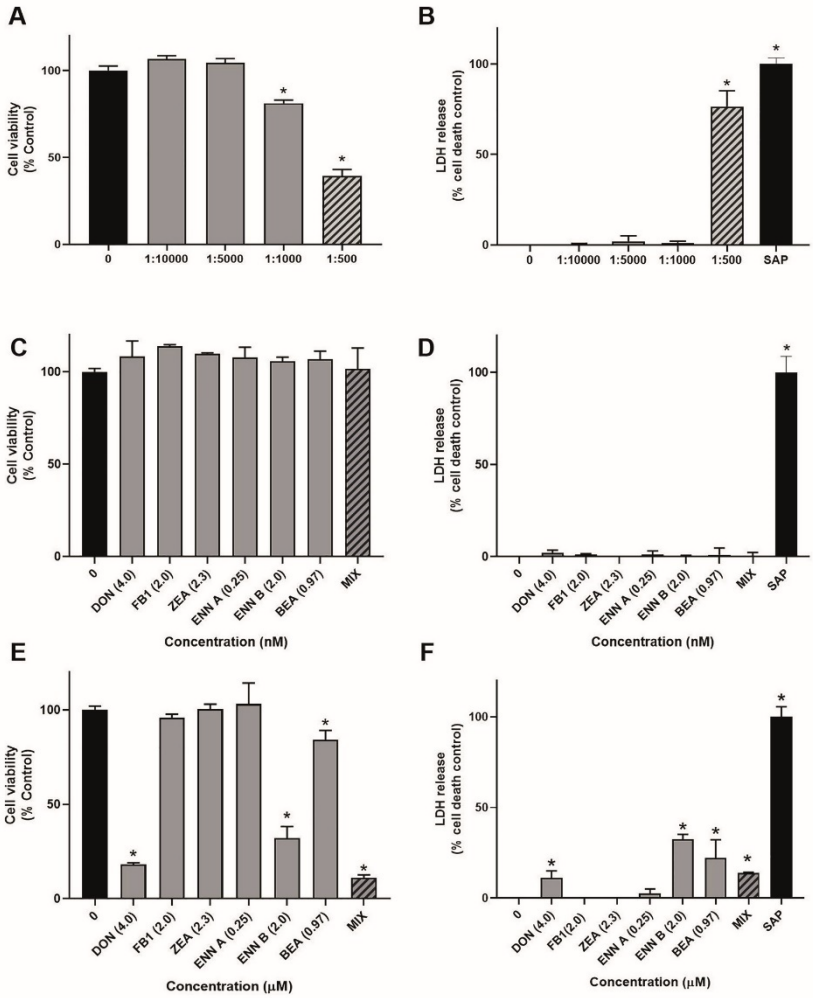


Fig. 11. Analysis of a cow feed contaminated extract and its equivalent mycotoxin standard mixture on cell viability and cytotoxicity of SH-SY5Y cells. Human neuroblastoma cells were treated for 24 h and MTT and LDH tests were carried out. (A) Effect on cell viability of a concentrated cow feed extract at dilutions between 1:500–1:10000. (B) Cytotoxicity, assessed by LDH assay, of SH-SY5Y cells treated with the concentrated extract. (C) Cell viability of cells treated with commercial mycotoxins, alone and in mixture, at the concentrations found in the 1:500 dilution of cow feed extract. (D) Effects of the standard mycotoxin mixture on cytotoxicity of neuroblastoma cells. (E) Cell viability of cells treated with commercial mycotoxins at concentrations 1000 times higher than those found in the 1:500 extract. (F) Cytotoxicity of SH-SY5Y cells treated with mycotoxins at doses 1000 times higher than those found in the cow feed extract. SAP (saponin) was used as cell death control. Mean ± SEM of three independent experiments. Cell viability aata are expressed as percentage of untreated control cells, whilst LDH test results are presented as percentage of cell death control cells- Statistical differences were determined by Student's *t*-test. *$p \leq 0.05$.

results agree with previous studies, which have reported these emerging mycotoxins to produce apoptosis through the mitochondrial pathway in other cell lines (Manyes et al., 2018; Prosperini et al., 2013). To our knowledge, this is the first report of ENN A and ENN B pro-apoptotic effects in neuronal cells.

With regard to BEA, its cytotoxicity has been recently reported in SH-SY5Y cells (Agahi et al., 2020a, 2020b; Juan et al., 2020; Montesano et al., 2020). These authors reported IC_{50} values among 2.5–3.2 µM, in the range of the data obtained in our study. The same authors described an increase in the expression of the apoptotic gene *Bcl-2* after treatment with BEA, which agrees with our results (Agahi et al., 2020b).

In summary, the analysis of individual mycotoxins revealed that ENN B was the most damaging molecule, followed by DON, BEA, ENN A, ZEA and FB1, which did not affect to SH-SY5Y cells. With the exception of DON, our results suggest that emerging mycotoxins produce a greater mitochondrial impairment and neurotoxicity than the regulated ones and could suppose a health hazard. In this sense, EFSA experts stress that chronic exposure to emerging mycotoxins could pose a public health problem, in fact, repeated oral exposure to ENN B and BEA produced genotoxic effects in mice (Maranghi et al., 2018).

USC UNIVERSIDADE DE SANTIAGO DE COMPOSTELA

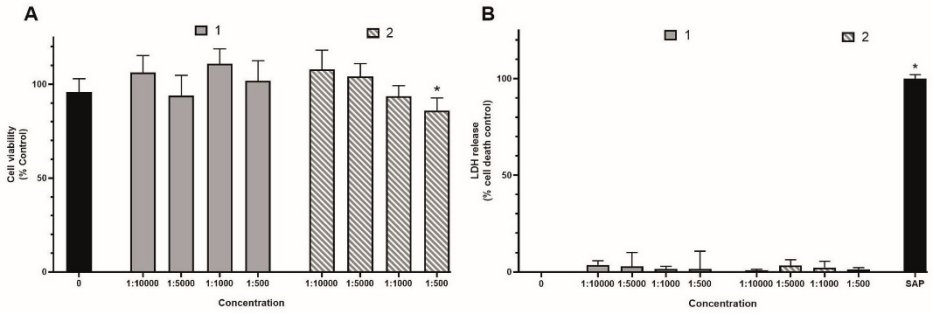


Fig. 12. Analysis of milk contaminated extracts effect on cell viability and cytotoxicity of SH-SY5Y cells. Human neuroblastoma cells were treated for 24 h and MTT and LDH tests were carried out. (A) Effect on cell viability of concentrated milk extracts at dilutions between 1:500–1:10000. (B) Cytotoxicity, assessed by LDH assay, of SH-SY5Y cells treated with the concentrated extracts. SAP (saponin) was used as cell death control. Mean ± SEM of three independent experiments. Data expressed as percentage of untreated control cells. Cell viability aata are expressed as percentage of untreated control cells, whilst LDH test results are presented as percentage of cell death control cells- Statistical differences were determined by Student's *t*-test. *p ≤ 0.05.

European multi-mycotoxin contamination studies indicate that 75–100% of animal feed samples contain more than one mycotoxin (Streit et al., 2012). Moreover, human bio-monitoring studies have found that 100% of human urine samples contained biomarkers of 2 or more mycotoxins, and up to 5 mycotoxins were detected in a severe case of co-exposure (Alassane-Kpembi et al., 2017). In this context, the effects of binary combinations of regulated and non-regulated mycotoxins were analysed. Antagonistic effects were found for the binary mixtures between DON, ZEA and emerging mycotoxins. Regarding FB1, although the combination index could not be calculated, the effects its mixture with emerging mycotoxins are almost the same observed with non-regulated toxins alone, suggesting an additive effect. Our results coincide with previous data in other cell types, in which antagonism was found. This is the case of DON and ENN B combination in intestinal cells (Fernández-Blanco et al., 2016; Vejdovszky et al., 2016), or BEA and DON mixture in CHO–K1 cells (EFSA, 2014).

Finally, contaminated cow feed and milk extracts were tested in our *in vitro* model. All the extracts tested were analysed by methods previously in-house validated for the quantification of regulated, emerging and modified mycotoxins. The sensitivity of the methods is high, allowing the detection of compounds at concentrations lower than the maximum residue levels established in European regulations. In addition, the accuracy and precision are good enough to fulfil the performance characteristics established in the legislation (Commission Regulation (EC) No 401/2006). In the cow feed extract, it was detected the presence of regulated and emerging mycotoxins, although in concentrations lower than the maximum levels recommended in the UE for animal feed (Commission Recommendation 2006/576/EC). It can be highlighted the presence of the emerging BEA and ENNs, which were found in low amounts. The extract decreased cell viability and generated cytotoxicity in SH-SY5Y cells, despite the fact that the regulated mycotoxins present are below the established maximum limits. When the commercial standard equivalent mixture was tested, no effects were found in cell viability. Only when commercial standards were mixed at concentrations 1000-fold higher than those found on the extract, similar results on cell viability were obtained. This may be due to the presence of other mycotoxins in the sample which could be enhancing the effect of the mycotoxins selected for this study. As ENN A1, ENN B1 and FB2 were also detected in the contaminated extract, the difference could be linked to the presence of these mycotoxins. Since the toxicity produced by the cow feed sample could be due to the presence of ENN A1 and ENN B1, two milk samples naturally contaminated with ENNs and BEA, in much lower concentrations than those found in cow feed, were tested. Both milk samples contained similar amounts of mycotoxins, being the main difference between them the presence of ENN B1 in extract **2**. This sample reduced SH-SY5Y cells viability at the highest dilution tested, whilst extract **1** did not show any significant effect on this cell line. These results indicate that ENN B1 possibly exhibits neuronal cytotoxicity and could be potentiating the effect of other mycotoxins on this cell line. In fact, ENNs combination is known to produce a greater damage than the toxins separately (EFSA, 2014), and ENN A1 and ENN B1 have displayed higher toxicity than ENN A and ENN B in several cell types (Ivanova et al., 2006; Khoshal et al., 2019; Krug et al., 2018; Prosperini et al., 2013). On the other hand, FB2 has synergistic effects with FB1 in human cells (Yu et al., 2020). Moreover, the decrease on cell viability at such low toxin concentrations suggests that matrix is influencing mycotoxin cytotoxicity. Particularly, the milk extract presented a greater reduction on cell viability than expected, indicating that the lipophilic properties of emerging mycotoxins could be related to this damaging effect. In view of these results and due to their prevalence on natural samples, it would be interesting to study the individual and combined effects of ENN A1 and B1 in this cell line in future studies. Moreover, the analysis of different contaminated matrixes such as cheese or beef would help to better understand if the presence of emerging mycotoxins in food could be considered a public health hazard, as is being suggested by our results.

In conclusion, our results denote that emerging mycotoxins and DON produce mitochondrial-mediated cytotoxicity in human neuroblastoma cells, indicating that non-regulated mycotoxins could pose a health hazard. Binary combinations of regulated and emerging mycotoxins resulted in antagonistic effects, but when they co-occur on natural matrixes, a greater damaging effect than expected is observed. In view of these results, it would be of particular interest to further study the neurotoxic mechanism of action of emerging mycotoxins and to compare their effects on different natural matrixes, which will help to better understand their impact on human health and, consequently, to decide if maximum legal limits in food should be established.

Disclosure statement

The authors have no conflicts of interest to declare.

CRediT authorship contribution statement

Nadia Pérez-Fuentes: Investigation, Writing – original draft, Writing – review & editing. **Rebeca Alvariño:** Conceptualization, Methodology, Writing – review & editing. **Amparo Alfonso:** Conceptualization, Methodology, Writing – review & editing. **Jesús González-**

USC UNIVERSIDADE DE SANTIAGO DE COMPOSTELA

Jartín: Investigation. **Sandra Gegunde:** Investigation. **Mercedes R. Vieytes:** Methodology. **Luis M. Botana:** Funding acquisition, Supervision.

Declaration of competing interest

The authors declare that they have no known competing financial interests or personal relationships that could have appeared to influence the work reported in this paper.

Acknowledgments

The research leading to these results has received funding from the following FEDER cofunded-grants. From Consellería de Cultura, Educación e Ordenación Universitaria, Xunta de Galicia, 2017 GRC GI-1682 (ED431C 2017/01). From Ministerio de Ciencia e Innovación IISCIII/PI19/001248. From European Union Interreg AlertoxNet EAPA-317-2016, Interreg Agritox EAPA-998-2018, and H2020 778069-EMERTOX. Sandra Gegunde was supported by a fellowship from FIDIS, Spain.

Appendix A. Supplementary data

Supplementary data to this article can be found online at https://doi.org/10.1016/j.fct.2021.112308.

References

Agahi, F., Font, G., Juan, C., Juan García, A., 2020a. Individual and combined effect of zearalenone derivates and beauvericin mycotoxins on SH-SY5Y cells. Toxins 12.
Agahi, F., Álvarez Ortega, N., Font, G., Juan García, A., Juan, C., 2020b. Oxidative stress, glutathione, and gene expression as key indicators in SH-SY5Y cells exposed to zearalenone metabolites and beauvericin. Toxicol. Lett. 334, 44–52.
Alassane-Kpembi, I., Schatzmayr, G., Taranu, I., Marin, D., Puel, O., Oswald, I.P., 2017. Mycotoxins co-contamination: methodological aspects and biological relevance of combined toxicity studies. Crit. Rev. Food Sci. Nutr. 57, 3489–3507.
Alvariño, R., Alonso, E., Bornancin, L., Bonnard, I., Inguimbert, N., Banaigs, B., Botana, L.M., 2020. Biological activities of cyclic and acyclic B type laxaphycins in SH-SY5Y human neuroblastoma cells. Mar. Drugs 18.
Alvariño, R., Alonso, E., Tribalat, M.A., Gegunde, S., Thomas, O.P., Botana, L.M., 2017. Evaluation of the protective effects of sarains on H(2)O(2)-induced mitochondrial dysfunction and oxidative stress in SH-SY5Y neuroblastoma cells. Neurotox. Res. 32, 368–380.
Arroyo-Manzanares, N., Rodríguez-Estévez, V., Arenas-Fernández, P., García-Campaña, A.M., Gámiz-Gracia, L., 2019. Occurrence of mycotoxins in swine feeding from Spain. Toxins 11.
Bensassi, F., Gallerne, C., Sharaf El Dein, O., Lemaire, C., Hajlaoui, M.R., Bacha, H., 2012. Involvement of mitochondria-mediated apoptosis in deoxynivalenol cytotoxicity. Food Chem. Toxicol. 50, 1680–1689.
Bertero, A., Fossati, P., Tedesco, D.E.A., Caloni, F., 2020. Beauvericin and enniatins: in vitro intestinal effects. Toxins 12.
Bonnet, M.S., Roux, J., Mounien, L., Dallaporta, M., Troadec, J.D., 2012. Advances in deoxynivalenol toxicity mechanisms: the brain as a target. Toxins 4, 1120–1138.
Bornancin, L., Alonso, E., Alvariño, R., Inguimbert, N., Bonnard, I., Botana, L.M., Banaigs, B., 2019. Structure and biological evaluation of new cyclic and acyclic laxaphycin-A type peptides. Bioorg. Med. Chem. 27, 1966–1980.
Chou, T.C., 2010. Drug combination studies and their synergy quantification using the Chou-Talalay method. Canc. Res. 70, 440–446.
Dagnac, T., Latorre, A., Fernández Lorenzo, B., Llompart, M., 2016. Validation and application of a liquid chromatography-tandem mass spectrometry based method for the assessment of the co-occurrence of mycotoxins in maize silages from dairy farms in NW Spain. Food Addit. Contam. 33, 1850–1863.
Domijan, A.M., 2012. Fumonisin B(1): a neurotoxic mycotoxin. Arh. Hig. Rada. Toksikol. 63, 531–544.
EFSA, 2012. Scientific Opinion on the risks for animal and public health related to the presence of phomopsins in feed and food. EFSA J. 10, 2567.
EFSA, 2013. Scientific Opinion on the risk for public and animal health related to the presence of sterigmatocystin in food and feed. EFSA J. 11, 3254.
EFSA, 2014. Scientific Opinion on the risks to human and animal health related to the presence of beauvericin and enniatins in food and feed. EFSA J. 12, 3802.
Fernández-Blanco, C., Font, G., Ruiz, M.J., 2016. Interaction effects of enniatin B, deoxinivalenol and alternariol in Caco-2 cells. Toxicol. Lett. 241, 38–48.
Fotakis, G., Timbrell, J.A., 2006. In vitro cytotoxicity assays: comparison of LDH, neutral red, MTT and protein assay in hepatoma cell lines following exposure to cadmium chloride. Toxicol. Lett. 160, 171–177.
Gammelsrud, A., Solhaug, A., Dendelé, B., Sandberg, W.J., Ivanova, L., Kocbach Bølling, A., Lagadic-Gossmann, D., Refsnes, M., Becher, R., Eriksen, G., Holme, J.A., 2012. Enniatin B-induced cell death and inflammatory responses in RAW 267.4 murine macrophages. Toxicol. Appl. Pharmacol. 261, 74–87.
González Jartín, J.M., Alfonso, A., Sainz, M.J., Vieytes, M.R., Botana, L.M., 2020. Multi detection Method for Mycotoxins with a Modified QuEChERS Extraction in Feed and Development of a Simple Detoxification Procedure. Animal Feed Science and Technology, p. 114745.
González-Jartín, J.M., Rodríguez-Cañás, I., Alfonso, A., Sainz, M.J., Vieytes, M.R., Gomes, A., Ramos, I., Botana, L.M., 2021. Multianalyte method for the determination of regulated, emerging and modified mycotoxins in milk: QuEChERS extraction followed by UHPLC-MS/MS analysis. Food Chem. 356, 129647.
Hashizume, H., Nishimura, Y., 2008. Cyclic lipopeptide antibiotics. Stud. Nat. Prod. Chem. 35, 693–751.
Huang, D., Cui, L., Dai, M., Wang, X., Wu, Q., Hussain, H.I., Yuan, Z., 2019. Mitochondrion: a new molecular target and potential treatment strategies against trichothecenes. Trends Food Sci. Technol. 88, 33–45.
Ivanova, L., Egge-Jacobsen, W.M., Solhaug, A., Thoen, E., Fæste, C.K., 2012. Lysosomes as a possible target of enniatin B-induced toxicity in Caco-2 cells. Chem. Res. Toxicol. 25, 1662–1674.
Ivanova, L., Skjerve, E., Eriksen, G.S., Uhlig, S., 2006. Cytotoxicity of enniatins A, A1, B, B1, B2 and B3 from Fusarium avenaceum. Toxicon 47, 868–876.
Janik, E., Niemcewicz, M., Ceremuga, M., Stela, M., Saluk-Bijak, J., Siadkowski, A., Bijak, M., 2020. Molecular aspects of mycotoxins-A serious problem for human health. Int. J. Mol. Sci. 21.
Jia, R., Liu, W., Zhao, L., Cao, L., Shen, Z., 2020. Low doses of individual and combined deoxynivalenol and zearalenone in naturally moldy diets impair intestinal functions via inducing inflammation and disrupting epithelial barrier in the intestine of piglets. Toxicol. Lett. 333, 159–169.
Juan, C., de Simone, G., Sagratini, G., Caprioli, G., Mañes, J., Juan-García, A., 2020. Reducing the effect of beauvericin on neuroblastoma SH-SY5Y cell line by natural products. Toxicon 188, 164–171.
Juan-García, A., Carbone, S., Ben-Mahmoud, M., Sagratini, G., Mañes, J., 2020. Beauvericin and ochratoxin A mycotoxins individually and combined in HepG2 cells alter lipid peroxidation, levels of reactive oxygen species and glutathione. Food Chem. Toxicol. 139, 111247.
Khan, R.B., Phulukdaree, A., Chuturgoon, A.A., 2018. Fumonisin B(1) induces oxidative stress in oesophageal (SNO) cancer cells. Toxicon 141, 104–111.
Khoshal, A.K., Novak, B., Martin, P.G.P., Jenkins, T., Neves, M., Schatzmayr, G., Oswald, I.P., Pinton, P., 2019. Co occurrence of DON and emerging mycotoxins in worldwide finished pig feed and their combined toxicity in intestinal cells. Toxins 11.
Krug, I., Behrens, M., Esselen, M., Humpf, H.U., 2018. Transport of enniatin B and enniatin B1 across the blood-brain barrier and hints for neurotoxic effects in cerebral cells. PloS One 13, e0197406.
Manyes, L., Escrivá, L., Ruiz, M.J., Juan-García, A., 2018. Beauvericin and enniatin B effects on a human lymphoblastoid Jurkat T-cell model. Food Chem. Toxicol. 115, 127–135.
Maranghi, F., Tassinari, R., Narciso, L., Tait, S., Rocca, C.L., Felice, G.D., Butteroni, C., Corinti, S., Barletta, B., Cordelli, E., 2018. In vivo toxicity and genotoxicity of beauvericin and enniatins. Combined approach to study in vivo toxicity and genotoxicity of mycotoxins beauvericin (BEA) and enniatin B (ENNB). EFSA Support. Publ. 15, 1406E.
Marin, S., Ramos, A.J., Cano-Sancho, G., Sanchis, V., 2013. Mycotoxins: occurrence, toxicology, and exposure assessment. Food Chem. Toxicol. 60, 218–237.
Montesano, D., Juan-García, A., Mañes, J., Juan, C., 2020. Chemoprotective effect of carotenoids from Lycium barbarum L. on SH-SY5Y neuroblastoma cells treated with beauvericin. Food Chem. Toxicol. 141, 111414.
Osuchowski, M.F., Edwards, G.L., Sharma, R.P., 2005a. Fumonisin B1-induced neurodegeneration in mice after intracerebroventricular infusion is concurrent with disruption of sphingolipid metabolism and activation of proinflammatory signaling. Neurotoxicology 26, 211–221.
Osuchowski, M.F., He, Q., Sharma, R.P., 2005b. Endotoxin exposure alters brain and liver effects of fumonisin B1 in BALB/c mice: implication of blood brain barrier. Food Chem. Toxicol. 43, 1389–1397.
Osuchowski, M.F., Sharma, R.P., 2005. Fumonisin B1 induces necrotic cell death in BV-2 cells and murine cultured astrocytes and is antiproliferative in BV 2 cells while N2A cells and primary cortical neurons are resistant. Neurotoxicology 26, 981–992.
Panel, M., Ghaleb, B., Morin, D., 2018. Mitochondria and aging: a role for the mitochondrial transition pore? Aging Cell 17, e12793.
Prosperini, A., Berrada, H., Ruiz, M.J., Caloni, F., Coccini, T., Spicer, L.J., Perego, M.C., Lafranconi, A., 2017. A review of the mycotoxin enniatin B. Front Public Health 5, 304.
Prosperini, A., Juan-García, A., Font, G., Ruiz, M.J., 2013. Reactive oxygen species involvement in apoptosis and mitochondrial damage in Caco-2 cells induced by enniatins A, A1, B and B1. Toxicol. Lett. 222, 36–44.
Sainz, M.J., González-Jartín, J.M., Aguín, O., Mansilla, J.P., Botana, L.M., 2018. 8. Isolation, Characterization, and Identification of Mycotoxin-Producing Fungi. De Gruyter, Berlin, Boston, pp. 202–245.
Streit, E., Schatzmayr, G., Tassis, P., Tzika, E., Marin, D., Taranu, I., Tabuc, C., Nicolau, A., Aprodu, I., Puel, O., Oswald, I.P., 2012. Current situation of mycotoxin contamination and co-occurrence in animal feed-focus on Europe. Toxins 4, 788–809.
Taevernier, L., Bracke, N., Veryser, L., Wynendaele, E., Gevaert, B., Peremans, K., De Spiegeleer, B., 2016. Blood brain barrier transport kinetics of the cyclic depsipeptide mycotoxins beauvericin and enniatins. Toxicol. Lett. 258, 175–184.
Tatay, E., Espín, S., García-Fernández, A.J., Ruiz, M.J., 2017. Oxidative damage and disturbance of antioxidant capacity by zearalenone and its metabolites in human cells. Toxicol. Vitro 45, 334–339.

USC UNIVERSIDADE DE SANTIAGO DE COMPOSTELA

Tonshin, A.A., Teplova, V.V., Andersson, M.A., Salkinoja Salonen, M.S., 2010. The Fusarium mycotoxins enniatins and beauvericin cause mitochondrial dysfunction by affecting the mitochondrial volume regulation, oxidative phosphorylation and ion homeostasis. Toxicology 276, 49–57.
Vejdovszky, K., Warth, B., Sulyok, M., Marko, D., 2016. Non-synergistic cytotoxic effects of Fusarium and Alternaria toxin combinations in Caco-2 cells. Toxicol. Lett. 241, 1–8.
Venkataramana, M., Chandra Nayaka, S., Anand, T., Rajesh, R., Aiyaz, M., Divakara, S.T., Murali, H.S., Prakash, H.S., Lakshmana Rao, P.V., 2014. Zearalenone induced toxicity in SHSY 5Y cells: the role of oxidative stress evidenced by N acetyl cysteine. Food Chem. Toxicol. 65, 335–342. https://doi.org/10.1016/j.fct.2013.12.042.
Walia, R., Madaan, R., Chaudhary, K., Mehta, B., Bala, R., 2021. Chapter 3 - molecular pathways of apoptotic cell death. In: Sodhi, R.K., Madan, J. (Eds.), Clinical Perspectives and Targeted Therapies in Apoptosis. Academic Press, pp. 79–109.
Yin, F., Boveris, A., Cadenas, E., 2014. Mitochondrial energy metabolism and redox signaling in brain aging and neurodegeneration. Antioxidants Redox Signal. 20, 353–371.
Yu, S., Jia, B., Liu, N., Yu, D., Wu, A., 2020. Evaluation of the individual and combined toxicity of fumonisin mycotoxins in human gastric epithelial cells. Int. J. Mol. Sci. 21.
Zhang, J., You, L., Wu, W., Wang, X., Chrienova, Z., Nepovimova, E., Wu, Q., Kuca, K., 2020. The neurotoxicity of trichothecenes T-2 toxin and deoxynivalenol (DON): current status and future perspectives. Food Chem. Toxicol. 145, 111676.
Zhou, H., Cheang, T., Su, F., Zheng, Y., Chen, S., Feng, J., Pei, Z., Chen, L., 2018. Melatonin inhibits rotenone-induced SH-SY5Y cell death via the downregulation of Dynamin-Related Protein 1 expression. Eur. J. Pharmacol. 819, 58–67.

USC UNIVERSIDADE DE SANTIAGO DE COMPOSTELA

Supporting Information

Single and combined effects of regulated and emerging mycotoxins on viability and mitochondrial function of SH-SY5Y cells

Nadia Pérez-Fuentes, Rebeca Alvariño, Amparo Alfonso Jesús González-Jartín, Sandra Gegunde, Mercedes R. Vieytes, Luis M. Botana

Figures

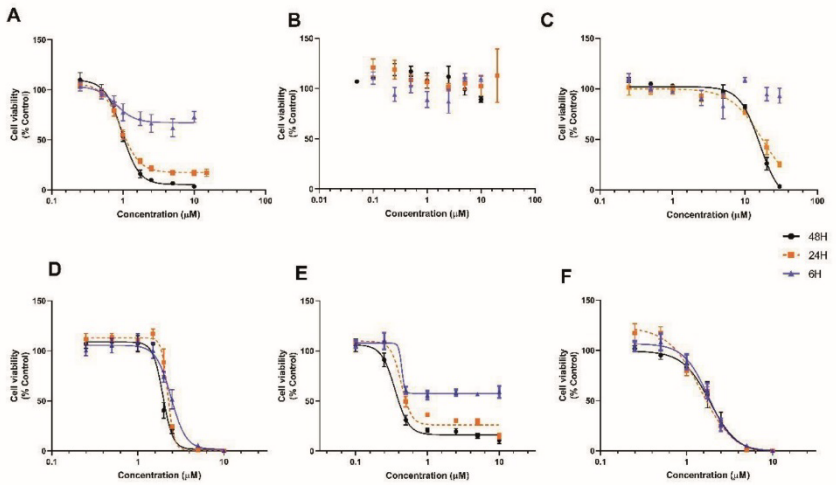


Figure S1. Dose-response curves of the effect of selected mycotoxins on cell viability of SH-SY5Y cells. Cells were incubated with mycotoxins for 6, 24 and 48 h and their effect on cell viability was assessed by MTT test. (A) DON, (B) FB1, (C) ZEA, (D) ENN A, (E) ENN B, (F) BEA. Data are mean ± SEM of three independent replicates expressed as percentage of control cells. IC_{50} values were determined by fitting the data with a log (inhibitor) *vs* response model.

USC UNIVERSIDADE DE SANTIAGO DE COMPOSTELA

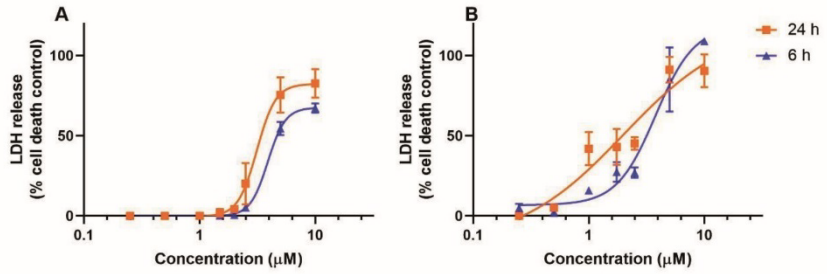


Figure S2. Dose-response curves of the effect of selected mycotoxins on cytotoxicity of SH-SY5Y cells. Cells were incubated with mycotoxins for 6 and 24 h and their effect on cytotoxicity was assessed by LDH test. (A) ENN A, (B) BEA. Data are mean ± SEM of three independent replicates expressed as percentage of cell death control. Data were fitting with a log (agonist) *vs* response model.

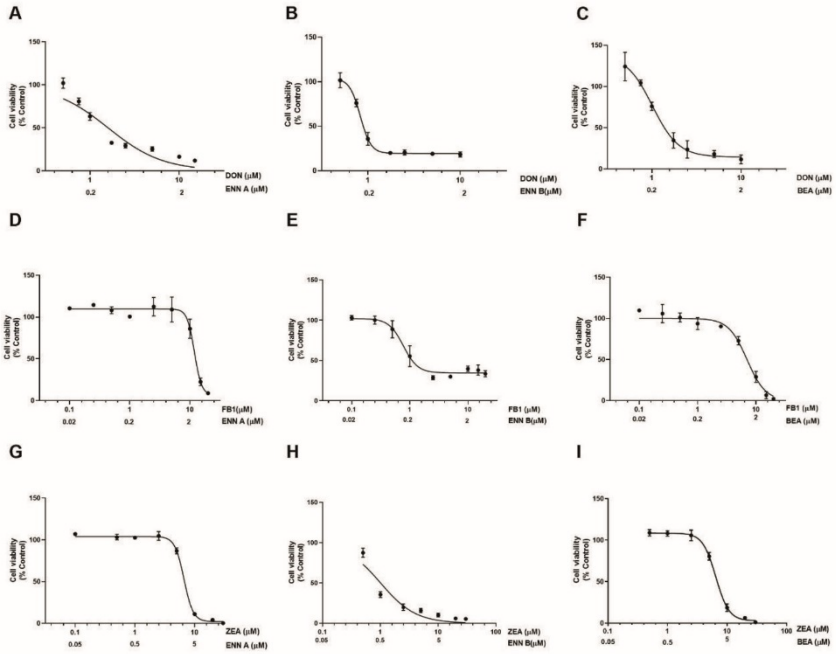


Figure S3. Effect of regulated and emerging mycotoxin binary combinations in cell viability. SH-SY5Y cells were treated with binary mixtures of regulated and non-regulated mycotoxins for 24 h and MTT assay was carried out. (A) DON + ENN A (5:1), (B) DON + ENN B (5:1), (C) DON + BEA (5:1), (D)

USC
UNIVERSIDADE
DE SANTIAGO
DE COMPOSTELA

FB1+ ENN A (5:1), (E) FB1 + ENN B (5:1), (F) FB1+ BEA (5:1), (G) ZEA + ENN A (2:1), (H) ZEA + ENN B (2:1), (I) ZEA + BEA (2:1). Mean ± SEM of three independent replicates performed by triplicate. Data were fitting with a log (inhibitor) *vs* response model.

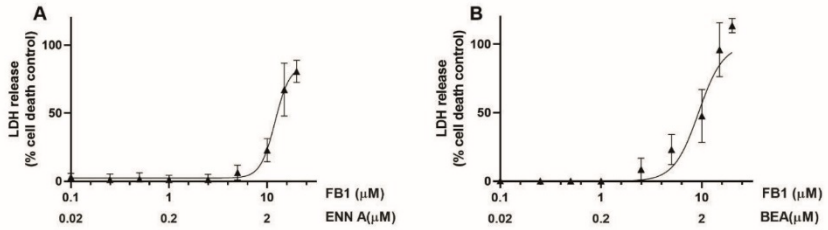


Figure S4. Dose-response curves of the effect of regulated and emerging mycotoxin binary combinations on cytotoxicity of SH-SY5Y cells. Cells were treated with binary mixtures of regulated and non-regulated mycotoxins for 24 h and LDH assay was carried out. (A) FB1+ ENN A (5:1), (B) FB1 + BEA (5:1). Data are mean ± SEM of three independent replicates expressed as percentage of cell death control. IC50 values were determined by fitting the data with a log (agonist) vs response model.

USC
UNIVERSIDADE
DE SANTIAGO
DE COMPOSTELA

USC
UNIVERSIDADE
DE SANTIAGO
DE COMPOSTELA

2. Enniatins A1 and B1 alter calcium homeostasis of neuronal cells leading to apoptotic death

Resumen:

Las eniatinas (ENNs) A1 y B1 son micotoxinas no reguladas producidas por *Fusarium* spp. que se encuentran comúnmente en diferentes tipos de alimentos. Estas toxinas son citotóxicas en varias líneas celulares, pero su mecanismo de acción no está claro. En este estudio, se analizaron los efectos citotóxicos de las ENNs A1 y B1 en células de neuroblastoma humano SH-SY5Y. Además, para comprender mejor su mecanismo de acción, se monitorizó la función mitocondrial, los niveles de especies reactivas de oxígeno (ROS) y los flujos de calcio. Las ENNs A1 y B1 redujeron la viabilidad celular, presentando valores de IC_{50} de 2.0 y 2.7 μM, respectivamente. Ambas toxinas indujeron apoptosis dependiente de caspasa, pero solo la ENN A1 aumentó la producción de ROS. La muerte celular apoptótica parece ser desencadenada por el aumento de calcio citosólico producido por ambas ENNs, ya que las toxinas alteraron la homeostasis del Ca^{2+} al vaciar los reservorios intracelulares. Finalmente, se probaron combinaciones binarias de ENN A1, ENN B1, ENN A y ENN B. Todas las mezclas resultaron en un efecto antagónico, con excepción de la combinación de ENN A y ENN B1, que produjo adición. Los resultados presentados en este estudio proporcionan la primera evidencia de los efectos de las ENNs A1 y B1 sobre los flujos de calcio, proporcionando nuevas perspectivas sobre el mecanismo de acción de estas micotoxinas.

USC
UNIVERSIDADE DE SANTIAGO DE COMPOSTELA

Información revista:

Enniatins A1 and B1 alter calcium homeostasis of neuronal cells leading to apoptotic death

Nadia Pérez-Fuentes[a], Rebeca Alvariño[a], Amparo Alfonso[a], Jesús González-Jartín[a], Sandra Gegunde[a,b], Mercedes R. Vieytes[c], Luis M. Botana[a]

[a] Departamento de Farmacología, Facultad de Veterinaria, Universidad de Santiago de Compostela, Lugo, 27002, Spain
[b] Fundación Instituto de Investigación Sanitario Santiago de Compostela (FIDIS), Hospital Universitario Lucus Augusti, Lugo, 27002, Spain
[c] Departamento de Fisiología, Facultad de Veterinaria, Universidad de Santiago de Compostela, Lugo, 27002, Spain

Revista: Food and Chemical Toxicology
Fecha de publicación: 12 de agosto de 2022
Enlace: https://doi.org/10.1016/j.fct.2022.113361
Editorial: PERGAMON-ELSEVIER SCIENCE LTD, THE BOULEVARD, LANGFORD LANE, KIDLINGTON, OXFORD, ENGLAND, OX5 1GB
ISSN: 0278-6915

Índices de calidad de la revista:
Factor de impacto (2022): 4.3
Factor de impacto 5 años (2022): 5.1
Categoría (2022): "Ciencia y tecnología de los alimentos" Q2 (43/142), "Toxicología" Q1 (20/94)

Contribución doctorando:
N. P-F. llevó a cabo la realización de experimentos, análisis de datos, preparación de figuras, redacción del borrador original, revisión y edición.

Autorización revista:
Contenido reproducido con permiso:



Enniatins A1 and B1 alter calcium homeostasis of neuronal cells leading to apoptotic death

Author:
Nadia Pérez-Fuentes,Rebeca Alvariño,Amparo Alfonso,Jesús González-Jartín,Sandra Gegunde,Mercedes R. Vieytes,Luis M. Botana

Publication: Food and Chemical Toxicology

Publisher: Elsevier

Date: October 2022

© 2022 The Authors. Published by Elsevier Ltd.

Food and Chemical Toxicology 168 (2022) 113361

Contents lists available at ScienceDirect

Food and Chemical Toxicology

journal homepage: www.elsevier.com/locate/foodchemtox

Enniatins A1 and B1 alter calcium homeostasis of neuronal cells leading to apoptotic death

Nadia Pérez-Fuentes [a], Rebeca Alvariño [a,*], Amparo Alfonso [a,**], Jesús González-Jartín [a], Sandra Gegunde [a,b], Mercedes R. Vieytes [c], Luis M. Botana [a]

[a] Departamento de Farmacología, Facultad de Veterinaria, Universidad de Santiago de Compostela, Lugo, 27002, Spain
[b] Fundación Instituto de Investigación Sanitario Santiago de Compostela (FIDIS), Hospital Universitario Lucus Augusti, Lugo, 27002, Spain
[c] Departamento de Fisiología, Facultad de Veterinaria, Universidad de Santiago de Compostela, Lugo, 27002, Spain

ARTICLE INFO

Handling Editor: Dr. Jose Luis Domingo

Keywords:
Enniatins
Calcium fluxes
Apoptosis
Mitochondria
Combined toxicity

ABSTRACT

Enniatins (ENNs) A1 and B1 are non-regulated mycotoxins produced by *Fusarium* spp. that commonly occur in different types of food. These toxins are cytotoxic in several cell lines, but their mechanism of action is unclear. In this study, the cytotoxic effects of ENNs A1 and B1 in SH-SY5Y human neuroblastoma cells were analysed. Moreover, to better understand their mechanism of action, mitochondrial function, reactive oxygen species (ROS) levels and calcium fluxes were monitored. ENNs A1 and B1 reduced cell viability, presenting IC_{50} values of 2.0 and 2.7 μM, respectively. Both toxins induced caspase-dependent apoptosis, but only ENN A1 increased ROS production. Apoptotic cell death seems to be triggered by the increase in cytosolic calcium produced by both ENNs, since the toxins altered Ca^{2+} homeostasis by depleting intracellular reservoirs. Finally, binary combinations of ENN A1, ENN B1, ENN A and ENN B were tested. All mixtures resulted in an antagonistic effect, with the exception of ENN A and ENN B1 combination, which produced an additive effect. The results presented in this study provide the first evidence of ENNs A1 and B1 effects on calcium fluxes, providing new insights into the mechanism of action of these mycotoxins.

1. Introduction

Enniatins (ENNs) are cyclic hexadepsipeptidic mycotoxins mainly produced by *Fusarium* spp. This genus of fungus includes several species that affect crop and food contamination worldwide. Each *Fusarium* fungus can synthetize different types of mycotoxins including trichothecenes, fumonisins, zearalenone, beauvericin (BEA) and ENNs, among others (Sainz et al., 2018; Tonshin et al., 2010). The first three are included in the group of regulated mycotoxins by the European Commission (Commission Regulation (EC) No 1881/2006), so maximum limits of these toxins have been stablished in foodstuff. However, even though it was pointed out that ENNs are cytotoxic in the micromolar range (Prosperini et al., 2014), their concentrations in food are not regulated. This is due to the lack of information about the effects of these toxins, so they cannot be currently established as a health hazard (EFSA, 2014).

There are more than 29 ENNs analogues, being ENNs A, A1, B and B1 the most frequents ones. ENNs have similar chemical structures that consist in alternating a-hydroxy-D-isovaleric and N-methylamino acid moieties. ENN A1 is formed by a N-methyl-L valine moiety, two residues of N-methyl-L-isoleucine and three parts of a-hydroxy-D-isovaleric acid, whilst ENN B1 contains one moiety of N-methyl-L-isoleucine, two of N-methyl-L-valine and three of a-hydroxy-D-isovaleric acid (Wätjen et al., 2009) (Fig. 1). The non-regulated mycotoxin BEA is also a cyclohexadepsipeptide with three N-methyl-L-phenylalanine residues alternated with 2-hydroxy-D-isovaleric acid moieties (Bertero et al., 2020).

Due to their structural similarities, biological activities of ENNs and BEA have been traditionally related (Bertero et al., 2020). In 1973, it was proposed that ENN B formed complexes in biological membranes, allowing the passage of ions. Since then, ENNs and BEA cytotoxicity has been associated with their ionophoric properties (Ivanov et al., 1973; Kamyar et al., 2004). However, data about their ionophoric behaviour are scarce and most reports are focused on ENN B and BEA activities (Bertero et al., 2020; Tonshin et al., 2010). BEA induces apoptosis in

* Corresponding author.
** Corresponding author.
E-mail addresses: rebeca.alvarino@usc.es (R. Alvariño), amparo.alfonso@usc.es (A. Alfonso).

https://doi.org/10.1016/j.fct.2022.113361
Received 18 April 2022; Received in revised form 26 July 2022; Accepted 6 August 2022
Available online 12 August 2022
0278-6915/© 2022 The Authors. Published by Elsevier Ltd. This is an open access article under the CC BY-NC-ND license (http://creativecommons.org/licenses/by-nc-nd/4.0/).

several cell lines (Jow et al., 2004; Lu et al., 2016; Pérez-Fuentes et al., 2021) and its cytotoxicity could be related with calcium homeostasis disruption, as the addition of a calcium chelator prevented BEA-induced cell death in human leukaemia cells (Jow et al., 2004). With respect to ENNs, it has been suggested that the mixture of the four ENNs has selective ionophoric properties for K^+ (Tonshin et al., 2010). Additionally, ENN B1 was recently reported to permeabilize the lysosomal membrane (Oliveira et al., 2020).

On the other hand, ENNs A, A1, B and B1 cytotoxicity could be related with mitochondrial impairment. These mycotoxins affect oxidative phosphorylation and mitochondrial volume regulation and cause apoptotic death through the production of reactive oxygen species (ROS) (Huang et al., 2019; Prosperini et al., 2013; Tonshin et al., 2010). Neuronal cells are very sensible to mitochondrial dysfunction and ion dysregulation due to their great dependence on oxygen consumption (Yin et al., 2014). In fact, ENNs A and B produced mitochondrial-mediated cytotoxicity in neuronal cells, and the analysis of natural contaminated samples containing the four ENNs revealed greater effects on neuronal viability than expected (Pérez-Fuentes et al., 2021), suggesting that their co-occurrence could suppose a health risk. However, neither the single nor the combined effects of ENNs A1 and B1 have been tested in neuronal cells so far.

Due to the previous results that point to an involvement of ion imbalance and mitochondrial dysfunction in the mechanism of action of ENNs, as well as their ability to cross the blood brain barrier (BBB) (Alonso-Garrido et al., 2021), ENNs A1 and B1 are expected to affect neuronal function and viability. Moreover, the increasing prevalence of ENNs contamination in Europe (González-Jartín et al., 2021; Prusova et al., 2022; Reinholds et al., 2021), as well as their potential bioaccumulation (Rodríguez-Carrasco et al., 2020) makes these toxins an inherent health hazard. Currently, data about their toxicity and bioactivity are still scarce and the need to elucidate their mechanism of action is increasingly evident. The present study examines the effects of ENN A1 and ENN B1 on cell viability, mitochondrial function, and calcium homeostasis in the human neuroblastoma cell line SH-SY5Y. In addition, binary combinations between these mycotoxins and ENNs A and B were tested to determine the potential consequences of their co-occurrence.

2. Materials and methods

2.1. Chemicals and solutions

CyQUANT™ lactate dehydrogenase (LDH) Cytotoxicity Assay Kit, tetramethyl rhodamine methyl ester (TMRM), 5-(and-6-)-carboxy-2′,7′-dichlorodihydrofluerescein diacetate (carboxy-H_2DCFDA), Dulbecco's Modified Eagle Medium: F-12 nutrient Mix (DMEM/F-12), glutamax, trypsin/EDTA (0.05%) and penicillin-streptomycin (10,000 U/mL) were purchased from Thermo Fisher Scientific (Madrid, Spain). ENN B1 (purity >99%) was bought in Vitro S.A. (Sevilla, Spain). Thapsigargin (Tg) was obtained from ENZO Life Sciences (Lausen, Swiss). ENN A, ENN A1 and ENN B (purity >95%), Annexin V-FITC Apoptosis Detection Kit, 3-(4,5-dimethyl thiazol-2-yl)-2,5-diphenyl tetrazolium bromide (MTT), Z-VAD-FMK, staurosporine (STS), saponin (SAP), and another chemical reagent grade were purchased from Merck (Madrid, Spain). ENNs standards were diluted in DMSO, and serial dilutions were prepared in culture medium. DMSO concentration was kept under 0.05% in all experiments.

The composition of Locke's buffer was (mM): NaCl 154.0, HEPES 10.0, KCl 5.6, glucose 5.0, $NaHCO_3$ 3.6, $CaCl_2$ 1.3 and $MgCl_2$ 1.0. The composition of Umbreit solution was (mM): NaCl 119.0, $NaHCO_3$ 22.85, KCl 5.94, $Mg(SO)_4$ 1.2, NaH_2PO_4 1.2, Glucose 0.1% and $CaCl_2$ 1.0. The pH was adjusted between 7.2 and 7.4 in all the assays. Phosphate buffered saline (PBS) was composed of (mM): NaCl 137.0, Na_2HPO_4 8.2, KH_2PO_4 1.5 and KCl 3.2 (pH 7.4).

2.2. Cell culture and treatment

SH-SY5Y human neuroblastoma cells were obtained from American Type Culture Collection (ATCC), number CRL2266. Cells were maintained in DMEM/F-12 medium supplemented with 10% foetal bovine serum (FBS), 10,000 U/mL penicillin-streptomycin and 1% glutamax at 37 °C in a humidified atmosphere of 95% air and 5% CO_2. Cells were dissociated once a week using 0.05% trypsin/EDTA.

2.3. Cell viability assay

The effects of ENNs on SH-SY5Y cells viability was analysed using MTT assay as previously described (Kumar et al., 2018; Pérez-Fuentes et al., 2021). Cells were seeded at 5×10^4 cells per well in 96-well plates and allowed to grow for 24 h. Then, cells were treated with ENN A1 and B1 at concentrations ranging from 0.1 to 15 μM for 6 and 24 h. After treatment, cells were washed three times with 200 μL/well of Locke's solution. Then, 200 μL of MTT (500 μg/mL) were added to each well and the plate was incubated in an orbital shaker for 1 h at 300 rpm and 37 °C. Afterward, MTT was removed, and cells were lysed by adding 5% sodium dodecyl sulphate. The absorbance originated was read at 595 nm in a spectrophotometer plate reader. SAP from *Quillaja bark* (1 mg/mL) was used as cell death control and its absorbance was subtracted from the other data.

To determine if ENN A1 and ENN B1 produced caspase-mediated apoptosis, SH-SY5Y cells were pre-treated with the caspase inhibitor Z-VAD-FMK at 40 μM for 24 h. Then, ENN A1 and ENN B1 at half

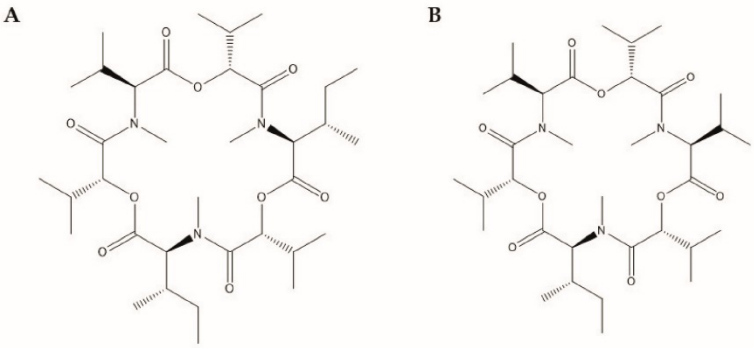


Fig. 1. Chemical structure of enniatins A1 (A) and B1 (B).

USC UNIVERSIDADE DE SANTIAGO DE COMPOSTELA

inhibitory concentrations (IC_{50}) were added for 24 h and MTT assay was performed.

For combination assays, ENNs (A, A1, B and B1) were mixed at 1:1 ratio, mimicking the proportion found in contaminated samples from NW Iberian Peninsula (González-Jartín et al., 2021). For this experiment, cells were seeded in 384-well plates at 2.5×10^4 cells per well. Neuroblastoma cells were treated with binary combinations for 24 h and MTT assay was carried out as described above.

All experiments were performed three times by triplicate.

2.4. Cytotoxicity assay

To analyse the effects of individual and mixed mycotoxins on cell cytotoxicity, CyQUANT™ LDH Cytotoxicity Assay Kit test was used, following manufacturer's instructions (Pérez-Fuentes et al., 2021). SAP from *Quillaja bark* at 1 mg/mL was used as cell death control. Cells were treated with ENNs A1 and B1 at concentrations from 0.1 to 15 μM for 6 and 24 h, whilst binary combinations were performed for 24 h, as described above. LDH release was evaluated after transferring 50 μL of cell medium to a 96-well flat-bottom. Absorbance was read at 490 and 680 nm in a plate reader. Finally, the background signal (680 nm absorbance value) was subtracted from the 490 nm absorbance value to determine LDH release to the medium. Experiments were performed three independent times by triplicate.

2.5. Mitochondrial membrane potential measurement

TMRM dye was used to analyse mitochondrial membrane potential ($\Delta\Psi_m$) (Pérez-Fuentes et al., 2021). Human neuroblastoma cells were seeded in 96-well plates at 5×10^4 cells per well and allowed to attach for 24 h. Then, cells were treated with ENN A1 and ENN B1 for 6 and 24 h. After this time, the plate was washed twice with Locke's solution, TMRM 20 μM was added, and the plate was incubated 30 min at 300 rpm and 37 °C. Then, the dye was removed, cells were dissolved in H_2O and DMSO (1:1) and fluorescence was read at 535 nm excitation and 590 nm emission in a plate reader. Rotenone (Rot) at 1 μM was used as positive control. Assays were performed by triplicate three independent times.

2.6. Measurement of intracellular reactive oxygen species levels

The fluorescent dye carboxy-H_2DCFDA was used to measure the levels of ROS produced by neuroblastoma cells as described before (Alvariño et al., 2021). After treatment with ENN A1 and ENN B1 for 6 and 24 h, cells were washed twice with serum-free medium. At that point, 20 μM carboxy-H_2DCFDA diluted in serum-free medium was added, and cells were incubated in an orbital shaker for 1 h at 300 rpm and 37 °C. Then, PBS was added to every well and the plate was incubated for 30 min at 300 rpm and 37 °C. Finally, fluorescence was read at 495 nm excitation and 527 nm emission in a plate reader. H_2O_2 150 μM was used as positive control. Experiments were performed in triplicate three times.

2.7. Cell death type analysis

To determine the cell death type produced by the toxins, Annexin V-FITC Apoptosis Detection Kit was used, following manufacturer's instructions (Pérez-Fuentes et al., 2021). For this assay, cells were seeded in 12-well plates at 5×10^5 cells per well. After 24 h, cells were treated with ENN A1 and ENN B1 and incubated another 24 h. STS at 0.1 μM was used as positive control. Then, cells were washed with PBS, resuspended in Annexin-binding buffer containing Annexin V-FITC and Propidium Iodide (PI) and incubated for 15 min at room temperature. Cells were resuspended in commercial PBS (pH 7.2) (Thermo Fisher Scientific), filtered, and kept on ice. Next, fluorescence was analysed by flow cytometry using the ImageStreamMKII instrument (Amnis Corporation, Luminex Corp, Austin, TX, USA). IDEAS Application 6.0 software was used to determine the fluorescence of 10,000 events (Amnis Corporation, Luminex Corp).

2.8. Measurement of cytosolic free calcium

Cells were seeded in 18-mm glass coverslips at 5×10^5 cells per well and incubated for 24 h. For calcium measurement, cells were washed twice with Umbreit solution, enriched with 0,1% BSA. SH-SY5Y cells were loaded with the fluorescent dye FURA-2 AM (0.5 μM) for 6.5 min at 300 rpm and 37 °C. Then, cells were washed twice with Umbreit solution and coverslips were placed in a thermostatic chamber (Life Sciences Resources, UK) (Sánchez et al., 2015). Cells were viewed in an inverted microscope Nikon Diphot 200, equipped with epifluorescence optics (Nikon 40x, immersion UV-fluor objective). Mycotoxin dilution was made in Umbreit solution without calcium, and compounds were directly added to the incubation chamber. Cytosolic calcium levels as FURA-2 ratio were obtained from the images collected by fluorescence equipment, consisting in an ultra-high-speed wavelength switcher (Lambda-DG4) for excitation and an optical filter changer Lambda 10–2 for emission (Sutter Instruments Co., USA). The light source was a xenon arc bulb and wavelengths used were selected with the filters. Cells were excited at 340 and 380 nm, with emission at 505 nm.

2.9. Statistical analysis

Data are presented as mean ± SEM of three independent experiments. Differences were evaluated by One-way ANOVA followed by Dunnett's or Tukey's multiple comparison tests. Statistical significance was established at $^*p < 0.05$, $^{**}p < 0.01$, and $^{***}p < 0.001$. IC_{50} and half maximal effective concentration (EC_{50}) values were calculated with GraphPad Prism 8 software by fitting the data with a log(inhibitor) *vs* response or a log(agonist) *vs* response models, respectively.

The combination index was calculated with Chou & Talalay equation (Chou and Talalay, 1983):

$$COMBINATION\ INDEX = \frac{D1}{(DX)1} + \frac{D2}{(DX)2}$$

where (DX)1 and (DX)2 are IC_{50} values of each mycotoxin alone, and D1 and D2 are IC_{50} values of each mycotoxin in combination. If the results of the equation are <1, =1 and >1, Chou & Talalay method considers synergism, additivity, or antagonism, respectively.

3. Results

3.1. Evaluation of ENN A1 and B1 effects on viability, mitochondrial function, and calcium homeostasis of SH-SY5Y cells

At first, effects of ENNs A1 and B1 on cell survival were evaluated with two assays. MTT dye was used to analyse the effects of ENNs in cell viability, whilst cytotoxicity was determined by LDH assay. Dose-response treatments were performed (0.1–15 μM) for 6 and 24 h and the experiments were carried out. Regarding MTT test, which determines cell viability based on cell metabolism, ENN A1 treatment for 6 h reduced cell viability between 36.2 and 99.7% at concentrations over 2.5 μM. After 24 h, cell viability decrease was greater, with a diminution of 88.3 ± 6.0% ($p < 0.001$) at 2.5 μM (Fig. 2 A). In the case of ENN B1, this toxin significantly decreased SH-SY5Y cell viability at 2.5, 5, 10 and 15 μM after 6 h of treatment. At longer incubation times (24 h), cell viability was reduced between 44.6 and 100% at doses higher than 2.5 μM (Fig. 2 B). With the data obtained in MTT assays, IC_{50} values for each toxin were calculated by fitting the data with a log(inhibitor) *vs* response model (Fig. S1 A-B). At 6 h of incubation, ENN A1 and ENN B1 showed similar IC_{50} values, 3.4 μM (CI: 2.8–4.4 μM) and 3.0 μM (CI: 2.4–3.6 μM), respectively. After 24 h incubation, IC_{50} values were lower, being ENN A1 (2.0 μM, CI: 1.2–3.3 μM) a little more damaging than ENN B1 (2.7

USC UNIVERSIDADE DE SANTIAGO DE COMPOSTELA

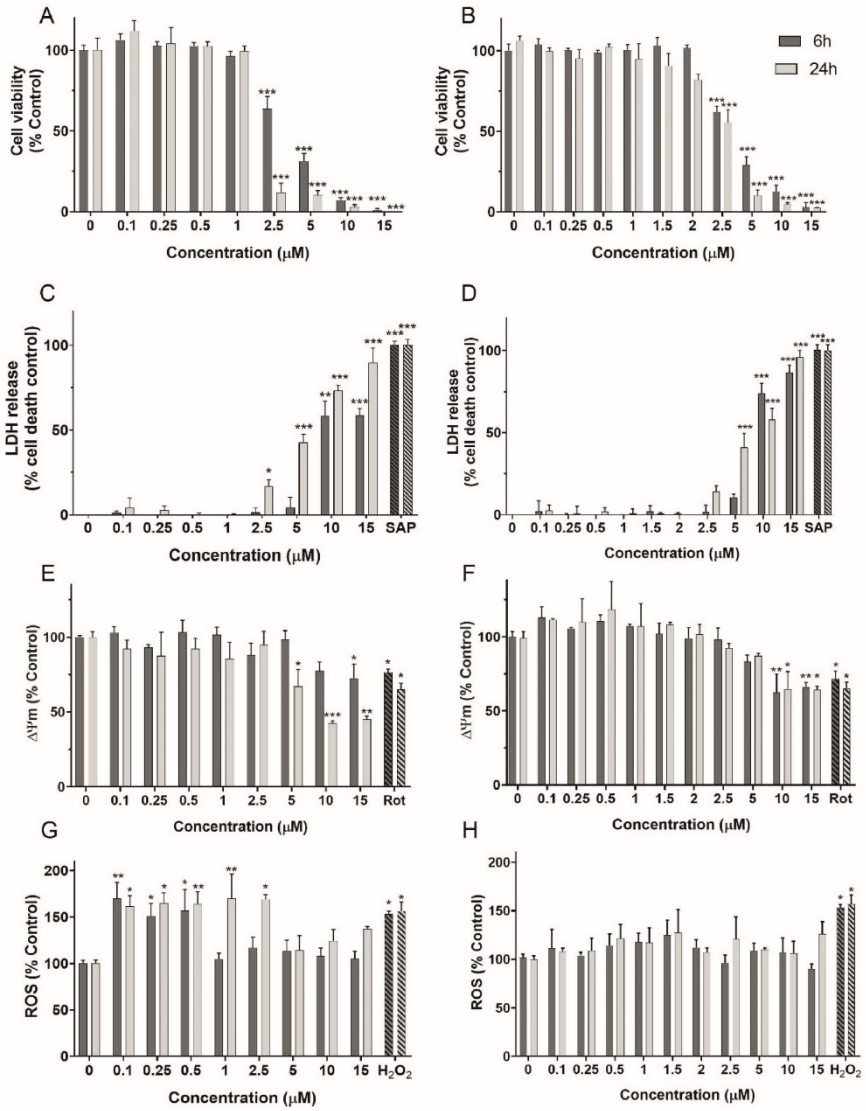


Fig. 2. Effects of ENNs A1 and B1 on viability and mitochondrial function of SH-SY5Y cells. Cells were treated with ENNs for 6 and 24 h. (A) Effect of ENN A1 and (B) ENN B1 on cell viability, assessed by MTT test. (C) Cytotoxicity of ENN A1 and (D) ENN B1, determined by LDH assay. Saponin (SAP) at 1 mg/mL was used as cell death control. (E) Mitochondrial membrane potential ($\Delta\Psi_m$) after treatment with ENN A1 and (F) ENN B1, measured using TMRM dye. Rot at 1 μM was used as positive control. (G) ROS levels after treatment with ENN A1 and (H) ENN B1, assessed by using carboxy-H_2DCFDA dye. 150 μM H_2O_2 was used as positive control for ROS production. Data are mean ± SEM of three independent replicates. Statistical differences determined by One-way ANOVA and Dunnett's multiple comparison test. *$p \leq 0.05$, **$p \leq 0.01$ and ***$p \leq 0.001$, significantly different from the control.

μM, CI: 2.4–3.1 μM).

As explained before, cytotoxicity was assessed with LDH assay, which provides information about cell membrane damage, and therefore has lower sensitivity than MTT assay. Results agreed with those obtained with MTT test, observing LDH release at the highest concentrations used (Fig. 2C–D). ENN A1 increased LDH liberation about 58% at concentrations above 10 μM after 6 h of treatment. At 24 h, the augmentation in LDH levels ranged between 20.2 and 89.9% at concentrations higher than 2.5 μM (Fig. 2 C). Finally, ENN B1 showed a significant increase in LDH release at doses above 10 μM after 6 h incubation, reaching levels of 88.7 ± 4.4% ($p < 0.001$) at 15 μM. After 24 h of exposure, ENN B1 induced a rise in LDH levels among 41.0–98.0%

USC UNIVERSIDADE DE SANTIAGO DE COMPOSTELA

(Fig. 2 D). From these data, EC_{50} values for each toxin were calculated by fitting the data with a log(agonist) *vs* response model (Fig. S1 C-D). ENN B1 presented an EC_{50} of 7.4 μM (CI: 6.4–8.3 μM) after 6 h of incubation. At longer treatments, EC_{50} of both toxins were similar, 6.2 μM (CI: 4.6–13.6 μM) and 6.7 μM (CI: 5.8–7.8 μM) for ENN A1 and ENN B1, respectively.

In view of the results obtained with MTT and LDH assays, the effects of ENNs on mitochondrial function were evaluated. Cells were treated with ENNs A1 and B1 for 6 and 24 h at the same concentrations used before. Then, $\Delta\Psi_m$ and ROS production were analysed. To study how compounds affected $\Delta\Psi_m$, the fluorescent dye TMRM was used, and the assay was validated with the inhibitor of the electronic transport chain Rot at 1 μM. Since $\Delta\Psi_m$ is maintained by oxidative phosphorylation, it is an indicator of mitochondrial function. As Fig. 2 E-F shows, both ENNs depolarized the mitochondrial membrane at the highest dosed used after 6 and 24 h of treatment. ENN A1 produced significant differences compared to control cells at 15 μM (72.4 ± 9.7%, $p < 0.05$) after 6 h of incubation. At 24 h, this toxin affected mitochondrial function at concentrations above 5 μM, reducing $\Delta\Psi_m$ by 45.2 ± 2.1% ($p < 0.01$) at 15 μM (Fig. 2 E). ENN B1 produced a lower effect, depolarizing mitochondrial membrane between 35.0 and 37.5% of control cells at 10 and 15 μM at both times of incubation (Fig. 2 F). These levels were similar to those observed after addition of the positive control Rot, which affected mitochondrial membrane at both times between 28.4 and 34.8% of control cells.

As mitochondria are the main producers of ROS in cells, effect of ENNs on release of these damaging molecules was analysed. ENN A1 induced an increase in ROS production at several concentrations (Fig. 2 G). At 6 h, this compound elevated ROS generation at doses between 0.1 and 0.5 μM about a 50% of control cells. Furthermore, treatment with ENN A1 for 24 h also augmented ROS at the lower doses, reaching an increase of 169.0 ± 4.9% ($p < 0.05$) at 2.5 μM. Conversely, ENN B1 did not produced ROS release at any concentration (Fig. 2 H). The assay was validated with H_2O_2 at 150 μM, treatment that increased ROS levels up to 153.0 ± 3.2 μM ($p < 0.05$) and 156.7 ± 9.5 μM ($p < 0.05$) at 6 and 24 h, respectively.

Since ENNs A1 and B1 affected cell viability, the type of death produced by these mycotoxins was evaluated. Cells were treated with ENNs for 24 h at IC_{50} values calculated with MTT test and the apoptosis inductor STS at 1 μM was used as positive control. Next, co-staining Annexin V-FITC and PI was carried out and fluorescence was analysed by flow cytometry (Fig. 3A–B). Percentages of early and late apoptotic cells (Annexin V-FITC positive and PI positive or negative) and necrotic cells (Annexin V-FITC negative and PI positive) were calculated. ENNs A1 and B1 produced a significant increase in apoptotic cells of 39.3 ± 5.1% ($p < 0.01$) and 36.3 ± 0.5% ($p < 0.05$), respectively, without any change in the percentage of necrotic cells, compared to control. As expected, the apoptotic inducer STS increased cells in apoptosis (45.2 ± 5.7%, $p < 0.01$).

To further confirm that ENNs were producing caspase-dependent apoptosis, the caspase inhibitor Z-VAD-FMK was used (Fig. 3 C). Cells were pre-treated with Z-VAD-FMK for 24 h, followed by exposure to ENNs A1 and B1, and cell viability was assessed. As observed in control cells, pre-treatment with the inhibitor did not affect cell viability. Regarding ENN A1, a decrease in cell viability of 16.8 ± 3.3% ($p < 0.05$) was observed when cells were pre-treated with Z-VAD-FMK. This reduction was significantly smaller ($p < 0.05$) than the diminution produced by the toxin alone (37.6 ± 0.9%, $p < 0.001$). Similar results were obtained with ENN B1, which presented a reduction of 18.5 ± 6.0% ($p < 0.05$) in cells pre-treated with the caspase inhibitor and a

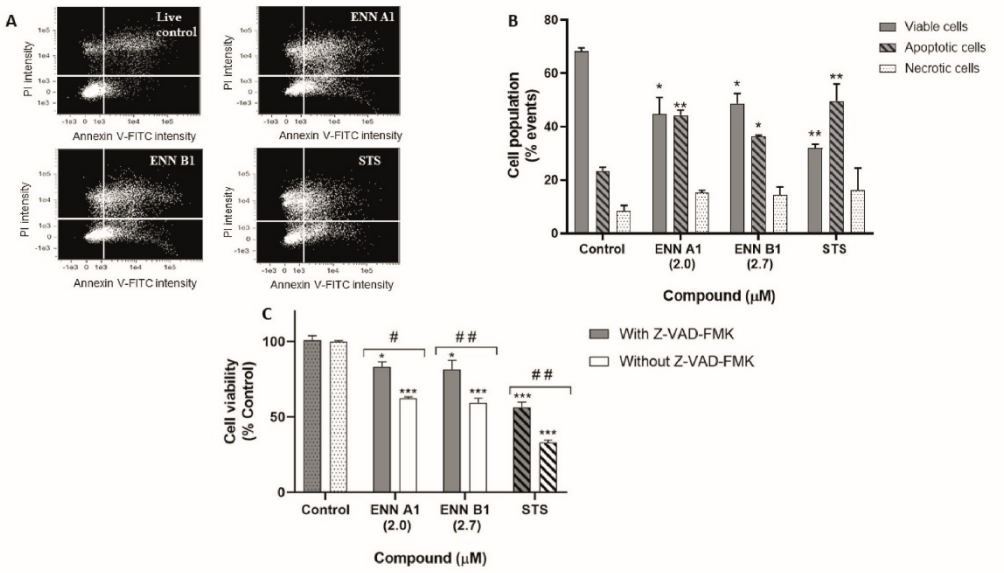


Fig. 3. Analysis of cell death type induced by ENNs A1 and B1 in SH-SY5Y cells. (A) Representative scatter plot of flow cytometry analysis. (B) Bar graph of the results obtained by flow cytometry. Cells were treated with mycotoxins at IC_{50} values for 24 h, co-stained with Annexin V-FITC and PI, and the fluorescence of 10000 cells was monitored. Percentages of viable cells (Annexin V-FITC -/PI -), apoptotic cells including early apoptosis (Annexin V-FITC + /PI –) and late apoptosis (Annexin V-FITC + /PI +), and necrotic cells (Annexin V-FITC –/PI+) were calculated. Data are mean ± SEM of three independent experiments, compared to control cells by One-way ANOVA followed by Dunnett tests (*$p \leq 0.05$ and **$p \leq 0.01$). (C) Evaluation of caspases involvement in ENNs-induced apoptosis. Cells were pre-treated with 40 μM Z-VAD-FMK for 24 h, followed by addition of ENNs at IC_{50} values, and cell viability was analysed. STS was used as positive control in these assays. Mean ± SEM of three independent experiments, expressed as percentage of control cells. Statistical significance determined by One-way ANOVA and Tukey's test (*$p \leq 0.05$ and ***$p \leq 0.001$, compared to control cells), (#$p \leq 0.05$ and ##$p \leq 0.01$, compared to their corresponding control).

USC UNIVERSIDADE DE SANTIAGO DE COMPOSTELA

decrease of 40.6 ± 3.1% ($p < 0.001$) when ENN B1 was added alone. These results were significantly different ($p < 0.01$), confirming that caspases are involved in the apoptosis generated by ENN B1. The assay was validated with STS (1 μM), which also presented a significant difference ($p < 0.01$) between pre-treated and non-pre-treated cells.

Finally, the effects of ENNs A1 and B1 on cytosolic Ca^{2+} were assessed. Tg at 2 μM was used as positive control. This compound inhibits irreversibly the Ca^{2+}-ATPase from the endoplasmic reticulum (ER), inducing Ca^{2+} pools depletion to cytosol and subsequently activating the entry of this ion through membrane store-operated channels (SOC). Tg effects were well documented and previously described in SH-SY5Y cells (Sánchez et al., 2015).

A dose-response assay was first performed with each mycotoxin. ENN A1 was tested at 0.5, 1 and 2 μM, while ENN B1 was used at 1, 2 and 5 μM. As Fig. 4 A-B shows, both ENNs act in a dose-dependent manner. However, each ENN seems to act differently. ENN A1 produced an acute Ca^{2+} depletion from intracellular compartments, and significantly increased Ca^{2+} uptake when this ion was added to the bath solution. At the highest dose employed (2 μM), Ca^{2+} uptake after adding the ion to the bath solution reached similar levels than Tg (Fig. 4 A). In the case of ENN B1, Ca^{2+} depletion from intracellular pools was smoother than the originated by ENN A1. Moreover, this toxin also induces Ca^{2+} entry when the ion was added to the bath solution, but it was smaller than the effect produced by ENN A1 (Fig. 4 B).

As ENN A1 exhibited a similar profile than the produced by Tg, it was checked if this mycotoxin was affecting the same reservoirs depleted by Tg. With this objective, ENN A1 and Tg and *vice versa*, were consecutively added to neuroblastoma cells. Fig. 4 C shows that pre-incubation with 2 μM ENN A1 did not inhibit Tg-induced Ca^{2+} depletion from ER. Moreover, pre-addition of ENN A1 increased calcium uptake when this ion was incorporated to the bath solution in comparison to cells treated with Tg alone. When Tg was added in first place, the effects of ENN A1 were reduced compared to those produced by the mycotoxin alone. When Ca^{2+} was added to the bath solution, the uptake of this ion was similar than the produced by ENN A1 and Tg alone (Fig. 4 D). However, this influx did not result in Ca^{2+} levels as high as those produced by adding first ENN A1, rather than Tg, to the cells.

3.2. Evaluation of ENNs binary combinations toxicity

In order to investigate interactions between ENNs, they were binary combined, and their toxic effects were determined. Concentration ratio (1:1) was selected based on the most frequent proportions found in samples from NW Iberian Peninsula (González-Jartín et al., 2021). As ENNs A1 and B1 usually appear in combination with ENN A and B, their combined effects were also tested. In this context, ENNs were combined as follows: ENN A1 + ENN A, ENN B1+ ENN A, ENN A1 + ENN B, ENN B1 + ENN B and ENN A1 + ENN B1. Concentration range (0.1–10 μM) and incubation time (24 h) were chosen based on the results obtained in the previous experiments.

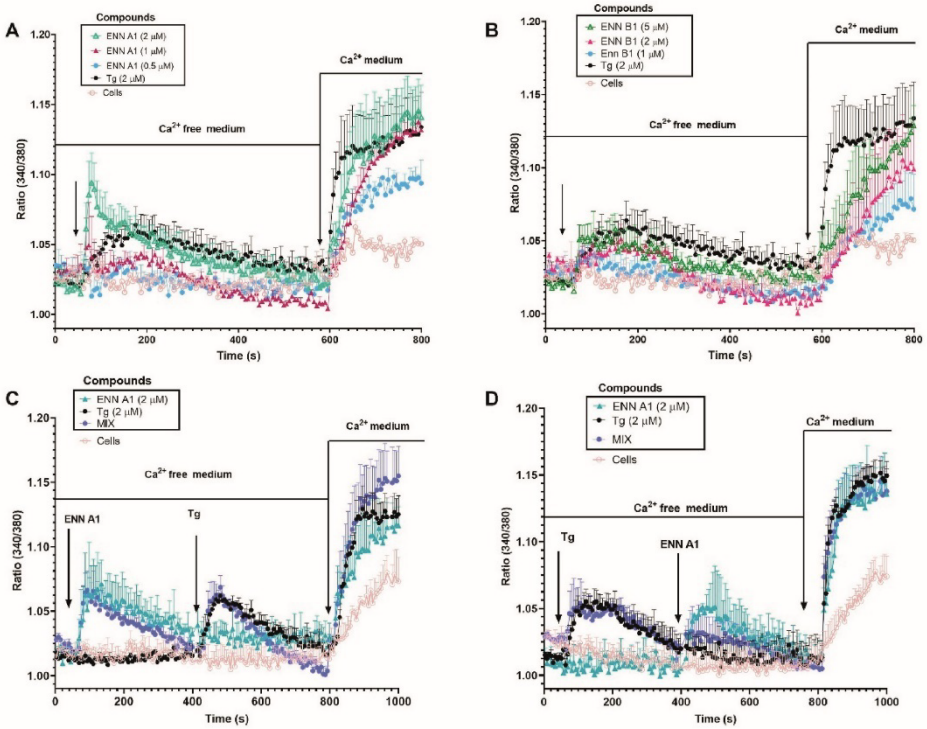


Fig. 4. Effects of ENNs A1 and B1 on cytosolic Ca^{2+} profile of SH-SY5Y cells. (A) ENN A1 dose-response assay. (B) ENN B1 dose-response assay. Tg at 2 μM was used as positive control. The first arrow indicates the addition of compounds. The second arrow shows the addition of 1 mM of Ca^{2+} to the bath solution. (C) Cytosolic Ca^{2+} profile of cells pre-incubated with 2 μM ENN A1 (first arrow) followed by addition of Tg at 2 μM (second arrow). Third arrow indicates the addition of 1 mM of Ca^{2+} to the bath medium. (D) Cytosolic Ca^{2+} profile of cells pre-treated with Tg at 2 μM (first arrow) followed by 2 μM ENN A1 (second arrow). Third arrow indicates the addition of 1 mM of Ca^{2+} to the bath medium. Mean ± SEM of three independent experiments performed by duplicate.

USC UNIVERSIDADE DE SANTIAGO DE COMPOSTELA

Initially, the effect of binary combinations on cell viability was determined with MTT test. The results obtained with ENN A1 + ENN A were similar to those observed after treatment with ENN A1 alone. This mixture caused a significant decrease on cell viability at concentrations above 1.5 μM, reaching a reduction of 96.6 ± 1.2% ($p < 0.001$) at 10 μM (Fig. 5 A). In the case of ENN B1 + ENN A, the results were quite similar to the previous mixture, inducing almost a complete decrease at the highest concentration used (Fig. 5 B). Regarding ENN A1 + ENN B, levels of cell viability ranged between 45.7 and 10.2% at concentrations higher than 1.5 μM (Fig. 5 C). On the other hand, the cell damage caused by ENN B1 + ENN B was less pronounced than in the previous mixtures, reducing cell viability by 86.2 ± 1.2% (Fig. 5 D) at 10 μM. Finally, ENN A1 + ENN B1 also injured cells at concentrations above 1 μM (Fig. 5 E).

With the results obtained in MTT assay, IC_{50} values for each combination were determined (Table 1, Fig. S2). With single and combined IC_{50} data, and following Chou & Talalay method, combination index was calculated (Chou and Talalay, 1983). IC_{50} values from ENN A and ENN B in SH-SY5Y cells after 24 h of incubation had been previously determined (2.3 and 0.4 μM, respectively) (Pérez-Fuentes et al., 2021). Chou & Talalay method establishes that if combination index is higher than 1, the toxins mixture produces antagonism, if it is equal to 1, it is an additive effect, and if it is lower than 1, it will be due to a synergistic effect. Except for ENN B1 + ENN A mixture, all combination indexes were higher than 1, indicating an antagonistic effect between the toxins. In the case of ENN B1 + ENN A, combination index value was 1.0, denoting an additive effect.

Finally, cytotoxicity of binary mixtures was assessed with LDH assay (Fig. 6). All the combinations originated an increase in LDH release at concentrations higher than 2.5 μM, but only ENN A1 + ENN A, ENN B1 + ENN A and ENN A1 + ENN B1 reached levels similar to the cell death control (94.0 ± 10.1%, 78.4 ± 9.8% and 91.1 ± 11.9%, $p < 0.001$, respectively). The other combinations produced a maximum augmentation of LDH levels in cell supernatant about 41%.

With the results obtained in LDH assay, EC_{50} values were calculated (Fig. S3). Except for ENN B combinations, whose EC_{50} value could not be calculated, the other mixtures showed lower or similar values to those of ENNs A1 and B1 alone. EC_{50} of ENN A1 + ENN A mixture was 4.4 μM (CI: 3.9–4.9 μM). ENN B1 + ENN A combination presented an EC_{50} of 6.8 μM (CI: 6.0–7.8 μM), whilst ENN A1 + ENN B1 showed a value of 4.3 μM (CI: 3.6–5.2 μM).

Table 1
IC_{50} and combination index of enniatins mixtures. ENN A: enniatin A, ENN A1: enniatin A1, ENN B: enniatin B and ENN B1: enniatin B1, CI: 95% confidence interval.

Binary combination (1:1)	IC_{50} (μM)	Combination index
ENN A1 + ENN A	1.7 (CI: 1.5–1.9) R^2: 0.94	1.7
ENN B1 + ENN A	1.3 (CI: 0.76–2.3) R^2: 0.89	1.0
ENN A1 + ENN B	1.4 (CI: 1.2–1.6) R^2: 0.92	4.2
ENN B1 + ENN B	1.4 (CI: 1.1–1.8) R^2: 0.88	4.1
ENN A1 + ENN B1	1.5 (CI: 1.2–1.8) R^2: 0.94	1.3

4. Discussion

ENNs are non-regulated mycotoxins that commonly occur in grain and another foodstuff at concentrations in the micromolar range. In the last decades, there have been few studies about ENNs toxicity and their mechanism of action is still unclear (Bertero et al., 2020). Most works analysed the cytotoxicity produced by ENNs in intestinal or liver cell lines because the main route of exposure is through ingestion (Meca et al., 2010, 2011). In this study, two of the most frequent ENNs found in cereals of Europe, ENN A1 and ENN B1, were chosen to determine how they affect SH-SY5Y human neuroblastoma cells (Gautier et al., 2020). Experiments were carried out in a neuronal cell line because it has been described that ENNs can cross the BBB due to their lipophilic nature (Alonso-Garrido et al., 2020). In these cells, ENN A1 and ENN B1 affected cell viability, presenting IC_{50} values in the micromolar range at both incubation times. These values were lower than those previously reported in intestinal or liver cells. SH-SY5Y cells were found to be 5–7 times more sensitive to ENNs A1 and B1, suggesting that they could be neurotoxic at concentrations found in contaminated samples. In fact, treatment with a mixture of ENNs and BEA in an *in vitro* model of BBB produced a downregulation in the expression of the complex I of the electronic transport chain. This impairment has been related to

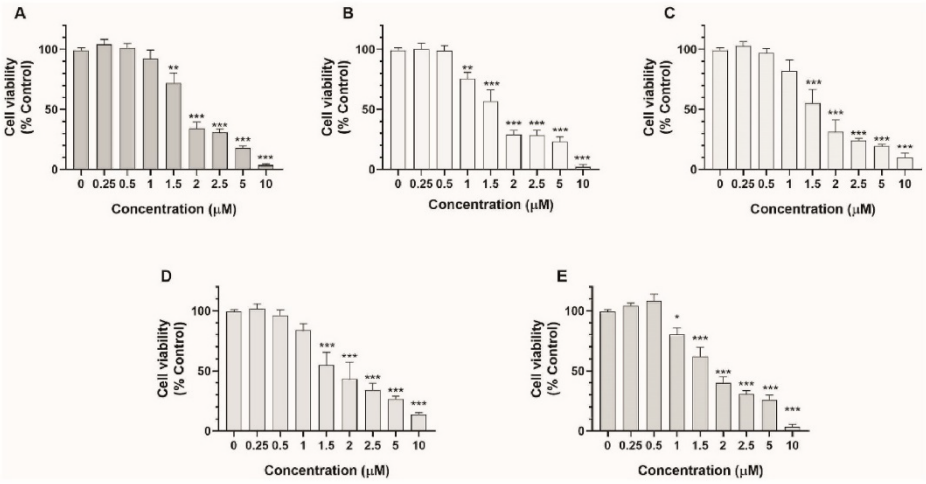


Fig. 5. Effects of ENNs binary combinations in cell viability of SH-SY5Y cells. Human neuroblastoma cells were treated with binary mixtures (1:1) of ENNs A1, B1, A, and B for 24 h and their effect on cell viability was assessed with MTT assay. (A) ENN A1 + ENN A, (B) ENN B1 + ENN A, (C) ENN A1 + ENN B, (D) ENN B1 + ENN B and (E) ENN A1 + ENN B1. Data are mean ± SEM of three independent replicates expressed as percentage of untreated control cells. Statistical differences determined by One-way ANOVA and Dunnett's multiple comparison tests. *$p \leq 0.05$, **$p \leq 0.01$ and ***$p \leq 0.001$, significantly different from the control.

USC UNIVERSIDADE DE SANTIAGO DE COMPOSTELA

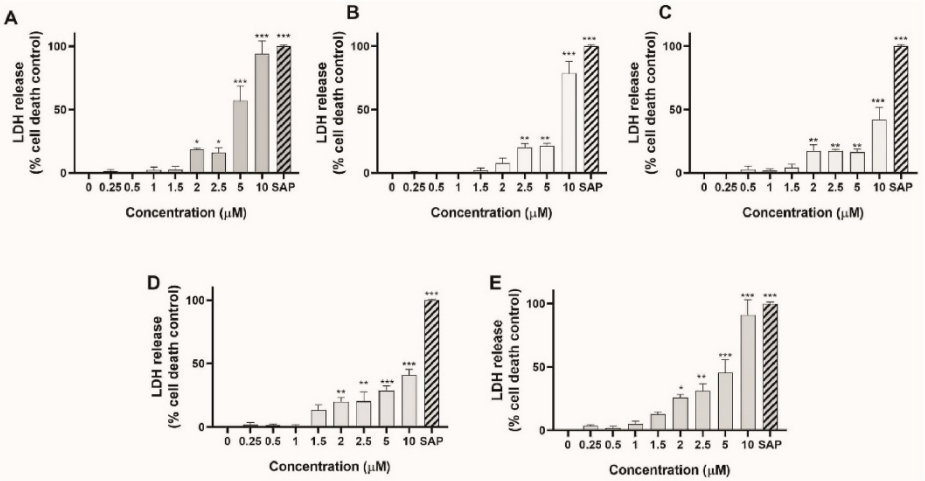


Fig. 6. Cytotoxic effects of ENNs binary combinations in human neuroblastoma cells. SH-SY5Y cells were treated with ENNs mixtures (1:1) for 24 h and cytotoxicity was determined by LDH assay. (A) ENN A1 + ENN A, (B) ENN B1 + ENN A, (C) ENN A1 + ENN B, (D) ENN B1 + ENN B and (E) ENN A1 + ENN B1. SAP (1 mg/mL) was used as cell death control. Data are mean ± SEM of three independent replicates expressed as percentage of cell death control. Statistical differences determined by One-way ANOVA and with Dunnett's multiple comparison test. *$p \leq 0.05$, **$p \leq 0.01$ and ***$p \leq 0.001$, significantly different from untreated control cells.

neurodegenerative diseases, supporting the assumption that ENNs exert neurotoxic effects (Alonso-Garrido et al., 2021).

The results obtained in MTT and LDH assays coincide for both mycotoxins, since the reduction of cell viability matches with the increase in LDH release. Considering that MTT is mainly metabolised by mitochondria (Fotakis and Timbrell, 2006), cytotoxicity produced by ENNs in neuroblastoma cells could be related with mitochondria impairment, as it was seen in the BBB model mentioned above (Alonso-Garrido et al., 2021). For this reason, the effects of ENNs A1 and B1 on $\Delta\Psi_m$ and ROS production were assessed. Surprisingly, both ENNs only affected $\Delta\Psi_m$ at highest doses used, so this reduction seems to be associated to the decrease in cell survival produced by these mycotoxins at those concentrations. Their analogues ENN A and ENN B produced mitochondrial depolarization at doses between 0.1 and 10 μM under the same conditions, suggesting that the mechanism of action of ENNs A and B is more related to mitochondria (Pérez-Fuentes et al., 2021). On the other hand, when analysing ROS production, ENN A1 elevated ROS levels in a wide range of concentrations while ENN B1 did not affect the release of these damaging molecules. In Caco-2 cells, ENN B1 was shown to elevate ROS generation, so intestinal cells seem to be more prone to originate ROS than neuronal cells after treatment with this toxin (Prosperini et al., 2013). Since ENN A1 increased ROS release at low doses without affecting $\Delta\Psi_m$, it seems that the toxin acts through a different pathway such as NADPH oxidase activation (Tarafdar and Pula, 2018). In any case, the lack of effect of ENN B1 on ROS release points to a different mechanism of action of each ENN.

Despite these differences, both ENNs A1 and B1 induced apoptotic death in human neuroblastoma cells, as did their analogues ENNs A and B (Pérez-Fuentes et al., 2021). Moreover, the results obtained with the caspase inhibitor suggest that ENNs A1 and B1 induce caspase-dependent apoptosis. The involvement of these enzymes in cytotoxicity of ENN A1, ENN B1 and ENN B had already been described in other cell types (Manyes et al., 2018; Wätjen et al., 2009). It is known that Ca^{2+} is involved in the activation of some caspases and that apoptosis could be associated with calcium signalling (Carreras-Sureda et al., 2018). Moreover, it has been suggested that ENNs have ionophoric properties and form membrane channels that permit the passage of ions (Kamyar et al., 2004). Therefore, the effects on calcium homeostasis of ENN A1 and B1, which had not been described before, were analysed. ENNs A1 and B1 produced Ca^{2+} depletion from intracellular reservoirs and increased Ca^{2+} uptake in a dose-dependent manner, but the way these toxins affected calcium homeostasis seems to be different. ENN A1 produced a depletion of Ca^{2+} from intracellular pools similar to the response observed when Tg, an inhibitor of the ER Ca^{2+}-ATPase, was added. Otherwise, ENN B1 generated a smaller ion depletion, suggesting that ENNs A1 and B1 altered ion homeostasis through different pathways. As the calcium profile of the ENN A1 resembled the response produced by Tg, it was determined if both compounds affected the same cell channels. The results obtained suggest that ENN A1 is affecting the ER and to other calcium reservoirs in a reversible way. When cells were treated with ENN A1 before Tg addition, the response of the latter was not altered, so the effects produced by the mycotoxin on ER seem to be reversible. Otherwise, when Tg, an irreversible inhibitor of ER Ca^{2+}-ATPase, was added before ENN A1, the effect of the toxin on intracellular pools depletion was smaller, but it was still a response, suggesting that it affects other cell compartments. As mitochondria are the second organelles with greater Ca^{2+} retention capacity, ENN A1 could be emptying this reservoir (Carreras-Sureda et al., 2018).

Therefore, the results point to a calcium-mediated apoptosis produced by ENN A1, in which ROS generation might be involved. Similar effects have been seen with the related mycotoxin BEA, whose effects on apoptosis were reversed by the addition of a calcium chelator (Chen et al., 2006). In the case of ENN B1, its cytotoxic effects on neuronal cells also occur through apoptosis. Calcium dysregulation seems to be involved in its mechanism of action, but mitochondrial dysfunction and oxidative stress are not implicated. With these data, it cannot be clearly confirmed if ENN A1 and ENN B1 are ionophores, but these toxins display different effects on calcium fluxes. Although ENN A1 and ENN B1 are structurally almost identical, dissimilarities in their chemical structure seem to lead to a different mechanism of action, a fact that has not been described to date.

Since food and feed samples commonly contain more than one

USC UNIVERSIDADE DE SANTIAGO DE COMPOSTELA

mycotoxin, as indicated by European multi-mycotoxin contamination studies (Streit et al., 2012), cytotoxic effects of binary combinations of the four ENNs were tested. In order to determine whether the co-ocurrence of toxins could enhance their toxicity, an approximation was made by combining them at 1:1 ratio. All the binary combinations tested resulted in an antagonistic effect, with the exception of ENN B1 and ENN A mixture, which presented an additive effect. This combination has been previously reported to produce additive effects in CHO–K1 and Caco-2 cells (EFSA, 2014). Therefore, co-occurrence of ENN B1 and ENN A could suppose a potential health hazard.

In conclusion, ENNs A1 and B1 alter calcium homeostasis leading to apoptotic cell death of SH-SY5Y human neuroblastoma cells. Although both ENNs present similar IC_{50} values, their mechanism of action differs since ENN A1 produced greater effects on calcium fluxes and increases ROS release. Therefore, the structural differences between ENN A1 and ENN B1 lead to dissimilarities in their mechanism of action that should be further investigated. These mechanisms of action could point to an anticancer effect of ENNs A1 and B1, however their effect in non-tumoral neurons should be assessed.

CRediT authorship contribution statement

Nadia Pérez-Fuentes: Investigation, Writing – original draft, Writing – review & editing. **Rebeca Alvariño:** Conceptualization, Methodology, Writing – review & editing. **Amparo Alfonso:** Conceptualization, Methodology, Writing – review & editing. **Jesús González-Jartín:** Investigation. **Sandra Gegunde:** Investigation. **Mercedes R. Vieytes:** Methodology. **Luis M. Botana:** Funding acquisition, Supervision.

Declaration of competing interest

The authors declare that they have no known competing financial interests or personal relationships that could have appeared to influence the work reported in this paper.

Data availability

Data will be made available on request.

Acknowledgments

The research leading to these results has received funding from the following FEDER cofunded-grants. From Conselleria de Cultura, Educacion e Ordenación Universitaria, Xunta de Galicia, GRC (ED431C 2021/01). From Ministerio de Ciencia e Innovación IISCIII/PI19/001248 and PID 2020-11262RB-C21. From European Union Interreg Agritox EAPA-998-2018, and H2020 778069-EMERTOX. R. Alvariño is supported by a postdoctoral fellowship from Xunta de Galicia (ED481B-2021-038), Spain. N.P–F. is supported by a fellowship from FIDIS, Spain.

Appendix A. Supplementary data

Supplementary data to this article can be found online at https://doi.org/10.1016/j.fct.2022.113361.

References

Alonso-Garrido, M., Frangiamone, M., Font, G., Cimbalo, A., Manyes, L., 2021. In vitro blood brain barrier exposure to mycotoxins and carotenoids pumpkin extract alters mitochondrial gene expression and oxidative stress. Food Chem. Toxicol. 153, 112261.

Alonso-Garrido, M., Tedeschi, P., Maietti, A., Font, G., Marchetti, N., Manyes, L., 2020. Mitochondrial transcriptional study of the effect of aflatoxins, enniatins and carotenoids in vitro in a blood brain barrier model. Food Chem. Toxicol. 137, 111077.

Alvariño, R., Alonso, E., Tabudravu, J.N., Pérez-Fuentes, N., Alfonso, A., Botana, L.M., 2021. Tavarua deoxyriboside A and jasplakinolide as potential neuroprotective agents: effects on cellular models of oxidative stress and neuroinflammation. ACS Chem. Neurosci. 12, 150–162.

Bertero, A., Fossati, P., Tedesco, D.E.A., Caloni, F., 2020. Beauvericin and enniatins: in vitro intestinal effects. Toxins 12.

Carreras-Sureda, A., Pihán, P., Hetz, C., 2018. Calcium signaling at the endoplasmic reticulum: fine-tuning stress responses. Cell Calcium 70, 24–31.

Chen, B.F., Tsai, M.C., Jow, G.M., 2006. Induction of calcium influx from extracellular fluid by beauvericin in human leukemia cells. Biochem. Biophys. Res. Commun. 340, 134–139.

Chou, T. C., Talalay, P., 1983. Analysis of combined drug effects: a new look at a very old problem. Trends Pharmacol. Sci. 4, 450–454.

EFSA, 2014. Scientific Opinion on the risks to human and animal health related to the presence of beauvericin and enniatins in food and feed. EFSA J. 12, 3802.

Fotakis, G., Timbrell, J.A., 2006. In vitro cytotoxicity assays: comparison of LDH, neutral red, MTT and protein assay in hepatoma cell lines following exposure to cadmium chloride. Toxicol. Lett. 160, 171–177.

Gautier, C., Pinson-Gadais, L., Richard-Forget, F., 2020. Fusarium mycotoxins enniatins: an updated review of their occurrence, the producing Fusarium species, and the abiotic determinants of their accumulation in crop harvests. J. Agric. Food Chem. 68, 4788–4798.

González-Jartín, J.M., Rodríguez-Cañás, I., Alfonso, A., Sainz, M.J., Vieytes, M.R., Gomes, A., Ramos, I., Botana, L.M., 2021. Multianalyte method for the determination of regulated, emerging and modified mycotoxins in milk: QuEChERS extraction followed by UHPLC-MS/MS analysis. Food Chem. 356, 129647.

Huang, C.H., Wang, F.T., Chan, W.H., 2019. Enniatin B1 exerts embryotoxic effects on mouse blastocysts and induces oxidative stress and immunotoxicity during embryo development. Environ. Toxicol. 34, 48–59.

Ivanov, V.T., Evstratov, A.V., Sumskaya, L.V., Melnik, E.I., Chumburidze, T.S., Portnova, S.L., Balashova, T.A., Ovchinnikov, Y.A., 1973. Sandwich complexes as a functional form of the enniatin ionophores. FEBS Lett. 36, 65–71.

Jow, G.M., Chou, C.J., Chen, B.F., Tsai, J.H., 2004. Beauvericin induces cytotoxic effects in human acute lymphoblastic leukemia cells through cytochrome c release, caspase 3 activation: the causative role of calcium. Cancer Lett. 216, 165–173.

Kamyar, M., Rawnduzi, P., Studenik, C.R., Kouri, K., Lemmens-Gruber, R., 2004. Investigation of the electrophysiological properties of enniatins. Arch. Biochem. Biophys. 429, 215–223.

Kumar, P., Nagarajan, A., Uchil, P.D., 2018. Analysis of cell viability by the MTT assay. Cold Spring Harb. Protoc. 2018, 6, 6.

Lu, C.L., Lin, H.I., Chen, B.F., Jow, G.M., 2016. Beauvericin-induced cell apoptosis through the mitogen-activated protein kinase pathway in human nonsmall cell lung cancer A549 cells. J. Toxicol. Sci. 41, 429–437.

Manyes, L., Escrivá, L., Ruiz, M.J., Juan-García, A., 2018. Beauvericin and enniatin B effects on a human lymphoblastoid Jurkat T-cell model. Food Chem. Toxicol. 115, 127–135.

Meca, G., Font, G., Ruiz, M.J., 2011. Comparative cytotoxicity study of enniatins A, A_1, A_2, B, B_1, B_4 and J_3 on Caco-2 cells, Hep-G_2 and HT-29. Food Chem. Toxicol. 49, 2464–2469.

Meca, G., Ruiz, M.J., Soriano, J.M., Ritieni, A., Moretti, A., Font, G., Mañes, J., 2010. Isolation and purification of enniatins A, A(1), B, B(1), produced by Fusarium tricinctum in solid culture, and cytotoxicity effects on Caco-2 cells. Toxicon 56, 418–424.

Oliveira, C.A.F., Ivanova, L., Solhaug, A., Fæste, C.K., 2020. Enniatin B(1)-induced lysosomal membrane permeabilization in mouse embryonic fibroblasts. Mycotoxin Res. 36, 23–30.

Prosperini, A., Font, G., Ruiz, M.J., 2014. Interaction effects of Fusarium enniatins (A, A1, B and B1) combinations on in vitro cytotoxicity of Caco-2 cells. Toxicol. Vitro 28, 88–94.

Prosperini, A., Juan-García, A., Font, G., Ruiz, M.J., 2013. Reactive oxygen species involvement in apoptosis and mitochondrial damage in Caco-2 cells induced by enniatins A, A_1, B and B_1. Toxicol. Lett. 222, 36–44.

Prusova, N., Dzuman, Z., Jelinek, L., Karabin, M., Hajslova, J., Rychlik, M., Stranska, M., 2022. Free and conjugated Alternaria and Fusarium mycotoxins during Pilsner malt production and double mash brewing. Food Chem. 369, 130926.

Pérez-Fuentes, N., Alvariño, R., Alfonso, A., González-Jartín, J., Gegunde, S., Vieytes, M. R., Botana, L.M., 2021. Single and combined effects of regulated and emerging mycotoxins on viability and mitochondrial function of SH-SY5Y cells. Food Chem. Toxicol. 154, 112308.

Reinholds, I., Jansons, M., Fedorenko, D., Pugajeva, I., Zute, S., Bartkiene, E., Bartkevics, V., 2021. Mycotoxins in cereals and pulses harvested in Latvia by nanoLC-Orbitrap MS. Food Addit. Contam. Part B Surveill 14, 115–123.

Rodríguez-Carrasco, Y., Narváez, A., Izzo, L., Gaspari, A., Graziani, G., Ritieni, A., 2020. Biomonitoring of enniatin B1 and its phase I metabolites in human urine: first large scale study. Toxins 12.

Sainz, M.J., González-Jartín, J.M., Aguín, O., Mansilla, J.P., Botana, L.M., 2018. 8. Isolation, Characterization, and Identification of Mycotoxin-Producing Fungi. De Gruyter, Berlin, Boston, pp. 202–245.

Streit, E., Schatzmayr, G., Tassis, P., Tzika, E., Marin, D., Taranu, I., Tabuc, C., Nicolau, A., Aprodu, I., Puel, O., Oswald, I.P., 2012. Current situation of mycotoxin contamination and co-occurrence in animal feed–focus on Europe. Toxins 4, 788–809.

Sánchez, J.A., Alfonso, A., Leirós, M., Alonso, E., Rateb, M.E., Jaspars, M., Houssen, W.E., Ebel, R., Botana, L.M., 2015. Spongionella secondary metabolites regulate store operated calcium entry modulating mitochondrial functioning in SH-SY5Y neuroblastoma cells. Cell. Physiol. Biochem. 37, 779–792.

Tarafdar, A., Pula, G., 2018. The role of NADPH oxidases and oxidative stress in neurodegenerative disorders. Int. J. Mol. Sci. 19.

USC UNIVERSIDADE DE SANTIAGO DE COMPOSTELA

Tonshin, A.A., Teplova, V.V., Andersson, M.A., Salkinoja Salonen, M.S., 2010. The Fusarium mycotoxins enniatins and beauvericin cause mitochondrial dysfunction by affecting the mitochondrial volume regulation, oxidative phosphorylation and ion homeostasis. Toxicology 276, 49–57.
Wätjen, W., Debbab, A., Hohlfeld, A., Chovolou, Y., Kampkötter, A., Edrada, R.A., Ebel, R., Hakiki, A., Mosaddak, M., Totzke, F., Kubbutat, M.H., Proksch, P., 2009. Enniatins A1, B and B1 from an endophytic strain of Fusarium tricinctum induce apoptotic cell death in H4IIE hepatoma cells accompanied by inhibition of ERK phosphorylation. Mol. Nutr. Food Res. 53, 431–440.
Yin, F., Boveris, A., Cadenas, E., 2014. Mitochondrial energy metabolism and redox signaling in brain aging and neurodegeneration. Antioxidants Redox Signal. 20, 353–371.

USC UNIVERSIDADE DE SANTIAGO DE COMPOSTELA

3. The Mode of Action of Enniatins A and B is Mediated by Interaction with SOC Reservoirs (A) and Mitochondrial Permeability Transition Pore (B)

Resumen:

Las eniatinas (ENNs) A y B han sido descritas durante mucho tiempo como ionóforos, pero su mecanismo de acción sigue sin estar claro. En este estudio, se analizaron sus efectos sobre los flujos de Ca^{2+} y la función mitocondrial de células de neuroblastoma humano SH-SY5Y. La ENN A causó una depleción aguda de Ca^{2+} de los reservorios intracelulares y una significativa entrada del ion desde el medio extracelular a través de canales operados por reservorios (SOC), lo cual se confirmó con el inhibidor de SOC SKF96365. La ENN B también liberó Ca^{2+} de los reservorios, pero no indujo el influjo de iones. Cuando se modularon los reservorios intracelulares dependientes de taspigargina (Tg) con este compuesto, el influjo de Ca^{2+} inducido por ENNs A y B se redujo entre un 38,8% y un 51,4%, respectivamente. Sin embargo, las micotoxinas actuaron de manera diferente. La ENN A parece actuar sobre los mismos reservorios, pero de manera distinta a la Tg, mientras que la ENN B parece afectar a los reservorios dependientes de Tg de manera similar al desacoplador mitocondrial cianuro de carbono 4-(trifluorometoxi) fenilhidrazona (FCCP). Al incubar las células con las ENNs y el FCCP, se observó que la ENN A afectó a los flujos de Ca^{2+} mitocondriales y que la ENN B mostró un comportamiento similar al FCCP. Por lo tanto, se determinaron los efectos de las ENNs sobre el poro de transición de permeabilidad mitocondrial, y se observó que ambas toxinas indujeron su apertura. Finalmente, en vista de los diferentes efectos observados sobre la homeostasis del calcio, se determinaron los efectos combinados del ENN A y ENN B sobre la viabilidad celular, resultando en antagonismo. Este estudio describe por primera vez los distintos efectos de los ENNs A y B sobre los flujos de Ca^{2+}, confirmando que estas toxinas no son ionóforos de calcio y tienen un mecanismo de acción diferente.

USC
UNIVERSIDADE DE SANTIAGO DE COMPOSTELA

Información revista:

The Mode of Action of Enniatins A and B is Mediated by Interaction with SOC Reservoirs (A) and Mitochondrial Permeability Transition Pore (B)

Nadia Pérez-Fuentes[1,2], Rebeca Alvariño[1,2], Amparo Alfonso[1,2], Jesús González-Jartín[1,2], Mercedes R. Vieytes[3], Luis M. Botana[1,2]

[1] Departamento de Farmacología, Facultad de Veterinaria, Universidad de Santiago de Compostela, 27002, Lugo, Spain
[2] Grupo de Investigación Biodiscovery, IDIS, 27002, Lugo, 27002, Spain
[3] Departamento de Fisiología, Facultad de Veterinaria, Universidad de Santiago de Compostela, 27002, Lugo, Spain

Revista: Exposure and Health
Fecha de publicación: 7 de noviembre de 2023
Enlace: https://doi.org/10.1007/s12403-023-00613-5
Editorial: SPRINGER
ISSN: 2451-9766

Índices de calidad de la revista:
Factor de impacto (2023): 4.5
Factor de impacto 5 años (2023): 5.8
Categoría (2023): "Recursos hídricos" Q1 (20/127)

Contribución doctorando:
N. P-F. llevó a cabo la realización de experimentos, análisis de datos, preparación de figuras, redacción del borrador original, revisión y edición.

Autorización revista:
Contenido reproducido con permiso:

SPRINGER NATURE

The Mode of Action of Enniatins A and B is Mediated by Interaction with SOC Reservoirs (A) and Mitochondrial Permeability Transition Pore (B)

Author: Nadia Pérez-Fuentes et al
Publication: Exposure and Health
Publisher: Springer Nature
Date: Nov 7, 2023

Copyright © 2023, The Author(s), under exclusive licence to Springer Nature B.V.

Exposure and Health
https://doi.org/10.1007/s12403-023-00613-5

ORIGINAL PAPER

The Mode of Action of Enniatins A and B is Mediated by Interaction with SOC Reservoirs (A) and Mitochondrial Permeability Transition Pore (B)

Nadia Pérez-Fuentes[1,2] · Rebeca Alvariño[1,2] · Amparo Alfonso[1,2] · Jesús González-Jartín[1,2] · Mercedes R. Vieytes[3] · Luis M. Botana[1,2]

Received: 22 May 2023 / Revised: 15 August 2023 / Accepted: 10 October 2023
© The Author(s), under exclusive licence to Springer Nature B.V. 2023

Abstract
Enniatins (ENNs) A and B have long been described as ionophores, but their mechanism of action remains unclear. In this study, their effects on Ca^{2+} fluxes and mitochondrial function were studied in SH-SY5Y human neuroblastoma cells. ENN A caused an acute Ca^{2+} depletion from intracellular pools and a significant Ca^{2+} influx from the extracellular media through store operated channels (SOC), confirmed with the SOC inhibitor SKF96365. ENN B also released Ca^{2+} from reservoirs, but it did not induce the ion influx. When thapsigargin (Tg)-dependent intracellular pools were modulated, Ca^{2+} influx induced by ENNs A and B was reduced between 38,8 and 51.4%, respectively. However, the mycotoxins acted differently. ENN A appears to act on the same reservoirs but in a different way than thapsigargin, while ENN B seems to affect thapsigargin-dependent pools similarly to the mitochondrial uncoupler carbonyl cyanide 4-(trifluoromethoxy) phenylhydrazone (FCCP). When incubating the cells with ENNs and FCCP, it was observed that ENN A affected mitochondrial Ca2 + fluxes and ENN B showed a similar behaviour to FCCP. Therefore, the effects of ENNs on mitochondrial permeability transition pore were determined, observing that both toxins induced the channel opening. Finally, in view of their different effects on calcium homeostasis, the combined effects of ENN A and ENN B on cell viability were determined, resulting in antagonism. This study describes for first time the distinct effects of ENNs A and B on Ca2 + fluxes, confirming that these toxins are not calcium ionophores and have a different mechanism of action.

Keywords Enniatins · Calcium fluxes · Mitochondria · Endoplasmic reticulum

Introduction

Calcium ion (Ca^{2+}) is a very important second messenger for neurons, it contributes to synaptic activity, it is involved in the transmission of depolarisation signals and is a key molecule in apoptosis. Cytoplasmic Ca^{2+} levels are tightly regulated by pumps, ion channels and exchangers in the plasma membrane, mitochondria, endoplasmic reticulum (ER), nucleus, Golgi apparatus and endolysosomes (Serwach and Gruszczynska-Biegala 2020; Zajac et al. 2022). In neuronal cells, the Ca^{2+} channels of the plasma membrane are divided into three main groups: voltage-gated Ca^{2+} channels, receptor-operated Ca^{2+} channels and store-operated Ca^{2+} (SOC) channels, the last type being responsible for the largest Ca^{2+} influx into these cells (Brini et al. 2014). Concerning the organelles, ER constitutes the main Ca^{2+} pool in cells. ER serves as a supply of Ca^{2+} to cytosol and mitochondria when the levels of the ion decrease (Serwach and Gruszczynska-Biegala 2020). In this regard, mitochondria are also essential for neuronal Ca^{2+} regulation because they accumulate this ion, but to a lesser extent than ER (Serwach and Gruszczynska-Biegala 2020). These organelles contribute to Ca^{2+} homeostasis by storing or releasing the ion in order to maintain its cytosolic levels. Importantly,

✉ Rebeca Alvariño
rebeca.alvarino@usc.es

✉ Amparo Alfonso
amparo.alfonso@usc.es

[1] Departamento de Farmacología, Facultad de Veterinaria, Universidad de Santiago de Compostela, 27002 Lugo, Spain

[2] Grupo de Investigación Biodiscovery, IDIS, 27002 Lugo, Spain

[3] Departamento de Fisiología, Facultad de Veterinaria, Universidad de Santiago de Compostela, 27002 Lugo, Spain

Published online: 07 November 2023

USC UNIVERSIDADE DE SANTIAGO DE COMPOSTELA

an increase in mitochondrial Ca^{2+} levels stimulates metabolism, but Ca^{2+} overload in the organelle leads to apoptosis through the opening of the mitochondrial permeability transition pore (mPTP) (Bauer and Murphy 2020; Serwach and Gruszczynska-Biegala 2020).

Enniatins (ENNs) are emerging mycotoxins produced by several fungal species, including the genera *Fusarium*, *Aspergillus* and *Penicillium*. They are N-methylated cyclic hexadepsipeptides with more than 29 described analogues, of which ENN A, ENN A1, ENN B and ENN B1 are the best known. These toxins contaminate food and feed worldwide, especially cereals, but also milk and fish, and are increasingly being detected in a growing number of foods (González-Jartín et al. 2020, 2021; Sá et al. 2023; Tolosa et al. 2014).

ENNs have a wide range of biological activities including antitumor, insecticidal, and antifungal properties. In addition, ENNs have displayed cytotoxic activity in several cell types and were recently found to produce impairment of reproductive function in cattle, so their co-occurrence in food could increasingly pose a health hazard (Chiminelli et al. 2022; Ivanova et al. 2006; Prosperini et al. 2014; Pérez-Fuentes et al. 2021). In this sense, the analysis of a milk extract containing ENNs A, A1, B and B1 has shown greater effects than expected on neuronal viability, as the presence of the four ENNs at picomolar concentrations displayed cytotoxicity, whereas the toxins alone did not affect neuronal survival up to micromolar doses in the same cell line. Moreover, the combination of ENN B1 and ENN A induced an additive effect in the same cell line (Pérez-Fuentes et al. 2021, 2022). Therefore, the risk associated to ENNs presence in natural samples could be higher than expected. Nevertheless, despite the great occurrence of these mycotoxins and their cytotoxicity, the mechanism of action of ENNs is still unknown.

ENNs effects have been traditionally related to their ionophoric nature, as in 1973 Ivanov et al. proposed that ENN B formed complexes on cell membranes that allowed the passage of ions (Ivanov et al. 1973). Since then, all ENNs have been considered as ionophores (Kamyar et al. 2004; Tonshin et al. 2010). However, the existing data on their ionophoric behaviour are scarce. It has been suggested that a mixture of ENNs A, A1, B and B1 has selective ionophoric properties for K^+ (Tonshin et al. 2010). In addition, ENNs A and ENN B affect Ca^{2+} levels in cells. ENN A augments cytosolic Ca^{2+} levels in erythrocytes while ENN B decreases the mitochondrial ion retention in boar sperm, pointing to an effect on Ca^{2+} homeostasis that has not been clarified (Jilani et al. 2011; Tonshin et al. 2010). The information on the ionophore behaviour of ENNs available to date does not clarify whether all analogues of these toxins act in the same way and how they affect ion homeostasis. On the other hand, although there is increasing data on these mycotoxins, there is insufficient recent information attempting to investigate its mechanism of action and most of them still focus only on ENN B (Aufy et al. 2023; Huang et al. 2022; Ojiro et al. 2023). It is know that ENNs also alter mitochondrial function by affecting the organelle volume regulation and impairing oxidative phosphorylation, which finally leads to apoptosis through the production of relative oxygen species (ROS) (Huang et al. 2019; Prosperini et al. 2013a, b). In this sense, we have previously proved that ENNs A and B induce apoptosis by depolarising the mitochondrial membrane in neuronal cells and that ENNs A1 and B1 affect Ca^{2+} fluxes in the same cell line (Pérez-Fuentes et al. 2021). In addition, the mechanism of action of ENN B has recently been linked to impairment of mitochondria and lysosomes, two calcium reservoirs (Søderstrøm et al. 2022).

Understanding how a compound affects calcium dynamics can help to elucidate its effects on specific cellular pathways and functions, contributing to both basic scientific knowledge and practical applications in fields such as drug development and toxicology.

In this context, and since the effect of these ENNs on calcium homeostasis has not been directly tested to date, the goal of this study was to disclose whether the mechanism of action of ENN A and ENN B is related to intracellular Ca^{2+} and mitochondria modulation in neuronal cells. In addition, the combined effects of ENNs A and B on neuronal viability were determined to analyse the potential consequences of their co-occurrence in food.

Materials and Methods

Reagents and Solutions

Cyclosporin A (CsA) was obtained from Abcam (Cambridge, UK). Dulbecco's Modified Eagle Medium: F-12 nutrient Mix (DMEM/F-12), penicillin–streptomycin (10,000 U/mL), glutamax, trypsin/EDTA (0.05%), MitoProbe™ transition pore assay kit (M34153), and CyQUANT™ lactate dehydrogenase (LDH) Cytotoxicity Assay Kit were obtained from Thermo Fisher Scientific (Madrid, Spain). ENN A, ENN B (purity > 95%), 3-(4,5-dimethyl thiazol-2-yl)-2,5-diphenyl tetrazolium bromide (MTT), saponin (SAP), 1-[β-(3-(4-methoxyphenyl) propoxy)-4-methoxyphenethyl]-1H-imidazole·HCl (SKF96365), carbonyl cyanide 4-(trifluoromethoxy) phenylhydrazone (FCCP) and other chemical reagents were purchased from Merck (Madrid, Spain). Thapsigargin (Tg) was bought in Enzo Life Sciences (Lausen, Swiss). Stock solutions of ENNs were prepared in DMSO, aliquoted, stored at -20ºC and used for the next three months. An aliquot of the stock solution was used for each experiment and serial dilutions were made in culture medium before

USC UNIVERSIDADE DE SANTIAGO DE COMPOSTELA

each treatment. The DMSO concentration varied between dilutions but was kept below 0.5% in all experiments.

Phosphate buffered saline (PBS) was composed of (in mM): 137.0 NaCl, 8.2 Na_2HPO_4, 1.5 KH_2PO_4 and 3.2 KCl (pH 7.4). The composition of Locke's buffer was (in mM): 154.0 NaCl, 10.0 HEPES, 5.6 KCl, 5.0 glucose, 3.6 $NaHCO_3$, 1.3 $CaCl_2$ and 1.0 $MgCl_2$. Umbreit solution was composed of (in mM): 119.0 NaCl, 22.85 $NaHCO_3$, 5.94 KCl, 1.2 $MgSO_4$, 1.2 NaH_2PO_4, 0.1% glucose and 1.0 $CaCl_2$. pH was adjusted between 7.2 and 7.4 in all the assays.

Cell Culture and Treatment

Human neuroblastoma cells SH-SY5Y were purchased from American Type Culture Collection (ATCC), number CRL2266. Cells were cultured in DMEM/F-12 medium supplemented with 10,000 U/mL penicillin–streptomycin, 10% foetal bovine serum (FBS) and 1% glutamax in a humidified atmosphere of 95% air and 5% CO_2 at 37ºC. Cells were dissociated weekly using 0.05% trypsin/EDTA.

Measurement of Cytosolic Free Calcium

Cytosolic calcium measurement was performed as previously described (Sánchez et al. 2015). Cells were seeded on 18-mm coverslips at a density of 5×10^5 cells per well and used after 24 h incubation. To measure Ca^{2+} levels, SH-SY5Y cells were washed twice with Umbreit solution supplemented with 0.1% BSA. The cells were then loaded with FURA-2 AM fluorescent dye at 0.5 µM. Neuroblastoma cells were plated on coverslips and shaken at 37 °C and 300 rpm for 6.5 min. Afterward, the loaded cells were washed twice with Umbreit solution and the coverslips were placed in a thermostatic chamber to maintain a constant temperature of 37 °C (Life Sciences Resources, UK). Cells were observed using a Nikon Diphot 200 inverted microscope equipped with epifluorescence optics (Nikon 40x, immersion UV-fluor objective). Compound dilutions were made in Umbreit solution without Ca^{2+} and added directly to the incubation chamber. In all the assays, the pH was adjusted between 7.2 and 7.4 using CO_2. Cells were alternately excited at 340 and 380 nm, and emission was collected at 505 nm using a fluorescence equipment composed by an ultra-high-speed wavelength switcher (Lambda-DG4) for excitation and an optical filter changer (Lambda 10–2) for emission (Sutter Instruments Co., USA). The light source was a xenon arc bulb and the wavelengths used were chosen with the filters. The fluorescence ratio (340/380) was used to determine variations in cytosolic calcium. All experiments were performed three independent times in duplicate.

Flow Cytometry Analysis of mPTP Opening

The effects of ENNs A and B on mPTP were assessed using the MitoProbe™ transition pore assay kit according to the manufacturer's instructions. For this assay, cells were seeded in 12-well plates at 1×10^6 cells per well for 24 h. SH-SY5Y cells were then resuspended in Umbreit solution, loaded with 0.01 µM calcein-AM dye and 0.4 mM $CoCl_2$, as a quencher, and treated with CsA at 0.2 µM to prevent mPTP opening. After 15 min incubation at 37 °C, cells were incubated with 2 µM ENN A and 10 µM ENN B for 10 min at 37 °C. Next, neuroblastoma cells were resuspended in commercial PBS (pH 7.2) (Thermo Fisher Scientific), filtered, and kept on ice. FCCP at 10 µM was used as a positive control for mPTP opening. Fluorescence of calcein was quantified by flow cytometry at 488 nm excitation and 517 nm emission wavelengths using the ImageStreamMKII instrument and ISX MKII software (Amnis Corporation, Luminex Corp, Austin, TX, USA). The fluorescence of 10,000 events was determined with IDEAS Application 6.0 software (Amnis Corporation, Luminex Corp).

Cell Viability Assay

The effect of ENN A and ENN B mixture on SH-Sy5Y cell viability was analysed using the MTT assay, as previously described (Pérez-Fuentes et al. 2021). Cells were seeded in 384-well plates at 2.5×10^4 cells per well and allowed to grow for 24 h. Cells were then treated with ENN A and ENN B mixed in a 1:1 ratio at concentrations ranging from 0.25 to 10 µM for 24 h, corresponding to the proportion found in naturally contaminated samples from the NW Iberian Peninsula (González-Jartín et al. 2021). Afterward, cells were washed three times with 200 µL/well of Locke's solution. Then, 200 µL/well of MTT (500 µg/mL) were added and the plate was incubated for 1 h at 37 °C and 300 rpm. MTT was removed and cells were lysed by adding 5% sodium dodecyl sulphate. Absorbance was read at 595 nm in a spectrophotometer plate reader. SAP from Quillaja bark (1 mg/mL) was used as cell death control and its absorbance was subtracted from the data obtained. All the experiments were performed in triplicate, three independent times.

Cytotoxicity Assay

CyQUANT™ LDH Cytotoxicity Assay Kit test was used to analyse the cytotoxic effects of ENN A + ENN B mixture on SH-SY5Y cells, following the manufacturer's instructions as previously described (Pérez-Fuentes et al. 2021). Cells were treated with the mixture as described above and 1 mg/mL SAP from Quillaja bark was used as death control. After 24 h treatment, LDH release was assessed by transferring 50 µL of medium from each well

USC UNIVERSIDADE DE SANTIAGO DE COMPOSTELA

to a 96-well flat-bottom plate. Absorbance was read at 490 and 680 nm in a plate reader, and the background signal (680 nm absorbance value) was subtracted from the 490 nm absorbance value to determine the release of LDH into the medium. Experiments were performed three independent times in triplicate.

Statistical Analysis

Data are expressed as the mean ± SEM of three independent experiments. Differences were assessed by one-way ANOVA followed by Dunnett's or Tukey's post hoc tests. Statistical significance was set at $*p < 0.05$, $**p < 0.01$ and $***p < 0.001$. The half maximal inhibitory concentration (IC_{50}) was calculated using GraphPad Prism 8 software by fitting the data with a log(inhibitor) vs response model, respectively.

The combination index was calculated using the Chou & Talalay equation (Chou & Talalay 1983):

$$\text{COMBINATION INDEX} = \frac{D1}{(DX)1} + \frac{D2}{(DX)2}$$

where (DX)1 and (DX)2 are the IC_{50} values of each mycotoxin alone, and D1 and D2 are the IC_{50} values of each mycotoxin in combination. If the results of the equation are < 1, = 1 and > 1, Chou & Talalay method considers synergism, additivity, or antagonism, respectively.

Results

ENNs A and B Affect Calcium Homeostasis in SH-SY5Y Cells

First, the effects of ENNs A and B on cytosolic Ca^{2+} levels were evaluated. To this end, a dose–response assay was performed with each toxin. ENN A was used at 0.5, 1 and 2 µM, while ENN B was analysed at 1, 5 and 10 µM. ENN A produced Ca^{2+} depletion from intracellular compartments at the higher dose tested. This toxin also increased ion uptake when Ca^{2+} was added to the bath solution at all the concentrations used (Fig. 1a). ENN B also caused a dose-dependent depletion of Ca^{2+} from intracellular pool, but it did not significantly increase Ca^{2+} uptake when the external ion was added to the medium, even at the higher dose tested (10 µM) (Fig. 1b).

Next, to analyse the intracellular Ca^{2+} reservoir on which ENNs A and B act, the highest doses of both toxins (2 and 10 µM, respectively) were used, and their effects were compared with those of the known control compounds. Thapsigargin (Tg), an inhibitor of the sarcoendoplasmic reticulum Ca^{2+}-ATPase (SERCA), was used at 2 µM to determine whether ENN A and ENN B affected the ER (Sánchez et al. 2015). Tg induces the depletion of Ca^{2+} from the ER to the cytosol and subsequently activates the entry of the ion through SOC channels (Luciani et al. 2009). Therefore, each ENN and Tg, and vice versa, were added sequentially to neuroblastoma cells and their

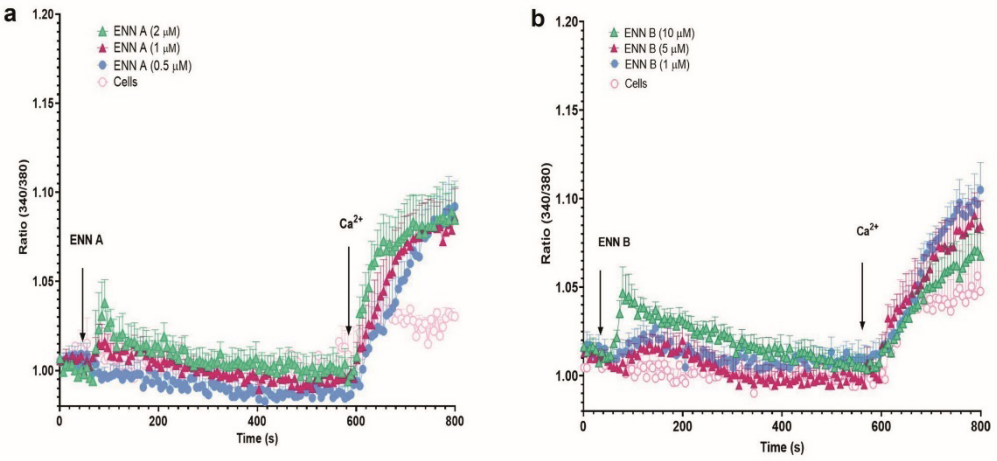


Fig. 1 Dose–response effect of ENNs A and B on cytosolic Ca^{2+} fluxes of SH-SY5Y cells. **a** ENN A dose–response assay. **b** ENN B dose–response assay. The 340/380 ratio indicates calcium cytosolic fluorescence. The first arrow shows the addition of compounds. The second arrow indicates the addition of Ca^{2+}. Mean ± SEM of three independent experiments performed by duplicate

USC UNIVERSIDADE DE SANTIAGO DE COMPOSTELA

effects on cytosolic Ca^{2+} were monitored. Regarding ENN A, the modulation of Tg-dependent intracellular Ca^{2+} pools reduced the ion depletion by 49.03% and the influx induced by this toxin by 38.8% (Fig. 2a). In addition, pre-incubation of cells with 2 µM ENN A did not inhibit the ER Ca^{2+} depletion caused by Tg. Moreover, the effects observed when the ion was added to the bath solution were similar to those produced by ENN A alone (Fig. 2b).

With respect to ENN B, its effects on intracellular Ca^{2+} pools were diminished by 73.0% when Tg was first added. Moreover, ENN B inhibited the Tg-induced Ca^{2+} influx by 51.4% (Fig. 2c). Similarly, when adding ENN B first, it also prevented the entry of Ca^{2+} produced by Tg by 52.07% but it only slightly reduced the depletion of Ca^{2+}-stores induced by the SERCA inhibitor to a 38.0% (Fig. 2d).

In view of ENN A effects on Ca^{2+} uptake, SKF96365, a known inhibitor of SOC channels, was used to determine

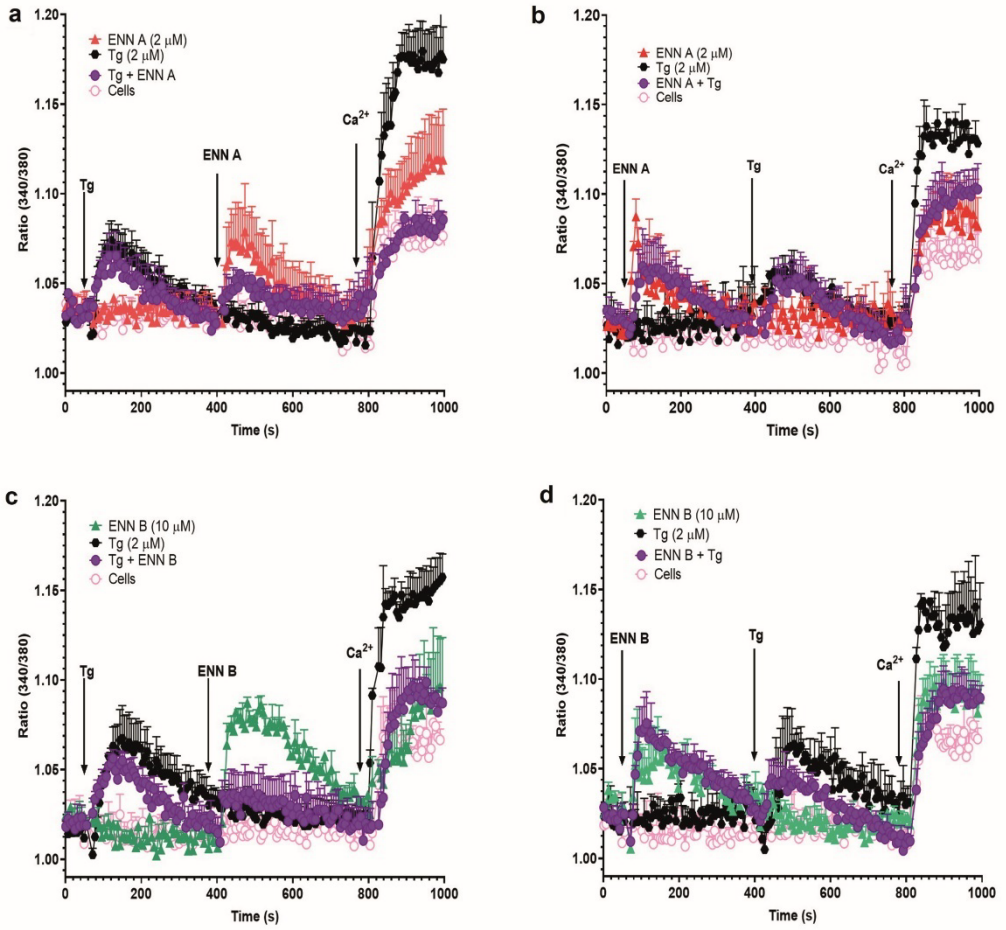


Fig. 2 Effects of ENNs and Tg on cytosolic Ca^{2+} profile of neuroblastoma cells. Cytosolic Ca^{2+} profiles of SH-SY5Y cells pre-incubated with 2 µM Tg followed by addition of 2 µM ENN A (**a**), cells pre-treated with 2 µM ENN A followed by incubation with 2 µM Tg (**b**), cells pre-incubated with 2 µM Tg followed by addition of 10 µM ENN B (**c**), and cells pre-incubated with 10 µM ENN B followed by 2 µM Tg (**d**). Arrows indicate the addition of each compound and 1 mM Ca^{2+} to the bath solution. Mean ± SEM of three independent experiments carried out by duplicate

USC UNIVERSIDADE DE SANTIAGO DE COMPOSTELA

if the mycotoxin was activating Ca^{2+} entry through these channels. At first, it was tested whether SKF96365 inhibited the Ca^{2+} influx induced by Tg, as previously described in SH-SY5Y cells (Audoin et al. 2014). As expected, addition of 30 µM SKF96365 after Tg produced a reduction in Ca^{2+} entry similar to that observed in control cells (Fig. 3a). Interestingly, a comparable blockage was observed when cells were treated with SKF96365 after ENN A addition (Fig. 3b), confirming an effect of this toxin on SOC channels.

Mitochondrial Function is Impaired by ENNs A and B in Neuronal Cells

Then, to understand the role of mitochondria in the effect of both ENNs, the mitochondrial uncoupler FCCP was used. This compound depolarises mitochondria and indirectly blocks SOC channels in different cell models (Jaiswal et al. 2009; Sánchez et al. 2015). Regarding ENN A, pre-incubation with 10 µM FCCP reduced the Ca^{2+} influx induced by the toxin when the ion was restored to the bath solution (Fig. 4a). When ENN A was added first, the toxin partially decreased FCCP-induced mitochondrial Ca^{2+} depletion by 46.2%. Interestingly, ENN A-induced Ca^{2+} entry was totally inhibited by FCCP (Fig. 4b). In the case of ENN B, pre-incubation with FCCP reduced the organelle Ca^{2+} depletion by 42.0%, while pre-incubation with the toxin did not affect the effect of the uncoupler. Both compounds caused a depletion of intracellular Ca^{2+} and they did not increase the uptake of the ion when added to the bath solution (Fig. 4c, d), which suggest that they affect the same cellular pool.

As both ENNs appear to alter the function of the mitochondria, the next step was to determine if they were affecting the opening of mPTP. For this purpose, cells were stained with calcein-AM, which diffuses into cytosol and accumulates in mitochondria. The cytosolic fluorescence was quenched with $CoCl_2$, which cannot diffuse into mitochondria and allows to monitor changes in fluorescence due to mPTP opening (Gillessen et al. 2002). In this assay, 10 µM FCCP was used as control to induce mPTP opening, and the pore inhibitor CsA was added to confirm the involvement of the channel in the mechanism of action of ENNs. As Fig. 5 shows, ENNs A and B significantly reduced calcein fluorescence by $16.1 \pm 3.07\%$ ($p < 0.01$) and $20.2 \pm 6.70\%$ ($p < 0.01$), respectively. Their effects were inhibited with a pre-treatment with 0.2 µM CsA, indicating a role of mPTP in ENNs effects. As expected, FCCP also reduced the calcein signal ($28.2 \pm 1.78\%$, $p < 0.01$), an effect inhibited by CsA.

Cytotoxic Effects of ENNs A and B Combination in SH-SY5Y Cells

In view of the different effects in cytosolic calcium of ENNs A and B, and our previous results with naturally contaminated samples, their combined cytotoxicity was determined. ENNs A and B were mixed in a 1:1 ratio, which was chosen to mimic their natural presence and based on the most common proportion found in samples from the NW Iberian Peninsula (González-Jartín et al. 2021). The concentration range (0.1–10 µM) and incubation time (24 h) were selected following our previous work (Pérez-Fuentes et al. 2021).

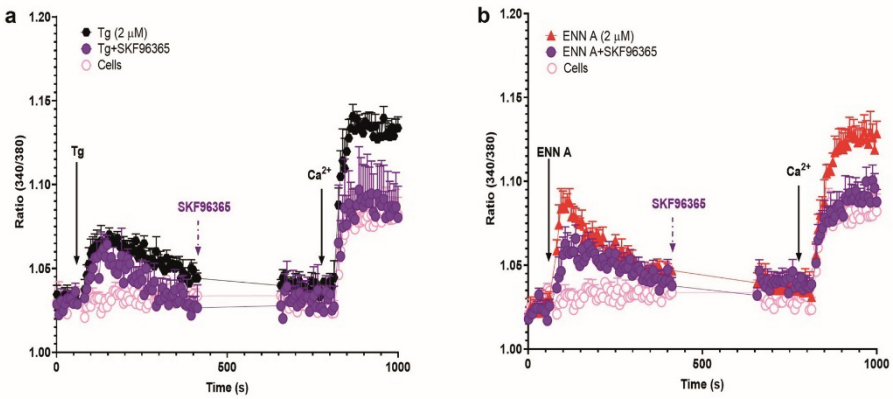


Fig. 3 Effect of ENN A and SKF96365 on cytosolic Ca^{2+} profile of SH-SY5Y cells. **a** Cytosolic Ca^{2+} profile of Tg-treated cells (solid hexagons), cells stimulated with 2 µM Tg and incubated for 5 min with 30 µM SKF96365 (solid circles) and untreated control cells (open circles). **b** Cytosolic Ca^{2+} profile of ENN A-treated cells (solid triangles), cells stimulated with 2 µM ENN A and incubated for 5 min with 30 µM SKF96365 (solid circles) and untreated control cells (open circles). Arrows indicate the addition of compounds and 1 mM Ca^{2+} to the bath medium. Mean ± SEM of three experiments performed by duplicate

USC UNIVERSIDADE DE SANTIAGO DE COMPOSTELA

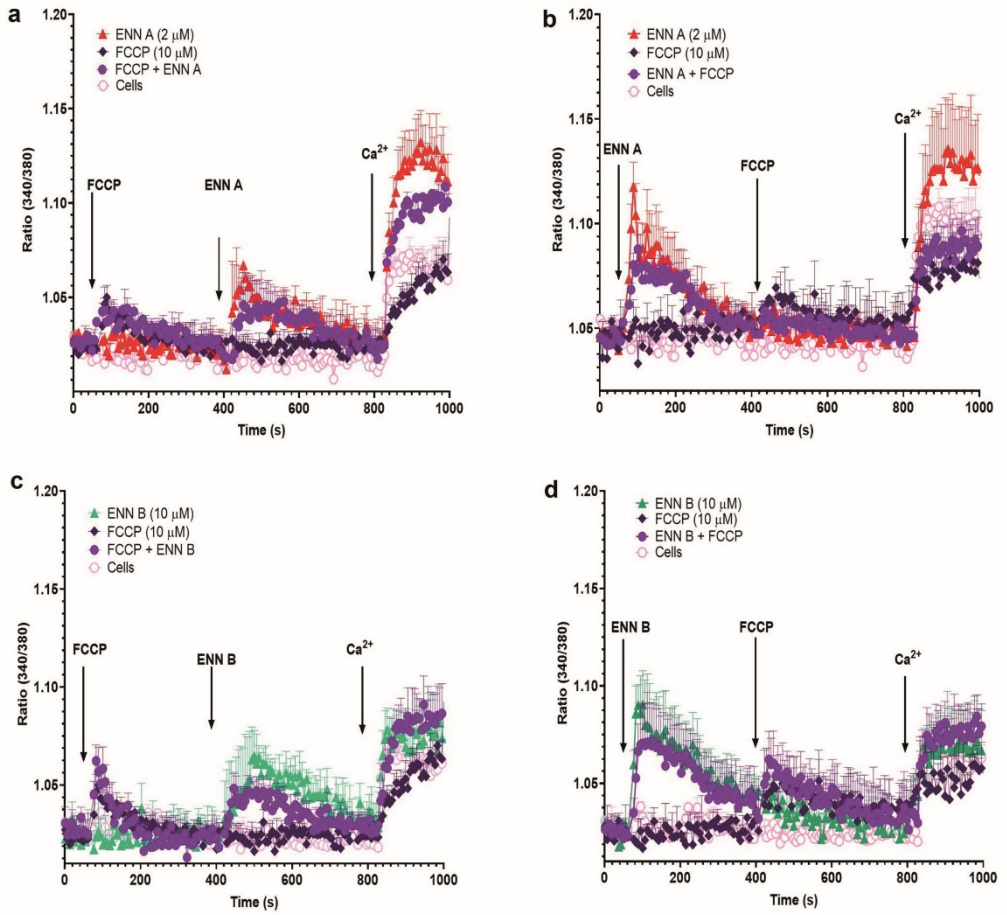


Fig. 4 Effects of ENNs A and B and FCCP on cytosolic Ca^{2+} profile of neuroblastoma cells. Cytosolic Ca^{2+} profiles of SH-SY5Y cells treated with 10 µM FCCP and 2 µM ENN A (**a**), cells pre-incubated with 2 µM ENN A followed by the addition of 10 µM FCCP (**b**), neuroblastoma cells treated with 10 µM FCCP and 10 µM ENN B (**c**), and cells incubated with 10 µM ENN B followed by 10 µM FCCP (**d**). Arrows indicate addition of compounds and 1 mM Ca^{2+} to the bath medium. Mean ± SEM of three independent replicates carried out by duplicate

The effect produced by ENN A + ENN B mixture on cell viability was determined with MTT assay. This mixture significantly injured cells at concentrations above 1.5 µM, reaching a reduction on cell viability of 93.2 ± 6.8% at 10 µM (Fig. 6a). With these results, the IC_{50} of the mixture was determined, obtaining a value of 1.5 µM (95% confidence interval: 1.4–1.7 µM). Then, combination index was calculated following Chou and Talalay method (Chou and Talalay 1983). IC_{50} values of ENN A and ENN B alone after 24 h incubation were previously determined in SH-SY5Y cells (2.3 and 0.4 µM, respectively) (Pérez-Fuentes et al. 2021). Chou and Talalay method states that if the combination index is higher than 1, it is due to an antagonistic effect, if it is equal to 1, the mixture of toxins produces an additive effect, and if it is lower than 1, it is synergistic. Applying the formula, the combination index was 4.2, so ENNs A and B presented an antagonistic effect in viability of SH-SY5Y cells.

Cytotoxicity of the binary combination was also determined with LDH assay. LDH release was increased at

USC UNIVERSIDADE DE SANTIAGO DE COMPOSTELA

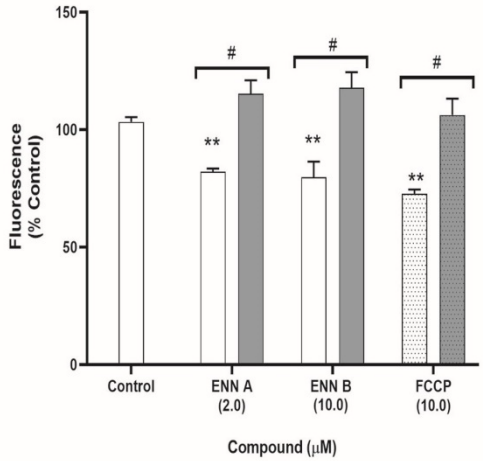


Fig. 5 Effects of ENN A and ENN B on mitochondrial permeability transition pore opening in SH-SY5Y cells. Cells were treated with 2 μM ENN A and 10 μM ENN B for 10 min and calcein fluorescence was monitored by flow cytometry. Pre-treatment with 0.2 μM CsA was used to confirm the effect of ENNs in the pore and 10 μM FCCP was included as a positive control. Mean ± SEM of three independent experiments expressed as a percentage of control cells. Statistical significance determined by one-way ANOVA and Tukey´s test (**$p \leq 0.01$, compared to control cells, (#$p \leq 0.05$, pairwise comparison)

concentrations above 2 μM, reaching a maximum level of 79.9 ± 7.1% at the highest concentration tested (Fig. 6b).

Discussion

ENNs have been described as ionophores since 1973, when it was proposed that ENN B formed complexes that allowed the passage of K^+ ions (Ivanov et al. 1973). Later, other authors adopted this assumption that the ENN family exhibited an ionophoric behaviour and continued their research on this basis. However, the present study refutes the claim of an ionophoric behaviour for Ca^{2+} of ENN A and ENN B and proposes a different new mechanism of action for these toxins based on their distinct effects on Ca^{2+} fluxes.

We have recently reported that the analogues ENN A1 and ENN B1 altered calcium homeostasis, each one showing a distinct mechanism of action (Pérez-Fuentes et al. 2022). Differences in the response to ENNs have also been described for ENN A and B, as their effects on cell survival and mitochondrial function diverge (Olleik et al. 2019). In the present work, it was observed that ENN A and B altered Ca^{2+} homeostasis in a different way, reinforcing previous results that indicated a distinct mechanism of action for each analogue (Pérez-Fuentes et al. 2021, 2022). In this sense, both ENNs induced Ca^{2+} depletion from intracellular compartments, but only ENN A caused Ca^{2+} entry when the ion was restored to the medium. The effect of ENN A in Ca^{2+} entry into cells was previously described in erythrocytes and was related to a severe depletion of ATP (Jilani et al. 2011). On the other hand, when analysing the effects of ENN B on

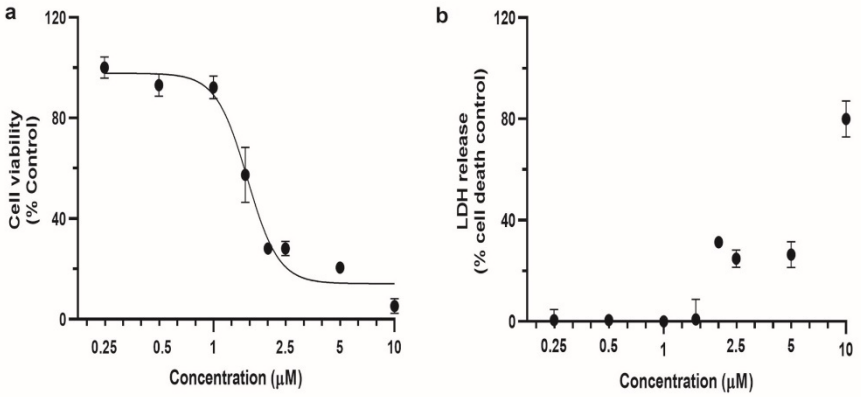


Fig. 6 Cytotoxic effects of ENN A and ENN B combination on neuroblastoma cells. **a** Effect of ENN A + ENN B (1:1) mixture on cell viability, determined by MTT test. **b** Cytotoxicity of ENN A + ENN B mixture (1:1), assessed by LDH assay. Cells were incubated with ENNs mixture for 24 h. Mean ± SEM of three independent experiments carried out by triplicate. IC50 value was determined by fitting the data with a log (inhibitor) vs response model

USC UNIVERSIDADE DE SANTIAGO DE COMPOSTELA

Ca^{2+} fluxes, it was observed that the higher the concentration of ENN B, the greater the depletion of intracellular pools, but the toxin did not induce Ca^{2+} influx from the extracellular medium.

To decipher the cellular reservoir on which ENNs A and B were acting, the effects of these mycotoxins were compared with Tg, an inhibitor of the ER Ca^{2+}-ATPase, and FCCP, a mitochondrial uncoupler. ENN A appears to act on the ER, but in a different way than Tg, because when cells were first treated with the mycotoxin, Tg-induced ER Ca^{2+} depletion was not affected. However, when cells were pre-incubated with Tg, whose effect is irreversible, ER depletion and Ca^{2+} uptake induced by ENN A were reduced (Pagliaro et al. 2021). Moreover, the Ca^{2+} influx caused by ENN A was lower than that produced by Tg. This compound inhibits the SERCA, which is responsible for the entry of Ca^{2+} into the ER. SERCA inhibition causes the release of the ion into the cytosol through IP3 and ryanodine receptor (RyR) channels and, secondarily, increases Ca^{2+} entry through SOCs (Luciani et al. 2009). Although ENN A and Tg activate SOC channels, the results suggest that ENN A acts in a different component of the ER, such as IP3 or RyR channels. In addition, ENN A seems to present a dual effect on SOC channels, as the mycotoxin alone activates calcium entry but, when it is combined with Tg, the effects of this drug were completely inhibited. ENN A may act primarily in the ER, activating proteins involved in Ca^{2+} signalling, but in the presence of another compound that affects the organelle, it would activate other signalling pathways. This dual effect suggests that ENN A could be acting on several cellular reservoirs and indirectly inducing different responses on SOC. However, the effect of ENN A on SOC channels is still unclear and demands further studies to clarify it.

On the other hand, when neuronal cells were treated with ENN A and the mitochondrial uncoupler FCCP, we observed that this mycotoxin also affected mitochondria. Pre-treatment with ENN A led to a decrease in FCCP-induced mitochondrial Ca^{2+} depletion, confirming the involvement of the organelle. Moreover, addition of FCCP after ENN A completely abolished the calcium entry induced by the toxin. Similar results have been described for the combination of Tg and FCCP in SH-SY5Y cells, where FCCP reduced the Tg-induced Ca^{2+} entry (Audoin et al. 2014). Otherwise, treatment with the mitochondrial uncoupler initially reduced, but not did not inhibit, ENN A-induced Ca^{2+} influx through SOCs. This effect in Ca^{2+} entry is lower than the observed when these cells were treated with Tg followed by FCCP (Sánchez et al. 2015). Thus, although ENN A appears to act similarly to Tg on calcium fluxes, their effects are different, reinforcing the idea that ENN A acts on a different component of the ER.

With regards to ENN B, its effects on Ca^{2+} fluxes were similar to those produced by FCCP. When cells were incubated with Tg and the toxin, there was a reduction in Tg-induced calcium efflux from reservoirs and influx through SOCs. In addition, when ENN B and FCCP were added to cells and vice versa, pre-incubation with FCCP induced a slight reduction in the ENN B-induced mitochondrial Ca^{2+} depletion, whereas the addition of the mycotoxin first had no effect on the release induced by FCCP. This suggests that ENN B may act on mitochondria similarly to FCCP, which causes a collapse of the mitochondrial membrane potential but allows a subsequent partial recovery of the organelle (Park et al. 2002). This effect could justify the damage induced by ENN B in the mitochondria, without producing total cell death, which was described in our previous study (Pérez-Fuentes et al. 2021). Therefore, the mechanism of action of ENN B could be similar to FCCP, which is a protonophore of H^+ (Benz and McLaughlin 1983).

As both ENN A and B altered mitochondrial Ca^{2+} homeostasis, which can trigger apoptosis by activating the mPTP, its effects on this channel were determined (Bauer and Murphy 2020). We had previously observed that ENN A and B depolarized mitochondria and induced apoptotic cell death in SH-SY5Y cells in the micromolar range (Pérez-Fuentes et al. 2021). In the present report, we describe that ENN A and ENN B caused mPTP opening, also in the micromolar range, in the same cell line, confirming that these mycotoxins induce mitochondrial-mediated apoptosis. The effects of ENN A on mPTP opening could be related to the increase in intracellular Ca^{2+} induced by the toxin, which would be responsible for the collapse of mitochondrial membrane potential and the decrease in ATP levels previously described in neuronal cells and erythrocytes (Jilani et al. 2011). However, the effects of ENN B appear to be predominantly associated to mitochondrial dysfunction. In this sense, ENN B has been described to alter the expression of genes related to mitochondrial electron transport chain pathway and to induce apoptosis mediated by mitochondrial disruption in different cell lines such as lymphoblasts or colorectal adenocarcinoma cells (Alonso-Garrido et al. 2018; Prosperini et al. 2013a, b; Tonshin et al. 2010). The effects of ENN B have also been linked to lysosomal impairment. Lysosomes are calcium-storing organelles, but the mechanism by which they regulate the ion homeostasis is still unclear. We have observed that ENN B has a similar effect on calcium fluxes than the protonophore FCCP, which could be due to toxin-induced proton imbalance affecting both organelles, lysosomes and mitochondria. On the other hand, ENN B has been related to inflammasome activation. These protein complexes can be stimulated by calcium signalling, so the effects on calcium fluxes induced by ENN B could be contributing to the inflammasome activation triggered by the toxin. In this sense, the role of calcium signalling in the mechanism of action of ENN B seems to be

USC UNIVERSIDADE DE SANTIAGO DE COMPOSTELA

crucial (Gammelsrud et al. 2012; Horng 2014; Ivanova et al. 2012; Søderstrøm et al. 2022).

The results obtained on calcium fluxes and mitochondrial dysfunction confirm that ENNs A and B are not calcium ionophores. In the case of ENN A, it was found to induce Ca^{2+} entry through SOC channels. Therefore, the changes in the Ca^{2+} equilibrium potential produced by a mixture of ENNs (A, A1, B and B1) observed by Kamyar et al. (2004) could be explained by the effect of ENNs A, A1 and B1 on Ca^{2+} release from intracellular pools described here and in a previous work (Kamyar et al. 2004; Pérez-Fuentes et al. 2022). In the case of ENN B, this mycotoxin did not increase Ca^{2+} influx from the extracellular medium and therefore, it cannot be considered as a Ca^{2+} ionophore. However, their possible action as ionophores for other ions should be considered. Previous studies have reported that ENN B has a pronounced preference for K^+ ions. This, together with the described effects on lysosomes and its similar mode of action to FCCP on calcium fluxes, suggests that ENN B could act as a mobile transporter for cations or protons. Consequently, it could trigger additional ion exchange mechanisms aimed at maintaining cellular homeostasis, which could justify the observed effects on calcium fluxes (Kamyar et al. 2004; Levy et al. 1995; Tonshin et al. 2010). Therefore, further studies are needed to definitively assess the ionophoric behaviour of each ENN with respect to other ions.

Finally, to gain further insights into the effects of ENNs A and B, and knowing that they affect Ca^{2+} fluxes, alter mitochondrial function and produce apoptosis, their combined effects on cell viability were determined. ENNs are commonly found together in food, and data on their joint toxicity are scarce, so there is a need to assess if their co-occurrence could pose a health hazard (Alassane-Kpembi et al. 2017; Streit et al. 2012). In neuroblastoma cells, the binary combination of ENN A and ENN B at 1:1 ratio resulted in an antagonistic effect. These results could be explained based on their effects in calcium fluxes, as ENN B presented a comparable behaviour to FCCP and ENN A act similarly to Tg in presence of the mitochondrial uncoupler (Sánchez et al. 2015). In this sense, the combination of FCCP and Tg results in a partial inhibition of Tg-induced Ca^{2+} influx through SOCs, so the mixture of both toxins could result in a reduction of ENN A-mediated Ca^{2+} entry that may explain the antagonistic effect.

In conclusion, this work clarifies that ENNs A and B have different mechanisms of action, highlighting their effects on specific cellular compartments, the ER and mitochondria. ENN B modulates calcium fluxes exclusively through the mitochondrial pathway, whereas ENN A affects both mitochondria and ER. Contrary to previous assumptions, these mycotoxins do not act as calcium ionophores, as ENN A releases Ca^{2+} through SOC channels, whereas ENN B has no effect on the ion entry. This study is a start point that demonstrates for first time that calcium fluxes are implicated in the mechanism of action of these toxins and opens a door to elucidate the signalling pathways that could be being activated by the toxins. Consequently, further research is needed to fully understand the complex effects of this family of mycotoxins.

Author Contributions All authors contributed to the study conception and design of the study. NP conducted the research and was involved in writing the original draft and in reviewing and editing the manuscript. RA and AA contributed to conceptualization, methodology, and writing, including review and editing. JG conducted investigations. MRV contributed to the methodology. Luis M. Botana was responsible for funding acquisition and provided supervision.

Funding The research leading to these results has received funding from the following FEDER cofunded-grants. From Campus Terra (USC), BreveRiesgo (2022-PU011), CLIMIGAL (2022- PU016). From Conselleria de Cultura, Educacion e Ordenación Universitaria, Xunta de Galicia, GRC (ED431C 2021/01). From Ministerio de Ciencia e Innovación IISCIII/PI19/001248, PID 2020-11262RB-C21, Grant CPP2021-008447 funded by MCIN/AEI/https://doi.org/10.13039/501100011033 and by the European Union NextGenerationEU/PRT. From European Union Interreg Agritox EAPA-998-2018, H2020 778069-EMERTOX and HORIZON-MSCA-2022-DN-01-MSCA Doctoral Networks 2022-101119901-BIOTOXDoc. R. A. is supported by a postdoctoral fellowship from Xunta de Galicia, Spain (ED481B-2021-038). N.P-F. is supported by a fellowship from FIDIS, Spain.

Data Availability All data used in this study are included in the manuscript figures.

Declarations

Competing interest The authors have no relevant financial or non-financial interests to disclose.

Ethical Approval NA.

Consent to Participate NA.

Consent to Publish NA.

References

Alassane-Kpembi I, Schatzmayr G, Taranu I, Marin D, Puel O, Oswald IP (2017) Mycotoxins co-contamination: methodological aspects and biological relevance of combined toxicity studies. Crit Rev Food Sci Nutr 57(16):3489–3507. https://doi.org/10.1080/10408398.2016.1140632

Alonso-Garrido M, Escrivá L, Manyes L, Font G (2018) Enniatin B induces expression changes in the electron transport chain pathway related genes in lymphoblastic T-cell line. Food Chem Toxicol 121:437–443. https://doi.org/10.1016/j.fct.2018.09.018

Audoin C, Sánchez JA, Genta-Jouve G, Alfonso A, Rios L, Vale C, Botana LM (2014) Autumnalamide, a prenylated cyclic peptide from the cyanobacterium Phormidium autumnale, acts on SH-SY5Y cells at the mitochondrial level. J Nat Prod 77(10):2196–2205. https://doi.org/10.1021/np500374a

USC UNIVERSIDADE DE SANTIAGO DE COMPOSTELA

Aufy M, Abdelaziz RF, Hussein AM, Topcagic N, Shamroukh H, Abdel-Maksoud MA, Studenik CR (2023) Impact of enniatin B and beauvericin on lysosomal cathepsin B secretion and apoptosis induction. Int J Mol Sci. https://doi.org/10.3390/ijms24032030

Bauer TM, Murphy E (2020) Role of Mitochondrial calcium and the permeability transition pore in regulating cell death. Circ Res 126(2):280–293. https://doi.org/10.1161/circresaha.119.316306

Benz R, McLaughlin S (1983) The molecular mechanism of action of the proton ionophore FCCP (carbonylcyanide p-trifluoromethoxyphenylhydrazone). Biophys J 41(3):381–398. https://doi.org/10.1016/s0006-3495(83)84449-x

Brini M, Calì T, Ottolini D, Carafoli E (2014) Neuronal calcium signaling: function and dysfunction. Cell Mol Life Sci 71(15):2787–2814. https://doi.org/10.1007/s00018-013-1550-7

Chiminelli I, Spicer LJ, Maylem ERS, Caloni F (2022) In Vitro Effects of Enniatin A on Steroidogenesis and Proliferation of Bovine Granulosa Cells. Toxins (basel). https://doi.org/10.3390/toxins14100714

Chou T-C, Talalay P (1983) Analysis of combined drug effects: a new look at a very old problem. Trends Pharmacol Sci 4:450–454. https://doi.org/10.1016/0165-6147(83)90490-X

Gammelsrud A, Solhaug A, Dendelé B, Sandberg WJ, Ivanova L, Kocbach Bølling A, Holme JA (2012) Enniatin B-induced cell death and inflammatory responses in RAW 2674 murine macrophages. Toxicol Appl Pharmacol 261(1):74–87. https://doi.org/10.1016/j.taap.2012.03.014

Gillessen T, Grasshoff C, Szinicz L (2002) Mitochondrial permeability transition can be directly monitored in living neurons. Biomed Pharmacother 56(4):186–193. https://doi.org/10.1016/s0753-3322(02)00184-1

González-Jartín JM, Alfonso A, Sainz MJ, Vieytes MR, Botana LM (2020) Multi-detection method for mycotoxins with a modified QuEChERS extraction in feed and development of a simple detoxification procedure. Animal Feed Sci Technol. https://doi.org/10.1016/j.anifeedsci.2020.114745

González-Jartín JM, Rodríguez-Cañás I, Alfonso A, Sainz MJ, Vieytes MR, Gomes A, Botana LM (2021) Multianalyte method for the determination of regulated, emerging and modified mycotoxins in milk: QuEChERS extraction followed by UHPLC-MS/MS analysis. Food Chem 356:129647. https://doi.org/10.1016/j.foodchem.2021.129647

Horng T (2014) Calcium signaling and mitochondrial destabilization in the triggering of the NLRP3 inflammasome. Trends Immunol 35(6):253–261. https://doi.org/10.1016/j.it.2014.02.007

Huang CH, Wang FT, Chan WH (2019) Enniatin B1 exerts embryotoxic effects on mouse blastocysts and induces oxidative stress and immunotoxicity during embryo development. Environ Toxicol 34(1):48–59. https://doi.org/10.1002/tox.22656

Huang CH, Wang FT, Chan WH (2022) Enniatin B induces dosage-related apoptosis or necrosis in mouse blastocysts leading to deleterious effects on embryo development. Drug Chem Toxicol 45(4):1449–1460. https://doi.org/10.1080/01480545.2020.1838537

Ivanov VT, Evstratov AV, Sumskaya LV, Melnik EI, Chumburidze TS, Portnova SL, Ovchinnikov YA (1973) Sandwich complexes as a functional form of the enniatin ionophores. FEBS Lett 36(1):65–71

Ivanova L, Egge-Jacobsen WM, Solhaug A, Thoen E, Fæste CK (2012) Lysosomes as a possible target of enniatin B-induced toxicity in Caco-2 cells. Chem Res Toxicol 25(8):1662–1674. https://doi.org/10.1021/tx300114x

Ivanova L, Skjerve E, Eriksen GS, Uhlig S (2006) Cytotoxicity of enniatins A, A1, B, B1, B2 and B3 from Fusarium avenaceum. Toxicon 47(8):868–876. https://doi.org/10.1016/j.toxicon.2006.02.012

Jaiswal MK, Zech WD, Goos M, Leutbecher C, Ferri A, Zippelius A, Keller BU (2009) Impairment of mitochondrial calcium handling in a mtSOD1 cell culture model of motoneuron disease. BMC Neurosci 10:64. https://doi.org/10.1186/1471-2202-10-64

Jilani K, Qadri SM, Lang E, Zelenak C, Rotte A, Bobbala D, Lang F (2011) Stimulation of erythrocyte phospholipid scrambling by enniatin A. Mol Nutr Food Res 55(2):S294-302. https://doi.org/10.1002/mnfr.201100156

Kamyar M, Rawnduzi P, Studenik CR, Kouri K, Lemmens-Gruber R (2004) Investigation of the electrophysiological properties of enniatins. Arch Biochem Biophys 429(2):215–223. https://doi.org/10.1016/j.abb.2004.06.013

Levy D, Bluzat A, Seigneuret M, Rigaud JL (1995) Alkali cation transport through liposomes by the antimicrobial fusafungine and its constitutive enniatins. Biochem Pharmacol 50(12):2105–2107. https://doi.org/10.1016/0006-2952(95)02045-4

Luciani DS, Gwiazda KS, Yang TL, Kalynyak TB, Bychkivska Y, Frey MH, Johnson JD (2009) Roles of IP3R and RyR Ca2+ channels in endoplasmic reticulum stress and beta-cell death. Diabetes 58(2):422–432. https://doi.org/10.2337/db07-1762

Ojiro R, Okano H, Ozawa S, Yamagata H, Zou X, Tang Q, Shibutani M (2023) Pharmacokinetics and 28-day repeated-dose toxicity of enniatin B after oral administration in mice. Food Chem Toxicol 177:113814. https://doi.org/10.1016/j.fct.2023.113814

Olleik H, Nicoletti C, Lafond M, Courvoisier-Dezord E, Xue P, Hijazi A, Maresca M (2019) Comparative Structure-Activity Analysis of the Antimicrobial Activity, Cytotoxicity, and Mechanism of Action of the Fungal Cyclohexadepsipeptides Enniatins and Beauvericin. Toxins (basel). https://doi.org/10.3390/toxins11090514

Pagliaro L, Marchesini M, Roti G (2021) Targeting oncogenic Notch signaling with SERCA inhibitors. J Hematol Oncol 14(1):8. https://doi.org/10.1186/s13045-020-01015-9

Park KS, Jo I, Pak K, Bae SW, Rhim H, Suh SH, Kim KW (2002) FCCP depolarizes plasma membrane potential by activating proton and Na+ currents in bovine aortic endothelial cells. Pflugers Arch 443(3):344–352. https://doi.org/10.1007/s004240100703

Prosperini A, Font G, Ruiz MJ (2014) Interaction effects of Fusarium enniatins (A, A1, B and B1) combinations on in vitro cytotoxicity of Caco-2 cells. Toxicol in Vitro 28(1):88–94. https://doi.org/10.1016/j.tiv.2013.06.021

Prosperini A, Juan-García A, Font G, Ruiz MJ (2013a) Reactive oxygen species involvement in apoptosis and mitochondrial damage in Caco-2 cells induced by enniatins A, A_1, B and B_1. Toxicol Lett 222(1):36–44. https://doi.org/10.1016/j.toxlet.2013.07.009

Prosperini A, Meca G, Font G, Ruiz MJ (2013b) Bioaccessibility of enniatins A, A_1, B, and B_1 in different commercial breakfast cereals, cookies, and breads of Spain. J Agric Food Chem 61(2):456–461. https://doi.org/10.1021/jf3044023

Pérez-Fuentes N, Alvariño R, Alfonso A, González-Jartín J, Gegunde S, Vieytes MR, Botana LM (2021) Single and combined effects of regulated and emerging mycotoxins on viability and mitochondrial function of SH-SY5Y cells. Food Chem Toxicol 154:112308. https://doi.org/10.1016/j.fct.2021.112308

Pérez-Fuentes N, Alvariño R, Alfonso A, González-Jartín J, Gegunde S, Vieytes MR, Botana LM (2022) Enniatins A1 and B1 alter calcium homeostasis of neuronal cells leading to apoptotic death. Food Chem Toxicol 168:113361. https://doi.org/10.1016/j.fct.2022.113361

Serwach K, Gruszczynska-Biegala J (2020) Target molecules of STIM proteins in the central nervous system. Front Mol Neurosci 13:617422. https://doi.org/10.3389/fnmol.2020.617422

Streit E, Schatzmayr G, Tassis P, Tzika E, Marin D, Taranu I, Oswald IP (2012) Current situation of mycotoxin contamination and co-occurrence in animal feed–focus on Europe. Toxins (basel) 4(10):788–809. https://doi.org/10.3390/toxins4100788

Sá SVM, Monteiro C, Fernandes JO, Pinto E, Faria MA, Cunha SC (2023) Emerging mycotoxins in infant and children foods: a

USC UNIVERSIDADE DE SANTIAGO DE COMPOSTELA

review. Crit Rev Food Sci Nutr 63(12):1707–1721. https://doi.org/10.1080/10408398.2021.1967282

Sánchez JA, Alfonso A, Leirós M, Alonso E, Ratcb ME, Jaspars M, Botana LM (2015) Spongionella secondary metabolites regulate store operated calcium entry modulating mitochondrial functioning in SH-SY5Y neuroblastoma cells. Cell Physiol Biochem 37(2):779–792. https://doi.org/10.1159/000430395

Søderstrøm S, Lie KK, Lundebye AK, Søfteland L (2022) Beauvericin (BEA) and enniatin B (ENNB)-induced impairment of mitochondria and lysosomes - Potential sources of intracellular reactive iron triggering ferroptosis in Atlantic salmon primary hepatocytes. Food Chem Toxicol 161:112819. https://doi.org/10.1016/j.fct.2022.112819

Tolosa J, Font G, Mañes J, Ferrer E (2014) Natural occurrence of emerging Fusarium mycotoxins in feed and fish from aquaculture. J Agric Food Chem 62(51):12462–12470. https://doi.org/10.1021/jf5036838

Tonshin AA, Teplova VV, Andersson MA, Salkinoja-Salonen MS (2010) The Fusarium mycotoxins enniatins and beauvericin cause mitochondrial dysfunction by affecting the mitochondrial volume regulation, oxidative phosphorylation and ion homeostasis. Toxicology 276(1):49–57. https://doi.org/10.1016/j.tox.2010.07.001

Zajac M, Modi S, Krishnan Y (2022) The evolution of organellar calcium mapping technologies. Cell Calcium 108:102658. https://doi.org/10.1016/j.ceca.2022.102658

Publisher's Note Springer Nature remains neutral with regard to jurisdictional claims in published maps and institutional affiliations.

Springer Nature or its licensor (e.g. a society or other partner) holds exclusive rights to this article under a publishing agreement with the author(s) or other rightsholder(s); author self-archiving of the accepted manuscript version of this article is solely governed by the terms of such publishing agreement and applicable law.

USC UNIVERSIDADE DE SANTIAGO DE COMPOSTELA

4. Enniatins A1 and B1 Modulate Calcium Flux through Alternative Pathways beyond Mitochondria

Resumen:

Las eniatinas (ENNs) A1 y B1, previamente consideradas ionóforos, son micotoxinas emergentes con efectos sobre la homeostasis de Ca^{2+}. Sin embargo, su mecanismo exacto de acción sigue sin estar claro. El presente estudio investigó cómo estas toxinas afectan al flujo de Ca^{2+} en las células SH-SY5Y. La ENN A1 indujo el influjo de Ca^{2+} a través de canales operados por reservorios (SOC). El desacoplador mitocondrial FCCP redujo este influjo, lo que sugiere que el estado mitocondrial influye en el efecto de la toxina. Por el contrario, la ENN B1 no afectó a los SOC, sino que actuó sobre otro canal de Ca^{2+}, como se demostró al añadir níquel, que bloquea directamente el poro del canal de Ca^{2+}. La función mitocondrial también influyó en los efectos de la ENN B1, ya que el tratamiento con FCCP redujo la depleción y captación de Ca^{2+} inducidas por la toxina. Además, ambas ENNs alteraron la función mitocondrial al producir la apertura del poro de transición de permeabilidad mitocondrial. Este estudio describe por primera vez que los ENNs A1 y B1 no son ionóforos de Ca^{2+} y sugiere un mecanismo de acción diferente para cada toxina.

USC
UNIVERSIDADE DE SANTIAGO DE COMPOSTELA

Información revista:

Enniatins A1 and B1 Modulate Calcium Flux through Alternative Pathways beyond Mitochondria

Nadia Pérez-Fuentes[1], Rebeca Alvariño[2], Amparo Alfonso[1], Jesús González-Jartín[1], Mercedes R. Vieytes[2], Luis M. Botana[1]

[1] Departamento de Farmacología, Facultad de Veterinaria, IDIS, Universidad de Santiago de Compostela, 27002, Lugo, Spain
[2] Departamento de Fisiología, Facultad de Veterinaria, Universidad de Santiago de Compostela, 27002, Lugo, Spain

Revista: Journal of Agricultural and Food Chemistry
Fecha de publicación: 10 de junio de 2024
Enlace: https://doi.org/10.1021/acs.jafc.4c04242
Editorial: American Chemical Society (ACS)

Índices de calidad de la revista:
Factor de impacto (2023): 5.7
Factor de impacto 5 años (2023): 6.0
Categoría (2023): "Agricultura multidisciplinaria" D1 (7/89), "Química aplicada" Q1 (12/74).

Contribución doctorando:
N. P-F. llevó a cabo la realización de experimentos, análisis de datos, preparación de figuras, redacción del borrador original, revisión y edición.

Autorización revista:
El presente artículo cuenta con una licencia creative commons CC-BY 4.0



JOURNAL OF AGRICULTURAL AND FOOD CHEMISTRY

Open Access
This article is licensed under CC-BY 4.0

pubs.acs.org/JAFC
Article

Enniatins A1 and B1 Modulate Calcium Flux through Alternative Pathways beyond Mitochondria

Nadia Pérez-Fuentes, Rebeca Alvariño,* Amparo Alfonso,* Jesús González-Jartín, Mercedes R. Vieytes, and Luis M. Botana

Cite This: https://doi.org/10.1021/acs.jafc.4c04242
Read Online

ACCESS | Metrics & More | Article Recommendations

ABSTRACT: Enniatins (ENNs) A1 and B1, previously considered ionophores, are emerging mycotoxins with effects on Ca^{2+} homeostasis. However, their exact mechanism of action remains unclear. This study investigated how these toxins affect Ca^{2+} flux in SH-SY5Y cells. ENN A1 induced Ca^{2+} influx through store-operated channels (SOC). The mitochondrial uncoupler FCCP reduced this influx, suggesting that the mitochondrial status influences the toxin effect. Conversely, ENN B1 did not affect SOC but acted on another Ca^{2+} channel, as shown when nickel, which directly blocks the Ca^{2+} channel pore, is added. Mitochondrial function also influenced the effects of ENN B1, as treatment with FCCP reduced toxin-induced Ca^{2+} depletion and uptake. In addition, both ENNs altered mitochondrial function by producing the opening of the mitochondrial permeability transition pore. This study describes for the first time that ENN A1 and B1 are not Ca^{2+} ionophores and suggests a different mechanism of action for each toxin.

KEYWORDS: *enniatin A1, enniatin B1, calcium fluxes, endoplasmic reticulum, mitochondria*

Downloaded via UNIV DE SANTIAGO DE COMPOSTELA on June 21, 2024 at 15:01:34 (UTC).
See https://pubs.acs.org/sharingguidelines for options on how to legitimately share published articles.

1. INTRODUCTION

Enniatins (ENNs) are a group of emerging mycotoxins produced by various fungi species, including *Fusarium*, *Aspergillus*, and *Penicillium* genera. These N-methylated cyclic hexadepsipeptides have over 29 analogues, with enniatin A (ENN A), enniatin A1 (ENN A1), enniatin B (ENN B), and enniatin B1 (ENN B1) being the best known. ENNs contaminate a wide range of food and feed, particularly cereals, milk, and fish, and exhibit diverse biological activities, including antifungal, insecticidal, and antitumor properties. These mycotoxins have shown cytotoxic effects in various cell types, raising concerns about their presence in food.[1−3] These studies indicate that ENNs A, A1, B, and B1 can reduce cell viability and induce apoptotic death in different cell lines at the micromolar range.[3−5] In Caco-2 cells, their effects were associated with the generation of reactive oxygen species (ROS) and with the disruption of mitochondrial function by altering the mitochondrial membrane potential (MMP).[5] In SH-SY5Y cells, ENNs A1 and B1 did not affect MMP, and only ENN A1 increased ROS production.[3,4]

Despite their widespread occurrence and cytotoxicity, the precise mechanism of action of ENNs remains unclear. Traditionally, ENNs have been identified as ionophores since it was proposed in 1973 that ENN B forms complexes on cell membranes, facilitating the passage of ions.[6] Subsequently, all ENNs were considered as ionophores.[7,8] However, information on their ionophoric behavior is limited. Some studies suggest that a mixture of ENNs A, A1, B, and B1 may exhibit potassium-selective ionophoric properties.[8] In addition, the effects of ENNs have been linked to fluctuations in divalent cations, such as calcium. Recently, ENNs A1 and B1 have been shown to alter Ca^{2+} fluxes in SH-SY5Y cells in a dose-dependent manner, and ENNs A and B were found to affect intracellular Ca^{2+} pools.[4] Furthermore, ENN A increases cytosolic Ca^{2+} levels in erythrocytes and affects store-operated channels (SOC) in human neuroblastoma cells.[9,10] Regarding ENN B, it decreases mitochondrial Ca^{2+} retention in boar spermatozoa and modifies calcium fluxes through the mitochondrial pathway in SH-SY5Y cells.[8,9]

Ca^{2+} is a crucial element for maintaining cellular homeostasis and plays a vital role at the neuronal level. Its precise regulation is essential for various cellular processes, including neurotransmission, gene expression, and cell survival. Ca^{2+} acts as a second messenger that influences synaptic plasticity and signal transmission.[11,12] The intricate control of cellular calcium levels involves dynamic interactions between various cellular compartments, which serve as reservoirs. The endoplasmic reticulum (ER) acts as a major intracellular calcium store, releasing the ion into the cytoplasm upon stimulation. It also accumulates the ion in response to specific cellular events, thereby maintaining calcium homeostasis. Mitochondria play a dual role by buffering cytoplasmic calcium and regulating their own calcium levels, which impacts energy production and cell fate. The nucleus, Golgi apparatus, peroxisomes, and endolysosomes also contribute to calcium storage and signaling, collectively orchestrating a finely tuned balance critical for neuronal function.[13]

Received: May 14, 2024
Revised: June 4, 2024
Accepted: June 10, 2024

ACS Publications
© XXXX The Authors. Published by American Chemical Society

USC UNIVERSIDADE DE SANTIAGO DE COMPOSTELA

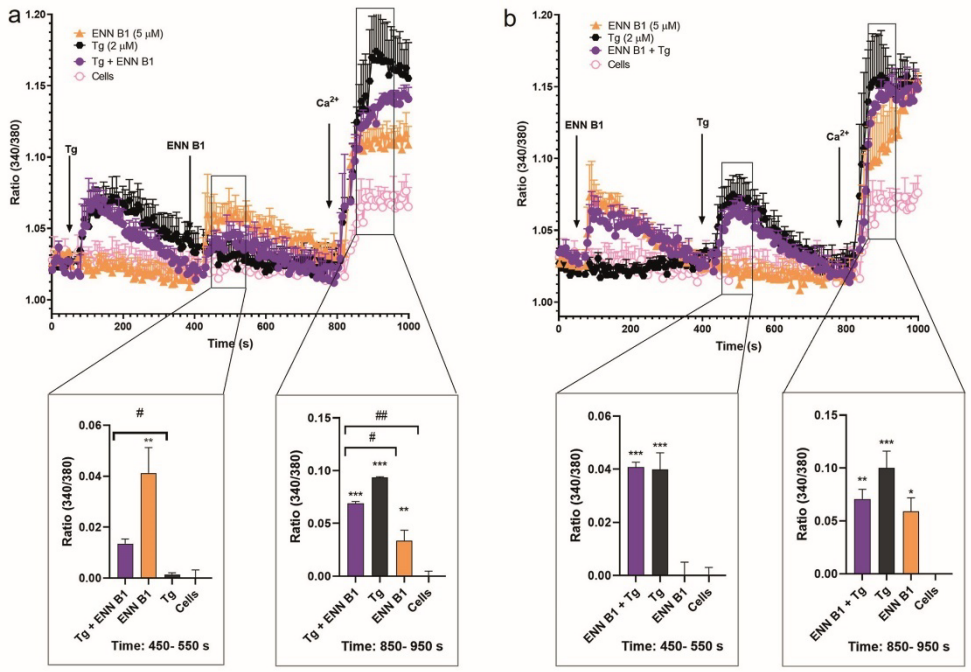


Figure 1. Effects of ENN B1 and Tg on the cytosolic Ca^{2+} profile on SH-SY5Y cells. (a) Cytosolic Ca^{2+} profiles of SH-SY5Y cells pretreated with 2 μM Tg, followed by the addition of 5 μM ENN B1. The left panel shows the quantification of Ca^{2+} release from intracellular pools between the seconds 450 and 550. The right panel presents the quantification of the Ca^{2+} plateau at the time interval 850−950 s. (b) Cytosolic Ca^{2+} profiles of cells preincubated with 5 μM ENN B1, followed by treatment with 2 μM Tg. The left panel presents the quantification of the Ca^{2+} peak (interval 450−550 s), and the right panel shows the quantification of the Ca^{2+} plateau (from 850 to 950 s). Arrows indicate the addition of compounds and 1 mM Ca^{2+} to the bath solution. Statistical significance was determined by one-way ANOVA and Dunnett's test (***$p \leq 0.001$, **$p \leq 0.01$, and *$p \leq 0.05$ compared to control cells; ###$p \leq 0.001$, #$p \leq 0.05$, pairwise comparison). The mean ± SEM of three experiments performed in duplicate.

Given this background, the objective of this study was to investigate the intracellular pools involved in the effects of ENN A1 and ENN B1 on Ca^{2+} homeostasis in SH-SY5Y human neuroblastoma cells. In a broader context, understanding the impact of ENNs on cellular processes, including Ca^{2+} homeostasis, is crucial for assessing their potential health risks and developing strategies to mitigate their effects.

2. MATERIALS AND METHODS

2.1. Reagents and Solutions. Thapsigargin (Tg) was bought from Enzo Life Sciences (Lausen, Swiss). Dulbecco's modified Eagle's medium: F-12 nutrient Mix (DMEM/F-12), penicillin−streptomycin (10,000 U/mL), trypsin/EDTA (0.05%), and glutamax were obtained from Thermo Fisher Scientific (Madrid, Spain). ENN A1, ENN B1 (purity >95%), 1-[β-(3-(4-methoxyphenyl)propoxy)-4-methoxyphenethyl]-1H-imidazole·HCl (SKF96365), carbonyl cyanide 4-(trifluoromethoxy) phenylhydrazone (FCCP), nickel chloride hexahydrate ($NiCl_2$), and other chemical reagents were purchased from Merck (Madrid, Spain). Stock solutions of ENNs were prepared in DMSO, and serial dilutions were made in a culture medium. The DMSO concentration was maintained under 0.05% in all experiments.

Umbreit solution was composed of (in mM) 119.0 NaCl, 22.85 $NaHCO_3$, 5.94 KCl, 1.2 $MgSO_4$, 1.2 NaH_2PO_4, 0.1% glucose, and 1.0 $CaCl_2$. Phosphate-buffered saline (PBS) was composed of (in mM) 137.0 NaCl, 8.2 Na_2HPO_4, 1.5 KH_2PO_4, and 3.2 KCl (pH 7.4). The composition of Locke's buffer was (in mM) 154.0 NaCl, 10.0 HEPES, 5.6 KCl, 5.0 glucose, 3.6 $NaHCO_3$, 1.3 $CaCl_2$, and 1.0 $MgCl_2$. The pH was adjusted between 7.2 and 7.4 in all the assays.

2.2. Cell Culture and Treatment. SH-SY5Y, human neuroblastoma cells were purchased from the American Type Culture Collection, number CRL2266. Cells were cultured in DMEM/F-12 medium enriched with 10,000 U/mL penicillin−streptomycin, 10% fetal bovine serum, and 1% glutamax in a humidified atmosphere of 5% CO_2 and 95% air at 37 °C. Cells were dissociated weekly using 0.05% trypsin/EDTA.

2.3. Measurement of Cytosolic-Free Calcium. Cells were plated onto 18 mm coverslips at a density of 5×10^5 cells per well and allowed to grow for 24 h. For the assessment of Ca^{2+} levels, SH-SY5Y cells were washed twice with Umbreit solution enriched with 0.1% BSA. Subsequently, the cells were loaded with FURA-2 AM fluorescent staining at a concentration of 0.5 μM for 6.5 min at 37 °C and 300 rpm. Then, cells were rinsed twice with Umbreit solution, and coverslips were positioned in a temperature-controlled chamber (Life Sciences Resources, UK) as previously explained.[4] The observation of cells was conducted using a Nikon Diaphot 200 inverted microscope equipped with epifluorescence optics (Nikon 40×, immersion UV-fluor objective).

Dilutions of compounds were prepared in an Umbreit solution lacking Ca^{2+} and directly added to the incubation chamber. Throughout the experiments, pH was maintained between 7.2 and 7.4. The cytosolic calcium ratio was determined from images captured by a fluorescence system consisting of an ultrahigh-speed wavelength switcher (Lambda-DG4) for excitation and an optical filter changer

https://doi.org/10.1021/acs.jafc.4c04242
J. Agric. Food Chem. XXXX, XXX, XXX−XXX

USC UNIVERSIDADE DE SANTIAGO DE COMPOSTELA

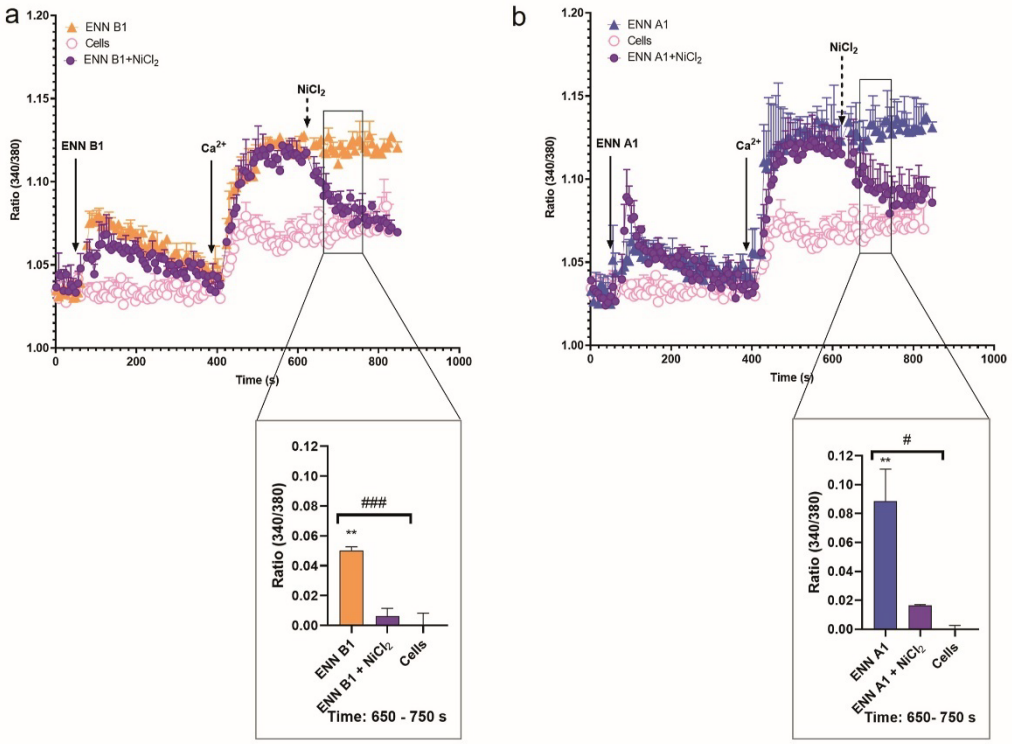


Figure 2. Effect of ENNs B1 and A1 and $NiCl_2$ on the cytosolic Ca^{2+} profile of neuroblastoma cells. (a) Cytosolic Ca^{2+} profile of ENN B1-treated cells (solid triangles), cells incubated with 5 μM ENN B1, followed by the addition of 1 mM $NiCl_2$ (solid circles), and untreated control cells (open circles). The bottom panel represents the Ca^{2+} quantification at the interval of 650−750 s. (b) Cytosolic Ca^{2+} profile of ENN A1-treated cells (solid triangles), cells incubated with 2 μM ENN A1, followed by the addition of 1 mM $NiCl_2$ (solid circles), and untreated control cells (open circles). The bottom panel represents the quantification of Ca^{2+} values from 650 to 750 s of the experiment. Arrows indicate the addition of compounds and 1 mM Ca^{2+} to the bath medium. Statistical significance was determined by one-way ANOVA and Dunnett's test (***$p \leq 0.001$, *$p \leq 0.05$ compared to control cells; ###$p \leq 0.001$, #$p \leq 0.05$, pairwise comparison). The mean ± SEM of three experiments performed in duplicate.

(Lambda 10−2) for emission (Sutter Instruments Co., USA). A xenon arc bulb served as the light source, and specific wavelengths were selected using filters. Cells were alternatively excited at 340 and 380 nm, with emission collected at 505 nm. Each experiment was performed three independent times in duplicate, with an average of 40 cells per visual field.

2.4. Flow Cytometry Analysis of Mitochondrial Permeability Transition Pore Opening. The effects of ENN A1 and B1 on mitochondrial permeability transition pore (mPTP) were assessed using the MitoProbe transition pore assay kit (Thermo Fisher Scientific), following the manufacturer's guidelines.[14,15] Cells were initially seeded in 12-well plates at a density of 1×10^6 cells per well and allowed to grow for 24 h. SH-SY5Y cells were then suspended in Umbreit solution, loaded with 0.01 μM calcein-AM and 0.4 mM $CoCl_2$, and treated with CsA at 0.2 μM and used to inhibit mPTP activation. After 15 min of incubation at 37 °C, cells were treated with 2 μM ENN A1 and 5 μM ENN B1 for 10 min at the same temperature. Then, neuroblastoma cells were suspended in commercial PBS (pH 7.2) (Thermo Fisher Scientific), filtered and kept on ice. FCCP at 10 μM was used as a positive control to induce mPTP opening. The fluorescence intensity of calcein was assessed by flow cytometry at excitation and emission wavelengths of 488 and 517 nm, respectively, using the ImageStreamMKII instrument and ISX MKII software (Amnis Corporation, Luminex Corp, Austin, TX, USA). Fluorescence from 10,000 events was quantified using IDEAS Application 6.0 software (Amnis Corporation, Luminex Corp).

2.5. Statical Analysis. The data are expressed as mean ± SEM of three independent experiments. Differences were assessed by a one-way ANOVA followed by Dunnett's or Tukey's post hoc tests. Statistical significance was set at *$p < 0.05$, **$p < 0.01$, and ***$p < 0.001$.

3. RESULTS

Based on previous work from our group, we extended our investigation into the effects of ENN A1 and ENN B1 on Ca^{2+} fluxes.[4,9] We have previously analyzed dose−response effects of these toxins and described their ability to deplete cellular Ca^{2+} stores and to induce an influx of this ion in a dose-dependent manner.[4] We have also investigated the behavior of ENN A1 in the presence of Tg, an inhibitor of the sarcoendoplasmic reticulum Ca^{2+}-ATPase (SERCA). Tg depletes Ca^{2+} from the ER, triggering the entry of the ions through the SOC. ENN A1 was found to have a calcium profile similar to Tg, suggesting that it may act on the same organelle as the SERCA inhibitor.[4]

The first step in this study was to determine the effect of ENN B1 on calcium fluxes in the presence of Tg in order to

https://doi.org/10.1021/acs.jafc.4c04242
J. Agric. Food Chem. XXXX, XXX, XXX−XXX

USC UNIVERSIDADE DE SANTIAGO DE COMPOSTELA

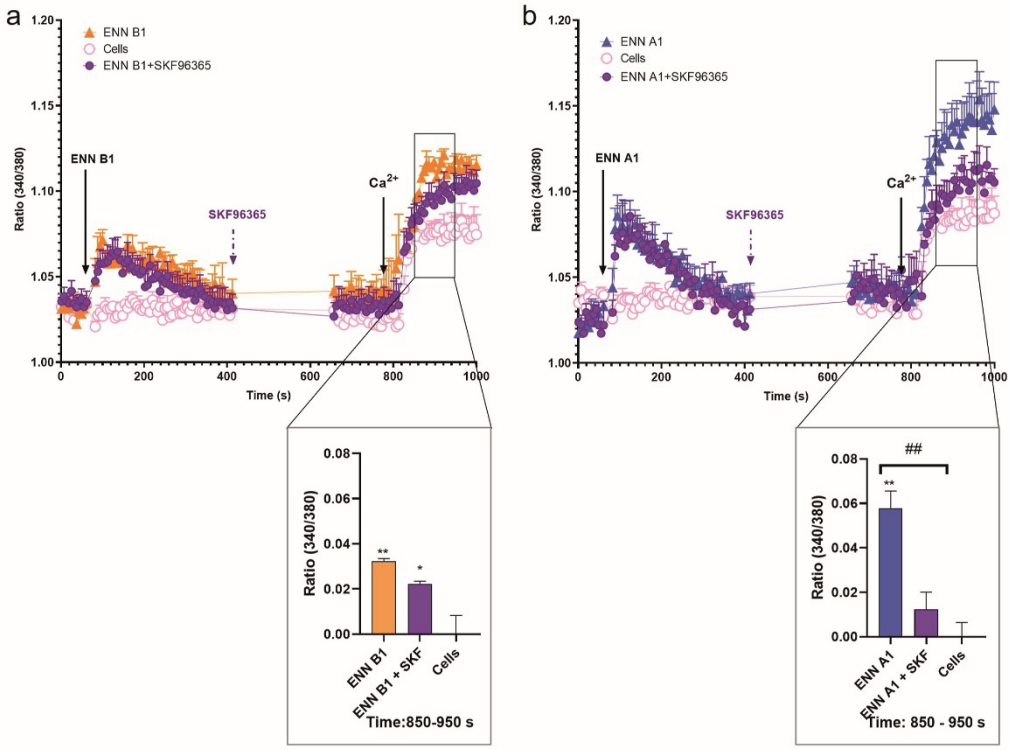


Figure 3. Effect of ENN B1, ENN A1, and SKF96365 on the cytosolic Ca^{2+} profile of neuroblastoma cells. (a) Cytosolic Ca^{2+} profile of ENN B1-treated cells (solid triangles), cells stimulated with 5 μM ENN B1 and incubated for 5 min with 30 μM SKF96365 (solid circles), and untreated control cells (open circles). The panel below represents Ca^{2+} uptake quantification at the region from 850 to 950 s. (b) Cytosolic Ca^{2+} profile of ENN A1-treated cells (solid triangles), cells stimulated with 2 μM ENN A1 and incubated for 5 min with 30 μM SKF96365 (solid circles), and untreated control cells (open circles). The panel below shows quantification of Ca^{2+} uptake at the interval of 850−950 s. Arrows indicate the addition of compounds and 1 mM Ca^{2+} to the bath medium. Statistical significance was determined by one-way ANOVA and Dunnett's test (***$p \leq 0.001$, *$p \leq 0.05$ compared to control cells; ###$p \leq 0.001$, #$p \leq 0.05$, pairwise comparison). The mean ± SEM of three experiments performed in duplicate.

elucidate its interaction with the cellular calcium regulation system. Cells were sequentially treated with 2 μM Tg and 5 μM ENN B1, concentrations that had previously shown pronounced effects on calcium fluxes in this cell line.[4,16]

The percentage of variation in the cytosolic calcium was calculated across different segments. The percentage of reduction or increase in calcium release from reservoirs and calcium uptake was calculated by comparing the effects of the compounds alone to the effects of the compound mixture. In all cases, the signal of the control cells in the corresponding interval was subtracted.

After pretreatment with Tg, the effects of ENN B1 on intracellular Ca^{2+} pools were reduced by 56.9%, and the Tg-induced Ca^{2+} influx was also diminished by 16.2% (Figure 1a). Then, cells were pretreated with the toxin, followed by the addition of Tg. In this case, there was no significant effect on Tg-induced Ca^{2+}-store depletion or Ca^{2+} influx, nor on the maximum peak of Ca^{2+} produced (Figure 1b).

Since both ENN A1 and ENN B1 resulted in an increase in Ca^{2+} uptake, $NiCl_2$, a Ca^{2+} channel blocker that inhibits Ca^{2+} channels by a direct blockade of the pore, was employed at a nontoxic concentration to determine whether the effects of ENN B1 and A1 on Ca^{2+} influx were mediated by cell membrane channels, in order to discard that the toxins were acting as ionophores.[17−20] The addition of 1 mM of $NiCl_2$ after ENN B1 significantly decreased the calcium entry produced by the toxin around 47.5%, achieving almost complete block, as observed in the interval between 650 and 750 s. These results confirmed that the Ca^{2+} uptake induced by the toxin was via a Ca^{2+} channel in the cell membrane (Figure 2a). A similar effect was observed in the case of ENN A1 (2 μM), in which $NiCl_2$ reduced the toxin-induced Ca^{2+} entry by 57.1% (Figure 2b), reaching almost basal levels.

To follow up with the study, the SOC inhibitor SKF96365 was used to determine whether ENNs A1 and B1 were activating the ion entry through these channels. The effect and concentration of SKF96365 had been previously validated in SH-SY5Y cells.[9] In the case of ENN B1, preincubation with 30 μM SKF96365 had no effect on the ion influx induced by the toxin, confirming that its effects were mediated by other

https://doi.org/10.1021/acs.jafc.4c04242
J. Agric. Food Chem. XXXX, XXX, XXX−XXX

USC UNIVERSIDADE DE SANTIAGO DE COMPOSTELA

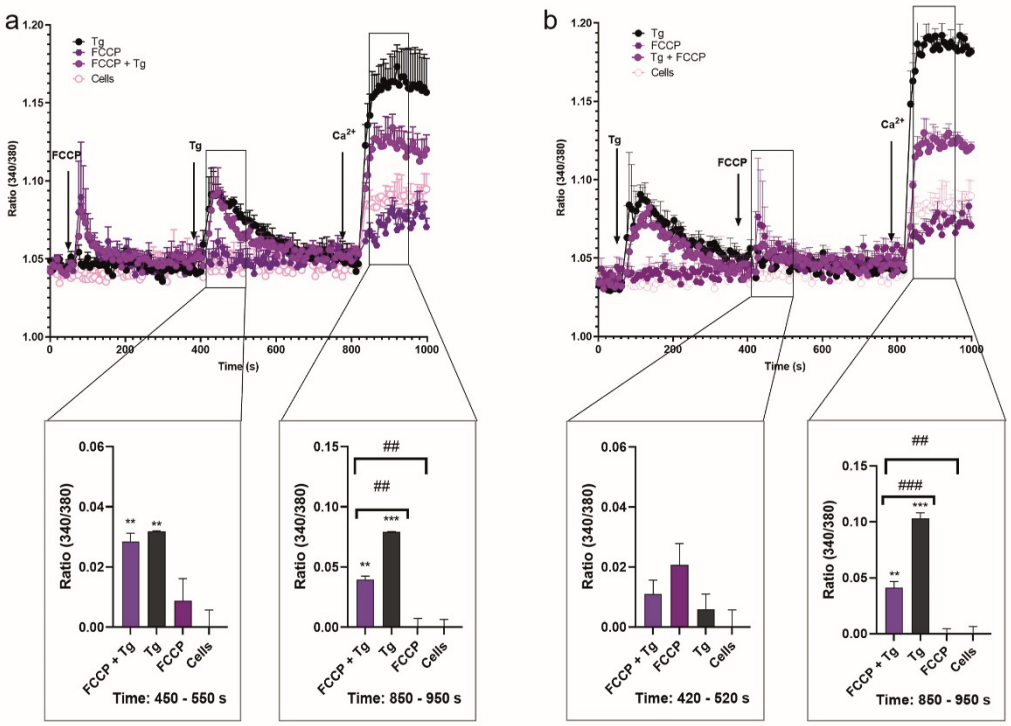


Figure 4. Effects of Tg and FCCP on the cytosolic Ca^{2+} profile of neuroblastoma cells. (a) Cytosolic Ca^{2+} profiles of SH-SY5Y cells pre-treated with 10 μM FCCP, followed by the incubation with 2 μM Tg. The left panel presents the quantification of Ca^{2+} release from intracellular pools (interval of seconds 450−550). The right panel represents the quantification of the Ca^{2+} uptake (seconds 850 to 950). (b) Cytosolic Ca^{2+} profiles of cells preincubated with 2 μM Tg, followed by the addition of 10 μM FCCP. The left panel shows the quantification of Ca^{2+} release at the seconds 420 to 520. The right panel presents the quantification of Ca^{2+} uptake (interval of seconds 850−950). Arrows indicate the addition of compounds and 1 mM Ca^{2+} to the bath medium. Statistical significance was determined by one-way ANOVA and Tukey's test (***$p \leq 0.001$, **$p \leq 0.01$ compared to control cells; ###$p \leq 0.001$, ##$p \leq 0.01$, pairwise comparison). The mean ± SEM of three independent experiments carried out in duplicate.

calcium channels (Figure 3a). By contrast, preincubation with the inhibitor resulted in an almost complete blockade of the Ca^{2+} influx produced by ENN A1, demonstrating its effect on SOC-mediated calcium entry (Figure 3b).

Then, the mitochondrial uncoupler FCCP, which releases calcium from mitochondrial stores through the opening of the mPTP, was used in the presence of both ENNs to determine whether the functional state of the organelle altered the effect produced by the toxins on the cytosolic calcium profile.[21] To this end, we first investigated how mitochondrial damage altered the Ca^{2+} profile of Tg, a compound with a known mechanism of action. Based on other assays performed by our research group, the concentration of 10 μM FCCP was chosen.[4,16] FCCP and Tg and vice versa were sequentially added to the bath solution. In both treatments, the depletion of intracellular stores induced by FCCP or Tg, compared to that produced by them alone, remained unaffected (Figure 4a,b). However, the addition of 10 μM FCCP initially resulted in a reduction of 33.2% in Tg-induced Ca^{2+} uptake (Figure 4a). On the other hand, when FCCP was added after the SERCA inhibitor, calcium influx was reduced by 43.6% when the ion was added to the bath solution (Figure 4b).

Next, the effects of ENNs A1 and B1 on Ca^{2+} fluxes were determined in the presence of the mitochondrial uncoupler. In the case of ENN A1, preincubation with 10 μM FCCP did not affect the Ca^{2+} release from intracellular reservoirs, but the ion uptake was reduced by 51.6% (Figure 5a). When ENN A1 was added first, neither ion depletion from stores nor the Ca^{2+} uptake was altered (Figure 5b). For ENN B1, preincubation with FCCP reduced the toxin-induced ion depletion to about 58.0% and decreased the ion uptake by 38.8% (Figure 5c). When ENN B1 was added first, the effects of FCCP on the intracellular pools were not diminished. However, the ENN B1-induced ion entry was reduced by 38.8% (Figure 5d).

As the mitochondrial damage induced by FCCP appeared to impact the effects of ENN A1 and ENN B1 on Ca^{2+} fluxes, it was investigated whether these toxins also affected organelle function by examining their effect on mPTP opening. With this objective, cells were stained with calcein-AM, which diffuses into the cytosol and accumulates in the mitochondria. Cytosolic fluorescence was quenched with $CoCl_2$, which

https://doi.org/10.1021/acs.jafc.4c04242
J. Agric. Food Chem. XXXX, XXX, XXX−XXX

USC UNIVERSIDADE DE SANTIAGO DE COMPOSTELA

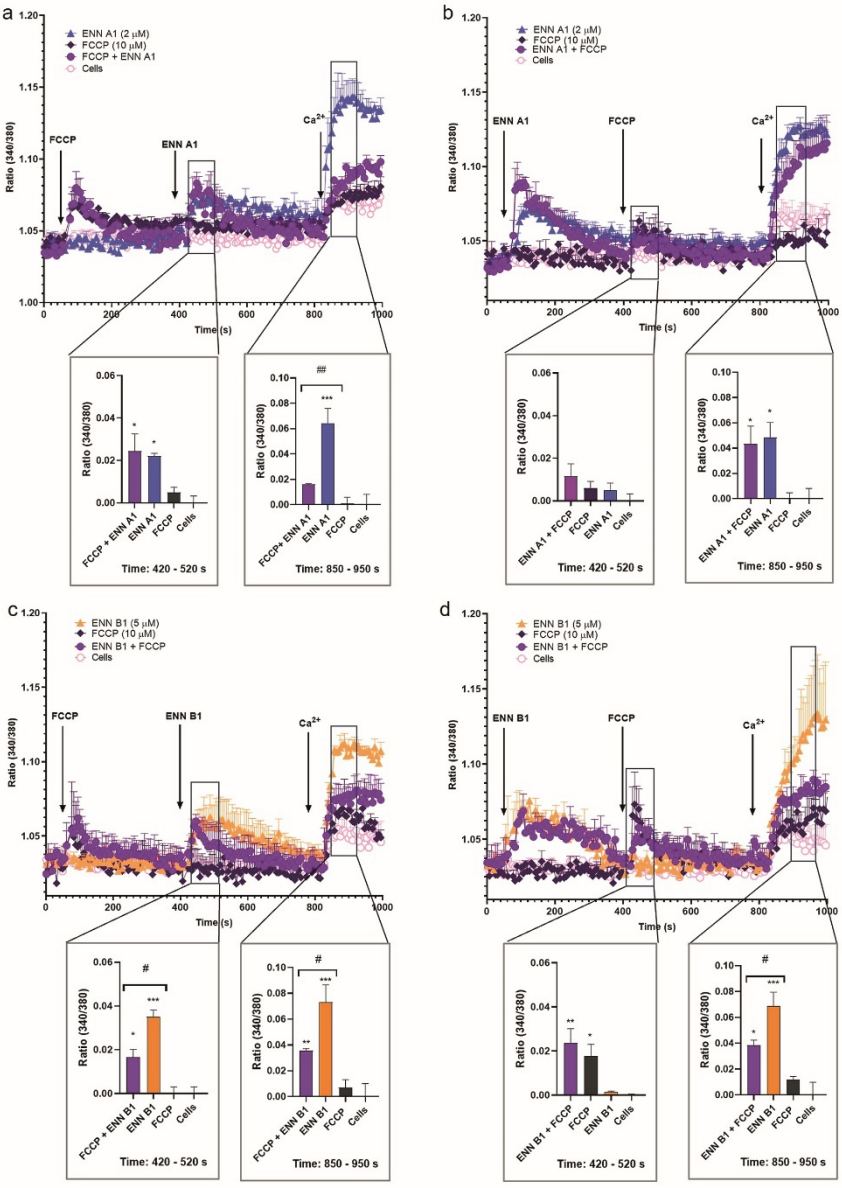


Figure 5. Effects of ENNs A1 and B1 and FCCP on the cytosolic Ca^{2+} profile of neuroblastoma cells. Cytosolic Ca^{2+} profiles of SH-SY5Y cells pretreated with 10 μM FCCP, followed by the incubation with 2 μM ENN A1 (a), cells preincubated with 2 μM ENN A1, followed by the addition of 10 μM FCCP (b), SH-SY5Y cells treated with 10 μM FCCP and 5 μM ENN B1 (c), and cells preincubated with 5 μM ENN B1, followed by 10 μM FCCP (d). Arrows indicate the addition of compounds and 1 mM Ca^{2+} to the bath medium. The left panels show Ca^{2+} peak values between the seconds 420 and 520, and the right panels present the quantification of Ca^{2+} uptake values from the second 850 to 950. Statistical significance was determined by one-way ANOVA and Dunnett's test (***$p \leq 0.001$, **$p \leq 0.01$, and *$p \leq 0.05$ compared to control cells; #$p \leq 0.05$, pairwise comparison). The mean ± SEM of three independent replicates carried out in duplicate.

https://doi.org/10.1021/acs.jafc.4c04242
J. Agric. Food Chem. XXXX, XXX, XXX−XXX

USC UNIVERSIDADE DE SANTIAGO DE COMPOSTELA

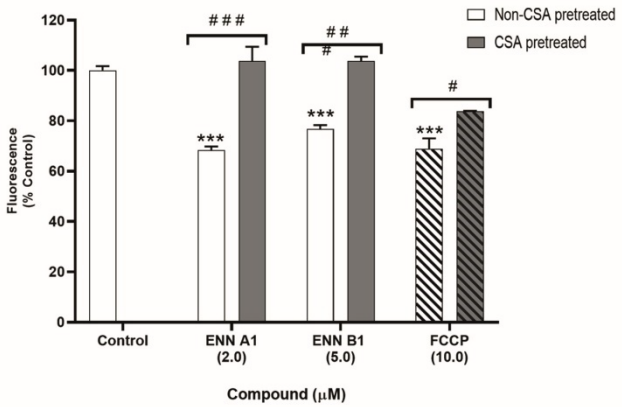


Figure 6. Effect of ENN A1 and ENN B1 on mPTP opening. SH-SY5Y cells were loaded with calcein-AM and $CoCl_2$ and treated with ENNs for 10 min. The fluorescence of 10,000 events was analyzed by flow cytometry. FCCP (bars with angled black lines) at 10 μM was used as positive control, and CsA (gray bars) at 0.2 μM was added as an inhibitor of mPTP opening. The mean ± SEM of three independent experiments expressed as a percentage of control cells. Statical significance determined by one-way ANOVA and Dunnett's test (***$p \leq 0.001$, compared to control cells; ###$p \leq 0.001$, #$p \leq 0.05$, pairwise comparison).

does not diffuse into mitochondria and allows one to monitor fluorescence changes due to mPTP opening.[22] In this assay, 10 μM FCCP was used as a control to induce mPTP opening, and the pore inhibitor CsA was added to confirm the involvement of the channel in the mode of action of ENNs. It was observed that ENN A1 and ENN B1 reduced calcein fluorescence by 32.2 ± 1.0% ($p < 0.001$) and 23.1 ± 2.2% ($p < 0.001$), respectively, and that their effects were blocked with pretreatment with 0.2 μM CsA. Similar effects were observed with the mitochondrial uncoupler FCCP, which also inhibited the calcein signal by 27.8 ± 4.2% ($p < 0.001$), an effect reversed by preincubation with CsA (Figure 6).

4. DISCUSSION

Although the cytotoxicity of ENNs A1 and B1 has been reported in different cell lines, the mode of action of these toxins has remained poorly explored. We had previously observed a proapoptotic effect of these compounds in human neuroblastoma cells, but the underlying mechanisms of this toxicity were only pointed out. Apoptosis appeared to be triggered by an increase in cytosolic calcium levels induced by toxins, as both led to a depletion of Ca^{2+} from intracellular stores and an increase in ion uptake. These observations suggested that their effects may be calcium-mediated.[4] ENNs have been described as ionophores for many years, but it has been recently demonstrated that ENN A and ENN B are not Ca^{2+} ionophores.[6,9] The current study also rejects the Ca^{2+} ionophoric behavior of ENNs A1 and B1 and highlights that, despite their structural similarities, the four analogues have different mechanisms of action, as it was suggested before.[3,4,9]

Regarding ENN A1, in our previous work, we proposed that its effect on calcium homeostasis could be mediated by the ER, as the toxin presented a Ca^{2+} profile similar to Tg[4]. In the present report, it was initially demonstrated that the toxin did not act as a calcium ionophore. First, the Ca^{2+} entry induced by the toxin was blocked with $NiCl_2$, which obstructs calcium channels of the cell membrane, especially voltage-gated ones, by direct blocking of the pore.[18] Subsequently, using SKF96365, a well-known SOC inhibitor, it was confirmed that the increase in the Ca^{2+} influx caused by the toxin was due to the activation of these channels. Then, the effects of ENN A1 were analyzed in the presence of FCCP, which uncouples the respiratory chain and is able to reduce Ca^{2+} entry through SOC in some cell models, such as SH-SY5Y cells.[16,23] It was observed that the functional state of the mitochondria affects the Ca^{2+} influx induced by ENN A1 since preincubation with the uncoupler reduces calcium uptake through SOC. Under physiological conditions, the mitochondrion serves as a regulator of Ca^{2+}, buffering its release into the cytosol from various pools and enabling the activation of SOC. Therefore, when FCCP disrupts the electron transport chain, the mitochondrion's capacity to store calcium is reduced, thereby affecting the influx through SOC.[24,25] In this sense, the effects of Tg on the induction of SOC-mediated Ca^{2+} entry were reduced when cells were treated with FCCP before and after the addition of the SERCA inhibitor. In the case of ENN A1, when the toxin has already acted, its effects on SOC entry are not reduced by FCCP. This effect could be due to the toxin acting on a component of the ER implicated in calcium efflux rather than on SERCA, which would be responsible for calcium entry into this organelle. When an inhibitor such as Tg blocks SERCA, it triggers the calcium exit pathways of the ER, leading to the activation of SOC entry and preventing the organelle from reabsorbing the ion. ENN A1 acts differently to Tg and also triggers SOC entry, suggesting that it may be involved in a calcium efflux mechanism from the ER. In this sense, inositol trisphosphate receptor (IP3R) and ryanodine receptor (RyR) are two channels involved in calcium release by ER that are expressed in human neuroblastoma cells.[26] IP3R is closely associated with mitochondria as they form a complex with the chaperone glucose-regulated protein 75 (GRP75) and voltage-dependent anion-selective channel 1 (VDAC1), one of the components of mPTP. When Ca^{2+} is released through IP3Rs, it is transferred to the mitochondria via this complex. If the levels of the ion are too high, it can lead to mPTP opening and cell death.[27] In this work, we have observed that ENN A1

https://doi.org/10.1021/acs.jafc.4c04242
J. Agric. Food Chem. XXXX, XXX, XXX−XXX

USC UNIVERSIDADE DE SANTIAGO DE COMPOSTELA

induced the pore opening so that it could act as a modulator of the IP3R−CRP75-VDAC complex. In addition, IP3R has been described as the major reticular Ca^{2+} channel in the mitochondrial-ER contact sites, regions where the ER transfers Ca^{2+} to mitochondria.[28] Therefore, IP3R could be a target of this toxin, which would explain why its effect on SOCs persists when administered prior to FCCP. Similar results were obtained with ENN A, which affects the ER and mitochondria, but the calcium profiles of the two toxins differ. These differences could be due to a distinct modulation of the IP3R-GRP75-VDAC1 complex by both analogues.[4,9]

The other analogue tested, ENN B1, was previously described to induce Ca^{2+} depletion from intracellular pools and ion entry in a dose-dependent manner.[4] In the current study, we observed that preincubation with Tg reduced the ion depletion from intracellular compartments caused by the toxin, and addition of the toxin decreased the Tg-induced Ca^{2+} uptake. These results could also indicate an effect on the ER, as observed with ENN A1. Moreover, it was verified that ENN B1 was not an ionophore as $NiCl_2$ decreased the ion uptake produced by the toxin. However, SKF96365 was unable to reduce the Ca^{2+} entry produced by the toxin, suggesting that ENN B1 activates a channel on the cell membrane other than SOC. Considering that Ca^{2+} release from the ER, either via IP3Rs or RyRs, triggers the entry of the ion via SOC, ENN B1 may be targeting another organelle, and the effects observed when preincubating with Tg may be due to interactions between different organelles, which could activate the RyRs in a secondary way.[29,30]

In this sense, the effects of ENN B1 on Ca^{2+} fluxes were also analyzed in the presence of the mitochondrial uncoupler FCCP. The addition of this compound was able to decrease the ENN B1-induced Ca^{2+} efflux from intracellular pools and the ion influx from the cell medium. However, when the toxin was added in the first place, no reduction in the mitochondrial emptying induced by FCCP was observed. Therefore, it appears that the mitochondrial status alters the effect of ENN B1 in calcium fluxes, but the toxin does not act directly in this organelle. These results are in agreement with previous studies that reported that ENN B1 did not affect MMP in either SH-SY5Y or HepG2 cells.[4,31] Therefore, the observed effects of ENN B1 on mPTP opening might be secondary due to the massive calcium entry induced by the toxin rather than a direct effect on the organelle. Interestingly, its analogue, ENN B, with small structural differences, modulates calcium by directly targeting the mitochondria, endorsing the hypothesis that each ENN has a different mechanism of action.[9]

Although the ER and the mitochondrion are the most studied intracellular calcium reservoirs, there are other organelles with calcium storage capacity, such as the nucleus, Golgi apparatus, peroxisomes, or endolysosomes, but there is limited data on their role.[13] A recent study in mouse embryonic fibroblasts suggests lysosomes as a possible early target of ENN B1, as the toxin seems to destabilize membrane-associated proteins, resulting in lysosomal alkalinization.[32] Since lysosomal Ca^{2+} channels are sensitive to pH variations, the effects produced by ENN B1 on Ca^{2+} fluxes could be related to an interaction with these organelles. Moreover, lysosomes can be associated with the ER and mitochondria, which could explain the observed long-term effects on mPTP induced by ENN B1.[13,33]

In conclusion, we describe the different effects on the calcium homeostasis of ENNs A1 and B1 in human neuroblastoma cells. Contrary to previous assumptions, neither toxin acts as a calcium ionophore. The effect of ENN A1 on Ca^{2+} signaling involves a complex interplay with the ER and mitochondria that could activate SOC entry. On the other hand, ENN B1 affects Ca^{2+} depletion from intracellular stores via a pathway different from those organelles, possibly involving lysosomes. These findings provide an important starting point for understanding the different mechanisms of action of ENNs A1 and B1 and highlight the need for further research to fully unravel the intricate complexities of their effects within cellular calcium signaling pathways.

■ ASSOCIATED CONTENT

Data Availability Statement

All data used in this study are included in the manuscript figures.

■ AUTHOR INFORMATION

Corresponding Authors

Rebeca Alvariño − *Departamento de Fisiología, Facultad de Veterinaria, IDIS, Universidad de Santiago de Compostela, Lugo 27002, Spain*; orcid.org/0000-0001-8796-1389; Email: rebeca.alvarino@usc.es

Amparo Alfonso − *Departamento de Farmacología, Facultad de Veterinaria, IDIS, Universidad de Santiago de Compostela, Lugo 27002, Spain*; orcid.org/0000-0003-1572-9016; Email: amparo.alfonso@usc.es

Authors

Nadia Pérez-Fuentes − *Departamento de Farmacología, Facultad de Veterinaria, IDIS, Universidad de Santiago de Compostela, Lugo 27002, Spain*; orcid.org/0000-0003-4660-2878

Jesús González-Jartín − *Departamento de Farmacología, Facultad de Veterinaria, IDIS, Universidad de Santiago de Compostela, Lugo 27002, Spain*; orcid.org/0000-0003-2882-504X

Mercedes R. Vieytes − *Departamento de Fisiología, Facultad de Veterinaria, IDIS, Universidad de Santiago de Compostela, Lugo 27002, Spain*

Luis M. Botana − *Departamento de Farmacología, Facultad de Veterinaria, IDIS, Universidad de Santiago de Compostela, Lugo 27002, Spain*

Complete contact information is available at: https://pubs.acs.org/10.1021/acs.jafc.4c04242

Author Contributions

All authors contributed to the conception and design of the study. Nadia Pérez-Fuentes carried out the research and was involved in writing the original draft and in reviewing and editing the manuscript. Rebeca Alvariño and Amparo Alfonso contributed to the conception, methodology, and drafting, including review and editing. Jesús González-Jartín carried out the research. Mercedes R. Vieytes contributed to the methodology. Luis M. Botana was responsible for fundraising and supervision.

Notes

The authors declare no competing financial interest.

■ ACKNOWLEDGMENTS

The research leading to these results has received funding from the following grants. From Conselleria de Cultura, Educacion e

https://doi.org/10.1021/acs.jafc.4c04242
J. Agric. Food Chem. XXXX, XXX, XXX−XXX

USC UNIVERSIDADE DE SANTIAGO DE COMPOSTELA

Ordenación Universitaria, Xunta de Galicia, GRC (ED431C 2021/01). From Ministerio de Ciencia e Innovación, PID 2020-11262RB-C21, Grant CPP2021-008447 funded by MCIN/AEI/10.13039/501100011033 and by The European Union NextGenerationEU/PRT. From European Union, Interreg EAPA-0032/2022 – BEAP-MAR, HORIZON-MSCA-2022-DN-01-MSCA Doctoral Networks 2022 101119901-BIOTOXDoc, and HORIZON-CL6-2023-CIRC-BIO-01 COMBO - 101135438.

REFERENCES

(1) Ivanova, L.; Skjerve, E.; Eriksen, G. S.; Uhlig, S. Cytotoxicity of enniatins A, A1, B, B1, B2 and B3 from Fusarium avenaceum. *Toxicon* **2006**, *47* (8), 868−876.
(2) Prosperini, A.; Font, G.; Ruiz, M. J. Interaction effects of Fusarium enniatins (A, A1, B and B1) combinations on in vitro cytotoxicity of Caco-2 cells. *Toxicol In Vitro* **2014**, *28* (1), 88−94.
(3) Pérez-Fuentes, N.; Alvariño, R.; Alfonso, A.; González-Jartín, J.; Gegunde, S.; Vieytes, M. R.; Botana, L. M. Single and combined effects of regulated and emerging mycotoxins on viability and mitochondrial function of SH-SY5Y cells. *Food Chem. Toxicol.* **2021**, *154*, 112308.
(4) Pérez-Fuentes, N.; Alvariño, R.; Alfonso, A.; González-Jartín, J.; Gegunde, S.; Vieytes, M. R.; Botana, L. M. Enniatins A1 and B1 alter calcium homeostasis of neuronal cells leading to apoptotic death. *Food Chem. Toxicol.* **2022**, *168*, 113361.
(5) Prosperini, A.; Juan-García, A.; Font, G.; Ruiz, M. J. Reactive oxygen species involvement in apoptosis and mitochondrial damage in Caco-2 cells induced by enniatins A, A_1, B and B_1. *Toxicol. Lett.* **2013**, *222* (1), 36−44.
(6) Ivanov, V. T.; Evstratov, A. V.; Sumskaya, L. V.; Melnik, E. I.; Chumburidze, T. S.; Portnova, S. L.; Balashova, T. A.; Ovchinnikov, Y. A. Sandwich complexes as a functional form of the enniatin ionophores. *FEBS Lett.* **1973**, *36* (1), 65−71.
(7) Kamyar, M.; Rawnduzi, P.; Studenik, C. R.; Kouri, K.; Lemmens-Gruber, R. Investigation of the electrophysiological properties of enniatins. *Arch. Biochem. Biophys.* **2004**, *429* (2), 215−223.
(8) Tonshin, A. A.; Teplova, V. V.; Andersson, M. A.; Salkinoja-Salonen, M. S. The Fusarium mycotoxins enniatins and beauvericin cause mitochondrial dysfunction by affecting the mitochondrial volume regulation, oxidative phosphorylation and ion homeostasis. *Toxicology* **2010**, *276* (1), 49−57.
(9) Pérez-Fuentes, N.; Alvariño, R.; Alfonso, A.; González-Jartín, J.; Vieytes, M. R.; Botana, L. M. The Mode of Action of Enniatins A and B is Mediated by Interaction with SOC Reservoirs (A) and Mitochondrial Permeability Transition Pore (B). *Expo. Health* **2023**.
(10) Jilani, K.; Qadri, S. M.; Lang, E.; Zelenak, C.; Rotte, A.; Bobbala, D.; Lang, F. Stimulation of erythrocyte phospholipid scrambling by enniatin A. *Mol. Nutr. Food Res.* **2011**, *55*, S294−S302.
(11) Burgoyne, R. D.; Helassa, N.; McCue, H. V.; Haynes, L. P. Calcium Sensors in Neuronal Function and Dysfunction. *Cold Spring Harbor Perspect. Biol.* **2019**, *11* (5), a035154.
(12) Serwach, K.; Gruszczynska-Biegala, J. Target Molecules of STIM Proteins in the Central Nervous System. *Front Mol. Neurosci* **2020**, *13*, 617422.
(13) Zajac, M.; Modi, S.; Krishnan, Y. The evolution of organellar calcium mapping technologies. *Cell Calcium* **2022**, *108*, 102658.
(14) Nguyen, T. T.; Stevens, M. V.; Kohr, M.; Steenbergen, C.; Sack, M. N.; Murphy, E. Cysteine 203 of Cyclophilin D Is Critical for Cyclophilin D Activation of the Mitochondrial Permeability Transition Pore. *J. Biol. Chem.* **2011**, *286* (46), 40184−40192.
(15) Alvariño, R.; Alonso, E.; Tribalat, M. A.; Gegunde, S.; Thomas, O. P.; Botana, L. M. Evaluation of the Protective Effects of Sarains on H(2)O(2)-Induced Mitochondrial Dysfunction and Oxidative Stress in SH-SY5Y Neuroblastoma Cells. *Neurotox Res.* **2017**, *32* (3), 368−380.
(16) Sánchez, J. A.; Alfonso, A.; Leirós, M.; Alonso, E.; Rateb, M. E.; Jaspars, M.; Houssen, W. E.; Ebel, R.; Botana, L. M. Spongionella Secondary Metabolites Regulate Store Operated Calcium Entry Modulating Mitochondrial Functioning in SH-SY5Y Neuroblastoma Cells. *Cell. Physiol. Biochem.* **2015**, *37* (2), 779−792.
(17) Pernas-Sueiras, O.; Alfonso, A.; Vieytes, M. R.; Orfao, A.; Escribano, L.; Francisca, S. J.; Botana, L. M. Calcium-pH crosstalks in the human mast cell line HMC-1: intracellular alkalinization activates calcium extrusion through the plasma membrane Ca2+-ATPase. *J. Cell. Biochem.* **2006**, *99* (5), 1397−1408.
(18) Obejero-Paz, C. A.; Gray, I. P.; Jones, S. W. Ni2+ Block of CaV3.1 (α1G) T-type Calcium Channels. *J. Gen Physiol* **2008**, *132* (2), 239−250.
(19) Fischer, M. J. E.; Paulussen, J. J. C.; de Mol, N. J.; Janssen, L. H. M. Dual Effect of the Anti-Allergic Astemizole on Ca2 Fluxes in Rat Basophilic Leukemia (RBL-2H3) Cells: Release of Ca2 from Intracellular Stores and Inhibition of Ca2 Release-Activated Ca2 Influx. *Biochem. Pharmacol.* **1998**, *55* (8), 1255−1262.
(20) Xu, S.; He, M.; Zhong, M.; Li, L.; Lu, Y.; Zhang, Y.; Zhang, L.; Yu, Z.; Zhou, Z. The neuroprotective effects of taurine against nickel by reducing oxidative stress and maintaining mitochondrial function in cortical neurons. *Neurosci. Lett.* **2015**, *590*, 52−57.
(21) Breitbart, H.; Rubinstein, S.; Gruberger, M. Calcium efflux mechanism in sperm mitochondria. *Biochim. Biophys. Acta* **1996**, *1312* (2), 79−84.
(22) Gillessen, T.; Grasshoff, C.; Szinicz, L. Mitochondrial permeability transition can be directly monitored in living neurons. *Biomed Pharmacother* **2002**, *56* (4), 186−193.
(23) Hernández-Morales, M.; Sobradillo, D.; Valero, R. A.; Muñoz, E.; Ubierna, D.; Moyer, M. P.; Núñez, L.; Villalobos, C. Mitochondria sustain store-operated currents in colon cancer cells but not in normal colonic cells: reversal by non-steroidal anti-inflammatory drugs. *Oncotarget* **2017**, *8* (33), 55332−55352.
(24) Demine, S.; Renard, P.; Arnould, T. Mitochondrial Uncoupling: A Key Controller of Biological Processes in Physiology and Diseases. *Cells* **2019**, *8* (8), 795.
(25) Glitsch, M. D.; Bakowski, D.; Parekh, A. B. Store-operated Ca2+ entry depends on mitochondrial Ca2+ uptake. *EMBO J* **2002**, *21* (24), 6744−6754.
(26) Liu, X.; Song, S.; Wang, Q.; Yuan, T.; He, J. A mutation in β-amyloid precursor protein renders SH-SY5Y cells vulnerable to isoflurane toxicity: The role of inositol 1,4,5-trisphosphate receptors. *Mol. Med. Rep* **2016**, *14* (6), 5435−5442.
(27) de Ridder, I.; Kerkhofs, M.; Lemos, F. O.; Loncke, J.; Bultynck, G.; Parys, J. B. The ER-mitochondria interface, where Ca(2+) and cell death meet. *Cell Calcium* **2023**, *112*, 102743.
(28) Ahumada-Castro, U.; Puebla-Huerta, A.; Cuevas-Espinoza, V.; Lovy, A.; Cardenas, J. C. Keeping zombies alive: The ER-mitochondria Ca(2+) transfer in cellular senescence. *Biochim Biophys Acta Mol. Cell Res.* **2021**, *1868* (11), 119099.
(29) Stanzione, R.; Forte, M.; Cotugno, M.; Bianchi, F.; Marchitti, S.; Rubattu, S. Relevance of stromal interaction molecule 1 (STIM1) in experimental and human stroke. *Pflugers Arch. Eur. J. Physiol.* **2022**, *474* (1), 141−153.
(30) Bootman, M. D.; Bultynck, G. Fundamentals of Cellular Calcium Signaling: A Primer. *Cold Spring Harbor Perspect. Biol.* **2020**, *12* (1), a038802.
(31) Juan-García, A.; Ruiz, M. J.; Font, G.; Manyes, L. Enniatin A1, enniatin B1 and beauvericin on HepG2: Evaluation of toxic effects. *Food Chem. Toxicol.* **2015**, *84*, 188−196.
(32) Oliveira, C. A. F.; Ivanova, L.; Solhaug, A.; Fæste, C. K. Enniatin B(1)-induced lysosomal membrane permeabilization in mouse embryonic fibroblasts. *Mycotoxin Res.* **2020**, *36* (1), 23−30.
(33) Galione, A.; Muallem, S. Preface. Endolysosomal calcium signalling. *Cell Calcium* **2023**, *110*, 102696.

https://doi.org/10.1021/acs.jafc.4c04242
J. Agric. Food Chem. XXXX, XXX, XXX−XXX

USC UNIVERSIDADE DE SANTIAGO DE COMPOSTELA

USC
UNIVERSIDADE
DE SANTIAGO
DE COMPOSTELA

5. In Vitro Testing of Lung Carcinogenicity for an In Silico-Identified Cluster of Mycotoxins

Resumen:

La presencia de micotoxinas emergentes en alimentos y piensos se ha reportado en todo el mundo, pero los estudios sobre sus efectos tóxicos aún son limitados. En un estudio previo basado en enfoques in silico se evidenció la asociación entre algunas micotoxinas emergentes y el cáncer de pulmón de células no pequeñas. En este trabajo, se realizó una investigación toxicológica in vitro de estas micotoxinas (eniatina A, eniatina B, beauvericina, apicidina y destruxina B). Se evaluaron varias vías involucradas en el cáncer de pulmón, incluídas en la base de datos KEGG de cáncer, en células de pulmón humano A549 y NCI-H226. Se determinaron los efectos sobre la viabilidad, apoptosis, ciclo celular, daño del ADN, especies reactivas de oxígeno y secreción de IL-8 después de un tratamiento de 24 horas con micotoxinas a concentraciones entre 0.01 y 100 μM. La eniatina A, beauvericina y apicidina presentaron una respuesta similar en todos los puntos evaluados. Además, fueron los compuestos más tóxicos, con una IC_{50} alrededor de 2.2 y 13.1 μM, e inducción de apoptosis en ambas líneas celulares. La eniatina B no indujo una disminución completa de la viabilidad celular y no provocó apoptosis. La destruxina B aumentó la actividad de la caspasa 3 y alteró el ciclo celular a concentraciones superiores a 6.25 μM en células A549, sugiriendo activación de apoptosis, aunque no redujo la viabilidad celular en ninguna de las líneas celulares. Finalmente, las eniatinas A y B, apicidina, beauvericina y destruxina B aumentaron la liberación de la IL-8 proinflamatoria. Los resultados in vitro de este trabajo confirmaron la predicción utilizando enfoques in silico, ya que algunos signos distintivos del cáncer pueden observarse después del tratamiento de células pulmonares con este grupo de micotoxinas. Los efectos tóxicos observados en células pulmonares humanas confirmaron que la presencia de estas micotoxinas emergentes en productos agrícolas, alimentos y piensos podría ser peligrosa para la salud humana y se perfiló aún más un vínculo con el cáncer de pulmón para tres de ellas.

USC
UNIVERSIDADE DE SANTIAGO DE COMPOSTELA

Información revista:

In Vitro Testing of Lung Carcinogenicity for an In Silico-Identified Cluster of Mycotoxins

Denis Habauzit[1], Rebeca Alvariño[2,3], Nadia Perez-Fuentes[2,3], Sylvie Huet[1], Amparo Alfonso[2,3], Kevin Hogeveen[1], Luis M. Botana[2,3], Valérie Fessard[1]

[1] French Agency for Food, Environmental and Occupational Health & Safety (ANSES), Fougères, France
[2] Departamento de Farmacología, Facultad de Veterinaria, Universidad de Santiago de Compostela, 27002, Lugo, Spain
Grupo de Investigación Biodiscovery, IDIS, 27002, Lugo, 27002, Spain
[3] Grupo Investigación Biodiscovery, IDIS, 27002, Lugo, Spain

Revista: Exposure and Health
Fecha de publicación: 22 de septiembre de 2023
Enlace: https://doi.org/10.1007/s12403-023-00601-9
Editorial: SPRINGER
ISSN: 2451-9766

Índices de calidad de la revista:
Factor de impacto (2023): 4.5
Factor de impacto 5 años (2023): 5.8
Categoría (2023): "Recursos hídricos" Q1 (20/127)

Contribución doctorando:
N. P-F. llevó a cabo la realización de experimentos en la línea NCI-H226, análisis de datos y preparación de figuras.

Autorización revista:
Contenido reproducido con permiso:

SPRINGER NATURE

In Vitro Testing of Lung Carcinogenicity for an In Silico-Identified Cluster of Mycotoxins
Author: Denis Habauzit et al
Publication: Exposure and Health
Publisher: Springer Nature
Date: Sep 22, 2023

Copyright © 2023, The Author(s), under exclusive licence to Springer Nature B.V.

USC UNIVERSIDADE DE SANTIAGO DE COMPOSTELA

Exposure and Health
https://doi.org/10.1007/s12403-023-00601-9

ORIGINAL PAPER

In Vitro Testing of Lung Carcinogenicity for an In Silico-Identified Cluster of Mycotoxins

Denis Habauzit[1] · Rebeca Alvariño[2,3] · Nadia Pérez-Fuentes[2,3] · Sylvie Huet[1] · Amparo Alfonso[2,3] · Kevin Hogeveen[1] · Luis M. Botana[2,3] · Valérie Fessard[1]

Received: 16 December 2022 / Revised: 17 May 2023 / Accepted: 5 September 2023
© The Author(s), under exclusive licence to Springer Nature B.V. 2023

Abstract
Occurrence of emerging mycotoxins in food and feed is reported worldwide, but studies on their toxic effects are still limited. Our previous study based on in silico approaches has evidenced an association between some cyclic peptidic mycotoxins and non-small cell lung cancer. In this work, an in vitro toxicological investigation of these mycotoxins (enniatin A, enniatin B, beauvericin, apicidin and destruxin B) was performed. Several pathways involved in lung cancer pathology, as revealed by the KEGG pathway map, were tested on A549 and NCI-H226 human lung cells. Effects on viability, apoptosis, cell cycle, DNA damage, reactive oxygen species, and IL-8 secretion were determined after 24-h mycotoxin treatment at concentrations between 0.01 and 100 µM. Enniatin A, beauvericin and apicidin presented a similar response for all endpoints. Moreover, they were the most toxic compounds, with IC_{50} around 2.2 and 13.1 µM, and apoptosis induction in both cell lines. Enniatin B did not induce a complete decrease in cell viability and did not provoke apoptosis. Destruxin B increased caspase 3 activity and altered cell cycle at concentrations above 6.25 µM in A549 cells, suggesting apoptosis activation, although it did not reduce cell viability in either cell line. Finally, enniatins A and B, apicidin, beauvericin and destruxin B increased the release of the pro-inflammatory IL-8. The in vitro results of this work confirmed the prediction using in silico approaches as some hallmarks of cancer can be observed after treatment of lung cells with this mycotoxin cluster. The toxic effects observed in human lung cells confirmed that the presence of these emerging mycotoxins in agricultural products, food and feed might be hazardous for human health and that a link with lung cancer was further outlined for three of them.

Keywords Hazard · In vitro testing · Viability · Apoptosis · Cell cycle · Inflammation

Introduction

Mycotoxins are secondary metabolites produced by fungi that are toxic against a large panel of organisms (bacteria, other fungi, animals and humans) (Goldblatt 1972). Their occurrence in agricultural products is a global challenge, since their presence in food and feed is dangerously increasing. Fungal infestation, and thus mycotoxin contamination, is favoured by increased humidity and temperature related to climate change (Azman et al. 2021; Liu and Van der Fels-Klerx 2021). Therefore, food and feed contamination at each step from seeds to transformed products (Pleadin et al. 2019; Pócsi et al. 2020) and, consequently, human health concerns associated to mycotoxins are expected to grow in the coming years (Liu and Van der Fels-Klerx 2021; Medina et al. 2017).

More than 500 mycotoxins have been described so far (Sulyok et al. 2020), but only some of them are present in food and feed and can be dangerous for animals and humans. Most of them are produced by filamentous fungi of the genera *Aspergillus*, *Fusarium* and *Penicillium* (Awuchi et al. 2021). Currently, maximum legal limits have been established for few mycotoxins, including aflatoxins, ergot alkaloids, fumonisins, ochratoxin A, patulin, trichothecenes and zearalenone (Commission Regulation (EC) No 1881/2006).

Denis Habauzit and Rebeca Alvariño have contributed equally to this work.

✉ Denis Habauzit
denis.habauzit@anses.fr; habauzit.denis@gmail.com

[1] French Agency for Food, Environmental and Occupational Health & Safety (ANSES), Fougères, France

[2] Departamento de Farmacología, Facultad de Veterinaria, Universidad de Santiago de Compostela, 27002 Lugo, Spain

[3] Grupo Investigación Biodiscovery, IDIS, 27002 Lugo, Spain

Published online: 22 September 2023

USC UNIVERSIDADE DE SANTIAGO DE COMPOSTELA

However, the presence of other non-regulated mycotoxins called emerging mycotoxins such as enniatins (ENNs) has been reported in different matrices (González-Jartín et al. 2021; Rocchetti et al. 2021; Taibon et al. 2015).

In the last decades, new approach methodologies (NAMs) have been developed in order to move forward from an animal-based hazard evaluation to in silico, in chemico and in vitro methodologies for toxicity investigation (Carstens et al. 2022; Escher et al. 2019; Watford et al. 2019). Previously, we used some in silico approaches (quantitative structure–activity relationships (QSAR) tools, gene expression analysis and text mining) to generate a cluster of mycotoxins showing similar effects (Habauzit et al. 2022). Based on a tiered approach, we highlighted a cluster of enniatin-like compounds, ENN A and B, beauvericin (BEA), apicidin (API) and destruxin B (DEST B), associated with lung cancer (Habauzit et al. 2022).

In fact, it is well known that mycotoxins can provoke acute and chronic effects to humans through ingestion or inhalation (Awuchi et al. 2022). If some mycotoxins were shown to reach the lung after ingestion and to cause inflammation (Wong et al. 2016), most of these studies have been carried out with regulated mycotoxins, whilst data on emerging mycotoxins are scarce (Behm et al. 2012; Ookawara et al. 2021). Although not volatile, mycotoxins can be present in airborne dust (Brera et al. 2002; Flannigan 1987) and in the fungal spores and fragments that can act as carriers of mycotoxins to the lungs (Brasel et al. 2005; Huttunen and Korkalainen 2017). Indeed, the handling of contaminated cereals, nuts, fruits… can provoke the exposure of workers (Viegas et al. 2018). If different fungi have been isolated from grain dust, the data on the amounts of mycotoxins found in dust are very scarce (Straumfors et al. 2015). Moreover, few studies have investigated the health effects of mycotoxins via inhalation and therefore the impacts for human health following exposure to grain dust contaminated with mycotoxins are hardly known (Ndaw et al. 2021; Straumfors et al. 2021). However, lungs are very sensitive to mycotoxin exposure by air, with induced injuries, such as pulmonary haemorrhage and chronic pulmonary inflammation (Agriopoulou et al. 2020; Awuchi et al. 2021). Some publications have evidenced an association between aflatoxin B1 (detected in lung biopsies) and lung cancer in agricultural, industrial and textile workers exposed to dust-contaminated material (Dvorácková 1976; Dvorácková and Píchová 1986; Georggiett et al. 2000; Hayes et al. 1984). In contrast, another study did not show such relationship, although aflatoxin B1 was involved in increased liver and biliary cancers (Olsen et al. 1988).

In this paper, we aimed testing the relationship between mycotoxins of the enniatin-like cluster (ENN A and B, BEA, API and DEST B) and non-small cell lung cancer. For this purpose, key toxicological endpoints, highlighted by in silico search on mycotoxins and involved in carcinogenesis (Habauzit et al. 2022), were evaluated on two different lung cell lines, A549 adenocarcinoma cells and NCI-H226 squamous cells. Cell viability, cell cycle disturbance, apoptosis, oxidative stress and inflammation were investigated.

Material and Methods

Chemicals and Solutions

Pierce ™ LDH-Cytotoxicity Assay Kit and EnzCheck® Caspase 3 Assay Kit were obtained from Thermo Fisher Scientific (Madrid, Spain). Annexin V-FITC Apoptosis Detection Kit was purchased in Immunostep (Salamanca, Spain). Cell culture flasks and plates were from JetBiofil (Guangzhou, China) or Corning (Thermo Fisher Scientific, Illkirch, France). ENN A, ENN B and BEA (purity > 96%) were obtained in Sigma-Aldrich (Saint Louis, USA), API (purity ≥ 99%) was purchased from Enzo Life Sciences (New York, USA) and DEST B (purity ≥ 96%) was from Cayman Chemical (Michigan, USA). Staurosporine (STS) (purity ≥ 98%) and the rest of reagent grade chemicals were obtained in Sigma-Aldrich. The primary and secondary antibodies (mouse monoclonal anti γH2AX ser139 (ab26350), rabbit monoclonal anti active caspase 3 antibody (ab13847), goat anti-rabbit IgG H&L AlexaFluor 647 (ab150079) and goat anti-mouse IgG H&L AlexaFluor 647 (ab150115)) were provided from Abcam (Cambridge, UK).

Cell Culture and Treatment

A549 (CCL185) and NCI-H226 (CRL5826) human non-small lung cancer cell lines were obtained from American Type Culture Collection (ATCC). A549 cells and NCI-H226 cells were cultured in Dulbecco's Modified Eagle Medium (DMEM) low-glucose medium and Roswell Park Memorial Institute (RPMI) 1640 medium, respectively, with 10% foetal bovine serum (FBS), 100 U/ml penicillin, and 100 µg/ml streptomycin. Cells were maintained at 37 °C in a humidified atmosphere of 5% CO_2 and dissociated weekly using 0.05% trypsin/EDTA. A549 and NCI-H226 cells were seeded in 96-well plates, at 1×10^4 cells/well and 1.5×10^4 cells/well, respectively, 24 h before a 24-h treatment with mycotoxins. For flow cytometry and caspase 3 assays, NCI-H226 cells were seeded at 5×10^5 cells/well in 12-well plates and treated with mycotoxins for 24 h. Mycotoxins were dissolved in DMSO and the final DMSO concentration in treatment medium was kept at 1% for A549 cells and below 0.5% for NCI-H226 cells.

USC UNIVERSIDADE DE SANTIAGO DE COMPOSTELA

Cell Viability

The effect of mycotoxins on cell viability after 24-h treatment was analysed with MTT (3-(4, 5-dimethyl thiazol-2-yl)-2, 5-diphenyl tetrazolium bromide) assay. For A549 cells, medium was replaced by MTT (500 µg/ml) dissolved in DMEM and incubated for 45 min. After a PBS wash, DMSO was added and the formazan salt was measured at 595 nm by a Fluostar Optima microplate reader (BMG labtech, Champigny-sur-Marne, France). After mycotoxin treatment, NCI-H226 cells were rinsed three times and incubated for 1 h at 37 °C with MTT (500 µg/ml) dissolved in Locke's buffer (154-mM NaCl, 5.6-mM KCl, 1.3-mM $CaCl_2$, 1-mM $MgCl_2$, 5.6-mM glucose and 10-mM HEPES, pH 7.4). After, 5 % sodium dodecyl sulphate was added to each well and absorbance was read at 595 nm by a Synergy 4 microplate reader (BioTek instruments, Vermont, USA).

Cytotoxicity in NCI-H226 cells was also assessed by lactate dehydrogenase (LDH) release. After mycotoxin treatment, cell medium was collected and LDH release was determined with Pierce™ LDH-Cytotoxicity Assay Kit, according to manufacturer's recommendations. Saponin at 1 mg/ml was used as positive control. Absorbance was measured at 490 nm by a Synergy 4 microplate reader (BioTek instruments). For each assay, at least three independent experiments were performed.

Active Caspase 3

After 24-h treatment with mycotoxins, A549 cell numbers were determined from DAPI staining, whilst active caspase 3 was quantified in the total cell compartment by High-Content Analysis (HCA) with an ArrayScan VTI HCS Reader (Thermo Scientific, Waltham, USA). Cells were scanned and analysed using the Compartmental Analysis module of the Bioapplication software. For each well, images from 10 fields (20×) were analysed for quantification of fluorescence. Four (ENNA and ENN B) to five (BEA, API, DEST B) independent experiments were carried out with duplicate wells.

After 24-h treatment with mycotoxins, the EnzCheck® Caspase 3 Assay Kit was used following manufacturer's instructions. Briefly, 150 µl of lysis buffer (10-mM Tris, 100-mM NaCl, 1-mM EDTA, 0.01% Triton x-100) were added to each well and samples were incubated on ice for 30 min. Next, cell lysates were centrifuged at 2300*g* and 4 °C for 5 min and supernatant was collected for caspase 3 activity and protein concentration analysis. Then, 50 µl of each sample were mixed with an equal volume of Z-DEVD-AMC substrate and incubated for 30 min at room temperature. Next, fluorescence at 342 nm excitation and 441 nm emission was measured in a microplate reader (Synergy 4, BioTek instruments). Caspase 3 activity data were corrected by protein concentration values, which were determined by Bradford method. STS at 0.05 µM was used as positive control and assays were carried out in duplicate three independent times.

Cell Death-Type Measurement

A commercial Annexin V-FITC Apoptosis Detection Kit was used following manufacturer's instructions. After 24-h treatment with toxins, cells were washed with PBS and suspended in annexin-binding buffer containing annexin V-FITC and propidium iodide (PI). Cells were incubated for 15 min at room temperature, suspended in PBS and filtered. The fluorescence was determined by flow cytometry using the ImageStreamMKII (Amnis Corporation, Luminex Corp, Austin, US). 10,000 events were analysed with IDEAS Application 6.0 software (Amnis Corporation, Luminex Corp, Austin, US). STS at 0.05 µM was used as control in this assay. Experiments were carried out in duplicate three independent times.

Cell Cycle Analysis

Effects of mycotoxin treatment on A549 cell cycle were quantified using the cell cycle BioApplication of the HCS studio software from 20 images per well. STS at 0.8 µM was used as positive control and experiments were performed in duplicate at least 4–5 independent times. For NCI-H226 cells, after 24 h of treatment, cells were detached, washed with ice-cold PBS and fixed with 70% ethanol for 1 h at 4 °C. After, cells were washed and resuspended in PBS containing propidium iodide (PI, 2.5 µg/ml) and RNase (0.1 mg/ml) for 30 min at room temperature. Then, cells were centrifuged at 550 g, 4 °C for 10 min and kept on ice. Fluorescence was analysed by flow cytometry using the ImageStreamMKII instrument (Amnis Corporation, Luminex Corp, Austin, US). 10,000 events were analysed with IDEAS Application 6.0 software (Amnis Corporation, Luminex Corp, Austin, US). STS at 0.01 µM was used as positive control in this assay. All experiments were carried out in duplicate and three independent times.

DNA Damage

DNA double-strand breaks were detected in A549 cells by the quantification of γH2AX in cell nuclei with HCA as described in "Active caspase 3". Experiments were carried out in duplicate and four (ENN A, B, BEA and API) to five (DEST B) independent experiments were performed.

Reactive Oxygen Species Levels Measurement

Reactive oxygen species (ROS) levels were assessed with the fluorescent dye carboxy-H_2DCFDA (5-(and-6)-carboxy-2′,

USC UNIVERSIDADE DE SANTIAGO DE COMPOSTELA

7′-dichlorodihydrofluorescein diacetate). After treatment with mycotoxins, NCI-H226 cells were washed twice with serum-free medium and loaded with 20-µM carboxy-H_2DCFDA dissolved in serum-free medium. After 1 h of incubation at 37 °C, PBS was added to each well for 30 min at 37 °C. Finally, fluorescence was read at 527-nm excitation, with an emission wavelength of 495 nm in a Synergy 4 microplate reader (BioTek instruments). H_2O_2 at 150 µM was used as positive control and three independent experiments were performed with duplicates for each condition.

IL-8 Enzyme-Linked Immunosorbent Assay (ELISA Assay)

After 24-h treatment, A549 cell culture media were collected and the levels of IL-8 were measured using ELISA as previously described (Jalili et al. 2022). Briefly, 96-well plates (Maxisorp, Nunc) were coated overnight at 4 °C with 1-µg/ml anti-human IL-8 monoclonal primary antibody (3IL8-H10, Fisher Scientific, Illkirch, France). SuperBlock blocking buffer (Thermo Scientific, Illkirch, France) was used to saturate wells for 1 h. Wells were then incubated with 90 µl of cell culture supernatant or recombinant human IL-8 standards for 2 h at room temperature. After three PBS-Tween 20 (0.05%) washes, wells were incubated with biotin-conjugated monoclonal anti-human 0.1 µg/ml IL-8 antibody (I8-S2, Fisher Scientific, Illkirch, France) for 1 h. Plates were then washed three times and 100 µl of streptavidin peroxidase polymer (Sigma-Aldrich) were added for 45 min. The chromogenic substrate Tetramethylbenzidine (TMB, 100 µl) was added, and plates were incubated for 5 min at room temperature. The reaction was then stopped with 100 µl of 1 M H_2SO_4. Absorbance was read at 405 nm using a FLUOstar Optima microplate reader (BMG Labtek). Cells treated with TNF-α (20 ng/ml) were used as positive controls. At least four independent experiments were performed with duplicate wells for each condition.

Statistical Analysis

Data are expressed as mean ± SEM. Statistical differences were evaluated by one-way ANOVA when data presented normal distribution and homoscedasticity, checked by Shapiro–Wilk and Brown–Forsythe tests, respectively. Data that did not meet distribution or variance criteria were compared with Kruskal–Wallis test. Dunnett's post hoc tests were used for multiple comparisons. p values ≤ 0.05 were considered statistically significant. Half inhibitory concentrations (IC_{50}) and half effective concentrations (EC_{50}) were determined by fitting the data with log(inhibitor) *vs* response and log(agonist) *vs* response models, respectively, with GraphPad Prism 8 software.

Results

Cell Viability

Firstly, cytotoxicity of selected mycotoxins was determined in A549 cells treated from 0.024 to 100 µM for 24 h. Two methods, cell count by HCA and MTT assay, were performed. As shown in Fig. 1a, ENN A produced a significant decrease in cell number at concentrations above 1 µM, with an $IC_{50} = 6.0$ µM (Table 1). ENN B also reduced cell number, but to a lesser extent, as the decrease did not exceed 50% for the highest concentration tested (Fig. 1b). Regarding BEA, a similar profile to ENN A was observed, with an effect on cell number starting above 1 µM (Fig. 1c). API was also cytotoxic to A549 cells, diminishing cell number at doses above 0.05 µM (Fig. 1d). Finally, DEST B treatment did not affect A549 cells (Fig. 1e). MTT assay confirmed these results, as the five mycotoxins presented similar profiles to those obtained for cell numbers (Fig. 2). ENN A and B decreased cell viability at concentrations above 1 µM, but the latter did not provoke a total inhibition (Fig. 2a, b). Treatment with BEA led to a reduction of cell survival at concentrations higher than 1 µM (Fig. 2c), as well as API (Fig. 2d). As expected, DEST B did not affect cell viability (Fig. 2e).

These results were confirmed in the NCI-H226 squamous cells. Analysis of cell viability by MTT test revealed that ENN A produced a reduction in cell survival at concentrations higher than 1 µM, as observed in A549 cells, with an $IC_{50} = 2.2$ µM (Fig. 3a, Table 1). The response of NCI-H226 cells to ENN B was also similar to the one of A549 cells, since cell viability was decreased down to 38.4 ± 4.5% at the highest concentration tested (Fig. 3b). Treatment with BEA and API diminished cell survival above 1 µM (Fig. 3c, d), whilst DEST B did not alter viability of NCI-H226 cells (Fig. 3e), as shown also in A549 cells. To further confirm the results in this cell line, LDH release (cell membrane integrity) was monitored (Fig. 4, Table 1). Only ENN A, BEA and API produced a concentration-dependent increase in LDH levels, although API did not induce a complete inhibition of cell survival (Fig. 4a, c, d).

Globally, the calculation of IC_{50} and EC_{50} for each mycotoxin in the different assays showed values within the same range (Table 1). For ENN A and BEA, the values were also similar in both cell lines: between 2.2 and 6.0 µM for ENN A and between 4.0 and 8.1 µM for BEA. For ENNB for which a complete inhibition was not reached, relative IC_{50} values were between 2.2 and 2.8 µM in all assays, whilst no LDH results were determined. Finally, API was the least toxic mycotoxin in MTT assay (IC_{50}: 7.0–13.1 µM); however, it reduced cell number at lower concentrations, with an IC_{50} of 1.4 µM.

USC UNIVERSIDADE DE SANTIAGO DE COMPOSTELA

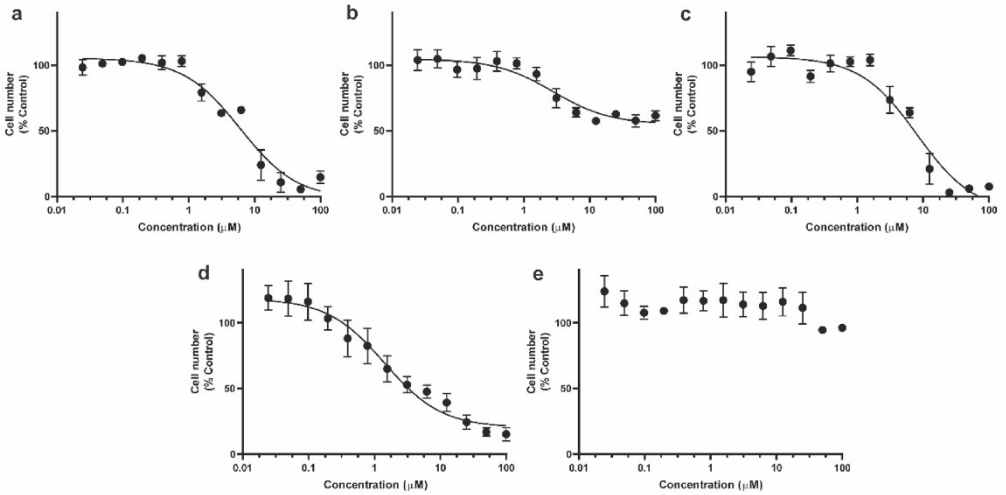


Fig. 1 Concentration–response effects of mycotoxins on A549 cell numbers. Non-small lung cancer cells were treated with toxins for 24 h and cell viability was determined by cell count by HCA. **a** ENN A, **b** ENN B, **c** BEA, **d** API and **e** DEST B. Data are mean ± SEM of four to five biological replicates performed in duplicate. Data were fitted with a log (inhibitor) *vs* response model

Table 1 IC_{50} and EC_{50} determined for cytotoxicity assessment of mycotoxins on the two lung cell lines

Cell line	A549		NCI-H226	
Toxin/Assay	Cell Number	MTT	MTT	LDH
	IC_{50} (μM)	IC_{50} (μM)	IC_{50} (μM)	EC_{50} (μM)
ENN A	6.0 (CI 4.1–9.0) R^2: 0.91	3.5 (CI 2.2–5.7) R^2: 0.87	2.2 (CI 1.3–3.6) R^2: 0.94	4.2 (CI 2.9–5.7) R^2: 0.94
ENN B[a]	2.8 (CI 1.5–5.3) R^2: 0.70	2.7 (CI 1.4–5.3) R^2: 0.67	2.2 (CI 1.2–4.0) R^2: 0.95	Nd
BEA	8.1(CI 5.4–12.2) R^2: 0.89	6.2 (CI 3.9–10.0) R^2: 0.83	4.0 (CI 2.1–7.7) R^2: 0.92	4.1 (CI 2.1–7.9) R^2: 0.88
API	1.4 (CI 0.7 – 3.0) R^2: 0.82	13.1 (CI 7.7–22.5) R^2: 0.85	7.0 (CI 2.9–16.7) R^2: 0.92	Nd
DEST B	Nd	Nd	Nd	Nd

ENN A enniatin A, *ENN B* enniatin B, *BEA* beauvericin, *API* apicidin, *DEST B* destruxin B, *CI 95%* confidence interval, *Nd* not determined

[a]For ENN B, a relative IC_{50} was calculated on the global effect, unless a total cell viability inhibition was not reached

Analysis of Cell Death

In view of the decrease in viability produced by mycotoxins in A549 and NCI-H226 cells, the type of cell death was further examined. Firstly, in contrast to the positive control STS, no increase in apoptosis as revealed by caspase 3 intensity was observed with ENN A, ENN B and BEA in A549 adenocarcinoma cells (Fig. 5a–c). However, a significant augmentation was obtained for both API and DEST B from 3.12 and 12.5 μM, respectively (Fig. 5d, e). Interestingly, API treatment induced caspase 3 intensity reaching a very high content at 25 μM ($p < 0.0001$), although this concentration was highly cytotoxic.

Caspase 3 activity was also assessed in NCI-H226 cells, but only at the IC_{50} values calculated from MTT testing, except for DEST B for which the highest concentration tested (50 μM) was used. If ENN A greatly increased caspase 3 activity until 369.1 ± 36.2%, ($p < 0.001$) (Fig. 6a), the enzyme activity was also augmented, but not statistically significant, with ENN B, BEA and API (Fig. 6a).

USC UNIVERSIDADE DE SANTIAGO DE COMPOSTELA

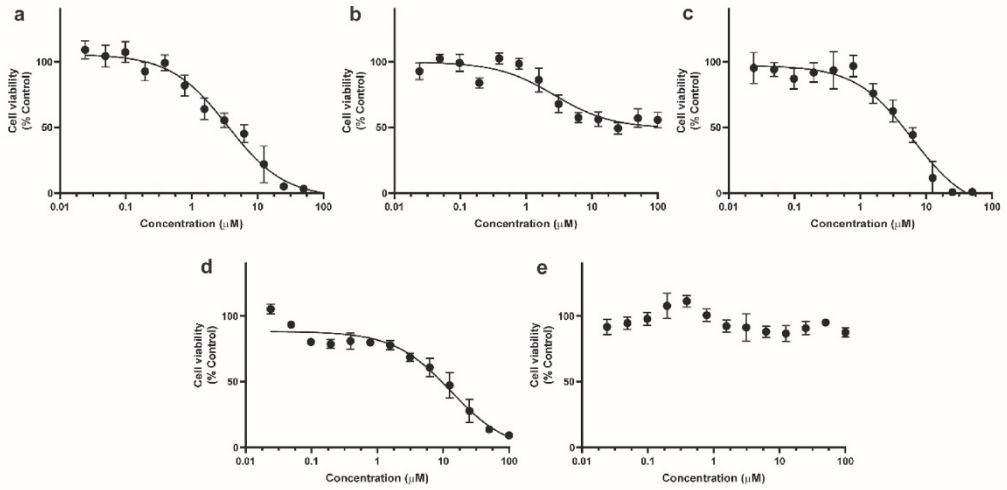


Fig. 2 Concentration–response effects of mycotoxins on A549 cell viability. Non-small lung cancer cells were treated with toxins for 24 h and cell viability was determined by MTT assay. **a** ENN A, **b** ENN B, **c** BEA, **d** API and **e** DEST B. Data are mean ± SEM of four to five biological replicates performed in duplicate. Data were fitted with a log (inhibitor) *vs* response model

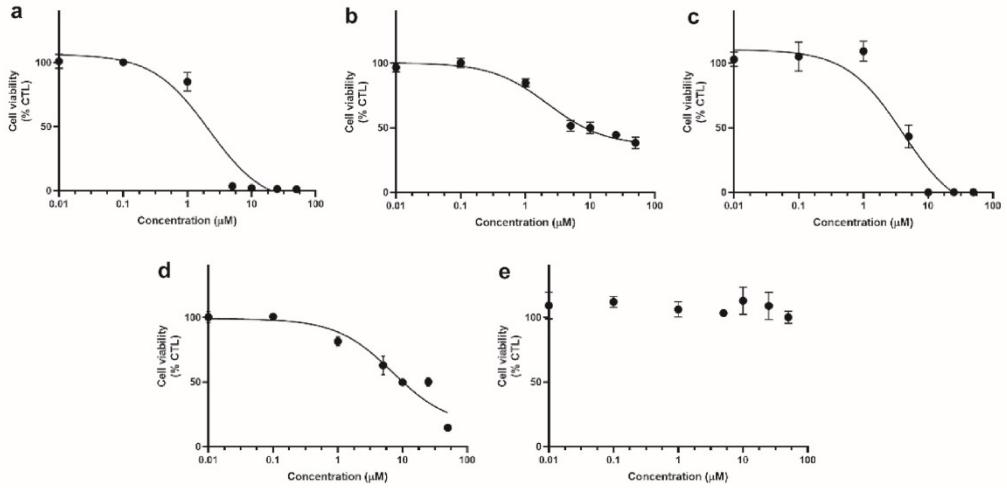


Fig. 3 Concentration–response effects of mycotoxins on NCI-H226 cells. Cell viability was determined by MTT assay after 24-h treatment. **a** ENN A, **b** ENN B, **c** BEA, **d** API and **e** DEST B. Data are mean ± SEM of three biological replicates performed in triplicate. Data were fitted with a log (inhibitor) *vs* response model

DEST B did not affect caspase 3 activation. As expected, the positive control STS significantly increased the enzyme activity (Fig. 6a).

In order to confirm the results obtained in caspase 3 assay in NCI-H226 cells, co-staining with annexin-FITC and PI was performed. As shown in Fig. 6b, treatment with ENN A,

USC UNIVERSIDADE DE SANTIAGO DE COMPOSTELA

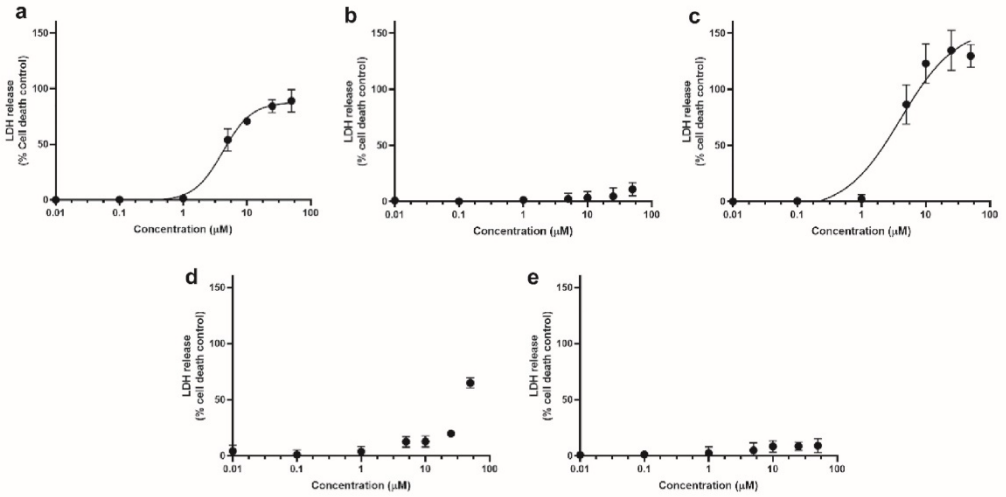


Fig. 4 Concentration–response curves of LDH release by NCI-H226 cells after treatment with mycotoxins. LDH levels were determined in cell medium after 24-h treatment with toxins. **a** ENN A, **b** ENN B, **c** BEA, **d** API and **e** DEST B. Data are mean ± SEM of three biological replicates performed in triplicate. Results expressed as percentage of cell death control and fitted with a log (agonist) *vs* response model

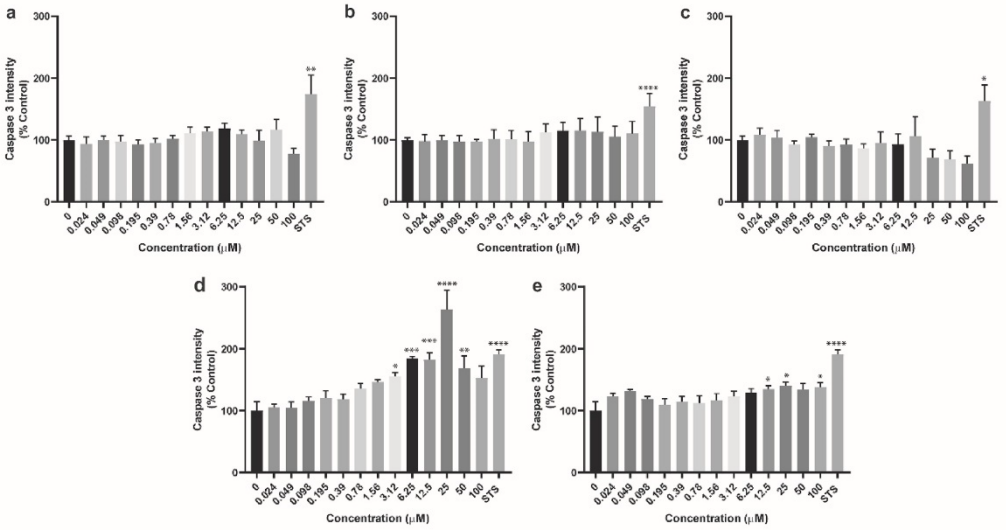


Fig. 5 Concentration–response effects of mycotoxins on caspase 3 intensity in A549 cells. Caspase 3 intensity was determined by the median of total intensity. **a** ENN A, **b** ENN B, **c** BEA, **d** API and **e** DEST B. Data are mean ± SEM of four to five biological replicates performed in duplicate. Results are expressed as percentage of control cells. Statistical differences determined by ANOVA and Dunnett's post hoc tests (*$p < 0.05$, **$p < 0.01$, ***$p < 0.001$, ****$p < 0.0001$) was performed. STS was used as positive control

USC
UNIVERSIDADE
DE SANTIAGO
DE COMPOSTELA

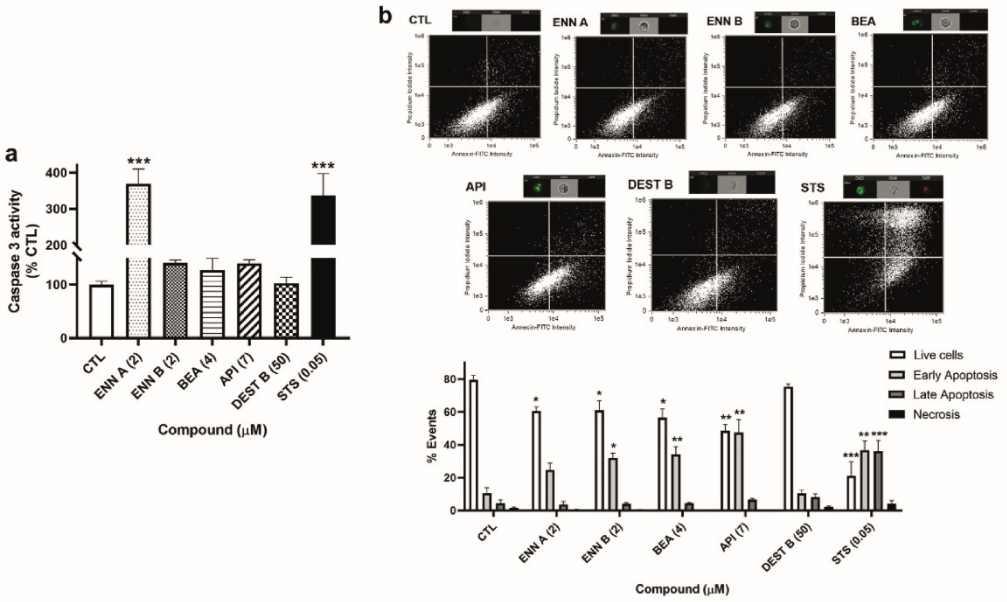


Fig. 6 Analysis of cell death type induced by mycotoxins on NCI-H226 cells. **a** Effect of mycotoxins on caspase 3 activity was determined 24 h after cell treatment. Data expressed as percentage of untreated control cells. **b** Representative scatter plot of each treatment and bar graph of cell death-type evaluation after 24 h of incubation. Cells were co-stained with annexin V-FITC and propidium iodide. Fluorescence was analysed by flow cytometry. Results expressed as percentage of total events. Percentages of live, early and late apoptotic and necrotic cells were calculated. STS was used as positive control in both assays. Mean ± SEM of three biological replicates. Statistical significance with respect to control cells was determined by one-way ANOVA and Dunnett's post hoc tests (*$p < 0.05$, **$p < 0.01$, ***$p < 0.001$)

ENN B, BEA, and API induced a decline of live cells compared to the control, with percentages ranging between 40.9 and 61.1%. This decrease was accompanied by a significant augmentation in early apoptotic cells when cells were treated with ENN B (27.4 ± 4.9%, $p < 0.05$), BEA (34.2 ± 4.5%, $p < 0.01$) and API (47.4 ± 8.0%, $p < 0.01$). ENN A also increased apoptosis up to 24.6 ± 4.4%, although it was not statistically significant. Finally, as expected from cytotoxicity data, DEST B did not induce apoptosis nor necrosis in this cell line. The positive control STS (0.05 µM) produced a significant decrease in live cells (21.1 ± 8.5%, $p < 0.001$) due to the activation of apoptosis, with an increase in both early and late apoptotic cells (37.7 ± 5.7% and 36.2 ± 3.7%, respectively).

Effects on Cell Cycle

Cell cycle analysis on A549 cells was carried out by HCA based on DAPI intensity. The positive control STS induced a significant decrease in G_0/G_1 cell population and a significant increase in G_2/M (Fig. 7). ENN A, BEA and API had similar effects on cell cycle for concentrations equal or greater than 12.5 µM. An increase in $subG_0$ phase, although not statistically significant, a significant decrease in G_0/G_1 population and a concomitant significant increase in S, G_2/M and sup G_2/M populations (illustrating polyploidy and cell division issue) were observed (Fig. 7a, c, d). In contrast, for lower concentrations (between 0.78 and 6.25 µM), API showed a concentration-dependent response, illustrated by a significant decrease in G_0/G_1 and a significant increase in G_2/M and sup G_2/M phases (at 6.25 µM) but with no effect on S phase. For ENN B, no significant effect on A549 cell cycle was identified (Fig. 7b). Finally, DEST B slightly but significantly increased the number of cells in G_0/G_1 phase in a concentration-dependent manner, which occurred simultaneously with a decrease in S and G_2/M phases (Fig. 7e).

NCI-H226 cell cycle was determined with PI staining by flow cytometry. In contrast to the positive control STS, no significant effect was observed for ENN A, ENN B, BEA and API tested at IC_{50} values as well as for DEST B at 50 µM (Fig. 8).

USC UNIVERSIDADE DE SANTIAGO DE COMPOSTELA

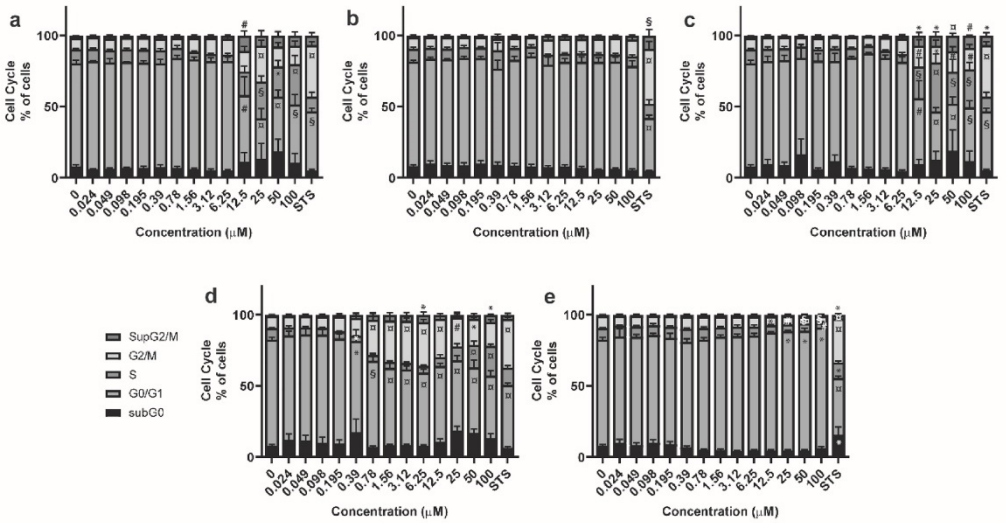


Fig. 7 Cell cycle analysis of A549 cells treated for 24 h with mycotoxins. Cell cycle phase was determined by HCA based on DAPI nucleus intensity. Percentages of cells in $SubG_0$, G_0/G_1, S, G_2/M and $SupG_2/M$ phases were calculated. **a** ENN A, **b** ENN B, **c** BEA, **d** API and **e** DEST B. Data are mean ± SEM of four to five biological replicates performed in duplicate, expressed as percentage of total events. STS was used as positive control. Statistics applied were ANOVA analysis followed by Dunnett's Post Hoc test ($^{*}p<0.05$, $^{\#}p<0.01$, $^{\S}p<0.001$, $^{¤}p<0.0001$)

DNA Damage

A significant increase in γH2AX level in A549 cells was observed with the positive control STS as well as with ENN A, BEA and API at concentrations above 12.5 µM (Fig. 9a, c, d), in agreement with the results obtained with cell cycle. For ENN B, only a trend increase in γH2AX intensity could be observed, whilst DEST B showed no effect up to 100 µM (Fig. 9b, e).

Reactive Oxygen Species (ROS) Generation

In NCI-H226 cells, ENN A increased the levels of ROS at 5 µM (142.4 ± 11.9%, $p<0.05$), but the augmentation was diminished at concentrations above 25 µM due to the decrease in cell viability (Fig. 10a). ENN B and API did not affect ROS generation (Fig. 10b), whilst BEA increased ROS levels only at 50 µM, reaching a percentage of 156.2 ± 10.7% ($p<0.05$) (Fig. 10c). Surprisingly, DEST B augmented ROS levels for concentrations above 10 µM (Fig. 10d, e). In this assay, H_2O_2 positive control increased ROS formation.

Pro-Inflammatory Response

IL-8 release was measured in A549 cell medium for all mycotoxins at the end of the treatment (Fig. 11). TNFα, used as positive control, produced a significant increase in IL-8 levels. ENN A, ENN B and BEA showed a concentration-dependent increase for concentrations above 3.12 µM (Fig. 11a–c). For API and DEST B, IL-8 release was maximal at 25 µM ($p<0.05$) (Fig. 11d, e). For ENN A, API and BEA, the IL-8 decrease observed at higher concentrations was associated with a decrease in cell viability (Fig. 11a, c, d).

Discussion

In our previous paper, we combined in silico methods and pointed out lung cancer-related effects for a small cluster of enniatin-like mycotoxins containing ENN A and B, BEA, API and DEST B (Habauzit et al. 2022). Amongst these compounds, ENN A and B and BEA are considered as emerging mycotoxins that are found more and more frequently in moulds processed for food and feed (Fraeyman

USC UNIVERSIDADE DE SANTIAGO DE COMPOSTELA

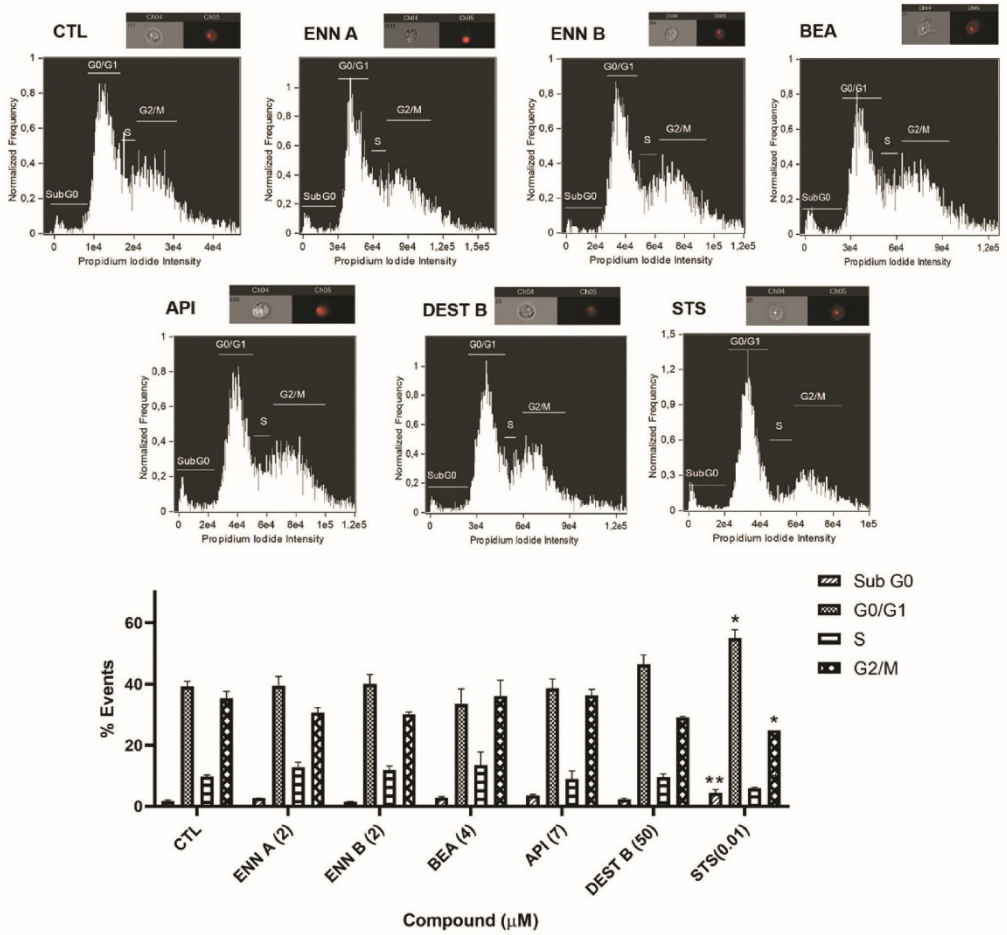


Fig. 8 Cell cycle analysis of NCI-H226 cells treated with mycotoxins. Cells were stained with propidium iodide after 24 h of incubation. Upper panels show histograms of a representative experiment. Bar plot of cell cycle evaluation is presented in the lower panel. Fluorescence of 10 000 events was analysed by flow cytometry. Percentages of cells in $SubG_0$, G_0/G_1, S and G_2/M phases were calculated. Results are mean ± SEM of three biological replicates, expressed as percentage of total events. STS was used as positive control. Statistical differences determined by one-way ANOVA and Dunnett's post hoc tests (*$p < 0.05$, **$p < 0.01$, compared to control cells)

et al. 2018; Pérez-Fuentes et al. 2021). Enniatins and their structural analogue BEA belong to the family of depsipeptides compounds. Although commonly reported in feed and food, data gaps on their toxicity do not allow to establish maximum limits (González-Jartín et al. 2021; Izzo et al. 2022). API, another depsipeptide also produced by *Fusarium* spp., has been found in different matrices including wheat and milk (Garcia-Cela et al. 2018; Rocchetti et al. 2021), but has been less studied. Finally, DEST B, produced by *Metarhizium brunneum* and used as biological control for maize and strawberries, has been suggested to be able to enter into the food chain and to be hazardous to humans (Taibon et al. 2015).

To investigate if the prediction linking lung cancer to the enniatin cluster of mycotoxins can be emphasized by in vitro testing, several endpoints (cell viability, apoptosis, cell cycle disturbance, ROS production and pro-inflammatory response), picked out in lung cancer KEGG pathways

USC UNIVERSIDADE DE SANTIAGO DE COMPOSTELA

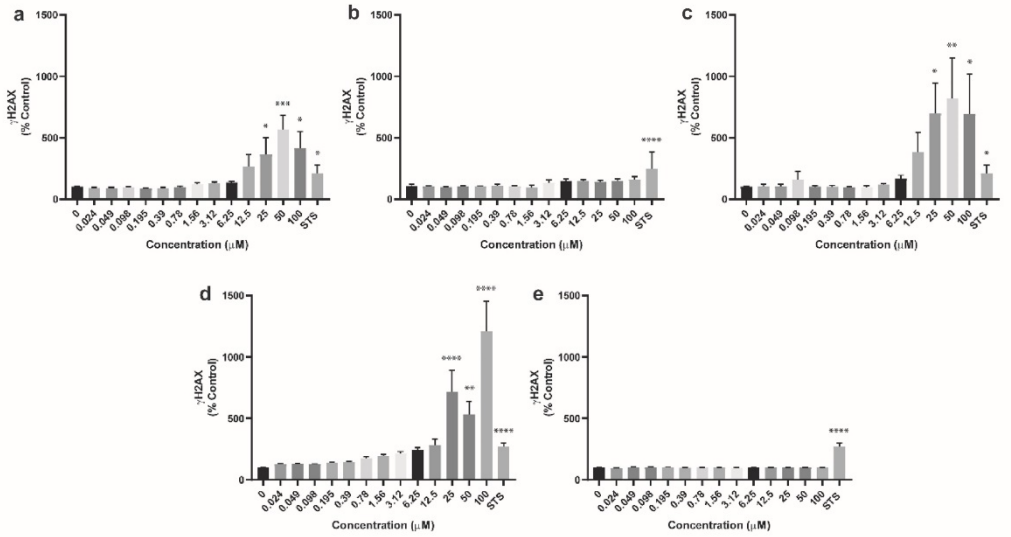


Fig. 9 Concentration–response effects of mycotoxins on γH2AX nucleus intensity in A549 cells. **a** ENN A, **b** ENN B, **c** BEA, **d** API and **e** DEST B. Data are mean ± SEM of four to five biological replicates performed in duplicate, expressed as percentage of control cells. Statistics applied were ANOVA analysis followed by Dunnett's Post Hoc test (*$p < 0.05$, **$p < 0.01$, ***$p < 0.001$, ****$p < 0.0001$)

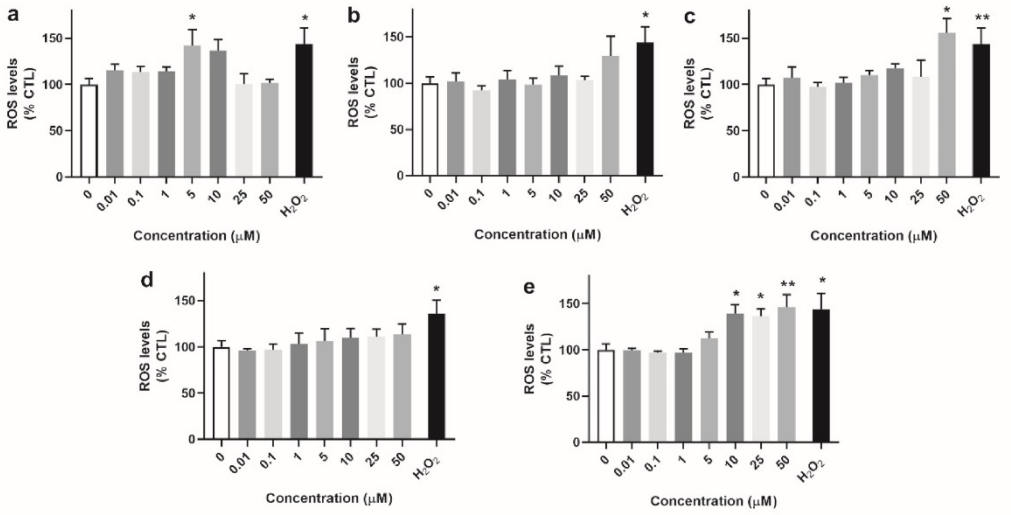


Fig. 10 Concentration–response effects of mycotoxins on ROS levels in NCI-H226 cells. Cells were treated with mycotoxins for 24 h and ROS content was measured with the fluorescent dye carboxy-H_2DCFDA. **a** ENN A, **b** ENN B, **c** BEA, **d** API and **e** DEST B. H_2O_2 at 150 μM was used as positive control. Data are mean ± SEM of three biological replicates performed in triplicate, expressed as percentage of control cells. Statistical significance analysed by ANOVA followed by Dunnett's post hoc test (*$p < 0.05$, **$p < 0.01$)

USC UNIVERSIDADE DE SANTIAGO DE COMPOSTELA

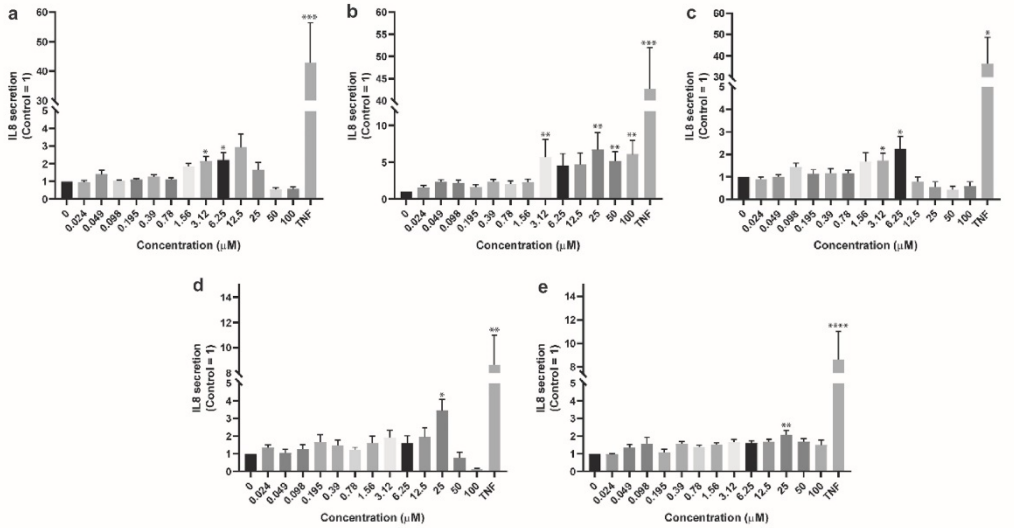


Fig. 11 Concentration–response effects of mycotoxins on IL-8 release in A549 cells. IL-8 release was quantified by ELISA. **a** ENN A, **b** ENN B, **c** BEA, **d** API and **e** DEST B. Data are mean ± SEM of four to five biological replicates performed in duplicate, expressed in fold change of control cells. Statistics applied were Kruskal–Wallis analysis (*$p < 0.05$, **$p < 0.01$, ***$p < 0.001$, ****$p < 0.0001$)

(Kanehisa and Goto 2000), were measured after mycotoxin treatment in two human lung cell lines, alveolar adenocarcinoma A549 and squamous carcinoma NCI-H226 cells.

First, we showed that, using 3 different methods to measure cell viability of mycotoxins, similar results were obtained for ENN A, BEA and API with a concentration-dependent decrease in cell viability in both cell models. ENN A was the most toxic compound (IC_{50}: 2.2–3.5 µM), followed by BEA (IC_{50}: 4.0–6.2 µM) and API (IC_{50}: 7.0–13.1 µM). Interestingly, squamous cells were more sensitive to these mycotoxins than adenocarcinoma cells, as IC_{50} were lower in NCI-H226 cells.

For the 3 mycotoxins, the increased cytotoxicity was concomitant with the activation of apoptosis in the two cell lines. In A549 cells, ENN A induced DNA double-strand breaks (γH2AX marker) and subG_0 phase and signs of apoptosis, although no modification of caspase 3 level was observed. In NCI-H226 cells, the mycotoxin induced a significant effect on caspase 3 activity at 2 µM as well as a slight but not significant increase in early apoptosis by annexin/PI staining and in the sub G_0 population.

A similar response on apoptotic endpoints (increase in γH2AX and sub G_0 phase without caspase 3 activation) was observed with BEA in A549 cells. No effect on caspase 3 activity and on sub G_0 population but an increase in early apoptosis by annexin/PI staining was reported in NCI-H226 cells. Apoptosis induction with BEA in A549 cells has been detected previously by caspase 3 activation, but a distinct method of measurement was employed, which can explain the discrepancy with our results on this marker (Lin et al. 2005).

In A549 cells, API augmented active caspase 3 level in a concentration-dependent manner from 3.12 µM. γH2AX level and cells in sub G_0 phase increased from 25 µM but this result must be taken with caution due to the high toxicity observed for these concentrations. If no modification of caspase 3 activity was observed in NCI-H226 cells, an increase in early apoptotic cells was obtained with annexin/PI staining. Moreover, subG_0 phase was slightly increased, although not significantly, in both cell lines. The same effects on viability, caspase 3 and cell cycle were also observed with API in fibrocystic breast MCF10A cell line for concentrations up to 0.3 µM (Park et al. 2008).The apoptotic effect observed for ENN B, BEA and API in this study was also reported in A549 cells for BEA (Lu et al. 2016), in human carcinoma from lung metastasis AT84 cell lines for API (Ahn 2018), and in neuronal SH-SY5Y cell line for ENN B and API (Pérez-Fuentes et al. 2021). Oxidative stress involvement in the apoptotic properties of several mycotoxins such as ENNs and BEA is still under debate. We showed that only ENN A and BEA induced a weak effect, whilst API did not show any increase in ROS levels in NCI-H226 cells at 24 h. Similar effect on ROS, and also related mitochondrial damage, was observed for ENN A and B in intestinal Caco-2 cells after

USC UNIVERSIDADE DE SANTIAGO DE COMPOSTELA

24–72-h treatment at EC50 concentrations (Prosperini et al. 2013). Disturbance of mitochondrial function was noticed in Jurkat lymphocytes after treatment with 1.5–5 µM ENN B for 24 h (Alonso-Garrido et al. 2018). However, BEA did not affect ROS levels in SH-SY5Y cells at 120 min (Agahi et al. 2020). It is worth mentioning that, in our study, measurement after 24 h might have been too short to detect a clear increase in ROS levels, mainly if this effect occurs as a late event of mycotoxin toxicity. Besides apoptosis, the 3 mycotoxins affected the cell cycle with a reduction of cells in G_0/G_1 phase and an arrest in S and G_2/M phases.

ENN B displayed a completely different pattern of toxicity on lung cell lines. First, it induced only a 50% decrease in cell viability for concentrations upper than 1 µM, as already reported in other cell lines, such as human astrocytoma CCF-STTG1 and neuroblastoma SH-SY5Y cells (Krug et al. 2018; Pérez-Fuentes et al. 2021; Søderstrøm et al. 2022). Nevertheless, no increase in LDH release was observed, suggesting that it did not affect cell integrity. A similar result on LDH release was obtained in the CCF-STTG1 cell line (Krug et al. 2018), but not in neuronal SH-SY5Y cells (Pérez-Fuentes et al. 2021). In contrast to the results obtained in rat hepatoma H4IIE cells (Wätjen et al. 2009) and in CCF-STTG1 cell line (Krug et al. 2018) where ENN B increases caspase 3 and DNA fragmentation, no effect of ENN B was observed on caspase 3 level and on cell cycle modifications, on DNA double-strand breaks, and on ROS levels. Only an increase in early apoptosis was obtained in NCI-H226 cells.

For DEST B, we did not evidence any decrease in cell viability in both cell lines. Although a decrease in cell viability was reported with DEST B in A549 cells for concentrations upper than 1 µM, it was only obtained after a 48-h treatment (Wu et al. 2013), suggesting that it occurred after a longer period of contact. Moreover, DEST B did not affect the apoptotic markers, except a slight increase in caspase 3 in A549 cells. However, a slight increase in G_0/G_1 phase was noticed at the highest concentrations tested, although without modification of the other phases, as already reported in A549 cells (Wu et al. 2013). In accordance to a delayed apoptosis, DEST B was the only toxin inducing ROS production in lung cells after 24-h treatment at concentrations above 10 µM. Therefore, oxidative stress may be involved as a secondary mechanism. Indeed, this mycotoxin has been described as an apoptotic inductor through mitochondria, implied in ROS production in A549 cells for 24 h (Wu et al. 2013) as well as in oral cancer cell lines at 72 h (Huang Liu et al. 2014).

Interestingly, increase in IL-8 secretion seems to be common to all molecules. However, data on the release of this cytokine after cell treatment with non-regulated mycotoxins are scarce. Increase in IL-8 levels has been observed in human adenocarcinoma Hela cells and colorectal carcinoma HCT116 cell line exposed to API (Kim et al. 2006a, 2006b; Kumar et al. 2019) but not in BEA-treated human intestinal Caco-2 cells (Albonico et al. 2016, 2015). Even, a reduction of IL-8 expression has been observed in blastocysts of mice treated with ENN B (Huang et al. 2022). IL-8 is involved in tumour inflammatory environment in lung cancer, by recruitment of inflammatory cells, and also plays a key role in tumour proliferation and metastasis (Chen and Chen 2022; Cui et al. 2022; Zhang et al. 2012). Therefore, the augmentation in IL-8 levels produced in A549 cells outlined a potential carcinogenic effect of these mycotoxins.

Amongst the tested mycotoxins, ENN A, BEA and API impacted mostly the different endpoints identified by KEGG as relevant for non-small cell lung cancer (Habauzit et al. 2022). ENN A, BEA and API have been reported to be widely present in food and feed (Khoshal et al. 2019). However, they were also detected in dust and in air, particularly in water-damaged indoor environment (Jakšić et al. 2021; Täubel et al. 2011), in ventilation systems (Hintikka et al. 2009) as well as in dust collected from wastewater treatment plans, harvest areas and farms (Limay-Rios and Schaafsma 2021; Skóra et al. 2016; Szulc et al. 2021, 2020). Nevertheless, the impact of these mycotoxins on human health following inhalation needs to be further investigated.

In silico combined approaches belong to the key methodologies that must be enforced in the next generation of risk assessment. Besides, it is necessary to carry out studies to decipher the pathways involved in the adverse outcomes (adverse outcome pathways) of mycotoxins. For this purpose, coupling in silico and in vitro improved methodologies will enable providing a more consistent and accurate prediction of toxicity.

Author contributions All authors contributed to the study conception and design. Material preparation, data collection and analysis were performed by Denis Habauzit, Rebeca Alvariño, Nadia Pérez-Fuentes and Sylvie Huet. The first draft of the manuscript was written by Denis Habauzit and Rebeca Alvariño and all authors commented on preliminary versions of the manuscript. Denis Habauzit and Rebeca Alvariño contributed equally to this work. All authors read and approved the final manuscript.

Funding The research leading to these results has received funding from the following FEDER cofunded-grants, from Conselleria de Cultura, Educacion e Ordenación Universitaria, Xunta de Galicia, GRC (ED431C 2021/01), from European Union Interreg Agritox EAPA-998-2018, and H2020 778069-EMERTOX, and from Ministerio de Ciencia e Innovación IISCIII/PI19/001248, PID 2020-11262RB-C21. N.P-F. is supported by a fellowship from FIDIS, Spain. R. A. is supported by a postdoctoral fellowship from Xunta de Galicia (ED481B-2021-038), Spain. This work was supported by ANSES.

Availability of data and material Not applicable.

Code availability Not applicable.

USC UNIVERSIDADE DE SANTIAGO DE COMPOSTELA

Declarations

Permission Not applicable.

Conflict of interest The authors declare that they have no competing interests.

Additional declarations for articles in life science journals that report the results of studies involving humans and/or animals Not applicable.

Ethics approval Not applicable.

Consent to participate Not applicable.

Consent for publication Not applicable.

References

Agahi F, Álvarez-Ortega N, Font G, Juan-García A, Juan C (2020) Oxidative stress, glutathione, and gene expression as key indicators in SH-SY5Y cells exposed to zearalenone metabolites and beauvericin. Toxicol Lett 334:44–52. https://doi.org/10.1016/j.toxlet.2020.09.011

Agriopoulou S, Stamatelopoulou E, Varzakas T (2020) Advances in occurrence, importance, and mycotoxin control strategies: prevention and detoxification in foods. Foods 9:137. https://doi.org/10.3390/foods9020137

Ahn M-Y (2018) HDAC inhibitor apicidin suppresses murine oral squamous cell carcinoma cell growth in vitro and in vivo via inhibiting HDAC8 expression. Oncol Lett 16:6552–6560. https://doi.org/10.3892/ol.2018.9468

Albonico M, Spicer L, Cortinovis C, Schutz LF, Caloni F (2015) In vitro toxicological effects of Fumonisin B1 and Beauvericin on bovine granulosa cells. Int J Health Anim Sci Food Saf. https://doi.org/10.13130/2283-3927/5039

Albonico M, Cortinovis C, Caloni F (2016) In vitro toxicity of beauvericin alone and combined with fumonisin B1 or deoxynivalenol on Caco-2 cells. Int J Health Anim Sci Food Saf. https://doi.org/10.13130/2283-3927/7089

Alonso-Garrido M, Escrivá L, Manyes L, Font G (2018) Enniatin B induces expression changes in the electron transport chain pathway related genes in lymphoblastic T-cell line. Food Chem Toxicol 121:437–443. https://doi.org/10.1016/j.fct.2018.09.018

Awuchi CG, Ondari EN, Ogbonna CU, Upadhyay AK, Baran K, Okpala COR, Korzeniowska M, Guiné RPF (2021) Mycotoxins affecting animals, foods, humans, and plants: types, occurrence, toxicities, action mechanisms, prevention, and detoxification strategies—a revisit. Foods 10:1279. https://doi.org/10.3390/foods10061279

Awuchi CG, Ondari EN, Nwozo S, Odongo GA, Eseoghene IJ, Twinomuhwezi H, Ogbonna CU, Upadhyay AK, Adeleye AO, Okpala COR (2022) Mycotoxins' toxicological mechanisms involving humans, livestock and their associated health concerns: a review. Toxins (basel) 14:167. https://doi.org/10.3390/toxins14030167

Azman NI, Wan-Mustapha WN, Goh YM, Hassim HA, Selamat J, Samsudin NIP (2021) Climatic conditions and farm practices affected the prevalence of Aspergillus section Flavi on different types of dairy goat's feed. Int J Food Microbiol 347:109205. https://doi.org/10.1016/j.ijfoodmicro.2021.109205

Behm C, Föllmann W, Degen GH (2012) Cytotoxic potency of mycotoxins in cultures of V79 lung fibroblast cells. J Toxicol Environ Health A 75:1226–1231. https://doi.org/10.1080/15287394.2012.709170

Brasel TL, Martin JM, Carriker CG, Wilson SC, Straus DC (2005) Detection of airborne *Stachybotrys chartarum* macrocyclic trichothecene mycotoxins in the indoor environment. Appl Environ Microbiol 71:7376–7388. https://doi.org/10.1128/AEM.71.11.7376-7388.2005

Brera C, Caputi R, Miraglia M, Iavicoli I, Salerno A, Carelli G (2002) Exposure assessment to mycotoxins in workplaces: aflatoxins and ochratoxin A occurrence in airborne dusts and human sera. Microchem J 73:167–173. https://doi.org/10.1016/S0026-265X(02)00061-9

Carstens KE, Carpenter AF, Martin MM, Harrill JA, Shafer TJ, Paul Friedman K (2022) Integrating data from in vitro new approach methodologies for developmental neurotoxicity. Toxicol Sci 187:62–79. https://doi.org/10.1093/toxsci/kfac018

Chen S, Chen M (2022) Schwann cells promote the migration and invasion of colorectal cancer cells via the activated NF-κB/IL-8 axis in the tumor microenvironment. Front Oncol 12:1026670. https://doi.org/10.3389/fonc.2022.1026670

Cui G, Wang Z, Liu H, Pang Z (2022) Cytokine-mediated crosstalk between cancer stem cells and their inflammatory niche from the colorectal precancerous adenoma stage to the cancerous stage: mechanisms and clinical implications. Front Immunol 13:1057181. https://doi.org/10.3389/fimmu.2022.1057181

Dvorácková I (1976) Aflatoxin inhalation and alveolar cell carcinoma. Br Med J 1:691. https://doi.org/10.1136/bmj.1.6011.691

Dvorácková I, Píchová V (1986) Pulmonary interstitial fibrosis with evidence of aflatoxin B1 in lung tissue. J Toxicol Environ Health 18:153–157. https://doi.org/10.1080/15287398609530856

Escher SE, Kamp H, Bennekou SH, Bitsch A, Fisher C, Graepel R, Hengstler JG, Herzler M, Knight D, Leist M, Norinder U, Ouédraogo G, Pastor M, Stuard S, White A, Zdrazil B, van de Water B, Kroese D (2019) Towards grouping concepts based on new approach methodologies in chemical hazard assessment: the read-across approach of the EU-ToxRisk project. Arch Toxicol 93:3643–3667. https://doi.org/10.1007/s00204-019-02591-7

Flannigan B (1987) Mycotoxins in the air. Int Biodeterior 23:73–78. https://doi.org/10.1016/0265-3036(87)90029-7

Fraeyman S, Meyer E, Devreese M, Antonissen G, Demeyere K, Haesebrouck F, Croubels S (2018) Comparative in vitro cytotoxicity of the emerging Fusarium mycotoxins beauvericin and enniatins to porcine intestinal epithelial cells. Food Chem Toxicol 121:566–572. https://doi.org/10.1016/j.fct.2018.09.053

Garcia-Cela E, Kiaitsi E, Medina A, Sulyok M, Krska R, Magan N (2018) Interacting environmental stress factors affects targeted metabolomic profiles in stored natural wheat and that inoculated with *F. graminearum*. Toxins (basel) 10:E56. https://doi.org/10.3390/toxins10020056

Georggiett OC, Muiño JC, Montrull H, Brizuela N, Avalos S, Gómez RM (2000) Relationship between lung cancer and aflatoxin B1. Rev Fac Cien Med Univ Nac Cordoba 57:95–107

Goldblatt LA (1972) Implications of mycotoxins. Clin Toxicol 5:453–464. https://doi.org/10.3109/15563657208991026

González-Jartín JM, Rodríguez-Cañás I, Alfonso A, Sainz MJ, Vieytes MR, Gomes A, Ramos I, Botana LM (2021) Multianalyte method for the determination of regulated, emerging and modified mycotoxins in milk: QuEChERS extraction followed by UHPLC-MS/MS analysis. Food Chem 356:129647. https://doi.org/10.1016/j.foodchem.2021.129647

Habauzit D, Lemée P, Botana LM, Fessard V (2022) Toxicity predictions for mycotoxins: a combined in silico approach on enniatin-like cluster. Expo Health. https://doi.org/10.1007/s12403-022-00492-2

Hayes RB, van Nieuwenhuize JP, Raatgever JW, ten Kate FJ (1984) Aflatoxin exposures in the industrial setting: an epidemiological study of mortality. Food Chem Toxicol 22:39–43. https://doi.org/10.1016/0278-6915(84)90050-4

USC UNIVERSIDADE DE SANTIAGO DE COMPOSTELA

Hintikka E, Holopainen R, Asola A, Jestoi M, Peitzsch M, Kalso S, Larsson L, Reijula K, Tuomi T (2009) Mycotoxins in the ventilation systems of four schools in Finland. World Mycotoxin J. https://doi.org/10.3920/WMJ2009.1155

Huang Liu R, Chen S-P, Lu T-M, Tsai W-Y, Tsai C-H, Yang C-C, Tzeng Y-M (2014) Selective apoptotic cell death effects of oral cancer cells treated with destruxin B. BMC Complement Altern Med 14:207. https://doi.org/10.1186/1472-6882-14-207

Huang CH, Wang FT, Chan WH (2022) Enniatin B induces dosage-related apoptosis ornecrosis in mouse blastocysts leading to deleterious effects on embryo development, Drug and Chemical-Toxicology, 45:4, 1449–1460. https://doi.org/10.1080/01480545.2020.1838537

Huttunen K, Korkalainen M (2017) Microbial secondary metabolites and knowledge on inhalation effects. In: Viegas C, Viegas S, Gomes A, Täubel M, Sabino R (eds) Exposure to microbiological agents in indoor and occupational environments. Springer International Publishing, Cham, pp 213–234. https://doi.org/10.1007/978-3-319-61688-9_10

Izzo L, Mikušová P, Lombardi S, Sulyok M, Ritieni A (2022) Analysis of mycotoxin and secondary metabolites in commercial and traditional Slovak cheese samples. Toxins (basel) 14:134. https://doi.org/10.3390/toxins14020134

Jakšić D, Sertić M, Kifer D, Kocsubè S, Mornar Turk A, Nigović B, Šarkanj B, Krska R, Sulyok M, Šegvić Klarić M (2021) Fungi and their secondary metabolites in water-damaged indoors after a major flood event in eastern Croatia. Indoor Air 31:730–744. https://doi.org/10.1111/ina.12777

Jalili P, Krause B-C, Lanceleur R, Burel A, Jungnickel H, Lampen A, Laux P, Luch A, Fessard V, Hogeveen K (2022) Chronic effects of two rutile TiO_2 nanomaterials in human intestinal and hepatic cell lines. Part Fibre Toxicol 19:37. https://doi.org/10.1186/s12989-022-00470-1

Kanehisa M, Goto S (2000) KEGG: kyoto encyclopedia of genes and genomes. Nucleic Acids Res 28:27–30. https://doi.org/10.1093/nar/28.1.27

Khoshal AK, Novak B, Martin PGP, Jenkins T, Neves M, Schatzmayr G, Oswald IP, Pinton P (2019) Co-occurrence of DON and emerging mycotoxins in worldwide finished pig feed and their combined toxicity in intestinal cells. Toxins (basel) 11:E727. https://doi.org/10.3390/toxins11120727

Kim YK, Lee EK, Kang JK, Kim JA, You J-S, Park JH, Seo D-W, Hwang JW, Kim S-N, Lee HY, Lee HW, Han J-W (2006a) Activation of NF-kappaB by HDAC inhibitor apicidin through Sp1-dependent de novo protein synthesis: its implication for resistance to apoptosis. Cell Death Differ 13:2033–2041. https://doi.org/10.1038/sj.cdd.4401915

Kim YK, Seo D-W, Kang D-W, Lee HY, Han J-W, Kim S-N (2006b) Involvement of HDAC1 and the PI3K/PKC signaling pathways in NF-kappaB activation by the HDAC inhibitor apicidin. Biochem Biophys Res Commun 347:1088–1093. https://doi.org/10.1016/j.bbrc.2006.06.196

Krug I, Behrens M, Esselen M, Humpf H-U (2018) Transport of enniatin B and enniatin B1 across the blood-brain barrier and hints for neurotoxic effects in cerebral cells. PLoS ONE 13:e0197406. https://doi.org/10.1371/journal.pone.0197406

Kumar S, O'Malley J, Chaudhary AK, Inigo JR, Yadav N, Kumar R, Chandra D (2019) Hsp60 and IL-8 axis promotes apoptosis resistance in cancer. Br J Cancer 121:934–943. https://doi.org/10.1038/s41416-019-0617-0

Limay-Rios V, Schaafsma AW (2021) Relationship between mycotoxin content in winter wheat grain and aspirated dust collected during harvest and after storage. ACS Omega 6:1857–1871. https://doi.org/10.1021/acsomega.0c04256

Lin H-I, Lee Y-J, Chen B-F, Tsai M-C, Lu J-L, Chou C-J, Jow G-M (2005) Involvement of Bcl-2 family, cytochrome c and caspase 3 in induction of apoptosis by beauvericin in human non-small cell lung cancer cells. Cancer Lett 230:248–259. https://doi.org/10.1016/j.canlet.2004.12.044

Liu C, Van der Fels-Klerx HJ (2021) Quantitative modeling of climate change impacts on mycotoxins in cereals: a review. Toxins (basel) 13:276. https://doi.org/10.3390/toxins13040276

Lu C-L, Lin H-I, Chen B-F, Jow G-M (2016) Beauvericin-induced cell apoptosis through the mitogen-activated protein kinase pathway in human nonsmall cell lung cancer A549 cells. J Toxicol Sci 41:429–437. https://doi.org/10.2131/jts.41.429

Medina Á, González-Jartín JM, Sainz MJ (2017) Impact of global warming on mycotoxins. Curr Opin Food Sci Food Toxicol Food Saf 18:76–81. https://doi.org/10.1016/j.cofs.2017.11.009

Ndaw S, Jargot D, Antoine G, Denis F, Melin S, Robert A (2021) Investigating multi-mycotoxin exposure in occupational settings: a biomonitoring and airborne measurement approach. Toxins (basel). https://doi.org/10.3390/toxins13010054

Olsen JH, Dragsted L, Autrup H (1988) Cancer risk and occupational exposure to aflatoxins in Denmark. Br J Cancer 58:392–396. https://doi.org/10.1038/bjc.1988.226

Ookawara T, Aihara R, Morimoto A, Iwashita N, Kurata K, Takagi Y, Miyasaka A, Kushiro M, Miyake S, Fukuyama T (2021) Acute and subacute oral toxicity of deoxynivalenol exposure in a *Dermatophagoides farinae*-induced murine asthma model. Toxicol Sci 179:229–240. https://doi.org/10.1093/toxsci/kfaa168

Park H, Im JY, Kim J, Choi WS, Kim HS (2008) Effects of apicidin, a histone deacetylase inhibitor, on the regulation of apoptosis in H-ras-transformed breast epithelial cells. Int J Mol Med 21:325–333

Pérez-Fuentes N, Alvariño R, Alfonso A, González-Jartín J, Gegunde S, Vieytes MR, Botana LM (2021) Single and combined effects of regulated and emerging mycotoxins on viability and mitochondrial function of SH-SY5Y cells. Food Chem Toxicol 154:112308. https://doi.org/10.1016/j.fct.2021.112308

Pleadin J, Frece J, Markov K (2019) Mycotoxins in food and feed. Adv Food Nutr Res 89:297–345. https://doi.org/10.1016/bs.afnr.2019.02.007

Pócsi I, Giacometti F, Ambrus Á, Logrieco AF (2020) Editorial: aspergillus-derived mycotoxins in the feed and food chain. Front Microbiol 11:606108. https://doi.org/10.3389/fmicb.2020.606108

Prosperini A, Juan-García A, Font G, Ruiz MJ (2013) Reactive oxygen species involvement in apoptosis and mitochondrial damage in Caco-2 cells induced by enniatins A, A_1, B and B_1. Toxicol Lett 222:36–44. https://doi.org/10.1016/j.toxlet.2013.07.009

Rocchetti G, Ghilardelli F, Masoero F, Gallo A (2021) Screening of regulated and emerging mycotoxins in bulk milk samples by high-resolution mass spectrometry. Foods 10:2025. https://doi.org/10.3390/foods10092025

Skóra J, Matusiak K, Wojewódzki P, Nowak A, Sulyok M, Ligocka A, Okrasa M, Hermann J, Gutarowska B (2016) Evaluation of microbiological and chemical contaminants in poultry farms. Int J Environ Res Public Health 13:192. https://doi.org/10.3390/ijerph13020192

Søderstrøm S, Lie KK, Lundebye A-K, Søfteland L (2022) Beauvericin (BEA) and enniatin B (ENNB)-induced impairment of mitochondria and lysosomes—potential sources of intracellular reactive iron triggering ferroptosis in Atlantic salmon primary hepatocytes. Food Chem Toxicol 161:112819. https://doi.org/10.1016/j.fct.2022.112819

Straumfors A, Uhlig S, Eriksen GS, Heldal KK, Eduard W, Krska R, Sulyok M (2015) Mycotoxins and other fungal metabolites in grain dust from Norwegian grain elevators and compound feed mills. World Mycotoxin J 8:361–373. https://doi.org/10.3920/WMJ2014.1799

Straumfors A, Mundra S, Foss OAH, Mollerup SK, Kauserud H (2021) The airborne mycobiome and associations with mycotoxins and

USC UNIVERSIDADE DE SANTIAGO DE COMPOSTELA

inflammatory markers in the Norwegian grain industry. Sci Rep 11:9357. https://doi.org/10.1038/s41598-021-88252-1

Sulyok M, Stadler D, Steiner D, Krska R (2020) Validation of an LC-MS/MS-based dilute-and-shoot approach for the quantification of > 500 mycotoxins and other secondary metabolites in food crops: challenges and solutions. Anal Bioanal Chem 412:2607–2620. https://doi.org/10.1007/s00216-020-02489-9

Szulc J, Okrasa M, Dybka-Stępień K, Sulyok M, Nowak A, Otlewska A, Szponar B, Majchrzycka K (2020) Assessment of microbiological indoor air quality in cattle breeding farms. Aerosol Air Qual Res 20:1353–1373. https://doi.org/10.4209/aaqr.2019.12.0641

Szulc J, Okrasa M, Majchrzycka K, Sulyok M, Nowak A, Ruman T, Nizioł J, Szponar B, Gutarowska B (2021) Microbiological and toxicological hazards in sewage treatment plant bioaerosol and dust. Toxins 13:691. https://doi.org/10.3390/toxins13100691

Taibon J, Sturm S, Seger C, Strasser H, Stuppner H (2015) Quantitative assessment of destruxins from strawberry and maize in the lower parts per billion range: combination of a QuEChERS-based extraction protocol with a fast and selective UHPLC-QTOF-MS assay. J Agric Food Chem 63:5707–5713. https://doi.org/10.1021/acs.jafc.5b01562

Täubel M, Sulyok M, Vishwanath V, Bloom E, Turunen M, Järvi K, Kauhanen E, Krska R, Hyvärinen A, Larsson L, Nevalainen A (2011) Co-occurrence of toxic bacterial and fungal secondary metabolites in moisture-damaged indoor environments. Indoor Air 21:368–375. https://doi.org/10.1111/j.1600-0668.2011.00721.x

Viegas S, Viegas C, Oppliger A (2018) Occupational exposure to mycotoxins: current knowledge and prospects. Ann Work Expo Health 62:923–941. https://doi.org/10.1093/annweh/wxy070

Watford S, Edwards S, Angrish M, Judson RS, Paul Friedman K (2019) Progress in data interoperability to support computational toxicology and chemical safety evaluation. Toxicol Appl Pharmacol 380:114707. https://doi.org/10.1016/j.taap.2019.114707

Wätjen W, Debbab A, Hohlfeld A, Chovolou Y, Kampkötter A, Edrada RA, Ebel R, Hakiki A, Mosaddak M, Totzke F, Kubbutat MHG, Proksch P (2009) Enniatins A1, B and B1 from an endophytic strain of *Fusarium tricinctum* induce apoptotic cell death in H4IIE hepatoma cells accompanied by inhibition of ERK phosphorylation. Mol Nutr Food Res 53:431–440. https://doi.org/10.1002/mnfr.200700428

Wong J, Magun BE, Wood LJ (2016) Lung inflammation caused by inhaled toxicants: a review. Int J Chron Obstruct Pulmon Dis 11:1391–1401. https://doi.org/10.2147/COPD.S106009

Wu C-C, Chen T-H, Liu B-L, Wu L-C, Chen Y-C, Tzeng Y-M, Hsu S-L (2013) Destruxin B isolated from entomopathogenic fungus metarhizium anisopliae induces apoptosis via a Bcl-2 family-dependent mitochondrial pathway in human nonsmall cell lung cancer cells. Evid Based Complement Alternat Med 2013:548929. https://doi.org/10.1155/2013/548929

Zhang Y, Wang L, Zhang M, Jin M, Bai C, Wang X (2012) Potential mechanism of interleukin-8 production from lung cancer cells: an involvement of EGF-EGFR-PI3K-Akt-Erk pathway. J Cell Physiol 227:35–43. https://doi.org/10.1002/jcp.22722

Publisher's Note Springer Nature remains neutral with regard to jurisdictional claims in published maps and institutional affiliations.

Springer Nature or its licensor (e.g. a society or other partner) holds exclusive rights to this article under a publishing agreement with the author(s) or other rightsholder(s); author self-archiving of the accepted manuscript version of this article is solely governed by the terms of such publishing agreement and applicable law.

USC UNIVERSIDADE DE SANTIAGO DE COMPOSTELA

SECCIÓN II: ARTÍCULO EN REVISIÓN

6. In vitro assessment of emerging mycotoxins co-occurring in cheese: A potential health hazard

Resumen:
Algunas cepas de *Penicillium* utilizadas en la maduración del queso producen micotoxinas emergentes, principalmente la roquefortina C (ROQC) y el ácido ciclopiazónico (CPA), así como eniatinas (ENNs) y beauvericina (BEA). La co-ocurrencia de estas micotoxinas en muestras naturales se ha reportado en todo el mundo; sin embargo, la mayoría de los estudios se centran en la toxicidad de una sola micotoxina. En el presente estudio, se analizaron los efectos de la ROQC y el CPA, solos y en combinación con BEA y ENNs A, A1, B y B1, en células de neuroblastoma humano. La ROQC y el CPA redujeron la viabilidad celular, con valores de IC_{50} de 49.5 y 7.3 μM, respectivamente, e indujeron apoptosis mediada por caspasa-8. Cuando la ROQC y el CPA se combinaron de forma binaria con las ENNs, se observó un aumento de sus efectos individuales. Además, se produjo un claro sinergismo cuando la ROQC y el CPA se mezclaron con las cuatro ENNs. También se describió un efecto aditivo para la combinación de CPA + ENNs (A, A1, B, B1) + BEA. Finalmente, se evaluaron los efectos de extractos de queso comercial que contenían las micotoxinas mencionadas, encontrando una fuerte reducción en la viabilidad celular. Estos resultados sugieren que la co-ocurrencia de micotoxinas emergentes en matrices naturales podría representar un riesgo potencial para la salud.

USC
UNIVERSIDADE DE SANTIAGO DE COMPOSTELA

USC
UNIVERSIDADE
DE SANTIAGO
DE COMPOSTELA

In vitro assessment of emerging mycotoxins co-occurring in cheese: A potential health hazard

Nadia Pérez-Fuentes[1], Rebeca Alvariño[2,*], Amparo Alfonso[1,*] Jesús González-Jartín[1], Mercedes R. Vieytes [2], Luis M. Botana[1]

[1]Departamento de Farmacología, Facultad de Veterinaria, IDIS, Universidad de Santiago de Compostela, Lugo 27002, Spain

[2]Departamento de Fisiología, Facultad de Veterinaria, IDIS, Universidad de Santiago de Compostela, Lugo 27002, Spain

*Corresponding authors. Email addresses: rebeca.alvarino@usc.es, amparo.alfonso@usc.es

Abstract:

Some *Penicillium* strains used in cheese ripening produce emerging mycotoxins, notably roquefortine C (ROQC) and cyclopiazonic acid (CPA), as well as enniatins (ENNs) and beauvericin (BEA). Co-occurrence of these mycotoxins in natural samples has been reported worldwide, however, most studies focus on the toxicity of a single mycotoxin. In the present study, the effects of ROQC and CPA alone and in combination with BEA and ENNs A, A1, B, and B1 were analysed in human neuroblastoma cells. ROQC and CPA reduced cell viability, with IC_{50} values of 49.5 and 7.3 µM, respectively, and induced caspase-8-mediated apoptosis. When ROQC and CPA were binary combined with ENNs, an enhancement of their individual effects was observed. Furthermore, a clear synergism was produced when ROQC and CPA were mixed with the four ENNs. An additive effect was also described for the combination of CPA + ENNs (A, A1, B, B1) + BEA. Finally, the effects of commercial cheese extracts containing the mentioned mycotoxins were evaluated, finding a strong reduction in cell viability. These results suggest that the co-occurrence of emerging mycotoxins in natural matrices could pose a potential health risk.

Keywords: Roquefortine C, cyclopiazonic acid, toxicity, enniatins, apoptosis, synergism

Statements and Declarations

Competing Interests

The authors have no relevant financial or non-financial interests to disclose.

Author Contributions

All authors contributed to the conception and design of the study. Nadia Pérez-Fuentes carried out the research and was involved in writing the original draft and in reviewing and editing the manuscript. Rebeca Alvariño and Amparo Alfonso contributed to the conception, methodology and drafting, including review and editing. Jesús González-Jartín carried out the research and was involved in writing the manuscript. Mercedes R. Vieytes contributed to the methodology. Luis M. Botana was responsible for fundraising and supervision.

USC UNIVERSIDADE DE SANTIAGO DE COMPOSTELA

Data Availability

All data used in this study are included in the manuscript Figs.

Acknowledgments

The research leading to these results has received funding from the following grants. From Conselleria de Cultura, Educacion e Ordenación Universitaria, Xunta de Galicia, GRC (ED431C 2021/01). From Ministerio de Ciencia e Innovación, PID 2020-11262RB-C21, Grant CPP2021-008447 funded by MCIN/AEI/10.13039/501100011033 and by The European Union NextGenerationEU/PRT. From European Union, Interreg EAPA-0032/2022 – BEAP-MAR, HORIZON-MSCA-2022-DN-01-MSCA Doctoral Networks 2022 101119901-BIOTOXDoc, and HORIZON-CL6-2023-CIRCBIO-01 COMBO - 101135438.

Disclosure Statement

The authors do not have conflicts of interest to declare.

USC UNIVERSIDADE DE SANTIAGO DE COMPOSTELA

1. Introduction

Fungal-derived compounds represent a great percentage of active natural products. Some of these metabolites, produced by species from the genera *Aspergillus*, *Fusarium* and *Penicillium*, are toxic to animals and humans. These molecules, named mycotoxins, are naturally present in contaminated matrices, so they can be found in cereals such as maize or rye, but also in other foods like milk, cheese or even fish (El-Sayed et al., 2022; Marin et al., 2013). *Penicillium* genus represents the most common contaminating mould in dairy products, followed by *Aspergillus*, and it is particularly well adapted to grow in cheese matrix (Kure and Skaar, 2019). Some *Penicillium* species that are used in cheese elaboration, such as *P. roqueforti* or *P. camemberti,* produce emerging mycotoxins, including roquefortines, cyclopiazonic acid (CPA) or even regulated mycotoxins like patulin (Izzo et al., 2022; Perrone and Susca, 2017). Emerging mycotoxins are molecules not routinely assessed, but their presence in food and feed is increasing. In the case of cheese, a recent study detected several non-regulated mycotoxins in commercial preparations, standing out the presence of CPA and roquefortine C (ROQC) in combination with other emerging mycotoxins like beauvericin (BEA) or enniatins (ENNs) (Rodríguez-Cañás et al., 2023).

ROQC is a 2,5-diketopiperazine (Figure 1a), usually detected in cheese at low concentrations and mainly produced by *P. roqueforti*. A neurotoxic effect after ROQC administration has been described in mice and its presence has been associated with intoxications in dogs and cattle (Tiwary et al., 2009; N. Hymery et al., 2018). However, there are not enough data on ROQC toxicity, and its mechanism of action remains unclear. CPA, an indole tetrameric acid mycotoxin (Figure 1b), is one of the most common and stable mycotoxins in cheese (Casquete et al., 2021; Nolwenn Hymery et al., 2014). This compound inhibits the Ca^{2+}-ATPase of the sarcoplasmic reticulum and produces hepatotoxic, neurotoxic, and nephrotoxic effects in different animal models (Fliszár-Nyúl et al., 2022). CPA is produced by several *Aspergillus* species and has presented cytotoxicity at high concentrations in different cell lines, so it is not considered a health issue (Chang et al., 2009) . However, its combination with aflatoxins produces additive effects, so its toxicity could be currently underestimated since its mixed effects with other mycotoxins have not been extensively studied (Chang et al., 2009; Pier et al., 1989).

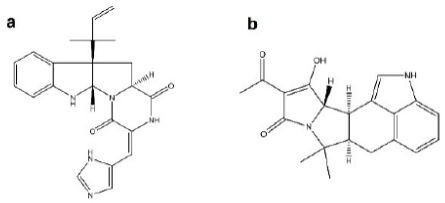


Figure 1. Chemical structures of roquefortine C (a) and cyclopiazonic acid (b).

In this sense, we have recently described that the mechanism of action of ENNs is mediated by an effect in calcium fluxes, so the co-occurrence of CPA with these emerging mycotoxins could represent a health risk that is not being considered.

USC UNIVERSIDADE DE SANTIAGO DE COMPOSTELA

ENNs, along with BEA, are cyclic hexadepsipeptides produced by *Fusarium* spp. that have been considered as ionophores for a long time, but the exact mechanism of action of each toxin has not been widely explored (Shin et al., 2009). In recent works, we have observed that the four most common ENNs (A, B, A1 and B1) present a different mode of action despite their structural similarities. All the toxins alter calcium homeostasis, but by affecting different intracellular pools (N. Pérez-Fuentes et al., 2022; Nadia Pérez-Fuentes et al., 2023). Moreover, ENNs interfere with mitochondrial function and induce apoptosis through mechanisms involving oxidative stress and cell cycle disruption (Qinghua Wu et al., 2018; Hamza Olleik et al., 2019b). Regarding BEA, it forms ion-selective channels with several metallic cations leading to an increase in cell membrane permeability (Caloni et al., 2020; Kouri et al., 2003). BEA has a wide range of biological properties, including the induction of cytotoxicity, oxidative stress, and disruption of mitochondrial function in several cell lines (Mallebrera et al., 2018; Hasuda et al., 2023; Søderstrøm et al., 2022; Caloni et al., 2020).

Although ROQC, CPA, ENNs and BEA presence is increasing and they naturally co-contaminate different types of cheese, there are not enough data on their combined toxicity. In this context, the objective of this study was to evaluate the combined effect of these naturally occurring emerging toxins in SH-SY5Y human neuroblastoma cells. To this end, the single effects of ROQC and CPA on cell viability were initially assessed, followed by the evaluation of dose-response combinations of the emerging mycotoxins. Finally, contaminated cheese extracts were tested in order to analyse the effect of these toxins in a natural sample.

2. Methods and material

2.1. Chemicals and solutions

CyQUANT™ lactate dehydrogenase (LDH) Cytotoxicity Assay Kit, Dulbecco's Modified Eagle Medium: F-12 nutrient Mix (DMEM/F-12), trypsin/EDTA (0.05%), glutamax, penicillin-streptomycin (10,000 U/mL), SuperSignal West Pico, SuperSignal West Femto, Pierce TM Protease Inhibitor Mini Tablets and Pierce TM Phosphatase Inhibitor Mini Tablets were bought in Thermo Fisher Scientific (Madrid, Spain). Durapore membrane centrifugal filters (0.22 µm pore size), ENN A, ENN A1, ENN B, ENN B1, CPA and ROQC (purity >95 %), 3-(4,5-dimethyl thiazol-2-yl)-2,5-diphenyl tetrazolium bromide (MTT), carbonyl cyanide 4-(trifluoromethoxy) phenylhydrazone (FCCP), saponin (SAP), staurosporine (STS), Annexin V-FITC Apoptosis Detection Kit, anti-beta actin monoclonal antibody and another chemical reagent grade were purchased from Merck (Madrid, Spain). Cheese samples were obtained in local supermarkets and storaged at 4ºC until analysis. Cyclosporin A (CsA) and anti-caspase 9 antibody were obtained from Abcam (Cambridge, UK). Anti-caspase-8 antibody was purchased in Cell Signalling Technology (Massachusetts, USA).

The composition of Locke´s buffer was: 154 mM NaCl, 5.6 mM KCl, 3.6 mM $NaHCO_3$, 1 mM $MgCl_2$ 1.3 mM $CaCl_2$, 5 mM glucose and 10 mM HEPES. Phosphate buffered saline (PBS) was composed of (in mM): 137.0 NaCl, 8.2 Na_2HPO_4, 1.5 KH_2PO_4 and 3.2 KCl (pH 7.4). Hypotonic lyses buffer was composed of 50 mM Tris-HCl (pH 7.4), 150 mM NaCl, 1% Triton X-100 and 1 mM EDTA. Stock solutions of mycotoxins were prepared in DMSO, and serial dilutions were carried out in culture medium. DMSO concentration was kept under 0.8% in all experiments.

2.2. Cheese extracts and analysis

USC UNIVERSIDADE DE SANTIAGO DE COMPOSTELA

Cheese samples were analysed utilizing a method previously validated for the simultaneous detection of 32 mycotoxins in this matrix (Rodríguez-Cañás et al., 2023). Briefly, samples were homogenized, and 1 g of each cheese was subjected to extraction using a QuEChERS (quick, easy, cheap, effective, rugged, and safe) protocol. Initially, 4 mL of 2% acetic acid solution were added, followed by 4 mL of acetonitrile, vigorous mixing was applied after each solvent addition using a vortex mixer. Phase separation was achieved with 1.6 g of MgSO4 and 0.4 g of NaCl. Subsequently, the organic phase was diluted 1:2 with 2% acetic acid and filtered through a 0.22 µm centrifugal filters. The resulting extracts were then analysed using an ultra-high liquid chromatography-tandem mass spectrometry (UHPLC-MS/MS) protocol. Cheese extracts (500 µL) were further subjected to drying in a centrifugal evaporator, followed by reconstitution in 500 µL of DMSO.

2.3. Cell Culture

SH-SY5Y human neuroblastoma cell line was purchased from American Type Culture Collection (ATCC), number CRL2266. Cells were cultured in DMEM/F-12 supplemented with 1% glutamax, 10% fetal bovine serum (FBS) and 10,000 U/mL penicillin-streptomycin. Cells were maintained at 37 °C in a humidified atmosphere of 95% air and 5% CO_2 and dissociated once a week using 0.05% trypsin/EDTA.

2.4. Cell viability assay

SH-SY5Y cells were cultured in 384-well plates at concentration of 2.5×10^4 cells/well in complete cell growth medium. After 24 h of incubation, cell medium was changed to DMEM/F-12 supplemented with 1% glutamax, 2% fetal bovine serum (FBS) and 10,000 U/mL penicillin-streptomycin.
Concentrated cheese extracts were prepared as described above and SH-SY5Y cells were treated at 1:200, 1:300, 1:400, 1:500 and 1:1000 dilutions. The less contaminated cheese sample (corresponding to camembert cheese) was used as a control, as no mycotoxin-free matrix was found. In individual mycotoxin assays, cells were treated at concentrations ranging from 0.01 to 100 µM. In the case of mycotoxin combinations, the ratio among different mycotoxins was selected based on the most frequent proportions found in contaminated cheese (Rodríguez-Cañás et al., 2023). In binary mixtures, CPA and ROQC were combined at 10:1 ratio with ENN A, ENN A1, ENN B or ENN B1. Then, the effects of a 1:1:1:1 mixture of ENNs A, A1, B and B1, and a combination of the four ENNs with BEA (1:1:1:1:1) were assessed. Finally, ROQC and CPA were combined with ENNs A, A1, B, and B1 at 10:1:1:1:1 proportion, and with the four ENNs and BEA at 10:1:1:1:1:1 ratio. Combined concentration ranges were selected based on the results obtained with individual mycotoxins to include their half maximal inhibitory concentration (IC_{50}) values in the concentration range analysed.

The effect of individual and mixed mycotoxins on SH-SY5Y cell viability was determined using the MTT assay, as previously described (Alvariño et al., 2017). Cells were treated for 24 h and SAP from *Quillaja bark* at 1mg/mL was used as cell death control. After treatment, SH-SY5Y cells were washed three times with Locke´s solution and 200 µL of MTT (500 µg/mL) were added per well. Then, cells were incubated at 37ºC for 1 h and 300 rpm in an orbital shaker. After incubation, MTT was removed, and 5% sodium dodecyl sulphate was added to lysate the cells. Absorbance was read in a spectrophotometer plate reader at 595 nm. All the experiments were performed in triplicate at least three independent times.

USC UNIVERSIDADE DE SANTIAGO DE COMPOSTELA

2.5. *Cytotoxicity assay*

Cell cytotoxicity induced by mycotoxins, alone and in combination, was determined by CyQUANT™ LDH Cytotoxicity Assay Kit test, following manufacturer´s instructions (N. Pérez-Fuentes et al., 2021). Cells were treated with cheese extracts, single toxins and mixtures as described above for 24 h. Then, 50 µL of cell medium were transferred to a 96-well flat-bottomed well and the kit reaction mixture was added. After 30 minutes, the stop solution was added, and LDH release was assessed. SAP from *Quillaja bark* at 1mg/mL was used as cell death control. Absorbance was read at 490 and 680 nm in a plate reader. Finally, the background signal (680 nm absorbance) was subtracted from the 490 nm absorbance to determine LDH release into the medium. Experiments were performed three independent times in triplicate.

2.6. *Cell death type assessment*

Annexin V-FITC Apoptosis Detection Kit was used to determine the cell death type induced by ROQC and CPA, following manufacturer´s instructions (Alvariño et al., 2020). For this assay, cells were seeded in 12-well plates at 5×10^5 cells per well. After 24 h, cells were treated with ROQC and CPA and incubated for 24 h. STS at 0.1 µM was used as a positive control. The cells were then washed with PBS, resuspended in annexin binding buffer containing annexin V-FITC and propidium iodide (PI) and incubated for 15 minutes at room temperature. Then, cells were resuspended in commercial PBS (pH 7.2) (Thermo Fisher Scientific), filtered, and kept on ice. Fluorescence was then analysed by flow cytometry using the ImageStreamMKII instrument (Amnis Corporation, Luminex Corp, Austin, TX, USA). IDEAS Application 6.0 software was used to determine the fluorescence of 10,000 events (Amnis Corporation, Luminex Corp).

2.7. *Western blot analysis*

Cells were seeded in a 12-well plate at 5×10^5 cells per well and allowed to attach for 24 h. After this time, CPA and ROQC were added for 24 h. SH-SY5Y cells were then rinsed twice with cold PBS, cells were scrapped and 100 µL of ice-cold hypotonic lysis buffer containing protease and phosphatase inhibitor cocktails were added. Samples were sonicated for 1 min and centrifugated for 20 min at 4 °C and 12000 rpm. Then, the supernatant was collected as the cytosolic fraction. Electrophoresis was performed on 4-20% sodium dodecyl sulphate polyacrylamide gels containing 15 µg of cytosolic protein and transferred onto PVDF membranes. Precision Plus Protein Standards Kaleidoscope molecular weight marker was used to determine the protein size. The membranes were then blocked with 0.5% BSA and antibody incubation was performed using the SNAP i.d. protein detection system. Caspase-8 was detected with anti-caspase-8 antibody (1:1000) and anti-caspase 9 (1:2000) antibody was used to detect caspase-9. Signal was normalized by β-actin with anti-β-actin antibody (1:5000). Immunoreactive bands were detected using Supersignal West Pico or Supersignal West Femto and Diversity GeneSnap software (Syngene). Experiments were performed three independent times by duplicate.

2.8. *Statistical analysis*

Data are expressed as mean ± SEM of three independent experiments. Differences were assessed by one-way ANOVA followed by Dunnett's or Tukey's multiple comparison tests. Statistical significance was set at *$p< 0.05$, **$p< 0.01$ and ***$p< 0.001$. IC_{50} and half maximal effective concentration (EC_{50}) values were

USC UNIVERSIDADE DE SANTIAGO DE COMPOSTELA

calculated using GraphPad Prism 8 software by fitting the data with a log(inhibitor) *vs* response or log(agonist) *vs* response model, respectively.

The combination index was calculated with Chou & Talalay equation (Ting-Chao Chou and Talalay, 1983):

$$Combination\ index = \frac{D1}{D(X)1} + \frac{D2}{D(X)2}$$

where (DX)1 and (DX)2 are the IC_{50} values of each mycotoxin alone, and D1 and D2 are the IC_{50} values of each mycotoxin in binary combination. According to Chou & Talalay method, synergism, additivity, and antagonism were considered when the combination index was <1, =1 and >1, respectively.

3. Results

3.1. Single effects of ROQC and CPA in human neuroblastoma cells

Based on a previous analysis of cheese samples, in which CPA and ROQC were frequently detected, these toxins were selected to test their toxicity in SH-SY5Y cells (Rodríguez-Cañás et al., 2023). At first, the effects of these two metabolites on cell viability and cytotoxicity were determined. Cells were treated with ROQC and CPA at concentrations ranging from 0.1 to 100 µM for 24 h. MTT was used to analyse the effects of these toxins on cell viability while cytotoxicity was determined by measuring the LDH release into the culture medium.

In MTT assay, ROQC reduced cell viability between 16.3 – 99.4 % at concentrations over 40 µM (Figure 2a), while CPA seemed to be more toxic, decreasing cell viability between 64.6 – 96.0 % at doses higher than 5 µM (Figure 2b). With the data obtained in MTT assays, IC_{50} values for each toxin were calculated by fitting the data with a log(inhibitor) *vs* response model. ROQC presented an IC_{50} of 49.5 µM (CI: 45.6 – 53.5 µM) and CPA was more toxic, with a value of 7.3 µM (CI: 5.9 – 8.8 µM).

Regarding LDH assay, the results were consistent with those obtained when measuring cell viability, as LDH release was observed at the highest concentrations used (Figure 2 c, d). ROQC increased LDH at concentrations above 40 µM, reaching a reduction of 100 % at the 100 µM dose. Although CPA seemed to affect more the cell metabolism, its effects on LDH release were lower (84.5 ± 5.9 % at 100 µM). With the data obtained with this assay, EC_{50} values for each toxin were calculated by fitting the data with a log(agonist) *vs* response model. ROQC showed an EC_{50} value of 49.5 µM (CI: 45.4– 53.0 µM). In the case of CPA, its EC_{50} was higher (84.1 µM, CI: 77.3 – 91.5 µM).

USC UNIVERSIDADE DE SANTIAGO DE COMPOSTELA

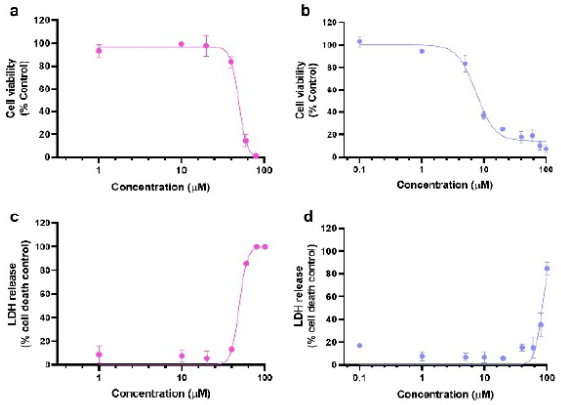


Figure 2. Single effects of ROQC and CPA on cell viability and cytotoxicity of SH-SY5Y cells. Cells were treated with mycotoxins for 24 h. (a) Effect of ROQC and (b) CPA on cell viability, assessed by MTT test. (c) Cytotoxicity of ROQC and (d) CPA, determined by LDH assay. Saponin at 1 mg/mL was used as cell death control. Data are mean ± SEM of three independent replicates expressed as percentage of untreated control cells. Data were fitted with a log (inhibitor) *vs* response and a log (agonist) *vs* response model for cell viability and LDH assays, respectively.

Next, the type of death induced by ROQC and CPA was assessed. Cells were treated for 24 h with mycotoxins at IC_{50} concentrations determined by MTT assay. Therefore, ROQC at 49.5 µM and CPA at 7.3 µM were added to cells for 24 h. The apoptotic inducer STS was used at 0.1 µM as a positive control. Samples were then co-stained with Annexin V-FITC and PI and the fluorescence was analysed by flow cytometry (Figure 3a). The percentages of necrotic cells (Annexin V-FITC negative and PI positive) and apoptotic cells (Annexin V-FITC positive and PI positive and negative) were calculated. ROQC and CPA induced a significant increase in apoptotic cells, with percentages of 52.7 ± 1.9 % ($p<0.01$) and 43.8 ± 8.0 % ($p<0.05$), respectively, without changing the proportion of necrotic cells compared to the control. These effects were similar to the results of the apoptotic inducer STS, that increased the number of cells undergoing apoptosis until 59.5 ± 3.6% ($p<0.001$).

Then, to decipher the type of apoptosis produced by ROQC and CPA, the expression of caspase-8 and caspase-9 were determined. The first one is involved in the extrinsic apoptotic pathway, whilst caspase-9 participates in the intrinsic or mitochondrial pathway. As Figure 3b shows, the expression of cleaved caspase-8 (41-43 KDa band) was increased by CPA (31.0 ± 16.8 %, $p<0.05$), while active caspase-8 expression (18 KDa band) was augmented by ROQC a 61.1 ± 36.9 %, compared to control cells. No significant differences were found in the expression of caspase-9 after treatment with these toxins.

USC UNIVERSIDADE DE SANTIAGO DE COMPOSTELA

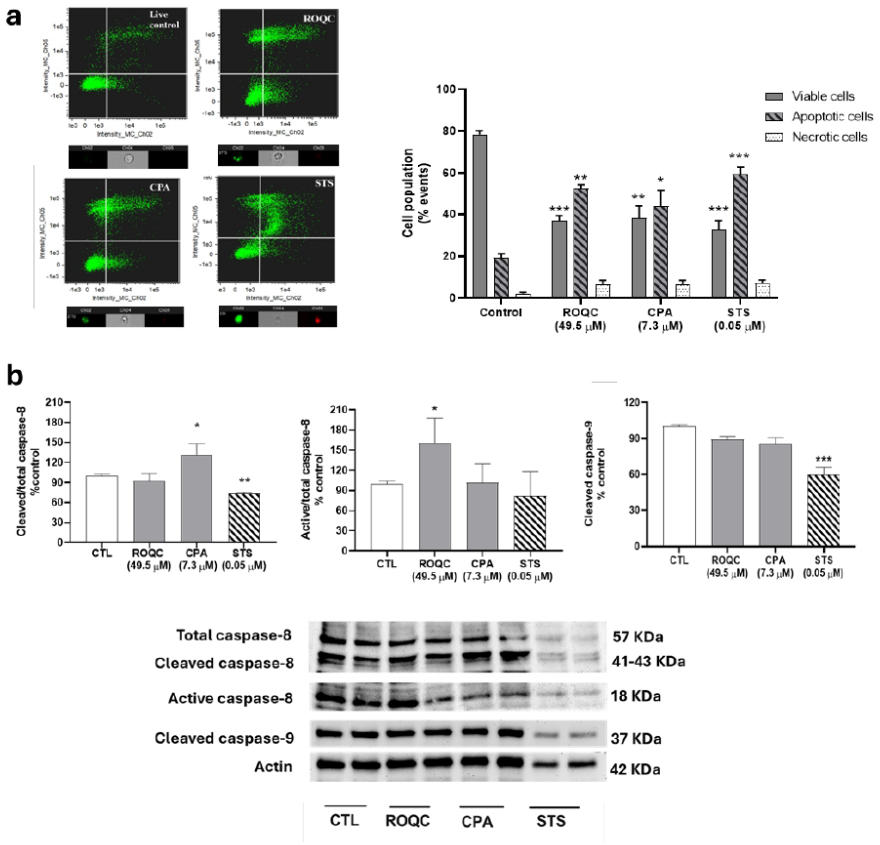


Figure 3. Cell death type induced by ROQC and CPA. (a) Results obtained by flow cytometry of SH-SY5Y cells treated with ROQC and CPA for 24 h at IC_{50} values, co-stained with Annexin V-FITC and PI. Fluorescence of 10000 cells was monitored. Percentages of viable cells (Annexin V-FITC -/PI), apoptotic cells (Annexin V-FITC + /PI – and +), and necrotic cells (Annexin V-FITC – /PI+) were calculated. STS was used as a positive control. (b) Expression of cleaved caspase -8, active caspase-8 and cleaved caspase-9 measured by western blot. Cleaved and active caspase-8 are expressed as ratio between its total levels. Protein band expression is normalized by actin levels. Values are mean ± SEM of three independent replicates, carried out by duplicate, and compared to control cells by one-way ANOVA followed by Dunnett test (*$p \leq 0.05$, **$p \leq 0.01$ and ***$p \leq 0.001$).

3.2. Effects of combined emerging mycotoxins on viability and cytotoxicity of SH-SY5Y cells

As cheese samples are commonly contaminated with ROQC and CPA in combination with other emerging mycotoxins, these two compounds where binary combined with ENNs A, A1, B and B1 at 10:1 ratio. The proportion was selected based on the most common proportions found in cheeses (Rodríguez-Cañás et al., 2023).

USC UNIVERSIDADE DE SANTIAGO DE COMPOSTELA

Before starting with the combined effects, the cytotoxicity of ENNs was tested. We had previously performed dose-response assays with these toxins in SH-SY5Y cells cultured in medium with 10% FBS (N. Pérez-Fuentes et al., 2021; 2022). Recently, we observed that the reduction of FBS concentration to 2%improves the results and reduces the variability between replicates (Figure 1S)(Mengual Gómez et al., 2010; Khasawneh et al., 2019; Lopes et al., 2010). In this sense, both MTT and LDH assays were repeated with ENNs A, A1, B and B1 in cell medium with 2% FBS (Figure 2S). No significant variations were observed in the data obtained with MTT assay, except for ENN B. This toxin did not produce a complete inhibition of cell viability in our previous results, but with a lower percentage of FBS we observed a total reduction at the highest dose tested, obtaining an IC_{50} of 1.5 µM (CI: 0.93 – 3.5 µM), in the same range than the previous one (0.43 µM). Regarding LDH release, no differences were detected, as EC_{50} values are similar to the previously reported for ENNs A, A1 and B1, whilst ENN B did not produce cell leakage(N. Pérez-Fuentes et al., 2022; 2021).

After confirming that FBS concentration did not affect ENNs results, the effects on cell viability and cytotoxicity of ROQC binary combined with ENNs (10:1) were determined. Regarding cell viability, the results obtained with the combination ROQC + ENN A were higher than those of ROQC alone, but similar to those of ENN A alone, which caused cell damage at concentrations higher than 2 µM (Figure 4 a). In ROQC + ENN A1 mixture, the effect of both toxins alone was enhanced, with a reduction in cell viability of 42.7 ± 13.5% at a concentration of 20 µM + 2 µM (Figure 4 b). In the case of ROQC + ENN B and ROQC + ENN B1 combinations, a decrease in cell viability similar to the effect produced by both ENNs alone was obtained. However, this reduction in cell survival was higher than the induced by ROQC alone (Figure 4 c, d).

Data obtained with LDH assay for ROQC combinations were consistent with those of cell viability. ROQC + ENN A and ROQC + ENN A1 mixtures showed greater effects than the emerging mycotoxins alone, inducing cytotoxicity at concentrations higher than 20 µM + 2 µM (Figure 4 e, f). ROQC + ENN B combination produced complete death at the highest concentrations used (80 µM + 8 µM and 100 µM + 10 µM), potentiating the effects of ENN B alone (Figure 4 g). For ROQC + ENN B1 mixture, the effects observed were slightly higher than those of both mycotoxins alone, showing a LDH release of 46.2 ±15.5 % at 40 µM + 4 µM (Figure 4 h).

USC UNIVERSIDADE DE SANTIAGO DE COMPOSTELA

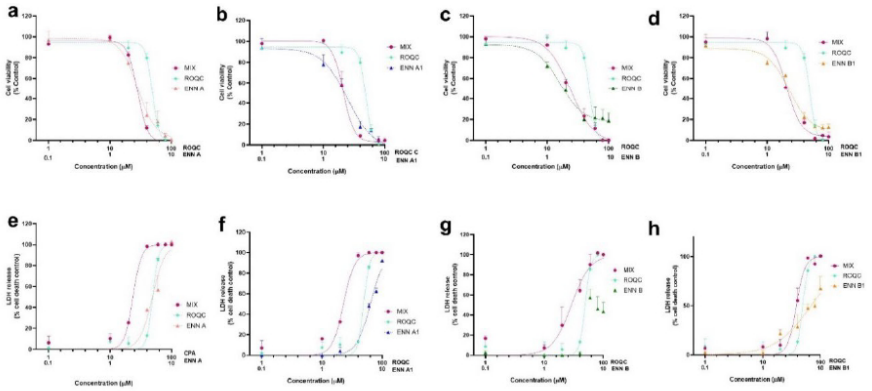


Figure 4. Effects on cell viability and cytotoxicity of binary combinations of ROQC with ENNs A, A1, B and B1. Cells were treated with binary mixtures of mycotoxins for 24 h. (a) Effect of ROQC + ENN A (10:1), (b) ROQC+ ENN A1 (10:1), (c) ROQC + ENN B (10:1) and (d) ROQC + ENN B1 (10:1) on cell viability, assessed by MTT test. (e) Cytotoxicity of ROQC + ENN A (10:1), (f) ROQC+ ENN A1 (10:1), (g) ROQC + ENN B (10:1) and (h) ROQC + ENN B1 (10:1), determined by LDH assay. Saponin at 1 mg/mL was used as cell death control. Pointed lines show the effects of each toxin alone while purple line represents the mixture. Data are mean ± SEM of three independent replicates. Data were fitted with a log (inhibitor) *vs* response and a log (agonist) *vs* response model for cell viability and LDH assays, respectively.

Then, the effects of CPA and ENNs (10:1) binary mixtures were determined. In MTT assay, all combinations showed a dose-response curve similar to the produced by CPA alone. The effects of ENNs were slightly increased since a reduction on cell viability was induced at concentrations above 1 µM + 0.1 µM (Figure 5 a-d). By contrast, when cytotoxicity was determined, CPA effects were intensified in all combinations, reaching a 100% of LDH release in CPA + ENN A and CPA + ENN A1 mixtures (Figure 5 e-h).

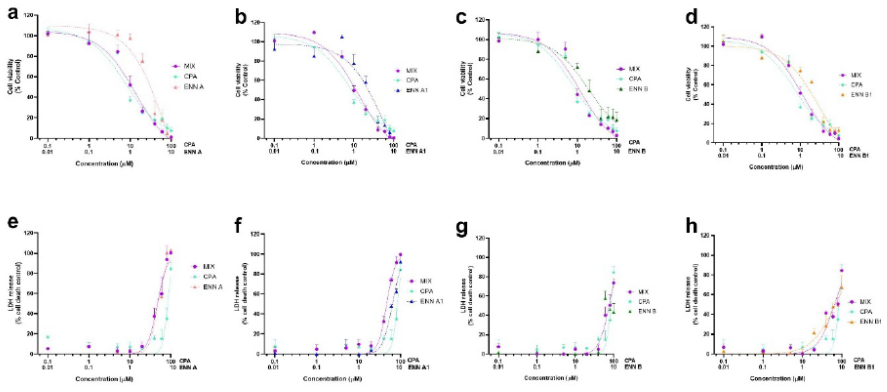


Figure 5. Cell viability and cytotoxicity of CPA binary combinations with ENNs A, A1, B and B1. SH-

USC UNIVERSIDADE DE SANTIAGO DE COMPOSTELA

SY5Y cells were treated with binary mixtures of mycotoxins for 24 h. (a) Effect of CPA + ENN A (10:1), (b) CPA+ ENN A1 (10:1), (c) CPA + ENN B (10:1) and (d) CPA + ENN B1 (1:10) on cell viability, assessed by MTT test. (e) Cytotoxicity of CPA + ENN A (10:1), (f) CPA+ ENN A1 (10:1), (g) CPA + ENN B (10:1) and (h) CPA + ENN B1 (10:1), determined by LDH assay. Saponin at 1 mg/mL was used as cell death control. Pointed lines show the effects of each toxin alone while purple line represents the mixture. Data are mean ± SEM of three independent replicates. Data were fitted with a log (inhibitor) *vs* response and a log (agonist) *vs* response model for cell viability and LDH assays, respectively.

Then, IC_{50} and EC_{50} values were calculated for each mixture by fitting the data with a log(inhibitor) *vs* response model and with a log(agonist) *vs* response model, respectively (Table 1S). With these results, combination index was obtained following Chou & Talalay method, and the value obtained was higher than 1 in all cases, indicating antagonism (Ting-Chao Chou and Talalay, 1983).

Since ROQC and CPA are usually detected in cheese combined with ENNs A, B, A1 and B1, as well as with BEA, all the toxins were tested together at ratios according to their natural proportions. As MTT test is more sensitive, it was performed to determine the effects of mixtures on cell viability. Then, IC_{50} values and combination index for each mixture were calculated as described above.
Before proceeding with the combination of all toxins, the four ENNs (A, A1, B and B1) were mixed in a 1:1:1:1 ratio at concentrations ranging from 0.01 to 10 µM. We had previously tested binary combinations of these toxins at 1:1 proportion and most of them produced antagonism, except ENN B1 and ENN A mixture, that resulted in an additive effect (Nadia Pérez-Fuentes et al., 2023; N. Pérez-Fuentes et al., 2022). As Figure 6 a shows, treatment with the four ENNs together enhanced the effects of the single toxins, presenting IC_{50} values of 1.1 µM (CI: 0.6 – 2.0 µM), slightly lower than the IC_{50} of each toxin alone (among 1.5 and 2.7 µM). Nevertheless, the combination index for this mix was 2.0, indicating antagonism. Then, ROQC was mixed with the four ENNs at 10:1:1:1:1 ratio (ROQC+ENN A+ENN A1+ENN B+ENN B1). With this combination, an increase greater than 15% on their individual effects was observed (Figure 6 b). The IC_{50} obtained was 3.0 µM (CI: 1.2 - 5.5 µM) for ROQC and 0.3 µM (CI: 0.12 - 0.55 µM) for each ENN. Then, a combination index of 0.6 was obtained, revealing a synergistic effect among these toxins. CPA was also combined with ENNs A, A1, B and B1 at a 10:1:1:1:1 proportion. In this case, CPA effects were potentiated about a 9%. The IC_{50} for CPA was 0.82 µM (CI: 0.1 – 1.7 µM) and a value of 0.08 µM (CI: 0.01 - 0.17 µM) was obtained for each ENN (Figure 6 c). In this case, the combination index was 0.26, indicating synergism.

Next, BEA was added to the previously described mixtures at the same proportion as ENNs. Combinations were performed as follows: ENN A+ ENN A1+ ENN B+ ENN B1 + BEA (1:1:1:1:1), ROQC+ ENN A+ ENN A1+ ENN B+ ENN B1 + BEA (10:1:1:1:1:1) and CPA + ENN A+ ENN A1+ ENN B+ ENN B1 + BEA (10: 1:1:1:1:1). The effects observed for the first mixture were similar to the obtained with the four ENNs, showing an IC_{50} of 1.1 µM (CI: 0.6 – 1.8 µM) for each toxin (Figure 6 d). The same occurred when ROQC was combined with ENNs and BEA, whose individual effects were increased (Figure 6 e). The IC_{50} of this combination was 4.8 µM (CI: 2.3 – 8.4 µM) for ROQC and 0.5 µM (CI: 0.23 – 0.84 µM) for ENNs and BEA. The mixture of CPA with ENNs and BEA also intensified the effects of individual mycotoxins,

USC UNIVERSIDADE DE SANTIAGO DE COMPOSTELA

but it seems to present a lower effect than CPA and ENNs combination (Figure 6 f). In this case, the IC_{50} was 2.4 µM (CI: 0.74 – 5.0 µM) for CPA and 0.24 µM (CI: 0.07 – 0.5µM) for each ENN and BEA, respectively. Although potentiation of the individual effects of the mycotoxins was observed in all BEA mixtures, the combination index was higher than 1 in all cases, except for the mixture of CPA with ENNs and BEA, which presented a value of 0.9, indicating an additive effect.

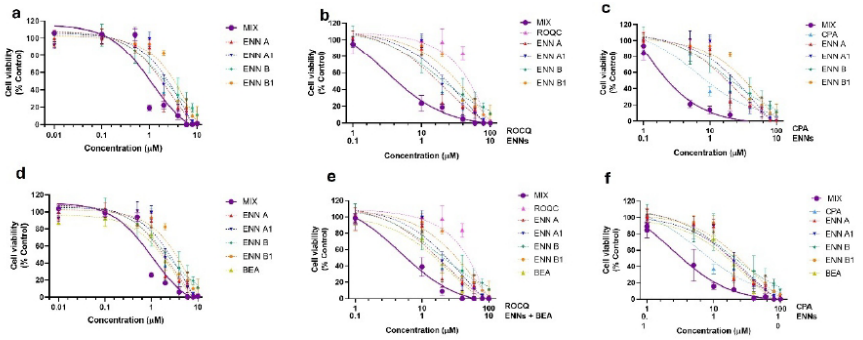


Figure 6. Effects of emerging mycotoxins multiple combinations on viability of SH-SY5Y cells. Cells were treated with combined mycotoxins for 24 h and MTT assay was carried out. Pointed lines showed the effects of each toxin alone while purple line represents the mixture of all. (a) ENN A+ ENN A1+ ENN B + ENN B1 (1:1:1:1), (b) ROQC + ENN A+ ENN A1+ ENN B + ENN B1 (10:1:1:1:1), (c) CPA + ENN A+ ENN A1+ ENN B + ENN B1 (10:1:1:1:1), (d) ENN A+ ENN A1+ ENN B + ENN B1 + BEA (1:1:1:1:1), (e) ROQC + ENN A+ ENN A1+ ENN B + ENN B1 + BEA (10:1:1:1:1:1) and (f) CPA + ENN A+ ENN A1+ ENN B + ENN B1 + BEA (10:1:1:1:1:1). Mean ± SEM of three independent replicates expressed as percentage of untreated control cells. Data were fitted with a log (inhibitor) *vs* response model

3.3. Analysis of mycotoxin content and cytotoxicity of three cheese samples

In view of the results obtained with mycotoxin combinations, the cytotoxicity of cheese extracts was studied in the same cell model to test the effect of a real mixture. At first, cheese samples were analysed using an in-house validated method designed for the quantification of 32 mycotoxins, including regulated, emerging, and modified compounds. Notably, the method exhibits high sensitivity, enabling the detection of compounds at concentrations below the maximum residue levels specified in European regulations. Moreover, the method demonstrates satisfactory accuracy and precision, meeting the performance criteria defined in legislation (Jesús M. González-Jartín et al., 2020; EC, 2006).

Several mycotoxins were detected in the extracts (Figure 3S), and their quantification was done by using linear 1/X calibration curves. Results were adjusted for matrix effects and recovery, and expressed in nM, as shown in Table 2S. No regulated or modified mycotoxins were detected, however, several emerging compounds were identified, including trace amounts (< 20 µg/kg) of *Fusarium* toxins namely BEA and ENNs, which were consistently found across all cheese types. Additionally, low levels of alternariol methyl-

USC UNIVERSIDADE DE SANTIAGO DE COMPOSTELA

ether (AME) and sterigmatocystin (STG) were detected. Furthermore, ROQC was detected in the Emmental sample at levels close to 2500 µg/kg and CPA was found in blue cheese at 800 µg/kg.

Then, the three cheese extracts were tested in human neuroblastoma cells. Camembert sample was used as a matrix control, since it was the less contaminated cheese, and it did not present ROQ and CPA. The effects of the extracts on cell viability and cytotoxicity were determined with MTT and LDH, respectively. Cells were treated with the extracts at dilutions between 1:200 and 1:1000 for 24 h. In MTT assay, Emmental extract reduced cell viability between 20.0 and 99.9% at concentrations above 1:500 compared to the Camembert control. On the other hand, blue cheese extract caused a smaller reduction in viability (40.1 - 66.0% at concentrations between 1:400 and 1:200) (Figure 7 a). LDH release was increased by 84.8 ± 6.4 % and 13.9 ± 4.8 % at the highest concentration used for Emmental and blue cheese extracts, respectively, in agreement with the results obtained in the MTT test (Figure 7 b).

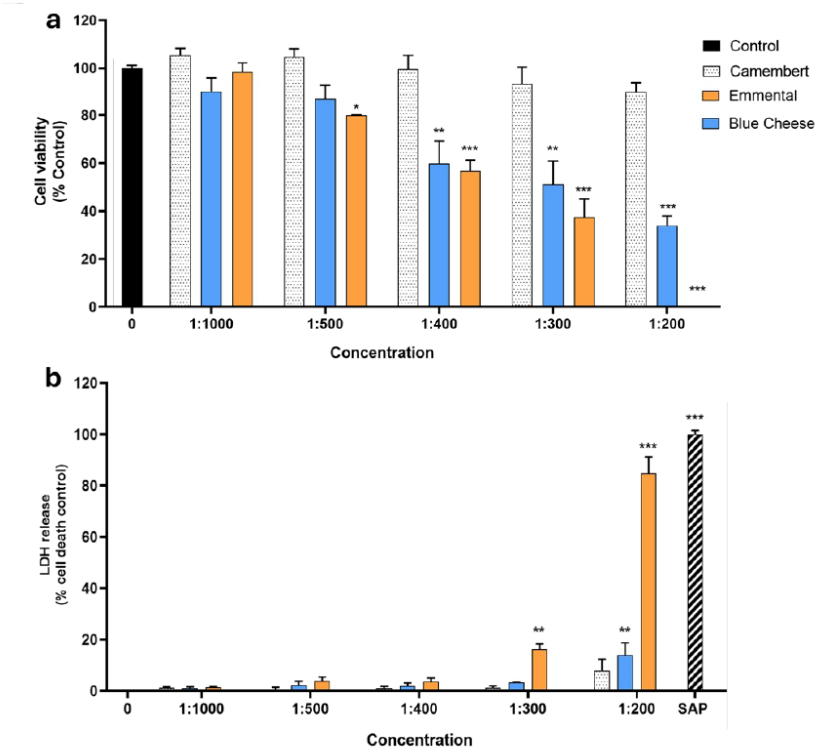


Figure 7. Effect of cheese extracts on cell viability and cytotoxicity of SH-SY5Y cells. Cells were treated with dilutions between 1:200 - 1:1000 of each cheese extract for 24 h. Effects of emmental extract (orange), blue cheese extract (blue) and camembert extract as blank (white) where determined on (a) cell viability and (b)cytotoxicity by MTT test and LDH assay, respectively. Saponin (SAP) at 1 mg/mL was used as cell death control. Data are mean ± SEM of three independent replicates expressed as percentage of untreated

USC
UNIVERSIDADE DE SANTIAGO DE COMPOSTELA

control cells. IC_{50} values were determined by fitting the data with a log (inhibitor) vs response model. EC_{50} values were determined by fitting the data with a log (agonist) vs response model.

4. Discussion

Mould growth on cheese is a major concern as it raises both food quality and safety issues. While several genera of fungi can affect cheese in terms of decomposition, some species are used in the ripening process. *Penicillium* is the most commonly used genus in this process. These cheese-contaminating moulds have the potential to produce mycotoxins such as ochratoxin A, STG and CPA, that remain stable under processing conditions, retaining their cytotoxic activity (Izzo et al., 2022; Rodríguez-Cañás et al., 2023; Kure and Skaar, 2019). To date, the EU legislation does not regulate levels of mycotoxins in cheese, and only aflatoxin M1 is regulated in milk and milk-derived products (EC, 2023). However, recent studies have highlighted the presence of emerging mycotoxins in both milk and cheese at a wide range of concentrations, including ENNs, BEA, ROQC and CPA (Izzo et al., 2022; Rodríguez-Cañás et al., 2023; J. M. González-Jartín et al., 2021). In this sense, we have previously analysed the effects of two milk extracts, contaminated with ENNs and BEA at concentrations in the picomolar range, observing that their co-occurrence had a greater effect on cell viability than expected (N. Pérez-Fuentes et al., 2021).

In the present study, the first step was to study the single effects of ROQC and CPA, as these toxins have been detected in different cheese samples (Rodríguez-Cañás et al., 2023). Neither ROQC nor CPA are considered a potential health concern because they do not cause significant toxicological effects at the concentrations commonly found in food. However, data on their cytotoxicity are insufficient (N. Hymery et al., 2018; Maragos et al., 2023). In our assays, CPA was more toxic than ROQC, presenting an IC_{50} of 7.3 µM. This finding contrasts with a recent study on the same cell line which reported an IC_{50} of 40.8 µM for CPA after 72 h treatment (de Sá et al., 2024). It is important to note that the discrepancy in IC_{50} values could be due to differences in experimental conditions between the two studies. Key variables such as the solvent used, the number of cells, the percentage of FBS in the culture medium and the duration of the assay were not consistent between the experiments. These factors can significantly influence cell viability results (Ghasemi et al., 2021; Mengual Gómez et al., 2010; Khasawneh et al., 2019). As the toxin stock in the current work was prepared in DMSO, which has the ability to interact with phospholipids in cell membranes and enables the diffusion of molecules across the cell membrane, the use of this vehicle could facilitate the uptake of the toxin into the cell, allowing it to exert its effects more rapidly (Nguyen et al., 2020; Nolwenn Hymery et al., 2014). Indeed, in a study using DMSO as a solvent for CPA, a nanomolar reduction in cell viability was observed in several cell lines (Nolwenn Hymery et al., 2014).Then, to support the cell viability data, a cytotoxicity assay was performed. In this sense, CPA had an EC_{50} of 84.1 µM. The cytotoxicity method used measures the release of LDH into the culture media after cell membrane disruption, whereas MTT assay is more sensitive because it measures the cellular metabolic activity (Fotakis and Timbrell, 2006). Therefore, our data may indicate that CPA interrupts cellular metabolism without compromising plasma membrane integrity until high concentrations are reached. In the case of ROQC, it shows the same value in both assays (49.5 µM), indicating that this compound produces metabolic and cell membrane disruption simultaneously, which suggest a different mechanism of action than CPA. The exact mode of action of ROQC toxicity is not yet understood, but it inhibits rat and human cytochrome P450, involved in

USC UNIVERSIDADE DE SANTIAGO DE COMPOSTELA

cellular metabolism and homeostasis, which could be related to the effects observed (Metin, 2023; Zhao et al., 2021).Both ROQC and CPA induced apoptotic cell death, involving the extrinsic pathway of apoptosis, as they increased the expression of active and cleaved caspase -8, respectively (Y. Wu et al., 2016). While there are no data on the type of death induced by ROQC, CPA has been described to induce p53-dependent apoptosis and to enhance IL-1β apoptosis in several cell lines, supporting our findings (Suzuki et al., 2024; Bonyadi et al., 2021; Miani et al., 2013).

On the other hand, ENNs and BEA, common mycotoxins found in cheese samples, have also been described to induce apoptosis of human neuroblastoma cells (N. Pérez-Fuentes et al., 2021; 2022; Rodríguez-Cañás et al., 2023; Izzo et al., 2022). ENNs and BEA have been the subject of recent studies due to their increasing prevalence in various foods. These toxins induce cytotoxicity in the micromolar range, affect mitochondrial function and alter calcium homeostasis in various cell lines (N. Pérez-Fuentes et al., 2022; Nadia Pérez-Fuentes et al., 2023; Alonso-Garrido et al., 2020; Aufy et al., 2023; Caloni et al., 2020). Although some studies reported additive or synergistic effects of these toxins in combination with other mycotoxins, these data are insufficient (EFSA, 2014). In a recent study, we observed an additive effect of the combination of ENN A + ENN B1 in SH-SY5Y cells (N. Pérez-Fuentes et al., 2022). However, the toxicity of all ENNs (A, A1, B and B1) together has not yet been evaluated in this cell line. In this sense, the present study describes for first time a greater combined effect of ENNs A, A1, B and B1 mixture than the observed when each toxin was added alone. Given their cytotoxicity and high prevalence in many natural samples, the co-occurrence of ENNs in food could pose a significant health risk. It should be noted that these four ENNs often contaminate natural matrices together, increasing the need to further evaluate their effects in combination in other cell lines and even in animal models (Izzo et al., 2022; Chalyy et al., 2021; H. Olleik et al., 2019a; Maranghi et al., 2018; Fraeyman et al., 2017).

Regarding CPA, it has shown additive effects with aflatoxins, but data on its joint toxicity with other mycotoxins is even scarcer than for ENNs (Pier et al., 1989). In the case of ROQC, to our knowledge, there are no studies about its combinations. Considering that both compounds are used in cheese ripening and that they are cytotoxic by themselves, we first tested their effects in binary combination with ENNs.

In all the mixtures, a shift in the combination curve is observed, suggesting an enhancement of their individual effects. Nevertheless, when the combination index was calculated, the value was greater than 1 in all cases, indicating antagonism. This discrepancy could be due to the fact that synergism is mutual for all compounds, whereas potentiation, enhancement or augmentation is unilateral (T. C. Chou, 2010). In some of the binary mixtures performed, we observed potentiation for one of the compounds but not for the other, as occurs in ROQC and ENN A mixture or in the combination of ROQC, ENNs and BEA, in which the combined IC_{50} is much lower than the individual value of each toxin. Synergism was only achieved in two of the mixtures tested (ROQC+ ENN A+ENN A1+ ENN B+ ENN B1 and CPA+ ENN A+ENN A1+ ENN B+ ENN B1), in which the combined IC_{50} was at least 9 times lower than the individual IC_{50} of each toxin. In the case of CPA+ ENN A+ENN A1+ ENN B+ ENN B1+ BEA mixture, an additive effect was observed. While ROQCs and CPAs are not considered a potential health hazard, existing toxicity data are limited to studies of these compounds alone without contemplating potential interactions with other mycotoxins (N. Hymery et al., 2018; Suzuki et al., 2024; Nolwenn Hymery et al., 2014). Here we observed that the co-occurrence of ENNs with CPA and ROQC, often observed in cheeses, significantly increases

USC UNIVERSIDADE DE SANTIAGO DE COMPOSTELA

the effects of these two toxins, up to concentrations that could be found in natural samples (Rodríguez-Cañás et al., 2023; Maragos et al., 2023; Izzo et al., 2022). Hence, as they could be a health concern, it would be interesting to deep into their combined effects.

Considering that mycotoxins are liposoluble substances and cheese is mainly fat, the effects of the combination of these toxins could be further enhanced by the matrix (Taevernier et al., 2016; Krug et al., 2018; Alonso-Garrido et al., 2021). Interestingly, the analysis of extracts from cheese commercial samples showed a strong reduction in cell viability, especially with the Emmental extract. As an academic exercise with no real-world implications, the 1:200 concentration of this extract rich in ROQC would be equivalent to approximately 45 g of cheese consumed. This estimation is based on a 60 kg woman with a body composition of 60% water. Therefore, even a small amount of cheese could potentially cause cellular damage. Although this calculation does not reflect a food risk evaluation, which was not the purpose of the article, it is worth mentioning that an extreme value from a commercial product could pose cytotoxic levels. Therefore, the role of emerging mycotoxins in food, cheese in this article, is clearly in need of risk evaluation, as their combined presence increases several folds the toxicity of certain mycotoxins. Also, this article provides experimental evidence that cheese should be included in the list of mycotoxins-regulated products.

In conclusion, our results indicate that ROQC and CPA are cytotoxic to human neuroblastoma cells and induce apoptosis via the extrinsic pathway. Their binary combination with ENNs A, A1, B and B1 results in an enhancement of the individual effects of each toxin. In addition, the mixture of emerging mycotoxins produced a higher effect than the cytotoxicity induced by ROQC, CPA, ENNs A, A1, B and B1 alone, and even greater damage was observed when they co-occurred on a natural matrix. In view of these results, it would be of particular interest to compare their effects on different natural matrices, which would help to better understand their impact on human health and consequently decide whether legal limits should be set in food.

5. References

Alonso-Garrido, M., Frangiamone, M., Font, G., Cimbalo, A., & Manyes, L. (2021). In vitro blood brain barrier exposure to mycotoxins and carotenoids pumpkin extract alters mitochondrial gene expression and oxidative stress. *Food Chem Toxicol*, 153, 112261. doi:10.1016/j.fct.2021.112261.

Alonso-Garrido, M., Manyes, L., Pralea, I. E., & Iuga, C. A. (2020). Mitochondrial proteomics profile points oxidative phosphorylation as main target for beauvericin and enniatin B mixture. *Food Chem Toxicol*, 141, 111432. doi:10.1016/j.fct.2020.111432.

Alvariño, R., Alonso, E., Bornancin, L., Bonnard, I., Inguimbert, N., Banaigs, B., et al. (2020). Biological Activities of Cyclic and Acyclic B-Type Laxaphycins in SH-SY5Y Human Neuroblastoma Cells. *Mar Drugs*, 18(7). doi:10.3390/md18070364.

Alvariño, R., Alonso, E., Tribalat, M. A., Gegunde, S., Thomas, O. P., & Botana, L. M. (2017). Evaluation of the Protective Effects of Sarains on H(2)O(2)-Induced Mitochondrial Dysfunction and Oxidative Stress in SH-SY5Y Neuroblastoma Cells. *Neurotox Res*, 32(3), 368-380. doi:10.1007/s12640-017-9748-3.

Aufy, M., Abdelaziz, R. F., Hussein, A. M., Topcagic, N., Shamroukh, H., Abdel-Maksoud, M. A., et al. (2023). Impact of Enniatin B and Beauvericin on Lysosomal Cathepsin B Secretion and Apoptosis Induction. *Int J Mol Sci*, 24(3). doi:10.3390/ijms24032030.

Bonyadi, F., Hasanzadeh, S., & Malekinejad, H. (2021). Cyclopiazonic acid induced p53-dependent apoptosis in the testis of mice: Another male related risk factor of infertility. *Environ Toxicol*, 36(5), 903-913. doi:10.1002/tox.23092.

Caloni, F., Fossati, P., Anadón, A., & Bertero, A. (2020). Beauvericin: The beauty and the beast. *Environmental Toxicology and Pharmacology*, 75, 103349. doi:https://doi.org/10.1016/j.etap.2020.103349.

USC UNIVERSIDADE DE SANTIAGO DE COMPOSTELA

Casquete, R., Benito, M. J., Aranda, E., Martín, A., Hernández, A., & Córdoba, M. G. (2021). Cyclopiazonic acid gene expression as strategy to minimizing mycotoxin contamination in cheese. *Fungal Biol*, 125(2), 160-165. doi:10.1016/j.funbio.2019.06.011.
Chalyy, Z. A., Kiseleva, M. G., Sedova, I. B., Minaeva, L. P., Sheveleva, S. A., & Tutelyan, V. A. (2021). [Dried fruits marketed in Russia: multi-mycotoxin contamination]. *Vopr Pitan*, 90(1), 33-39. doi:10.33029/0042-8833-2021-90-1-33-39.
Chang, P. K., Ehrlich, K. C., & Fujii, I. (2009). Cyclopiazonic acid biosynthesis of Aspergillus flavus and Aspergillus oryzae. *Toxins (Basel)*, 1(2), 74-99. doi:10.3390/toxins1020074.
Chou, T.-C., & Talalay, P. (1983). Analysis of combined drug effects: a new look at a very old problem. *Trends in Pharmacological Sciences*, 4, 450-454. doi:https://doi.org/10.1016/0165-6147(83)90490-X.
Chou, T. C. (2010). Drug combination studies and their synergy quantification using the Chou-Talalay method. *Cancer Res*, 70(2), 440-6. doi:10.1158/0008-5472.can-09-1947.
de Sá, S. V. M., Sousa Monteiro, C., Fernandes, J. O., Pinto, E., Faria, M. A., & Cunha, S. C. (2024). Evaluating the human neurotoxicity and toxicological interactions impact of co-occurring regulated and emerging mycotoxins. *Food Research International*, 184, 114239. doi:https://doi.org/10.1016/j.foodres.2024.114239.
EC (2006) 'EC (2006). Commission Regulation (EC) No 401/2006 of 23 February 2006 laying down the methods of sampling and analysis for the official control of the levels of mycotoxins in foodstuffs (Text with EEA relevance). Official Journal of theEuropean Union, L 70/12.'.

EC (2023) 'EC (2023). Commission Regulation (EU) 2023/915 of 25 April 2023 on maximum levels for certain contaminants in food and repealing Regulation (EC)N1881/2006. Official Journal of theEuropean Union, L 119/103.'.

EFSA (2014). Scientific Opinion on the risks to human and animal health related to the presence of beauvericin and enniatins in food and feed. *EFSA Journal*, 12(8), 3802. doi:10.2903/j.efsa.2014.3802.
El-Sayed, R. A., Jebur, A. B., Kang, W., & El-Demerdash, F. M. (2022). An overview on the major mycotoxins in food products: characteristics, toxicity, and analysis. *Journal of Future Foods*, 2(2), 91-102. doi:https://doi.org/10.1016/j.jfutfo.2022.03.002.
Fliszár-Nyúl, E., Faisal, Z., Skaper, R., Lemli, B., Bayartsetseg, B., Hetényi, C., et al. (2022). Interaction of the Emerging Mycotoxins Beauvericin, Cyclopiazonic Acid, and Sterigmatocystin with Human Serum Albumin. *Biomolecules*, 12(8). doi:10.3390/biom12081106.
Fotakis, G., & Timbrell, J. A. (2006). In vitro cytotoxicity assays: comparison of LDH, neutral red, MTT and protein assay in hepatoma cell lines following exposure to cadmium chloride. *Toxicol Lett*, 160(2), 171-7. doi:10.1016/j.toxlet.2005.07.001.
Fraeyman, S., Croubels, S., Devreese, M., & Antonissen, G. (2017). Emerging Fusarium and Alternaria Mycotoxins: Occurrence, Toxicity and Toxicokinetics. *Toxins (Basel)*, 9(7). doi:10.3390/toxins9070228.
Ghasemi, M., Turnbull, T., Sebastian, S., & Kempson, I. (2021). The MTT Assay: Utility, Limitations, Pitfalls, and Interpretation in Bulk and Single-Cell Analysis. *Int J Mol Sci*, 22(23). doi:10.3390/ijms222312827.
González-Jartín, J. M., Alfonso, A., Sainz, M. J., Vieytes, M. R., & Botana, L. M. (2020). Multi-detection method for mycotoxins with a modified QuEChERS extraction in feed and development of a simple detoxification procedure. *Animal Feed Science and Technology*, 114745. doi:https://doi.org/10.1016/j.anifeedsci.2020.114745.
González-Jartín, J. M., Rodríguez-Cañás, I., Alfonso, A., Sainz, M. J., Vieytes, M. R., Gomes, A., et al. (2021). Multianalyte method for the determination of regulated, emerging and modified mycotoxins in milk: QuEChERS extraction followed by UHPLC-MS/MS analysis. *Food Chem*, 356, 129647. doi:10.1016/j.foodchem.2021.129647.
Hasuda, A. L., Person, E., Khoshal, A., Bruel, S., Puel, S., Oswald, I. P., et al. (2023). Emerging mycotoxins induce hepatotoxicity in pigs' precision-cut liver slices and HepG2 cells. *Toxicon*, 231, 107195. doi:10.1016/j.toxicon.2023.107195.
Hymery, N., Masson, F., Barbier, G., & Coton, E. (2014). Cytotoxicity and immunotoxicity of cyclopiazonic acid on human cells. *Toxicology in Vitro*, 28(5), 940-947. doi:https://doi.org/10.1016/j.tiv.2014.04.003.
Hymery, N., Mounier, J., & Coton, E. (2018). Effect of Penicillium roqueforti mycotoxins on Caco-2 cells: Acute and chronic exposure. *Toxicol In Vitro*, 48, 188-194. doi:10.1016/j.tiv.2018.01.017.
Izzo, L., Mikušová, P., Lombardi, S., Sulyok, M., & Ritieni, A. (2022). Analysis of Mycotoxin and Secondary Metabolites in Commercial and Traditional Slovak Cheese Samples. *Toxins (Basel)*, 14(2). doi:10.3390/toxins14020134.

USC UNIVERSIDADE DE SANTIAGO DE COMPOSTELA

Khasawneh, R. R., Al Sharie, A. H., Abu-El Rub, E., Serhan, A. O., & Obeidat, H. N. (2019). Addressing the impact of different fetal bovine serum percentages on mesenchymal stem cells biological performance. *Molecular Biology Reports*, 46(4), 4437-4441. doi:10.1007/s11033-019-04898-1.
Kouri, K., Lemmens, M., & Lemmens-Gruber, R. (2003). Beauvericin-induced channels in ventricular myocytes and liposomes. *Biochimica et Biophysica Acta (BBA) - Biomembranes*, 1609(2), 203-210. doi:https://doi.org/10.1016/S0005-2736(02)00689-2.
Krug, I., Behrens, M., Esselen, M., & Humpf, H. U. (2018). Transport of enniatin B and enniatin B1 across the blood-brain barrier and hints for neurotoxic effects in cerebral cells. *PLoS One*, 13(5), e0197406. doi:10.1371/journal.pone.0197406.
Kure, C. F., & Skaar, I. (2019). The fungal problem in cheese industry. *Current Opinion in Food Science*, 29, 14-19. doi:https://doi.org/10.1016/j.cofs.2019.07.003.
Lopes, F. M., Schröder, R., da Frota, M. L., Jr., Zanotto-Filho, A., Müller, C. B., Pires, A. S., et al. (2010). Comparison between proliferative and neuron-like SH-SY5Y cells as an in vitro model for Parkinson disease studies. *Brain Res*, 1337, 85-94. doi:10.1016/j.brainres.2010.03.102.
Mallebrera, B., Prosperini, A., Font, G., & Ruiz, M. J. (2018). In vitro mechanisms of Beauvericin toxicity: A review. *Food Chem Toxicol*, 111, 537-545. doi:10.1016/j.fct.2017.11.019.
Maragos, C. M., Probyn, C., Proctor, R. H., & Sieve, K. K. (2023). Cyclopiazonic acid in soft-ripened and blue cheeses marketed in the USA. *Food Addit Contam Part B Surveill*, 16(1), 14-23. doi:10.1080/19393210.2022.2109213.
Maranghi, F., Tassinari, R., Narciso, L., Tait, S., Rocca, C. L., Felice, G. D., et al. (2018). In vivo toxicity and genotoxicity of beauvericin and enniatins. Combined approach to study in vivo toxicity and genotoxicity of mycotoxins beauvericin (BEA) and enniatin B (ENNB). *EFSA Supporting Publications*, 15(5), 1406E.
Marin, S., Ramos, A. J., Cano-Sancho, G., & Sanchis, V. (2013). Mycotoxins: occurrence, toxicology, and exposure assessment. *Food Chem Toxicol*, 60, 218-37. doi:10.1016/j.fct.2013.07.047.
Mengual Gómez, D. L., Belaich, M. N., Rodríguez, V. A., & Ghiringhelli, P. D. (2010). Effects of fetal bovine serum deprivation in cell cultures on the production of Anticarsia gemmatalis multinucleopolyhedrovirus. *BMC Biotechnol*, 10, 68. doi:10.1186/1472-6750-10-68.
Metin, B. (2023). Penicillium roqueforti Secondary Metabolites: Biosynthetic Pathways, Gene Clusters, and Bioactivities.
Miani, M., Barthson, J., Colli, M. L., Brozzi, F., Cnop, M., & Eizirik, D. L. (2013). Endoplasmic reticulum stress sensitizes pancreatic beta cells to interleukin-1β-induced apoptosis via Bim/A1 imbalance. *Cell Death Dis*, 4(7), e701. doi:10.1038/cddis.2013.236.
Nguyen, S. T., Nguyen, H. T.-L., & Truong, K. D. (2020). Comparative cytotoxic effects of methanol, ethanol and DMSO on human cancer cell lines. *Biomedical Research and Therapy*, 7(7), 3855-3859.
Olleik, H., Nicoletti, C., Lafond, M., Courvoisier-Dezord, E., Xue, P., Hijazi, A., et al. (2019a). Comparative Structure-Activity Analysis of the Antimicrobial Activity, Cytotoxicity, and Mechanism of Action of the Fungal Cyclohexadepsipeptides Enniatins and Beauvericin. *Toxins (Basel)*, 11(9). doi:10.3390/toxins11090514.
Olleik, H., Nicoletti, C., Lafond, M., Courvoisier-Dezord, E., Xue, P., Hijazi, A., et al. (2019b). Comparative structure–activity analysis of the antimicrobial activity, cytotoxicity, and mechanism of action of the fungal cyclohexadepsipeptides enniatins and beauvericin. *Toxins*, 11(9), 514.
Perrone, G., & Susca, A. (2017). Penicillium Species and Their Associated Mycotoxins. *Methods Mol Biol*, 1542, 107-119. doi:10.1007/978-1-4939-6707-0_5.
Pier, A. C., Belden, E. L., Ellis, J. A., Nelson, E. W., & Maki, L. R. (1989). Effects of cyclopiazonic acid and aflatoxin singly and in combination on selected clinical, pathological and immunological responses of guinea pigs. *Mycopathologia*, 105(3), 135-42. doi:10.1007/bf00437245.
Pérez-Fuentes, N., Alvariño, R., Alfonso, A., González-Jartín, J., Gegunde, S., Vieytes, M. R., et al. (2021). Single and combined effects of regulated and emerging mycotoxins on viability and mitochondrial function of SH-SY5Y cells. *Food Chem Toxicol*, 154, 112308. doi:10.1016/j.fct.2021.112308.
Pérez-Fuentes, N., Alvariño, R., Alfonso, A., González-Jartín, J., Gegunde, S., Vieytes, M. R., et al. (2022). Enniatins A1 and B1 alter calcium homeostasis of neuronal cells leading to apoptotic death. *Food Chem Toxicol*, 168, 113361. doi:10.1016/j.fct.2022.113361.
Pérez-Fuentes, N., Alvariño, R., Alfonso, A., González-Jartín, J., Vieytes, M. R., & Botana, L. M. (2023). The Mode of Action of Enniatins A and B is Mediated by Interaction with SOC Reservoirs (A) and Mitochondrial Permeability Transition Pore (B). *Exposure and Health*. doi:10.1007/s12403-023-00613-5.
Rodríguez-Cañás, I., González-Jartín, J. M., Alvariño, R., Alfonso, A., Vieytes, M. R., & Botana, L. M. (2023). Detection of mycotoxins in cheese using an optimized analytical method based on a QuEChERS extraction and UHPLC-MS/MS quantification. *Food Chemistry*, 408, 135182. doi:https://doi.org/10.1016/j.foodchem.2022.135182.

USC UNIVERSIDADE DE SANTIAGO DE COMPOSTELA

Shin, C. G., An, D. G., Song, H. H., & Lee, C. (2009). Beauvericin and enniatins H, I and MK1688 are new potent inhibitors of human immunodeficiency virus type-1 integrase. *J Antibiot (Tokyo)*, 62(12), 687-90. doi:10.1038/ja.2009.102.

Suzuki, S., Saito, S., Narushima, Y., Kodani, S., Kagaya, N., Suenaga, H., et al. (2024). Notch activator cyclopiazonic acid induces apoptosis in HL-60 cells through calcineurin activation. *J Antibiot (Tokyo)*, 77(1), 30-38. doi:10.1038/s41429-023-00673-4.

Søderstrøm, S., Lie, K. K., Lundebye, A. K., & Søfteland, L. (2022). Beauvericin (BEA) and enniatin B (ENNB)-induced impairment of mitochondria and lysosomes - Potential sources of intracellular reactive iron triggering ferroptosis in Atlantic salmon primary hepatocytes. *Food Chem Toxicol*, 161, 112819. doi:10.1016/j.fct.2022.112819.

Taevernier, L., Bracke, N., Veryser, L., Wynendaele, E., Gevaert, B., Peremans, K., et al. (2016). Blood-brain barrier transport kinetics of the cyclic depsipeptide mycotoxins beauvericin and enniatins. *Toxicol Lett*, 258, 175-184. doi:10.1016/j.toxlet.2016.06.1741.

Tiwary, A. K., Puschner, B., & Poppenga, R. H. (2009). Using roquefortine C as a biomarker for penitrem A intoxication. *J Vet Diagn Invest*, 21(2), 237-9. doi:10.1177/104063870902100210.

Wu, Q., Patocka, J., Nepovimova, E., & Kuca, K. (2018). A review on the synthesis and bioactivity aspects of beauvericin, a Fusarium mycotoxin. *Frontiers in pharmacology*, 9, 1338.

Wu, Y., Zhao, D., Zhuang, J., Zhang, F., & Xu, C. (2016). Caspase-8 and Caspase-9 Functioned Differently at Different Stages of the Cyclic Stretch-Induced Apoptosis in Human Periodontal Ligament Cells. *PLoS One*, 11(12), e0168268. doi:10.1371/journal.pone.0168268.

Zhao, M., Ma, J., Li, M., Zhang, Y., Jiang, B., Zhao, X., et al. (2021). Cytochrome P450 Enzymes and Drug Metabolism in Humans. *Int J Mol Sci*, 22(23). doi:10.3390/ijms222312808.

USC UNIVERSIDADE DE SANTIAGO DE COMPOSTELA

Supporting Information

In vitro assessment of emerging mycotoxins co-occurring in cheese: A potential health hazard

Nadia Pérez-Fuentes[1], Rebeca Alvariño[1,*], Amparo Alfonso[1,*] Jesús González-Jartín[1], Mercedes R. Vieytes [2], Luis M. Botana[1]

[1]Departamento de Farmacología, Facultad de Veterinaria, IDIS, Universidad de Santiago de Compostela, Lugo 27002, Spain

[2]Departamento de Fisiología, Facultad de Veterinaria, IDIS, Universidad de Santiago de Compostela, Lugo 27002, Spain

*Corresponding authors. Email addresses: rebeca.alvarino@usc.es, amparo.alfonso@usc.es

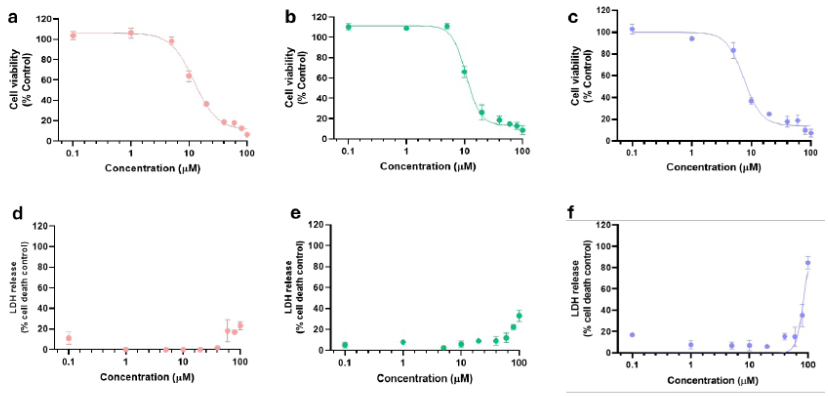


Figure 1S. Effect of CPA on cell viability and cytotoxicity of SH-SY5Y cells at different concentrations of FBS. Cells were treated with mycotoxins for 24 h. Effects of CPA on cell viability, assessed by MTT assay, in culture medium containing (a) 10% FBS, (b) 5% FBS and (c) 2% FBS. Cytotoxicity of CPA determined by LDH assay, in culture medium with (d) 10% FBS, (e) 5% FBS and (f) 2% FBS. Saponin at 1 mg/mL was used as cell death control. Data are mean ± SEM of three independent replicates expressed as percentage of untreated control cells. IC_{50} values were determined by fitting the data with a log (inhibitor) vs response model. EC_{50} values were determined by fitting the data with a log (agonist) vs response model.

USC UNIVERSIDADE DE SANTIAGO DE COMPOSTELA

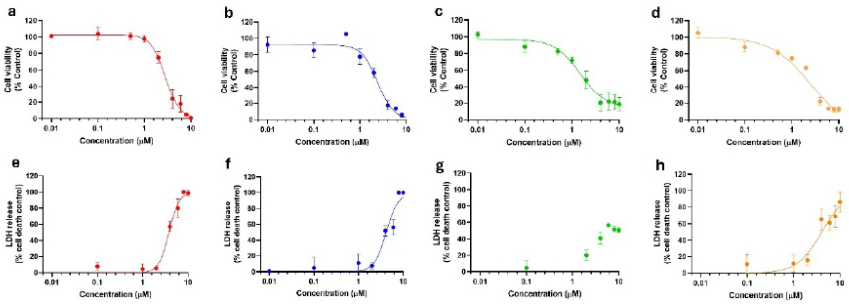


Figure 2S. Effects of ENNs on viability and cytotoxicity of SH-SY5Y cells. Cells were treated with mycotoxins for 24 h. (a) Effect of ENN A, (b) ENN A1, (c) ENN B and (d) ENN B1 on cell viability, assessed by MTT test. (e) Cytotoxicity of ENN A, (f) ENN A1, (g) ENN B and (h) ENN B1, determined by LDH assay. Saponin at 1 mg/mL was used as cell death control. Data are mean ± SEM of three independent replicates expressed as percentage of untreated control cells. IC_{50} values were determined by fitting the data with a log (inhibitor) vs response model. EC_{50} values were determined by fitting the data with a log (agonist) vs response model.

USC UNIVERSIDADE DE SANTIAGO DE COMPOSTELA

Table 1S. IC_{50} and EC_{50} of binary combinations of ROQC and CPA with ENNs

	IC_{50} (µM)		EC_{50} (µM)	
ROQC + ENN A	ROQC	ENN A	ROQC	ENN A
	28.3 µM (26.3 – 30.4)	2.8 µM (2.6 – 3.0)	42.4 µM (18.4 – 130.3)	4.2 µM (1.8– 13.0)
ROQC + ENN A1	ROQC	ENN A1	ROQC	ENN A1
	20.9 µM (19.1 – 23.3)	2.1 µM (1.9 – 2.3)	22.8 µM (20.4– 25.5)	2.3 µM (2.0– 2.5)
ROQC + ENN B	ROQC	ENN B	ROQC	ENN B
	24.0 µM (18.8 – 34.8)	2.4 µM (1.9 – 3.5)	25.5 µM (19.5– 32.8)	2.5 µM (1.9– 3.3)
ROQC + ENN B1	ROQC	ENN B1	ROQC	ENN B1
	20.0 µM (17.7 – 22.9)	2.0 µM (1.8 – 2.3)	38.2 µM (31.2 – 41.7)	3.8 µM (3.1 – 4.2)
CPA+ ENN A	CPA	ENN A	CPA	ENN A
	13.6 µM (9.1 – 20.7)	1.4 µM (0.9 – 2.1)	47.5 µM (39.5 – 55.5)	4.7 µM (3.9 – 5.5)
CPA + ENN A1	CPA	ENN A1	CPA	ENN A1
	10.4 µM (8.8 – 12-6)	1.0 µM (0.88 – 1. 26)	46.9 µM (42.9 – 50.6)	4.7 µM (4.3 – 5.1)
CPA + ENN B	CPA	ENN B	CPA	ENN B
	11.9 µM (7.8 – 18.8)	1.2 µM (0.78 – 1.9)	75.4 µM (68.7 – 82.4)	7.5 µM (6.9 – 8.2)
CPA + ENN B1	CPA	ENN B1	CPA	ENN B1
	9.5 µM (7.8 – 11.8)	0.95 µM (0.78 – 1.2)	65.1 µM (57.0 – 74.7)	6.5 µM (5.7 – 7.5)

USC UNIVERSIDADE DE SANTIAGO DE COMPOSTELA

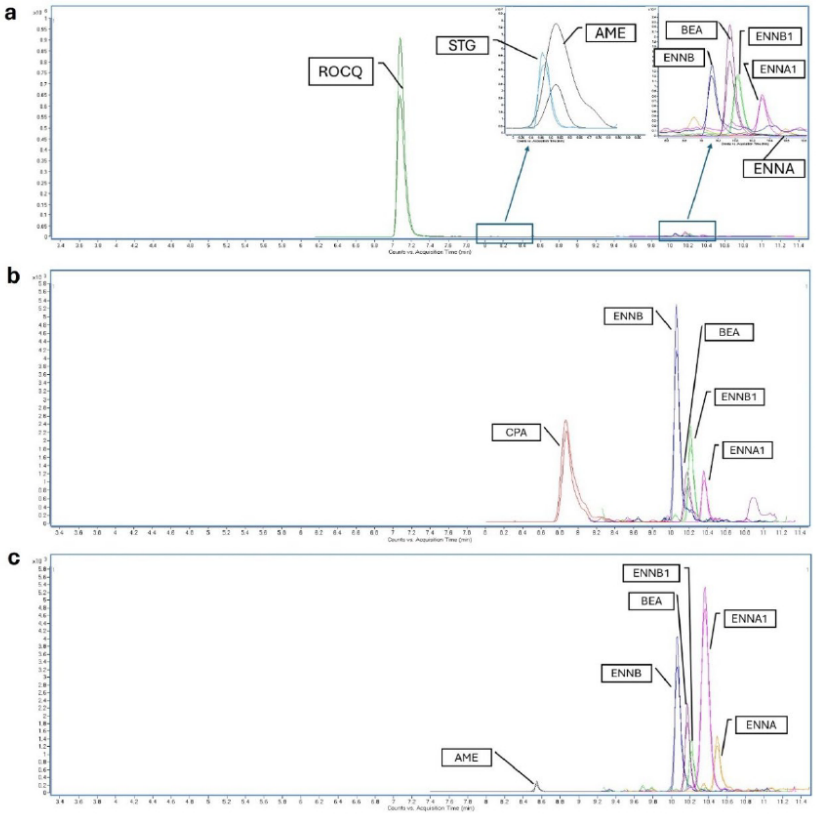


Figure 3S. UHPLC-MS/MS chromatogram of the extracts. Emmental (a), blue cheese (b), and camembert (c) samples

Table 2S. Amount of emerging mycotoxins (nM) present in three cheese extracts

	Emmental	Blue cheese	Camembert
BEA	-	0.67 nM	0.12 nM
ENN A	-	-	0.26 nM
ENN A1	0.05 nM	0.31 nM	0.72 nM
ENN B	0.18 nM	1.04 nM	0.62 nM
ENN B1	0.11 nM	0.6 nM	0.61nM
ROQC	911.5 nM	0.59 nM	-
CPA	-	301.2 nM	-

USC UNIVERSIDADE DE SANTIAGO DE COMPOSTELA

5 DISCUSIÓN

La contaminación por micotoxinas es un problema global; la FAO estima que aproximadamente el 25% de los cereales producidos en el mundo contienen micotoxinas, las cuales pueden provocar daños a humanos y animales tanto mediante ingestión como por inhalación, siendo la primera la principal vía de exposición a estos compuestos (36, 282). El consumo de alimentos contaminados con micotoxinas supone un riesgo importante para la salud, ya que se sabe que estas producen enfermedades como patologías renales, pulmonares, cáncer y enfermedades neurológicas (283). En este sentido, varios estudios *in vitro* e *in vivo* han demostrado que las micotoxinas pueden atravesar la BHE debido a sus propiedades físicas, causando daños a nivel del sistema nervioso central (38, 39, 284). Por otro lado, aunque las micotoxinas no son volátiles, pueden estar presentes en el polvo transportado por el aire y en las esporas y fragmentos de hongos, alcanzando de este modo los pulmones (285-288). De hecho, los trabajadores que manipulan cereales, frutas o frutos secos contaminados, están expuestos a estos compuestos (289). Aunque los datos sobre las cantidades de micotoxinas encontradas en polvo son escasos y apenas existen estudios sobre sus efectos inhalatorios, se sabe que los pulmones son muy sensibles a la exposición a estos compuestos (2, 290-293). Sin ir más lejos, se ha descrito la presencia de AFB1 en biopsias pulmonares de pacientes con cáncer de pulmón expuestos a polvo de distintos materiales (294-297). Por consiguiente, en la presente tesis doctoral se eligieron dos líneas celulares, una de neuroblastoma humano y otra de células de cáncer de pulmón para evaluar los distintos efectos producidos por micotoxinas reguladas y/o emergentes, con el fin de profundizar en el estudio de sus efectos toxicológicos.

La línea celular de neuroblastoma humano SH-SY5Y se empleó para evaluar cómo algunas micotoxinas pueden producir neurotoxicidad, especialmente las emergentes, ya que los datos existentes sobre sus efectos a nivel central son escasos. De hecho, no existen límites legales máximos establecidos para estas toxinas en alimentos y piensos debido a la falta de información sobre su toxicidad (298). Se comenzó analizando los efectos sobre la viabilidad celular y la función mitocondrial de las células de neuroblastoma de las toxinas reguladas (DON, FB1 y ZEA) y emergentes (BEA y ENNs A, B, A1 y B1), que aparecen frecuentemente en piensos y leche del noroeste ibérico. En cuanto a las micotoxinas reguladas, el DON produjo el mayor daño celular, con una IC_{50} de 0,94 µM. La ZEA presentó un valor casi 20 veces mayor (17,4 µM), mientras que la FB1 no mostró efectos tóxicos en esta línea celular hasta concentraciones de 10 µM después de 24 h de tratamiento. Sin embargo, cuando se analizaron sus efectos citotóxicos mediante el ensayo LDH así como el tipo de muerte celular producida, el DON y la ZEA no mostraron efectos dañinos en las células de neuroblastoma humano. Considerando que el MTT se metaboliza por la mitocondria y es un ensayo más sensible que el de LDH (270), estos resultados podrían indicar que las mitocondrias están siendo afectadas por el DON y la ZEA, pero que la integridad de la membrana plasmática no se ve comprometida a las concentraciones probadas. La neurotoxicidad del DON se había descrito con anterioridad tanto en ensayos *in vitro* como *in vivo* y datos recientes confirman que esta toxina causa daño mitocondrial mediante la producción de estrés oxidativo (299, 300). Además, a una concentración de 100 µM, se describió que el DON induce apoptosis dependiente de las mitocondrias en células de carcinoma humano, mediante la apertura del mPTP (108). No obstante, los resultados de la presente tesis doctoral no permiten confirmar la apoptosis, ya que en el ensayo de citometría de flujo se usó una dosis más baja (0,94 µM) y un tipo celular diferente. Sin embargo, se observó una disminución en el $\Delta\Psi m$ a concentraciones entre 1-10

USC UNIVERSIDADE DE SANTIAGO DE COMPOSTELA

μM después de 24 h de incubación, lo que indica que la toxina afecta a las mitocondrias de las células SH-SY5Y.

En el caso de la FB1, los resultados obtenidos indican que esta toxina no afecta ni a la viabilidad celular ni a la función mitocondrial de las células SH-SY5Y, lo cual coincide con resultados previos (301). La FB1 se considera neurotóxica debido a su implicación en la ELEM, ya que induce desmielinización y elevación de esfinganina. Sin embargo, no hay evidencia de su citotoxicidad en líneas neuronales, lo que podría estar relacionado con una ausencia de mielina en las células cultivadas (301). Además, se ha hipotetizado que los efectos neurotóxicos de la FB1 podrían deberse a su capacidad para activar las células gliales (302). Con respecto a la ZEA, se obtuvieron resultados similares a los presentados por Venkataramana et al. (2014) en células SH-SY5Y, en los que la toxina reduce la viabilidad celular a concentraciones inferiores a 25 μM (303). Además, los resultados presentados en esta tesis confirman que la citotoxicidad de la ZEA está mediada por la disfunción mitocondrial, ya que se produce despolarización de la membrana a las concentraciones más altas.

Las micotoxinas emergentes causaron efectos citotóxicos y alteraron significativamente la función mitocondrial de las células SH-SY5Y, lo cual condujo a apoptosis. Las ENNs A, B, A1, B1 y la BEA, redujeron notablemente la viabilidad de las células, presentando valores de IC_{50} de 2.2, 0.43, 2.0, 2.7 y 1.7 μM, respectivamente, tras 24 h de tratamiento. Estos valores fueron más bajos que los reportados previamente en células intestinales o hepáticas (304, 305). En este sentido, las células SH-SY5Y resultaron ser 5-7 veces más sensibles a las ENNs, lo que sugiere que podrían ser neurotóxicas a las concentraciones encontradas en muestras contaminadas. De hecho, el tratamiento con una mezcla de ENNs y BEA en un modelo *in vitro* de la BHE produjo una disminución en la expresión del complejo I de la cadena de transporte electrónico, lo cual se ha relacionado con enfermedades neurodegenerativas, apoyando la suposición de que estas toxinas ejercen efectos neurotóxicos (41). Cabe destacar el efecto producido por la ENN B tras 6 h de incubación, ya que indujo una disminución repentina en la viabilidad celular a la concentración de 0.5 μM que se mantuvo hasta dosis de 10 μM, sin observarse un efecto dosis-dependiente. Esta respuesta también se reportó previamente en células Caco-2 y macrófagos murinos tratados con la toxina (174, 306). De hecho, aunque la ENN B presentó la IC_{50} más baja en el ensayo de MTT, cuando se evaluaron sus efectos citotóxicos con el ensayo de LDH, fue la única toxina emergente de las analizadas que no mostró una respuesta dependiente de la dosis. La ENN B produjo una respuesta prácticamente constante, con un aumento en la liberación de LDH de alrededor del 30% a concentraciones superiores a 0.5 μM. Este efecto sostenido podría estar relacionado con la unión de la ENN B a un receptor específico, que mostraría una alta sensibilidad y especificidad para la toxina a bajas concentraciones o por un daño mitocondrial que permitiese una posterior recuperación parcial del orgánulo (307). Pese a esta diferencia, que apunta a un distinto modo de acción para la ENN B, los resultados obtenidos en los ensayos de MTT y LDH fueron consistentes para todas las toxinas, ya que la reducción de la viabilidad celular concuerda con el aumento en la liberación de LDH. Considerando que el MTT es principalmente metabolizado por las mitocondrias (270), la citotoxicidad producida por ENNs y BEA en células de neuroblastoma podría estar relacionada con un daño mitocondrial, como se observó en el modelo de BHE mencionado anteriormente (41). Por esta razón, se evaluaron los efectos de las cuatro ENNs y la BEA sobre el $\Delta\Psi m$ y se observó que todas despolarizaron la mitocondria, lo cual podría estar relacionado con los efectos de estas toxinas sobre los flujos iónicos. Las ENNs y la BEA son péptidos cíclicos con una estructura similar. Se ha descrito que la BEA afecta a las membranas biológicas formando complejos con metales como K^+, Na^+ y Ca^{2+}, provocando un aumento en la permeabilidad celular, mientras que las ENNs han sido consideradas tradicionalmente como

ionóforos (161, 176). Por lo tanto, la membrana mitocondrial podría ser una posible diana de estas toxinas. En este sentido, las células neuronales son muy susceptibles a la disfunción mitocondrial debido a su gran consumo de energía, por lo que una ligera disminución en el ΔΨm podría tener un gran impacto en la función neuronal (308). En este sentido, las ENNs A, A1, B1 y la BEA a las dosis más altas probadas, inhibieron completamente la viabilidad celular, lo cual podría estar relacionado con los efectos observados sobre el ΔΨm. Sin embargo, no todas las toxinas actuaron igual. Mientras que la ENN A y la ENN B despolarizaron la mitocondria a todas las concentraciones probadas, sugiriendo que su toxicidad podría estar mediada por las mitocondrias, la ENN A1, la ENN B1 y la BEA redujeron el ΔΨm solo a las dosis más altas utilizadas, lo cual podría deberse a la disminución de la viabilidad celular producida a esas concentraciones (178).

Por otro lado, dado que las ENNs A1 y B1 parecen actuar de forma similar (en MTT, LDH y ΔΨm), se evaluó su efecto sobre la producción de ROS y se observó que la ENN A1 elevó los niveles de ROS en un amplio rango de concentraciones mientras que la ENN B1 no afectó la liberación de estas moléculas. En células Caco-2, se ha demostrado que la ENN B1 aumenta la producción de ROS, por lo que, después del tratamiento con esta toxina, las células intestinales parecen ser más propensas a originar ROS que las células neuronales (173). Dado que la ENN A1 incrementó la producción de ROS a dosis bajas sin afectar al ΔΨm, parece que la toxina actúa a través de una vía diferente, como la activación de la NADPH oxidasa (309). En cualquier caso, la falta de efecto de la ENN B1 sobre la liberación de ROS apunta a un mecanismo de acción diferente para cada ENN.

Finalmente, se analizó el tipo de muerte celular producida por estos compuestos, y se observó que todos (ENN A, ENN B, ENN A1, ENN B1 y BEA) causaban muerte celular apoptótica. Además, se describió la implicación de caspasas, al usar el inhibidor de caspasas Z-VAD-FMK, en la apoptosis producida por las ENNs A1 y B1. Estos resultados coinciden con estudios previos, en los que se describió que estas micotoxinas emergentes producen apoptosis a través de la vía mitocondrial en otras líneas celulares (155, 173). La presente tesis recoge por primera vez los efectos pro-apoptóticos de la ENN A, la ENN B, la ENN A1 y la ENN B1 en células neuronales. Con respecto a la BEA, su citotoxicidad ya había sido reportada previamente en células SH-SY5Y (224, 310, 311). Estos autores obtuvieron valores de IC_{50} entre 2.5-3.2 μM, en el rango de los datos obtenidos en esta tesis, y describieron un aumento en la expresión del gen apoptótico Bcl-2 después del tratamiento con BEA, lo que concuerda con los resultados aquí presentados (312).

Estudios recientes han resaltado también la presencia de ENNs y otras micotoxinas emergentes, entre las que se incluyen BEA, ROQC y CPA, en queso en una amplia gama de concentraciones (14, 164, 166). Aunque varios géneros de hongos pueden afectar al queso en términos de descomposición, algunas especies se utilizan en el proceso de maduración. *Penicillium* es el género más comúnmente utilizado en este proceso y tiene el potencial de producir micotoxinas como la OTA, ROQC y CPA, que permanecen estables bajo las condiciones de procesamiento de los quesos, manteniendo su actividad citotóxica (164, 197). Pese a la elevada prevalencia de micotoxinas emergentes en quesos, hasta la fecha, la legislación de la UE no regula sus niveles en esta matriz, y solo la aflatoxina M1 está regulada en la leche y los productos derivados de la leche (EC, 2023).

Por lo tanto, se procedió a estudiar los efectos individuales de las micotoxinas emergentes ROQC y el CPA, frecuentemente detectadas en diferentes muestras de queso (166). Ni la ROQC ni el CPA se consideran un posible riesgo para la salud porque no causan efectos toxicológicos significativos a las concentraciones comúnmente encontradas en los alimentos. Sin embargo, los datos sobre su citotoxicidad son insuficientes (196, 216). En la prese te tesis doctoral, se

USC UNIVERSIDADE DE COMPOSTELA

observó que el CPA presentó una mayor toxicidad que la ROQC, presentando una IC_{50} de 7.3 µM (frente a 49.5 µM). Ambas IC_{50} resultaron superiores a las de las otras micotoxinas emergentes analizadas en la presente tesis, sugiriendo un menor efecto tóxico. Sin embargo, el CPA ha presentado una reducción de la viabilidad celular en el rango nanomolar en varias líneas celulares (313). A continuación, para respaldar los datos de viabilidad celular, se realizó un ensayo de citotoxicidad, obteniéndose una EC_{50} de 84.1 µM para el CPA. Por lo tanto, nuestros datos pueden indicar que el CPA interrumpe el metabolismo celular sin comprometer la integridad de la membrana plasmática hasta que se alcanzan concentraciones altas. En el caso de la ROQC, se obtuvo el mismo valor en ambos ensayos (49.5 µM), indicando que esta toxina produce la disrupción metabólica y de la membrana celular simultáneamente, lo que sugiere un mecanismo de acción diferente al del CPA. El modo exacto por el que se produce la toxicidad de la ROQC aún no se comprende, pero se sabe que inhibe el citocromo P450 de ratas y humanos, involucrado en el metabolismo y la homeostasis celular, lo que podría estar relacionado con los efectos observados (314, 315). Por otro lado, tanto la ROQC como el CPA indujeron la muerte celular apoptótica, involucrando la vía extrínseca de la apoptosis, ya que aumentaron la expresión de la caspasa-8 activa y escindida, respectivamente (316). Si bien no hay datos sobre el tipo de muerte inducida por la ROQC, se ha descrito que el CPA induce apoptosis dependiente de p53 y aumenta la expresión de IL-1β en varias líneas celulares, lo que respalda nuestros hallazgos (317-319).

En resumen, el análisis de micotoxinas individuales sobre la viabilidad celular reveló que la ENN B es la molécula más dañina, seguida por el DON, la BEA, la ENN A1, la ENN A, la ENN B1, el CPA, la ZEA, la ROQ C y la FB1, que no afectó a las células SH-SY5Y. Exceptuando el DON y la ROQC, los resultados de la presente tesis sugieren que las micotoxinas emergentes producen una mayor neurotoxicidad que las reguladas y podrían suponer un peligro para la salud. En este sentido, los expertos de la EFSA subrayan que la exposición crónica a micotoxinas emergentes podría representar un problema de salud pública; de hecho, la exposición oral repetida a la ENN B y la BEA se ha relacionado con efectos genotóxicos en ratones (175).

Los alimentos no suelen estar contaminados por un solo tipo de micotoxina. Estudios europeos sobre contaminación con estas toxinas indican que entre el 75% y el 100% de las muestras de piensos para animales contienen más de una micotoxina (320). Como se explicó en la introducción, estas toxinas pueden bioacumularse en el músculo o la leche animal y llegar al ser humano (18). Sin ir más lejos, estudios de biomonitorización humana encontraron que el 100% de muestras de orina analizadas contenían biomarcadores de dos o más micotoxinas, y se detectaron hasta 5 micotoxinas en un caso grave de co-exposición (321). Considerando la creciente incidencia de micotoxinas emergentes y la escasez de datos sobre su toxicidad conjunta, en la presente tesis doctoral se evaluaron combinaciones de varias de estas toxinas, basándose en su co-ocurrencia en la naturaleza. En este contexto, se analizaron los efectos de las combinaciones binarias de micotoxinas reguladas (DON, FB1, ZEA) y emergentes (ENN A, ENN B y BEA) que co-occurren con mayor frecuencia en piensos del noroeste ibérico (167). Se observaron efectos antagónicos para las mezclas binarias de DON y ZEA con las micotoxinas emergentes. En el caso de las mezclas de FB1, no pudo calcularse el índice de combinación, dado que no se obtuvo una IC_{50} para esta toxina. Sin embargo, los efectos de su mezcla con las micotoxinas emergentes son, en todos los casos, similares a los de las estas toxinas solas, lo que podría sugerir un efecto aditivo. Los resultados de la presente tesis doctoral coinciden con datos previos en los que se describieron efectos antagónicos en otros tipos celulares. Este es el caso de la combinación de DON y ENN B en células intestinales (322, 323), o la mezcla de BEA y DON en células ováricas de ratón (298).

USC DE COMPOSTELA

En base a los resultados de las combinaciones binarias de micotoxinas reguladas y emergentes, se decidió probar extractos de pienso y muestras de leche naturalmente contaminados con micotoxinas, en el mismo modelo *in vitro* empleado hasta ahora. Todos los extractos probados fueron analizados mediante métodos previamente validados para la cuantificación de micotoxinas. La sensibilidad de estos métodos es alta, permitiendo la detección de compuestos a concentraciones inferiores a los niveles máximos establecidos en las normativas europeas. Además, la precisión y exactitud son lo suficientemente buenas como para cumplir con las características de rendimiento establecidas en la legislación (324). En el extracto de pienso para vacas se detectó la presencia de micotoxinas emergentes y reguladas, aunque a unas concentraciones inferiores a los niveles máximos recomendados en la UE para piensos animales (48). Cabe destacar la presencia de BEA y ENNs, que se encontraron en pequeñas cantidades. El extracto redujo la viabilidad celular y generó citotoxicidad en las células SH-SY5Y, a pesar de que las micotoxinas reguladas presentes se hallaban por debajo de los límites máximos establecidos. Después, se probó una mezcla equivalente de estándares comerciales de micotoxinas (incluyendo DON, FB1, ZEA, ENN A, ENN B y BEA) y no se observaron efectos sobre la viabilidad celular. Solo cuando los estándares comerciales se mezclaron a concentraciones 1000 veces superiores a las encontradas en el extracto, se obtuvieron resultados similares a los producidos por el mismo. Esto puede deberse a la presencia de otras micotoxinas en la muestra que podrían estar potenciando el efecto de las micotoxinas seleccionadas en el presente estudio. Como en el extracto contaminado también se detectaron ENN A1, ENN B1 y FB2, la diferencia podría estar vinculada a la presencia de estas micotoxinas. Dado que la toxicidad producida por la muestra de pienso para vacas podría deberse a la presencia de ENN A1 y ENN B1, se probaron dos muestras de leche naturalmente contaminadas con las cuatro ENNs y BEA, a concentraciones mucho más bajas que las encontradas en el pienso de vaca. Ambas muestras de leche contenían cantidades similares de micotoxinas, siendo la principal diferencia entre ellas la presencia de ENN B1 en el extracto 2. Sorprendentemente, esta muestra redujo la viabilidad de las células SH-SY5Y a la concentración más alta, mientras que el extracto 1 no mostró ningún efecto significativo en esta línea celular. Estos resultados indican que la ENN B1 podría estar potenciando el efecto de otras micotoxinas en esta línea celular. De hecho, se ha descrito un mayor daño para combinaciones de ENNs que para las toxinas por separado. Por otro lado, la disminución en la viabilidad celular a concentraciones de toxinas tan bajas sugiere que la matriz podría influir en la citotoxicidad de las micotoxinas. En particular, el extracto de leche presentó una mayor reducción en la viabilidad celular de lo esperado, lo que indica que las propiedades lipofílicas de las micotoxinas emergentes podrían estar relacionadas con este efecto dañino.

A la vista de los resultados observados con los extractos de leche, se procedió a estudiar la actividad citotóxica de combinaciones binarias de las cuatro ENNs, para determinar si su coexistencia podría aumentar su toxicidad. Para esto, se hizo una aproximación combinándolas en una proporción 1:1. En este sentido, todas las combinaciones binarias probadas produjeron un efecto antagonista, con excepción de la mezcla de ENN B1 y ENN A, que presentó un efecto aditivo. Esta combinación ya se había reportado anteriormente como aditiva en otros tipos celulares (298). Por lo tanto, la mezcla de ENN B1 y ENN A podría ser la responsable de los efectos observados en el extracto 2 de leche, pero también podría serlo la de todas las ENNs (A, B, A1 y B1) juntas, ya que co-ocurren en dicho extracto. Como en la mayoría de alimentos contaminados con ENNs suelen co-ocurrir los cuatro análogos, se estudió también la toxicidad de los estos combinación, en una mezcla 1:1:1:1, lo cual no se había descrito previamente en esta línea celular. En este sentido, se describió por primera vez un mayor efecto combinado de la mezcla de ENNs A, A1, B y B1 que el observado con cada toxina individualmente. Dada su

USC DE COMPOSTELA

citotoxicidad y alta prevalencia en muchas muestras naturales, la co-ocurrencia de ENNs en los alimentos podría representar un riesgo significativo para la salud, como ya se viene apuntando a lo largo de la presente tesis doctoral (164, 175, 326-328).

Debido a que se ha descrito recientemente la co-ocurrencia de ENNs y BEA con toxinas producidas por hongos empleados en la maduración de quesos, como CPA y ROQC, se procedió a estudiar el efecto combinado de las micotoxinas más frecuentemente encontradas en estas matrices, todas ellas emergentes, con el fin de determinar si la contaminación conjunta con las mismas podría suponer un peligro. En lo que respecta al CPA, los datos sobre su toxicidad conjunta con otras micotoxinas son aún más escasos que los existentes para las ENNs, aunque se han descrito efectos aditivos con aflatoxinas (329). En el caso de la ROQC, no hay estudios sobre sus combinaciones. Considerando que ambos compuestos se utilizan en la maduración del queso y que son citotóxicos por sí mismos, primero se probaron sus efectos en combinación binaria con las ENNs. En todas las mezclas, se observó un desplazamiento en la curva de combinación hacia la izquierda, sugiriendo una potenciación de sus efectos individuales. Sin embargo, cuando se calculó el índice de combinación, el valor fue mayor a 1 en todos los casos, indicando antagonismo. Esta discrepancia podría deberse al hecho de que el sinergismo es mutuo para todos los compuestos, mientras que la potenciación es unilateral (330). En algunas de las mezclas binarias realizadas, observamos potenciación para uno de los compuestos, pero no para el otro, como ocurre en la mezcla de ROQC y ENN A o en la combinación de ROQC, ENNs y BEA, en la que la IC_{50} combinada es mucho menor que el valor individual de cada toxina. El sinergismo solo se logró en dos de las mezclas probadas (ROQC+ ENN A+ENN A1+ ENN B+ ENN B1 y CPA+ ENN A+ENN A1+ ENN B+ ENN B1), en las que la IC_{50} combinada fue al menos 9 veces menor que la IC_{50} individual de cada toxina. En el caso de la mezcla de CPA+ ENN A+ENN A1+ ENN B+ ENN B1+ BEA, se observó un efecto aditivo. Si bien la ROQC y el CPA no se consideran un riesgo potencial para la salud, los datos de toxicidad existentes están limitados a estudios de estos compuestos solos sin contemplar posibles interacciones con otras micotoxinas (216, 313, 317). En la presente tesis doctoral se observa que la co-ocurrencia de ENNs con CPA y ROQC, a menudo observada en quesos, aumenta significativamente los efectos de estas dos toxinas, hasta concentraciones que podrían encontrarse en muestras naturales (164, 166, 196).

Considerando que las micotoxinas son sustancias liposolubles y el queso es principalmente grasa, los efectos de la combinación de estas toxinas podrían ser aún mayores debido a la matriz, como ya habíamos hipotetizado al analizar los extractos de leche (39, 41, 168). En este sentido, el análisis de extractos de muestras comerciales de queso mostró una pronunciada reducción en la viabilidad celular, especialmente con un extracto de queso Emmental, con un alto contenido de ROQC. Como ejercicio teórico sin implicaciones en el mundo real, la concentración 1:200 de este extracto, sería equivalente a aproximadamente 45 g de queso consumido, para una mujer de 60 kg con una composición corporal del 60% de agua. Por lo tanto, incluso una pequeña cantidad de queso podría causar daño celular. Aunque este cálculo no refleja una evaluación de riesgo alimentario, vale la pena mencionar que un valor elevado de toxinas emergentes, presente en un producto comercial podría presentar niveles citotóxicos. Por lo tanto, la presencia de micotoxinas emergentes en distintos alimentos debería someterse a evaluación y el queso debería incluirse en la lista de productos regulados para micotoxinas.

Debido a la elevada ocurrencia de las ENNs en distintos alimentos y a las diferencias previamente descritas sobre la supervivencia celular y la función mitocondrial de las células SH-SY5Y, tras el tratamiento con cada ENN (A, A1, B y B1) (Tabla 3), se decidió profundizar en el estudio del mecanismo de acción de estas. Las ENNs se han considerado ionóforos desde 1973, cuando se propuso que la ENN B formaba complejos que permitían el paso de iones de

K^+ (177). Posteriormente, otros autores adoptaron la suposición de un comportamiento ionofórico para todos los análogos y continuaron sus investigaciones en base a este supuesto. Como se mencionó previamente, en células de neuroblastoma, las ENNs A, A1, B y B1 provocan apoptosis y, en algunos casos, se ha demostrado la implicación de caspasas en su citotoxicidad (155, 169). Se sabe que el Ca^{2+} está involucrado en la activación de algunas caspasas y que la apoptosis podría estar asociada con la señalización del calcio (331). Por lo tanto, se analizaron los efectos de las cuatro ENNs sobre la homeostasis del calcio. Pese a sus similitudes estructurales, todas las toxinas alteraron los flujos de Ca^{2+} de manera diferente, reforzando la hipótesis previa de un mecanismo de acción distinto para cada análogo. En este sentido, las ENNs A, A1 y B1 produjeron depleción de Ca^{2+} de los reservorios intracelulares y aumentaron la captación del ion de manera dependiente de la dosis. Sin embargo, la forma en que estas toxinas afectaron a la homeostasis del calcio difiere entre los análogos, observándose un mayor vaciamiento de los reservorios en el caso de la ENN A1 y diferencias significativas en el influjo de iones desde el medio extracelular para los tres. En el caso de la ENN B, se observó que a mayor concentración de toxina, mayor era la depleción de Ca^{2+} de los reservorios intracelulares, pero esta no indujo entrada del ion desde el medio extracelular.

Tabla 3. Resumen de los resultados obtenidos con las ENNs A, A1, B y B1 sobre la línea celular SH-SY5Y.

	Viabilidad	Citotoxicidad	Despolarización Ψm	Producción ROS	Tipo muerte
ENN A	IC_{50}= 2.2 µM	SI	Todas [ ]	-	Apoptosis
ENN B	IC_{50}=0.43 µM Daña mitocondria. No reduce al 100%	Poca (no rompe la célula)	Casi a todas [ ]	-	Apoptosis
ENN A1	IC_{50}=1.9 µM	SI	[ ] altas	[ ] bajas	Apoptosis dependiente de caspasas
ENN B1	IC_{50}=2.6 µM	SI	[ ] altas	NO	Apoptosis dependiente de caspasas

Para intentar esclarecer el origen de las diferencias observadas en los flujos de Ca^{2+} y cómo las cuatro ENNs afectaron al vaciamiento de los reservorios, se compararon sus efectos con los de distintos compuestos conocidos, con el objetivo de identificar sobre qué reservorio de calcio intracelular podrían estar actuando las toxinas.

En primer lugar, dado que la ENN A provocó tanto el vaciamiento de los reservorios de calcio como la entrada del ion desde el medio, se evaluaron los efectos de esta toxina en presencia de Tg, un inhibidor de la Ca^{2+}-ATPasa del RE. Este compuesto provoca la depleción de calcio del RE y aumenta la captación del ion del medio extracelular en las células SH-SY5Y(332, 333). Por lo tanto, se evaluó si la ENN A podría actuar de forma similar. En este sentido, la toxina parece afectar al RE, pero de manera diferente a la Tg, ya que cuando las células se trataron primero con la micotoxina, la depleción de Ca^{2+} del RE inducida por Tg no se vio afectada. Sin embargo, cuando las células se preincubaron con Tg, cuyo efecto es irreversible, la depleción del RE y la captación de Ca^{2+} inducidas por ENN A se redujeron (334). Además, el influjo de Ca^{2+} causado por ENN A fue menor que el producido por Tg. Este compuesto inhibe la SERCA, que es responsable de la entrada de Ca^{2+} en el RE. La inhibición de la SERCA provoca la liberación del ion al citosol a través de los canales IP3P y RyR y, secundariamente, aumenta la entrada de Ca^{2+} a través de los SOC (335). Aunque la ENN A

también activó la entrada SOC, como se demostró con el inhibidor de estos canales, SKF96365, los resultados sugieren que esta toxina actúa en un componente diferente del RE al SERCA, como los canales IP3R o RyR. Además, la ENN A parece presentar un efecto dual sobre los SOC, ya que la micotoxina sola activa la entrada de calcio, pero, cuando se combina con Tg, los efectos de este compuesto se inhiben por completo. La ENN A puede actuar principalmente en el RE, activando proteínas involucradas en la señalización de Ca^{2+}, pero en presencia de otro compuesto que afecta al orgánulo, activaría otras vías de señalización. Este efecto dual sugiere que la ENN A podría estar afectando a varios reservorios celulares e induciendo indirectamente diferentes respuestas en los SOC. Posteriormente, las células neuronales se trataron con ENN A y el desacoplador mitocondrial FCCP, y se observó que esta micotoxina también afecta a las mitocondrias, apoyando la hipótesis previamente formulada. El pretratamiento con ENN A condujo a una disminución de la depleción de Ca^{2+} mitocondrial inducida por el FCCP, confirmando la implicación del orgánulo. Además, la adición de FCCP después de la ENN A abolió por completo la entrada de calcio inducida por la toxina. Se obtuvieron efectos similares para la combinación de Tg y FCCP, donde el FCCP redujo la entrada de Ca^{2+} inducida por Tg (332). Por otro lado, el tratamiento con el desacoplador mitocondrial inicialmente redujo, pero no inhibió, el influjo de Ca^{2+} inducido por la ENN A a través de los SOC. Este efecto en la entrada de Ca^{2+} es bastante inferior al observado cuando las células se trataron con Tg seguido de FCCP. Por lo tanto, aunque la ENN A parece actuar de manera similar a la Tg en los flujos de calcio, sus efectos son diferentes, reforzando la idea de que esta micotoxina actúa sobre un componente diferente del RE. Los efectos de la ENN A sobre la homeostasis del Ca^{2+} mitocondrial podrían desencadenar la apoptosis descrita previamente al activar el mPTP (248). Por lo tanto, se evaluó la actividad de la toxina sobre este canal y se observó que a concentraciones en el rango micromolar, la ENN A provoca la apertura del mPTP, confirmando que la apoptosis producida está mediada por las mitocondrias. De este modo, el aumento del Ca^{2+} intracelular inducido por la toxina sería responsable del colapso del potencial de membrana mitocondrial y la disminución de los niveles de ATP descritos previamente en células neuronales y eritrocitos (336).

En cuanto a los efectos producidos por la ENN B sobre los flujos de Ca^{2+}, estos fueron similares a los producidos por el FCCP. Al incubar las células con Tg y la toxina, se observó una reducción en la liberación de calcio de los reservorios inducida por Tg y en la entrada a través de los SOCs. Además, cuando se añadieron la ENN B y el FCCP a las células, se observó que la preincubación con FCCP indujo una ligera reducción en la depleción de Ca^{2+} mitocondrial provocada por la ENN B, mientras que la adición de la micotoxina primero no tuvo efecto sobre la liberación del ion inducida por el FCCP. Esto sugiere que la ENN B puede actuar sobre las mitocondrias de manera similar al FCCP, provocando un colapso del potencial de membrana mitocondrial, pero permitiendo una recuperación parcial posterior del orgánulo (307). Este efecto podría justificar el daño inducido por la ENN B en las mitocondrias, sin producir la muerte celular total. Por lo tanto, el mecanismo de acción de la ENN B podría ser similar al de FCCP, que es un ionóforo de H^+ (337). Este compuesto también causó la apertura del mPTP, por lo que sus efectos parecen estar predominantemente asociados con la disfunción mitocondrial. En este sentido, algunos autores han descrito que la ENN B altera la expresión de genes relacionados con la cadena de transporte de electrones y que induce apoptosis mediada por la disrupción mitocondrial en diferentes líneas celulares, como linfoblastos o células de adenocarcinoma colorrectal (173, 178, 338). Los efectos de la ENN B también se han asociado con el deterioro de los lisosomas. Estos orgánulos almacenan calcio, pero el mecanismo mediante el cual regulan la homeostasis del ion aún no está claro. Debido al comportamiento de la ENN B sobre los flujos de calcio, similar al del protonóforo FCCP, esta toxina podría

USC DE COMPOSTELA

provocar un desequilibrio de protones que afecte tanto a los lisosomas como a las mitocondrias. Por otro lado, la ENN B se ha relacionado con la activación de los inflamasomas. Estos complejos proteicos pueden ser estimulados por la señalización de calcio, lo que sugiere que los efectos de la ENN B sobre los flujos de calcio podrían contribuir a dicha activación. Así, la señalización de calcio parece desempeñar un papel crucial en el mecanismo de acción de la ENN B (154, 174, 306, 339).

Con respecto a la ENN A1, esta toxina indujo una depleción de Ca^{2+} de los reservorios intracelulares similar a la producida por la Tg, por lo que se evaluaron sus efectos conjuntos para determinar si ambos compuestos podrían afectar a los mismos canales celulares. Los resultados obtenidos sugirieron que la ENN A1 afecta al RE de forma distinta a la Tg, ya que el pretratamiento con la toxina no produjo ningún efecto sobre la respuesta del inhibidor de la SERCA. Sin embargo, al añadir antes la Tg, se redujo la depleción de calcio de los reservorios intracelulares producida por la toxina. Para descartar el posible comportamiento ionofórico de la ENN A1, se empleó $NiCl_2$, que obstruye los canales de calcio de la membrana celular, especialmente los activados por voltaje, mediante un bloqueo directo del poro del canal (340). En este sentido, el $NiCl_2$ bloqueó la entrada de Ca^{2+} inducida por la toxina. Posteriormente, se confirmó que el aumento en la entrada de Ca^{2+} observado se debía a la activación de los SOC, utilizando SKF96365. Luego, se analizaron los efectos de la ENN A1 en presencia del FCCP, que desacopla la cadena respiratoria y es capaz de reducir la entrada de Ca^{2+} a través de los SOC en algunos modelos celulares como las células SH-SY5Y (333, 341). Se observó que el estado funcional de las mitocondrias afecta a la entrada de Ca^{2+} inducido por la ENN A1, ya que al preincubar las células con el desacoplador se redujo la captación de calcio. En condiciones fisiológicas, la mitocondria sirve como regulador de Ca^{2+}, amortiguando la liberación del ion desde varios reservorios al citosol y permitiendo la activación de los SOC. Cuando el FCCP interrumpe la cadena de transporte de electrones, la capacidad de la mitocondria para almacenar calcio se reduce, afectando así a la entrada del ion a través de estos canales (342, 343). En este sentido, el tratamiento con FCCP antes y después de la adición de Tg, redujo los efectos del inhibidor de la SERCA. En el caso de la ENN A1, el FCCP no redujo los efectos de la toxina en la entrada de SOC, después de que esta ya hubiese actuado. Este efecto podría deberse a que la toxina actúe sobre un componente del RE implicado en la salida de calcio en lugar de en la SERCA. En este sentido, cuando un inhibidor como la Tg bloquea la SERCA, activa las vías de salida de calcio del RE, lo que lleva a la entrada del ion a través de los SOC. Además, evita que el orgánulo vuelva a recaptar el ion. La ENN A1 actúa de manera diferente a la Tg, pero también desencadena la entrada de calcio a través de los SOC, sugiriendo que actúa sobre un mecanismo de salida de calcio del RE. En este sentido, los IP3R y los RyR, canales presentes en las células de neuroblastoma humano, son los canales involucrados en la liberación de calcio del RE (344). Los IP3R están estrechamente relacionados con las mitocondrias, ya que forman un complejo con la GRP75 y el VDAC1. Cuando el Ca^{2+} se libera a través de los IP3R, se transfiere a las mitocondrias a través de este complejo. Si los niveles del ion son demasiado altos, puede llevar a la apertura del mPTP y a la muerte celular (246). En este trabajo, hemos observado que la ENN A1 produce la apertura del poro, por lo que podría estar actuando como modulador del complejo IP3R-GRP75-VDAC. Además, los IP3R han sido descritos como los principales canales de Ca^{2+} reticulares en los sitios de contacto mitocondria-RE, regiones donde el RE transfiere el ion a las mitocondrias (242). Por lo tanto, los IP3R podrían ser una diana de esta toxina, lo que explicaría por qué su efecto en los SOC persiste cuando se administra antes del FCCP. Esta hipótesis explicaría los resultados previamente descritos con la ENN A, que también afectó al RE y a las mitocondrias,

USC UNIVERSIDADE DE SANTIAGO DE COMPOSTELA

pero el perfil de calcio de las dos toxinas difiere. Estas diferencias podrían deberse a una modulación distinta del complejo IP3R-GRP75-VDAC1 por ambos análogos.

El último análogo probado, ENN B1, también afectó a los flujos de calcio, induciendo la depleción del ion de los reservorios intracelulares y su entrada desde el medio extracelular de manera dosis-dependiente. Al combinarlo con Tg, observamos que la preincubación con el inhibidor de la SERCA redujo la depleción de iones de los compartimentos intracelulares causada por la toxina, y que la adición de la toxina en primer lugar disminuyó la captación de Ca^{2+} del medio inducida por la Tg. Estos resultados también podrían indicar un efecto en el RE, como se observó con las ENNs A y A1. Además, se verificó que la ENN B1 no era un ionóforo, ya que el $NiCl_2$ redujo la captación de iones producida por la toxina. Sin embargo, el SKF96365 no pudo disminuir la entrada de Ca^{2+} producida por la toxina, lo que sugiere que la ENN B1 activa un canal en la membrana celular distinto del SOC. Considerando que la liberación de Ca^{2+} del RE, ya sea a través de los IP3R o los RyR, desencadena la entrada de iones a través del SOC, la ENN B1 podría estar afectando a otro orgánulo y los efectos observados al preincubar con la Tg podrían deberse a interacciones entre diferentes componentes celulares que activarían los RyR secundariamente (239, 345). En este sentido, los efectos de la ENN B1 en los flujos de Ca^{2+} también se analizaron en presencia del desacoplador mitocondrial, FCCP. La adición de este compuesto fue capaz de disminuir la salida de Ca^{2+} de los reservorios intracelulares y la entrada de iones del medio celular inducidos por la ENN B1. Sin embargo, cuando la toxina se añadió primero, no se observó una reducción en el vaciamiento mitocondrial producido por el FCCP. Por lo tanto, parece que el estado de las mitocondrias altera el efecto de la ENN B1 en los flujos de calcio, pero la toxina no actúa directamente en este orgánulo. Estos resultados están en consonancia con los resultados obtenidos sobre el $\Delta\Psi m$ y con estudios previos que describieron que la ENN B1 no afectaba al $\Delta\Psi m$ en otras líneas celulares (346). Sin embargo, esta toxina produjo la apertura del mPTP, lo cual podría deberse a la entrada masiva de calcio inducida por la toxina, más que a un efecto directo en el orgánulo. Curiosamente, su análogo ENN B, con pequeñas diferencias estructurales, modula el calcio al dirigirse directamente a las mitocondrias, respaldando la hipótesis de que cada ENN tiene un mecanismo de acción diferente. Aunque el RE y la mitocondria son los reservorios de calcio intracelular más estudiados, existen otros orgánulos con capacidad de almacenamiento de calcio, como el núcleo, el aparato de Golgi, los peroxisomas o los endolisosomas, pero hay datos limitados sobre su función (241). Un estudio reciente en fibroblastos embrionarios de ratón sugiere que los lisosomas son una posible diana temprana de la ENN B1, ya que la toxina parece desestabilizar las proteínas asociadas a la membrana de estos, resultando en una alcalinización lisosómica (347). Dado que los canales de Ca^{2+} lisosomales son sensibles a las variaciones de pH, los efectos producidos por la ENN B1 en los flujos de Ca^{2+} podrían estar relacionados con una interacción con estos orgánulos. Además, los lisosomas pueden estar asociados con el RE y las mitocondrias, lo que podría explicar los efectos inducidos por la ENN B1 sobre la apertura del mPTP y el RE (241, 250).

Los resultados obtenidos sobre los flujos de calcio y la disfunción mitocondrial confirman que las ENNs A, B A1 y B1 no son ionóforos de calcio y que, a pesar de sus similitudes estructurales, los cuatro análogos tienen diferentes mecanismos de acción. En el caso de las ENNs A y A1, se descubrió que inducen la entrada de Ca^{2+} a través de los canales SOC, mientras que el $NiCl_2$ bloquea la entrada del ion inducida por la ENN B1. Por lo tanto, los cambios en el potencial de equilibrio de Ca^{2+} observados por Kamyar et al. (2004), producidos por una mezcla de ENNs (A, A1, B y B1), podrían explicarse por el efecto de las ENNs A, A1 y B1 sobre la liberación de Ca^{2+} de reservorios intracelulares descrita en la presente tesis doctoral y no por un comportamiento ionofórico (176). En el caso de la ENN B, esta micotoxina no aumentó el

influjo de Ca^{2+} desde el medio extracelular y, por lo tanto, no puede considerarse un ionóforo de Ca^{2+}. Sin embargo, debería considerarse su posible acción como ionóforo para otros iones. Estudios previos describen que la ENN B tiene una mayor afinidad por los iones de K^+. Esto, junto con los efectos descritos sobre los lisosomas y su modo de acción similar al de FCCP en los flujos de calcio, sugiere que la ENN B podría actuar como un transportador móvil para cationes o protones. En consecuencia, podría desencadenar mecanismos adicionales de intercambio de iones destinados a mantener la homeostasis celular, lo que podría justificar los efectos observados sobre los flujos de calcio (176, 178, 348).

Algunos de los resultados obtenidos sobre la homeostasis del calcio podrían explicar los efectos antagónicos o aditivos descritos previamente para las combinaciones binarias de ENNs. En lo que respecta a la combinación de ENN A y ENN B, el efecto antagónico podría explicarse en función de lo observado en los flujos de calcio, ya que la ENN B presentó un comportamiento comparable al del FCCP y la ENN A actuó de manera similar a la Tg en presencia del desacoplador mitocondrial. En este sentido, la combinación de FCCP y Tg resulta en una inhibición parcial de la entrada de Ca^{2+} inducida por Tg a través de SOCs, por lo que la mezcla de ambas toxinas podría resultar en una reducción de la entrada de Ca^{2+} mediada por ENN A. En cuanto a la mezcla de ENN B1 y ENN A, sus efectos sobre el vaciamiento de distintos reservorios de calcio podrían llevar a una mayor concentración del ion en el citosol, lo cual explicaría el efecto aditivo observado.

Por último, dado que las micotoxinas también pueden llegar al ser humano por vía inhalatoria y que los pulmones son especialmente sensibles a estos compuestos, se seleccionaron varias micotoxinas emergentes relacionadas con el cáncer de pulmón en un estudio previo *in silico*, para estudiar sus efectos sobre la línea celular de carcinoma escamoso de pulmón NCI-H226 (349). Este grupo incluyó ENN A, ENN B, BEA, API y DEST B. La API, es un depsipéptido, igual que las ENNs y BEA, producido por *Fusarium* spp., que contamina diferentes matrices, incluyendo trigo y leche, mientras que la DEST B, es un compuesto utilizado como control biológico en maíz y fresas. Por lo tanto, ambas pueden entrar en la cadena alimentaria y ser peligroso para los seres humanos (350-352).

La ENN A, la BEA y la API redujeron la viabilidad celular de manera dosis-dependiente, siendo la ENN A el compuesto más tóxico (IC_{50}: 2.2 μM), seguido de la BEA (IC_{50}: 4.0 μM) y la API (IC_{50}: 7.0 μM). Para estas tres micotoxinas, el aumento de la citotoxicidad fue acompañado de la activación de la apoptosis, lo cual ya se había descrito previamente en otras líneas celulares (354, 355). La ENN A mostró un efecto significativo en la actividad de la caspasa-3 a una concentración de 2 μM, así como un ligero, pero no significativo, aumento de la apoptosis temprana y en la población sub G_0 tras analizar el ciclo celular. En el caso de la BEA, no se observó efecto en la actividad de la caspasa 3 ni modificación en la población sub G_0, pero produjo un aumento en la apoptosis temprana. Por otro lado, la API indujo la apoptosis temprana de las células NCI-H226, sin modificar la actividad de la caspasa 3. Además, se produjo un aumento ligero, aunque no significativo de la fase subG_0. Esta toxina produjo efectos similares en n una línea de cáncer de mama (356).

La ENN B mostró un patrón de toxicidad en la línea pulmonar similar al descrito previamente en las células de neuroblastoma SH-SY5Y, induciendo una drástica disminución de la viabilidad a concentraciones superiores a 1 μM, sin llegar a producir una inhibición total. Sin embargo, no se observó un aumento en la liberación de LDH, lo que sugiere que no afectó a la integridad celular. Un resultado similar en la liberación de LDH se obtuvo en la línea celular CCF-STTG1 (168), pero no en células neuronales SH-SY5Y. A diferencia de los resultados obtenidos en células de hepatoma de rata y en la línea celular CCF-STTG1, donde la ENN B aumentó la actividad de la caspasa 3 y la fragmentación del ADN, en el presente estudio no se

USC DE COMPOSTELA

observó ningún efecto de esta toxina en los niveles de caspasa 3, el ciclo celular, ni en los niveles de ROS (168, 169).

Tras el tratamiento con DEST B, no se observó ninguna disminución en la viabilidad celular de la línea NCI-H226. No obstante, en un estudio llevado a cabo por Wu et al. (2013) se observó muerte de otras células pulmonares a concentraciones superiores a 1 μM de DEST B tras 48 horas de tratamiento (357). Dado que en la presente tesis los tiempos e incubación fueron menores, esta toxina puede ejercer toxicidad a tiempos de exposición prolongados. Por otro lado, la DEST B no afectó a los marcadores apoptóticos, pero se observó un leve incremento en la fase G_0/G_1 a las concentraciones más altas probadas, sin modificaciones en las otras fases, como ya se había descrito previamente (357). Por otro lado, la DEST B fue la única que indujo la producción de ROS a concentraciones superiores a 10 μM después de 24 h de tratamiento. Por lo tanto, el estrés oxidativo podría estar involucrado en sus efectos. De hecho, esta micotoxina ha sido descrita como un inductor apoptótico a través de las mitocondrias, implicadas en la producción de ROS, en otras líneas celulares (357, 358).

Por tanto, entre las micotoxinas probadas, la ENN A, la BEA y la API afectaron a la viabilidad y produjeron apoptosis de la línea celular NCI-H226, por lo que podrían suponer un problema para la salud. Estas toxinas están presentes en alimentos, pero también se han detectado en el polvo del aire, por lo que su impacto tras ser inhaladas necesita ser investigado más a fondo.

USC UNIVERSIDADE DE SANTIAGO DE COMPOSTELA

6 CONCLUSIONES

1. Las micotoxinas emergentes ENN A, ENN A1, ENN B, ENN B1y BEA son tan tóxicas como la micotoxina regulada DON.
2. Las micotoxinas emergentes ROQC y CPA producen citotoxicidad y apoptosis intrínseca.
3. La combinación de micotoxinas no reguladas da lugar a una potenciación de sus efectos individuales.
4. Las ENNs A, A1, B y B1 no son ionóforos de calcio, pero alteran la homeostasis de este ión, producen daño mitocondrial y apoptosis.
5. El efecto de las ENNs A y A1 activa la entrada del calcio a través de los calanes SOC.
6. La ENN B modula los flujos de calcio a través de la mitocondria y la ENN B1 actúa en la mitocondria y aumenta la entrada de calcio por un canal no SOC.

USC
UNIVERSIDADE DE SANTIAGO DE COMPOSTELA

USC
UNIVERSIDADE
DE SANTIAGO
DE COMPOSTELA

7 REFERENCIAS

1. El-Sayed RA, Jebur AB, Kang W, El-Demerdash FM. An overview on the major mycotoxins in food products: characteristics, toxicity, and analysis. Journal of Future Foods. 2022;2(2):91-102.
2. Awuchi CG, Ondari EN, Eseoghene IJ, Twinomuhwezi H, Amagwula IO, Morya S. Fungal growth and mycotoxins production: Types, toxicities, control strategies, and detoxification. Fungal reproduction and growth. 2021;100207.
3. EC. EC (2023). Commission Regulation(EU)2023/915 of 25 April 2023 on maximum levels for certain contaminants in food and repealing Regulation (EC) No 1881/2006. Official Journal of the European Union, L 11,p 103-157. 2023.
4. Jestoi M. Emerging Fusarium -Mycotoxins Fusaproliferin, Beauvericin, Enniatins, And Moniliformin—A Review. Critical Reviews in Food Science and Nutrition. 2008;48(1):21-49.
5. Bhat R, Rai RV, Karim AA. Mycotoxins in food and feed: present status and future concerns. Comprehensive reviews in food science and food safety. 2010;9(1):57-81.
6. Alshannaq A, Yu JH. Occurrence, Toxicity, and Analysis of Major Mycotoxins in Food. Int J Environ Res Public Health. 2017;14(6).
7. WHO WHO. Mycotoxins 2023 [Available from: https://www.who.int/news-room/fact-sheets/detail/mycotoxins.
8. Liew WP, Mohd-Redzwan S. Mycotoxin: Its Impact on Gut Health and Microbiota. Front Cell Infect Microbiol. 2018;8:60.
9. Fletcher MT, Blaney BJ. Mycotoxins. Reference Module in Food Science: Elsevier; 2016.
10. Guo X, Chen F, Zhang W. Analysis of 16 mycotoxins in genuine traditional Chinese medicine for five medicinal parts: Classification of analytical method based on PANI@CS extraction-UPLC-MS/MS. Heliyon. 2023;9(6):e17027.
11. Grzybowski A, Pawlikowska-Łagód K, Polak A. Ergotism and Saint Anthony's fire. Clin Dermatol. 2021;39(6):1088-94.
12. Aiko V, Mehta A. Occurrence, detection and detoxification of mycotoxins. J Biosci. 2015;40(5):943-54.
13. Bernal-Algaba E, Pulgarín-Alfaro M, Fernández-Cruz ML. Cytotoxicity of Mycotoxins Frequently Present in Aquafeeds to the Fish Cell Line RTGill-W1. Toxins (Basel). 2021;13(8).
14. González-Jartín JM, Rodríguez-Cañás I, Alfonso A, Sainz MJ, Vieytes MR, Gomes A, et al. Multianalyte method for the determination of regulated, emerging and modified mycotoxins in milk: QuEChERS extraction followed by UHPLC-MS/MS analysis. Food Chem. 2021;356:129647.
15. Reinholds I, Jansons M, Fedorenko D, Pugajeva I, Zute S, Bartkiene E, et al. Mycotoxins in cereals and pulses harvested in Latvia by nanoLC-Orbitrap MS. Food Addit Contam Part B Surveill. 2021;14(2):115-23.
16. Daou R, Joubrane K, Maroun RG, Khabbaz LR, Ismail A, Khoury AE. Mycotoxins: Factors influencing production and control strategies. AIMS Agriculture and Food. 2021;6(1):416-47.
17. Pandey AK, Samota MK, Kumar A, Silva AS, Dubey NK. Fungal mycotoxins in food commodities: present status and future concerns. Frontiers in Sustainable Food Systems. 2023;7:1162595.
18. Escrivá L, Font G, Manyes L, Berrada H. Studies on the Presence of Mycotoxins in Biological Samples: An Overview. Toxins (Basel). 2017;9(8).

USC UNIVERSIDADE DE SANTIAGO DE COMPOSTELA

19. Nji QN, Babalola OO, Ekwomadu TI, Nleya N, Mwanza M. Six Main Contributing Factors to High Levels of Mycotoxin Contamination in African Foods. Toxins (Basel). 2022;14(5).
20. Perdoncini M, Sereia MJ, Scopel FHP, Formigoni M, Rigobello ES, Beneti SC, et al. Growth of fungal cells and the production of mycotoxins. Cell growth. 2019;23.
21. Greeff-Laubscher MR, Beukes I, Marais GJ, Jacobs K. Mycotoxin production by three different toxigenic fungi genera on formulated abalone feed and the effect of an aquatic environment on fumonisins. Mycology. 2019;11(2):105-17.
22. Kokkonen M, Jestoi M, Rizzo A. The effect of substrate on mycotoxin production of selected Penicillium strains. International Journal of Food Microbiology. 2005;99(2):207-14.
23. Calvo AM, Duran RM, Cary JW. Role of the Osmotic Stress Regulatory Pathway in Morphogenesis and Secondary Metabolism in Filamentous Fungi. 2010.
24. Mannaa M, Kim KD. Effect of Temperature and Relative Humidity on Growth of Aspergillus and Penicillium spp. and Biocontrol Activity of Pseudomonas protegens AS15 against Aflatoxigenic Aspergillus flavus in Stored Rice Grains. Mycobiology. 2018;46(3):287-95.
25. Vylkova S. Environmental pH modulation by pathogenic fungi as a strategy to conquer the host. PLoS pathogens. 2017;13(2):e1006149.
26. Wang Y, Zhang W, Fu L. Food spoilage microorganisms: ecology and control: CRC Press; 2017.
27. Brzonkalik K, Hümmer D, Syldatk C, Neumann A. Influence of pH and carbon to nitrogen ratio on mycotoxin production by Alternaria alternata in submerged cultivation. AMB express. 2012;2:1-8.
28. Reverberi M, Ricelli A, Zjalic S, Fabbri AA, Fanelli C. Natural functions of mycotoxins and control of their biosynthesis in fungi. Applied microbiology and biotechnology. 2010;87:899-911.
29. Zingales V, Taroncher M, Martino PA, Ruiz MJ, Caloni F. Climate Change and Effects on Molds and Mycotoxins. Toxins (Basel). 2022;14(7).
30. Valencia-Quintana R, Milić M, Jakšić D, Šegvić Klarić M, Tenorio-Arvide MG, Pérez-Flores GA, et al. Environment changes, aflatoxins, and health issues, a review. International Journal of Environmental Research and Public Health. 2020;17(21):7850.
31. Giorni P, Battilani P, Magan N. Effect of solute and matric potential on in vitro growth and sporulation of strains from a new population of Aspergillus flavus isolated in Italy. Fungal Ecology. 2008;1(2):102-6.
32. Polano C, Sanseverino I, Ermolli M, Porcel RE, Bisselink B, Pozzoli L, et al. Mycotoxin fungal plant diseases and climate change: state of the art and beyond. 2024.
33. Eskola M, Kos G, Elliott CT, Hajšlová J, Mayar S, Krska R. Worldwide contamination of food-crops with mycotoxins: Validity of the widely cited 'FAO estimate' of 25. Crit Rev Food Sci Nutr. 2020;60(16):2773-89.
34. Gruber-Dorninger C, Jenkins T, Schatzmayr G. Global Mycotoxin Occurrence in Feed: A Ten-Year Survey. Toxins (Basel). 2019;11(7).
35. Silva JVBd, Oliveira CAFd, Ramalho LNZ. An overview of mycotoxins, their pathogenic effects, foods where they are found and their diagnostic biomarkers. Food Science and Technology. 2021;42.
36. Janik E, Niemcewicz M, Ceremuga M, Stela M, Saluk-Bijak J, Siadkowski A, et al. Molecular Aspects of Mycotoxins-A Serious Problem for Human Health. Int J Mol Sci. 2020;21(21).

UNIVERSIDADE DE SANTIAGO DE COMPOSTELA

37. Ostry V, Malir F, Toman J, Grosse Y. Mycotoxins as human carcinogens-the IARC Monographs classification. Mycotoxin Res. 2017;33(1):65-73.
38. Osuchowski MF, He Q, Sharma RP. Endotoxin exposure alters brain and liver effects of fumonisin B1 in BALB/c mice: implication of blood brain barrier. Food Chem Toxicol. 2005;43(9):1389-97.
39. Taevernier L, Bracke N, Veryser L, Wynendaele E, Gevaert B, Peremans K, et al. Blood-brain barrier transport kinetics of the cyclic depsipeptide mycotoxins beauvericin and enniatins. Toxicol Lett. 2016;258:175-84.
40. Zhang J, You L, Wu W, Wang X, Chrienova Z, Nepovimova E, et al. The neurotoxicity of trichothecenes T-2 toxin and deoxynivalenol (DON): Current status and future perspectives. Food Chem Toxicol. 2020;145:111676.
41. Alonso-Garrido M, Frangiamone M, Font G, Cimbalo A, Manyes L. In vitro blood brain barrier exposure to mycotoxins and carotenoids pumpkin extract alters mitochondrial gene expression and oxidative stress. Food Chem Toxicol. 2021;153:112261.
42. Magnoli AP, Poloni VL, Cavaglieri L. Impact of mycotoxin contamination in the animal feed industry. Current Opinion in Food Science. 2019;29:99-108.
43. Mavrommatis A, Giamouri E, Tavrizelou S, Zacharioudaki M, Danezis G, Simitzis PE, et al. Impact of Mycotoxins on Animals' Oxidative Status. Antioxidants (Basel). 2021;10(2).
44. EC. EC(2013). 2013/165/EU: Commission Recommendation of 27 March 2013 on the presence of T-2 and HT-2 toxin in cereals and cereal products Text with EEA relevance. Official Journal of the European Union, L 91, p. 12-15. 2013.
45. EC. EC (2016). Commission Recommendation (EU) 2016/1319 of 29 July 2016 amending Recommendation 2006/576/EC as regards deoxynivalenol, zearalenone and ochratoxin A in pet food. Official Journal of the European Union, L 208, p. 58 - 60 . 2016.
46. EC. EC (2006). Commission Recommendation of 17 August 2006 on the presence of deoxynivalenol, zearalenone, ochratoxin A, T-2 and HT-2 and fumonisins in products intended for animal feeding. Official Journal of the European Union, L 229, p. 7 - 9. 2006.
47. EC. EC (2002). Directive 2002/32/EC of the European Parliament and of the Council of 7 May 2002 on undesirable substances in animal feed - Council statement. Official Journal of the European Union. 2002.
48. Recomendación (UE) 2016/1319 de la Comisión, de 29 de julio de 2016, que modifica la Recomendación 2006/576/CE por lo que se refiere al deoxinivalenol, la zearalenona y la ocratoxina A en los alimentos para animales de compañía (Texto pertinente a efectos del EEE), (2016).
49. EC. EC (2002). Regulation (EC) No 178/2002 of the European Parliament and of the Council of 28 January 2002 laying down the general principles and requirements of food law, establishing the European Food Safety Authority and laying down procedures in matters of food safety. Official Journal of the European Union, L 31, p. 1-24. 2002.
50. Committee ES. Guidance on human health risk-benefit assessment of foods. EFSA Journal. 2010;8(7):1673.
51. Agriopoulou S. Ergot Alkaloids Mycotoxins in Cereals and Cereal-Derived Food Products: Characteristics, Toxicity, Prevalence, and Control Strategies. Agronomy [Internet]. 2021; 11(5).
52. Lorenz N, Wilson EV, Machado C, Schardl CL, Tudzynski P. Comparison of ergot alkaloid biosynthesis gene clusters in Claviceps species indicates loss of late pathway steps in evolution of C. fusiformis. Appl Environ Microbiol. 2007;73(22):7185-91.
53. Lee MR. The history of ergot of rye (Claviceps purpurea) II: 1900–1940. JR Coll Physicians Edinb. 2009;39(4):365-9.

USC DE COMPOSTELA

54. Schiff PL. Ergot and its alkaloids. Am J Pharm Educ. 2006;70(5):98.
55. Coufal-Majewski S, Stanford K, McAllister T, Blakley B, McKinnon J, Chaves AV, et al. Impacts of Cereal Ergot in Food Animal Production. Front Vet Sci. 2016;3:15.
56. Silva Â, Mateus ARS, Barros SC, Silva AS. Ergot Alkaloids on Cereals and Seeds: Analytical Methods, Occurrence, and Future Perspectives. Molecules. 2023;28(20).
57. Chain EPoCitF, Schrenk D, Bignami M, Bodin L, Chipman JK, del Mazo J, et al. Risks for animal health related to the presence of ergot alkaloids in feed. EFSA Journal. 2024;22(1):e8496.
58. Sainz MJ, González-Jartín JM, Aguín O, Mansilla JP, Botana LM. 8. Isolation, characterization, and identification of mycotoxin-producing fungi. Berlin, Boston: De Gruyter; 2018. p. 202-45.
59. Baron EP, Tepper SJ. Revisiting the role of ergots in the treatment of migraine and headache. Headache. 2010;50(8):1353-61.
60. Jones AJ, Federspiel JJ, Eke AC. Preventing postpartum hemorrhage with combined therapy rather than oxytocin alone. American Journal of Obstetrics & Gynecology MFM. 2023;5(2, Supplement):100731.
61. Reddy P, Hemsworth J, Guthridge KM, Vinh A, Vassiliadis S, Ezernieks V, et al. Ergot alkaloid mycotoxins: physiological effects, metabolism and distribution of the residual toxin in mice. Scientific Reports. 2020;10(1):9714.
62. Jaćević V, Dumanović J, Alomar SY, Resanović R, Milovanović Z, Nepovimova E, et al. Research update on aflatoxins toxicity, metabolism, distribution, and detection: A concise overview. Toxicology. 2023;492:153549.
63. Bennett JW, Klich M. Mycotoxins. Clin Microbiol Rev. 2003;16(3):497-516.
64. Filazi A, Sireli UT. Occurrence of aflatoxins in food. Aflatoxins—Recent Advances and Future Prospects. 2013:143-70.
65. Temba BA, Darnell RE, Gichangi A, Lwezaura D, Pardey PG, Harvey JJ, et al. The Influence of Weather on the Occurrence of Aflatoxin B1 in Harvested Maize from Kenya and Tanzania. Foods. 2021;10(2).
66. Valencia-Quintana R, Milić M, Jakšić D, Šegvić Klarić M, Tenorio-Arvide MG, Pérez-Flores GA, et al. Environment Changes, Aflatoxins, and Health Issues, a Review. Int J Environ Res Public Health. 2020;17(21).
67. Mahato DK, Lee KE, Kamle M, Devi S, Dewangan KN, Kumar P, et al. Aflatoxins in Food and Feed: An Overview on Prevalence, Detection and Control Strategies. Front Microbiol. 2019;10:2266.
68. Shabeer S, Asad S, Jamal A, Ali A. Aflatoxin Contamination, Its Impact and Management Strategies: An Updated Review. Toxins (Basel). 2022;14(5).
69. Popescu RG, Rădulescu AL, Georgescu SE, Dinischiotu A. Aflatoxins in Feed: Types, Metabolism, Health Consequences in Swine and Mitigation Strategies. Toxins (Basel). 2022;14(12).
70. Cabañes FJ, Bragulat MR, Castellá G. Ochratoxin A producing species in the genus Penicillium. Toxins (Basel). 2010;2(5):1111-20.
71. Ortiz-Villeda B, Lobos O, Aguilar-Zuniga K, Carrasco-Sánchez V. Ochratoxins in Wines: A Review of Their Occurrence in the Last Decade, Toxicity, and Exposure Risk in Humans. Toxins (Basel). 2021;13(7).
72. Dhungana B, Ali S, Byamukama E, Krishnan P, Caffe-Treml M. Incidence of Penicillium verrucosum in grain samples from oat varieties commonly grown in South Dakota. Journal of food protection. 2018;81(6):898-902.

USC UNIVERSIDADE DE SANTIAGO DE COMPOSTELA

73. Wang Y, Wang L, Liu F, Wang Q, Selvaraj JN, Xing F, et al. Ochratoxin A producing fungi, biosynthetic pathway and regulatory mechanisms. Toxins. 2016;8(3):83.
74. Bui-Klimke TR, Wu F. Ochratoxin A and human health risk: a review of the evidence. Crit Rev Food Sci Nutr. 2015;55(13):1860-9.
75. Tao Y, Xie S, Xu F, Liu A, Wang Y, Chen D, et al. Ochratoxin A: Toxicity, oxidative stress and metabolism. Food Chem Toxicol. 2018;112:320-31.
76. Hope JH, Hope BE. A review of the diagnosis and treatment of Ochratoxin A inhalational exposure associated with human illness and kidney disease including focal segmental glomerulosclerosis. J Environ Public Health. 2012;2012:835059.
77. Ferenczi S, Kuti D, Cserháti M, Krifaton C, Szoboszlay S, Kukolya J, et al. Effects of Single and Repeated Oral Doses of Ochratoxin A on the Lipid Peroxidation and Antioxidant Defense Systems in Mouse Kidneys. Toxins (Basel). 2020;12(11).
78. Kőszegi T, Poór M. Ochratoxin A: Molecular Interactions, Mechanisms of Toxicity and Prevention at the Molecular Level. Toxins (Basel). 2016;8(4):111.
79. Stoev SD. New Evidences about the Carcinogenic Effects of Ochratoxin A and Possible Prevention by Target Feed Additives. Toxins (Basel). 2022;14(6).
80. Ioi JD, Zhou T, Tsao R, M FM. Mitigation of Patulin in Fresh and Processed Foods and Beverages. Toxins (Basel). 2017;9(5).
81. Saleh I, Goktepe I. The characteristics, occurrence, and toxicological effects of patulin. Food Chem Toxicol. 2019;129:301-11.
82. Pal S, Singh N, Ansari KM. Toxicological effects of patulin mycotoxin on the mammalian system: an overview. Toxicol Res (Camb). 2017;6(6):764-71.
83. Singh N, Sharma G, Dev I, Shukla SK, Ansari KM. Study of the metabolic alterations in patulin-induced neoplastic transformation in normal intestinal cells. Toxicology Research. 2021;10(3):592-600.
84. McCormick SP, Stanley AM, Stover NA, Alexander NJ. Trichothecenes: from simple to complex mycotoxins. Toxins (Basel). 2011;3(7):802-14.
85. Ekwomadu TI, Akinola SA, Mwanza M. Fusarium Mycotoxins, Their Metabolites (Free, Emerging, and Masked), Food Safety Concerns, and Health Impacts. Int J Environ Res Public Health. 2021;18(22).
86. Proctor RH, McCormick SP, Kim HS, Cardoza RE, Stanley AM, Lindo L, et al. Evolution of structural diversity of trichothecenes, a family of toxins produced by plant pathogenic and entomopathogenic fungi. PLoS Pathog. 2018;14(4):e1006946.
87. Wannemacher RW, Wiener SL, Sidell FR, Takafuji ET, Franz DR. Trichothecene mycotoxins. Medical aspects of chemical and biological warfare. 1997;6:655-76.
88. Yoshizawa T. Thirty-five Years of Research on Deoxynivalenol, a Trichothecene Mycotoxin: with Special Reference to Its Discovery and Co-occurrence with Nivalenol in Japan. Food Safety. 2013;1(1):2013002-.
89. Miller JD. Mycotoxins in small grains and maize: old problems, new challenges. Food Addit Contam Part A Chem Anal Control Expo Risk Assess. 2008;25(2):219-30.
90. Janik E, Niemcewicz M, Podogrocki M, Ceremuga M, Stela M, Bijak M. T-2 Toxin-The Most Toxic Trichothecene Mycotoxin: Metabolism, Toxicity, and Decontamination Strategies. Molecules. 2021;26(22).
91. Rocha O, Ansari K, Doohan FM. Effects of trichothecene mycotoxins on eukaryotic cells: a review. Food Addit Contam. 2005;22(4):369-78.
92. Kimura M, Tokai T, Takahashi-Ando N, Ohsato S, Fujimura M. Molecular and Genetic Studies of Fusarium Trichothecene Biosynthesis: Pathways, Genes, and Evolution. Bioscience, Biotechnology, and Biochemistry. 2007;71(9):2105-23.

USC DE COMPOSTELA

93. Wu Q, Dohnal V, Huang L, Kuča K, Yuan Z. Metabolic pathways of trichothecenes. Drug metabolism reviews. 2010;42(2):250-67.
94. Adhikari M, Negi B, Kaushik N, Adhikari A, Al-Khedhairy AA, Kaushik NK, et al. T-2 mycotoxin: toxicological effects and decontamination strategies. Oncotarget. 2017;8(20):33933-52.
95. Yang L, Yu Z, Hou J, Deng Y, Zhou Z, Zhao Z, et al. Toxicity and oxidative stress induced by T-2 toxin and HT-2 toxin in broilers and broiler hepatocytes. Food and Chemical Toxicology. 2016;87:128-37.
96. Meneely J, Greer B, Kolawole O, Elliott C. T-2 and HT-2 Toxins: Toxicity, Occurrence and Analysis: A Review. Toxins (Basel). 2023;15(8).
97. Gurikar C, Shivaprasad DP, Sabillón L, Nanje Gowda NA, Siliveru K. Impact of mycotoxins and their metabolites associated with food grains. Grain & Oil Science and Technology. 2023;6(1):1-9.
98. Morooka N, Uratsuji N, Yoshizawa T, Yamamoto H. Studies on the Toxic Substances in Barley Infected with <I>Fusarium</I> spp. Food Hygiene and Safety Science (Shokuhin Eiseigaku Zasshi). 1972;13(5):368-75.
99. Munkvold GP. Fusarium species and their associated mycotoxins. Mycotoxigenic fungi: methods and protocols. 2017:51-106.
100. Zhang Y, Ouyang B, Zhang W, Guang C, Xu W, Mu W. Deoxynivalenol: Occurrence, toxicity, and degradation. Food Control. 2023:110027.
101. European Food Safety A. Deoxynivalenol in food and feed: occurrence and exposure. EFSA Journal. 2013;11(10):3379.
102. Côté LM, Dahlem AM, Yoshizawa T, Swanson SP, Buck WB. Excretion of deoxynivalenol and its metabolite in milk, urine, and feces of lactating dairy cows. Journal of Dairy Science. 1986;69(9):2416-23.
103. Kamle M, Mahato DK, Gupta A, Pandhi S, Sharma B, Dhawan K, et al. Deoxynivalenol: An Overview on Occurrence, Chemistry, Biosynthesis, Health Effects and Its Detection, Management, and Control Strategies in Food and Feed. Microbiology Research [Internet]. 2022; 13(2):[292-314 pp.].
104. Deng Y, You L, Wang X, Wu W, Kuca K, Wu Q, et al. Deoxynivalenol: Emerging Toxic Mechanisms and Control Strategies, Current and Future Perspectives. J Agric Food Chem. 2023;71(29):10901-15.
105. Ren ZH, Deng HD, Deng YT, Deng JL, Zuo ZC, Yu SM, et al. Effect of the Fusarium toxins, zearalenone and deoxynivalenol, on the mouse brain. Environ Toxicol Pharmacol. 2016;46:62-70.
106. Pinton P, Tsybulskyy D, Lucioli J, Laffitte J, Callu P, Lyazhri F, et al. Toxicity of Deoxynivalenol and Its Acetylated Derivatives on the Intestine: Differential Effects on Morphology, Barrier Function, Tight Junction Proteins, and Mitogen-Activated Protein Kinases. Toxicological Sciences. 2012;130(1):180-90.
107. Sobrova P, Adam V, Vasatkova A, Beklova M, Zeman L, Kizek R. Deoxynivalenol and its toxicity. Interdiscip Toxicol. 2010;3(3):94-9.
108. Bensassi F, Gallerne C, Sharaf El Dein O, Lemaire C, Hajlaoui MR, Bacha H. Involvement of mitochondria-mediated apoptosis in deoxynivalenol cytotoxicity. Food Chem Toxicol. 2012;50(5):1680-9.
109. Wang X, Xu W, Fan M, Meng T, Chen X, Jiang Y, et al. Deoxynivalenol induces apoptosis in PC12 cells via the mitochondrial pathway. Environ Toxicol Pharmacol. 2016;43:193-202.

USC UNIVERSIDADE DE SANTIAGO DE COMPOSTELA

110. Cao L, Jiang Y, Zhu L, Xu W, Chu X, Zhang Y, et al. Deoxynivalenol induces caspase-8-mediated apoptosis through the mitochondrial pathway in hippocampal nerve cells of piglet. Toxins. 2021;13(2):73.
111. Mwaniki AW, Buis QR, Trott D, Huber LA, Yang C, Kiarie EG. Comparative efficacy of commercially available deoxynivalenol detoxifying feed additives on growth performance, total tract digestibility of components, and physiological responses in nursery pigs fed diets formulated with naturally contaminated corn. Transl Anim Sci. 2021;5(2):txab050.
112. Smith GW. Chapter 71 - Fumonisins. In: Gupta RC, editor. Veterinary Toxicology (Third Edition): Academic Press; 2018. p. 1003-18.
113. Marasas WF. Discovery and occurrence of the fumonisins: a historical perspective. Environ Health Perspect. 2001;109 Suppl 2(Suppl 2):239-43.
114. Gelderblom WC, Jaskiewicz K, Marasas WF, Thiel PG, Horak RM, Vleggaar R, et al. Fumonisins--novel mycotoxins with cancer-promoting activity produced by Fusarium moniliforme. Appl Environ Microbiol. 1988;54(7):1806-11.
115. Kaltner F, Rampl C, Rychlik M, Zimmermann T, Rohe A. Development and validation of a cost-effective HPLC-FLD method for routine analysis of fumonisins B1 and B2 in corn and corn products. Food Analytical Methods. 2017;10(5):1349-58.
116. Kamle M, Mahato DK, Devi S, Lee KE, Kang SG, Kumar P. Fumonisins: Impact on Agriculture, Food, and Human Health and their Management Strategies. Toxins (Basel). 2019;11(6).
117. Damiani T, Righetti L, Suman M, Galaverna G, Dall'Asta C. Analytical issue related to fumonisins: A matter of sample comminution? Food Control. 2019;95:1-5.
118. Yu S, Zou L, Zhao J, Zhu Y. Individual and Combined Cytotoxic Effects of Co-Occurring Fumonisin Family Mycotoxins on Porcine Intestinal Epithelial Cell. Foods. 2023;12(13).
119. Shier WT. The fumonisin paradox: a review of research on oral bioavailability of fumonisin B1, a mycotoxin produced by Fusarium moniliforme. Journal of Toxicology: Toxin Reviews. 2000;19(2):161-87.
120. Sreenivasa MY. Fumonisins: A review on its global occurrence, epidemiology, toxicity and detection. Journal of Veterinary Medicine and Research. 2017;4(6).
121. Riley RT, Voss KA, Yoo HS, Gelderblom WCA, Merrill AH. Mechanism of Fumonisin Toxicity and Carcinogenesis. Journal of Food Protection. 1994;57(7):638-45.
122. Marasas WFO, Riley RT, Hendricks KA, Stevens VL, Sadler TW, Gelineau-van Waes J, et al. Fumonisins Disrupt Sphingolipid Metabolism, Folate Transport, and Neural Tube Development in Embryo Culture and In Vivo: A Potential Risk Factor for Human Neural Tube Defects among Populations Consuming Fumonisin-Contaminated Maize. The Journal of Nutrition. 2004;134(4):711-6.
123. Chu FS, Li GY. Simultaneous occurrence of fumonisin B1 and other mycotoxins in moldy corn collected from the People's Republic of China in regions with high incidences of esophageal cancer. Appl Environ Microbiol. 1994;60(3):847-52.
124. Domijan AM. Fumonisin B(1): a neurotoxic mycotoxin. Arh Hig Rada Toksikol. 2012;63(4):531-44.
125. Merrill AH, Wang E, Vales TR, Smith ER, Schroeder JJ, Menaldino DS, et al. Fumonisin Toxicity and Sphingolipid Biosynthesis. In: Jackson LS, DeVries JW, Bullerman LB, editors. Fumonisins in Food. Boston, MA: Springer US; 1996. p. 297-306.
126. Qu L, Wang L, Ji H, Fang Y, Lei P, Zhang X, et al. Toxic Mechanism and Biological Detoxification of Fumonisins. Toxins [Internet]. 2022; 14(3).

USC UNIVERSIDADE DE SANTIAGO DE COMPOSTELA

127. Chen J, Wei Z, Wang Y, Long M, Wu W, Kuca K. Fumonisin B1: Mechanisms of toxicity and biological detoxification progress in animals. Food and Chemical Toxicology. 2021;149:111977.
128. Scott PM. Recent research on fumonisins: a review. Food Addit Contam Part A Chem Anal Control Expo Risk Assess. 2012;29(2):242-8.
129. Domijan AM, Abramov AY. Fumonisin B1 inhibits mitochondrial respiration and deregulates calcium homeostasis--implication to mechanism of cell toxicity. Int J Biochem Cell Biol. 2011;43(6):897-904.
130. Stockmann-Juvala H, Mikkola J, Naarala J, Loikkanen J, Elovaara E, Savolainen K. Oxidative stress induced by fumonisin B1 in continuous human and rodent neural cell cultures. Free Radic Res. 2004;38(9):933-42.
131. Tardieu D, Bailly JD, Benard G, Tran TS, Guerre P. Toxicity of maize containing known levels of fumonisin B1 during force-feeding of ducks. Poultry Science. 2004;83(8):1287-93.
132. Haschek WM, Gumprecht LA, Smith G, Tumbleson ME, Constable PD. Fumonisin toxicosis in swine: an overview of porcine pulmonary edema and current perspectives. Environ Health Perspect. 2001;109 Suppl 2(Suppl 2):251-7.
133. Chen J, Wen J, Tang Y, Shi J, Mu G, Yan R, et al. Research Progress on Fumonisin B1 Contamination and Toxicity: A Review. Molecules [Internet]. 2021; 26(17).
134. Soriano JM, González L, Catalá AI. Mechanism of action of sphingolipids and their metabolites in the toxicity of fumonisin B1. Prog Lipid Res. 2005;44(6):345-56.
135. Wang SK, Wang TT, Huang GL, Shi RF, Yang LG, Sun GJ. Stimulation of the proliferation of human normal esophageal epithelial cells by fumonisin B1 and its mechanism. Experimental and Therapeutic Medicine. 2014;7(1):55-60.
136. Ajmal M, Hussain A, Ali A, Chen H, Lin H. Strategies for Controlling the Sporulation in Fusarium spp. J Fungi (Basel). 2022;9(1).
137. Stob M, Baldwin RS, Tuite J, Andrews FN, Gillette KG. Isolation of an anabolic, uterotrophic compound from corn infected with Gibberella zeae. Nature. 1962;196(4861).
138. Urry WH, Wehrmeister HL, Hodge EB, Hidy PH. The structure of zearalenone. Tetrahedron Letters. 1966;7(27):3109-14.
139. Cai P, Liu S, Tu Y, Shan T. Toxicity, biodegradation, and nutritional intervention mechanism of zearalenone. Science of The Total Environment. 2024;911:168648.
140. Shier WT, Shier AC, Xie W, Mirocha CJ. Structure-activity relationships for human estrogenic activity in zearalenone mycotoxins. Toxicon. 2001;39(9):1435-8.
141. Agahi F, Juan C, Font G, Juan-García A. In silico methods for metabolomic and toxicity prediction of zearalenone, α-zearalenone and β-zearalenone. Food Chem Toxicol. 2020;146:111818.
142. Minervini F, Dell'Aquila ME. Zearalenone and reproductive function in farm animals. International journal of molecular sciences. 2008;9(12):2570-84.
143. Han X, Huangfu B, Xu T, Xu W, Asakiya C, Huang K, et al. Research Progress of Safety of Zearalenone: A Review. Toxins (Basel). 2022;14(6).
144. Zhou J, Zhao L, Huang S, Liu Q, Ao X, Lei Y, et al. Zearalenone toxicosis on reproduction as estrogen receptor selective modulator and alleviation of zearalenone biodegradative agent in pregnant sows. J Anim Sci Biotechnol. 2022;13(1):36.
145. Bulgaru CV, Marin DE, Pistol GC, Taranu I. Zearalenone and the Immune Response. Toxins (Basel). 2021;13(4).
146. Ben Ammar R, Zahra HA, Abu Zahra AM, Alfwuaires M, Abdulaziz Alamer S, Metwally AM, et al. Protective Effect of Fucoxanthin on Zearalenone-Induced Hepatic Damage through Nrf2 Mediated by PI3K/AKT Signaling. Mar Drugs. 2023;21(7).

147. Kościelecka K, Kuć A, Kubik-Machura D, Męcik-Kronenberg T, Włodarek J, Radko L. Endocrine Effect of Some Mycotoxins on Humans: A Clinical Review of the Ways to Mitigate the Action of Mycotoxins. Toxins (Basel). 2023;15(9).
148. Kolawole O, Siri-Anusornsak W, Petchkongkaew A, Elliott C. A systematic review of global occurrence of emerging mycotoxins in crops and animal feeds, and their toxicity in livestock. Emerging Contaminants. 2024;10(3):100305.
149. Logrieco A, Moretti A, Castella G, Kostecki M, Golinski P, Ritieni A, et al. Beauvericin production by Fusarium species. Applied and Environmental Microbiology. 1998;64(8):3084-8.
150. Alves LFA, Bellon PP, Rheinheimer AR, Pietrowski V. First record of Beauveria bassiana (Hyphomycetes: Moniliales) on adults of cassava lace bug Vatiga manihotae (Drake)(Hemiptera: Tingidae) in Brazil. Arquivos do Instituto Biológico. 2012;79:309-11.
151. Lee K-E, Kim BH, Lee C. Occurrence of Fusarium mycotoxin beauvericin in animal feeds in Korea. Animal feed science and technology. 2010;157(3-4):190-4.
152. Klarić MS, Pepeljnjak S. Beauvericin: chemical and biological aspects and occurrence. Arhiv za higijenu rada i toksikologiju. 2005;56(4):343-50.
153. Mallebrera B, Prosperini A, Font G, Ruiz MJ. In vitro mechanisms of Beauvericin toxicity: A review. Food Chem Toxicol. 2018;111:537-45.
154. Søderstrøm S, Lie KK, Lundebye AK, Søfteland L. Beauvericin (BEA) and enniatin B (ENNB)-induced impairment of mitochondria and lysosomes - Potential sources of intracellular reactive iron triggering ferroptosis in Atlantic salmon primary hepatocytes. Food Chem Toxicol. 2022;161:112819.
155. Manyes L, Escrivá L, Ruiz MJ, Juan-García A. Beauvericin and enniatin B effects on a human lymphoblastoid Jurkat T-cell model. Food Chem Toxicol. 2018;115:127-35.
156. Wu Q, Patocka J, Nepovimova E, Kuca K. A review on the synthesis and bioactivity aspects of beauvericin, a Fusarium mycotoxin. Frontiers in pharmacology. 2018;9:1338.
157. Mallebrera B, Juan-Garcia A, Font G, Ruiz MJ. Mechanisms of beauvericin toxicity and antioxidant cellular defense. Toxicol Lett. 2016;246:28-34.
158. Bertero A, Fossati P, Tedesco DEA, Caloni F. Beauvericin and Enniatins: In Vitro Intestinal Effects. Toxins (Basel). 2020;12(11).
159. Çelik M, Aksoy H, Yılmaz S. Evaluation of beauvericin genotoxicity with the chromosomal aberrations, sister-chromatid exchanges and micronucleus assays. Ecotoxicology and Environmental Safety. 2010;73(7):1553-7.
160. Caloni F, Fossati P, Anadón A, Bertero A. Beauvericin: The beauty and the beast. Environmental Toxicology and Pharmacology. 2020;75:103349.
161. Kouri K, Lemmens M, Lemmens-Gruber R. Beauvericin-induced channels in ventricular myocytes and liposomes. Biochimica et Biophysica Acta (BBA) - Biomembranes. 2003;1609(2):203-10.
162. Lee SE, Park S-H, Oh SW, Yoo JA, Kwon K, Park SJ, et al. Beauvericin inhibits melanogenesis by regulating cAMP/PKA/CREB and LXR-α/p38 MAPK–mediated pathways. Scientific Reports. 2018;8(1):14958.
163. Agriopoulou S. Enniatins: An emerging food safety issue. EC Nutr. 2016;3:1142-6.
164. Izzo L, Mikušová P, Lombardi S, Sulyok M, Ritieni A. Analysis of Mycotoxin and Secondary Metabolites in Commercial and Traditional Slovak Cheese Samples. Toxins (Basel). 2022;14(2).
165. Khoshal AK, Novak B, Martin PGP, Jenkins T, Neves M, Schatzmayr G, et al. Co-occurrence of DON and Emerging Mycotoxins in Worldwide Finished Pig Feed and Their Combined Toxicity in Intestinal Cells. Toxins (Basel). 2019;11(12).

USC DE COMPOSTELA

166. Rodríguez-Cañás I, González-Jartín JM, Alvariño R, Alfonso A, Vieytes MR, Botana LM. Detection of mycotoxins in cheese using an optimized analytical method based on a QuEChERS extraction and UHPLC-MS/MS quantification. Food Chemistry. 2023;408:135182.
167. González-Jartín JM, Alfonso A, Sainz MJ, Vieytes MR, Botana LM. Multi-detection method for mycotoxins with a modified QuEChERS extraction in feed and development of a simple detoxification procedure. Animal Feed Science and Technology. 2020:114745.
168. Krug I, Behrens M, Esselen M, Humpf HU. Transport of enniatin B and enniatin B1 across the blood-brain barrier and hints for neurotoxic effects in cerebral cells. PLoS One. 2018;13(5):e0197406.
169. Wätjen W, Debbab A, Hohlfeld A, Chovolou Y, Kampkötter A, Edrada RA, et al. Enniatins A1, B and B1 from an endophytic strain of Fusarium tricinctum induce apoptotic cell death in H4IIE hepatoma cells accompanied by inhibition of ERK phosphorylation. Mol Nutr Food Res. 2009;53(4):431-40.
170. Dornetshuber R, Heffeter P, Kamyar M-R, Peterbauer T, Berger W, Lemmens-Gruber R. Enniatin exerts p53-dependent cytostatic and p53-independent cytotoxic activities against human cancer cells. Chemical Research in Toxicology. 2007;20(3):465-73.
171. Huang CH, Wang FT, Chan WH. Enniatin B1 exerts embryotoxic effects on mouse blastocysts and induces oxidative stress and immunotoxicity during embryo development. Environ Toxicol. 2019;34(1):48-59.
172. Prosperini A, Meca G, Font G, Ruiz MJ. Bioaccessibility of enniatins A, A_1, B, and B_1 in different commercial breakfast cereals, cookies, and breads of Spain. J Agric Food Chem. 2013;61(2):456-61.
173. Prosperini A, Juan-García A, Font G, Ruiz MJ. Reactive oxygen species involvement in apoptosis and mitochondrial damage in Caco-2 cells induced by enniatins A, A_1, B and B_1. Toxicol Lett. 2013;222(1):36-44.
174. Ivanova L, Egge-Jacobsen WM, Solhaug A, Thoen E, Fæste CK. Lysosomes as a possible target of enniatin B-induced toxicity in Caco-2 cells. Chem Res Toxicol. 2012;25(8):1662-74.
175. Maranghi F, Tassinari R, Narciso L, Tait S, Rocca CL, Felice GD, et al. In vivo toxicity and genotoxicity of beauvericin and enniatins. Combined approach to study in vivo toxicity and genotoxicity of mycotoxins beauvericin (BEA) and enniatin B (ENNB). EFSA Supporting Publications. 2018;15(5):1406E.
176. Kamyar M, Rawnduzi P, Studenik CR, Kouri K, Lemmens-Gruber R. Investigation of the electrophysiological properties of enniatins. Arch Biochem Biophys. 2004;429(2):215-23.
177. Ivanov VT, Evstratov AV, Sumskaya LV, Melnik EI, Chumburidze TS, Portnova SL, et al. Sandwich complexes as a functional form of the enniatin ionophores. FEBS letters. 1973;36(1):65-71.
178. Tonshin AA, Teplova VV, Andersson MA, Salkinoja-Salonen MS. The Fusarium mycotoxins enniatins and beauvericin cause mitochondrial dysfunction by affecting the mitochondrial volume regulation, oxidative phosphorylation and ion homeostasis. Toxicology. 2010;276(1):49-57.
179. Rodríguez-Carrasco Y, Narváez A, Izzo L, Gaspari A, Graziani G, Ritieni A. Biomonitoring of Enniatin B1 and Its Phase I Metabolites in Human Urine: First Large-Scale Study. Toxins (Basel). 2020;12(6).
180. Prusova N, Dzuman Z, Jelinek L, Karabin M, Hajslova J, Rychlik M, et al. Free and conjugated Alternaria and Fusarium mycotoxins during Pilsner malt production and double-mash brewing. Food Chem. 2022;369:130926.

181. Darkin-Rattray SJ, Gurnett AM, Myers RW, Dulski PM, Crumley TM, Allocco JJ, et al. Apicidin: A novel antiprotozoal agent that inhibits parasite histone deacetylase. Proceedings of the National Academy of Sciences. 1996;93(23):13143-7.
182. Von Bargen KW, Niehaus E-M, Bergander K, Brun R, Tudzynski B, Humpf H-U. Structure elucidation and antimalarial activity of apicidin F: an apicidin-like compound produced by Fusarium fujikuroi. Journal of natural products. 2013;76(11):2136-40.
183. Singh SB, Zink DL, Liesch JM, Mosley RT, Dombrowski AW, Bills GF, et al. Structure and chemistry of apicidins, a class of novel cyclic tetrapeptides without a terminal α-keto epoxide as inhibitors of histone deacetylase with potent antiprotozoal activities. The Journal of Organic Chemistry. 2002;67(3):815-25.
184. Han J-W, Ahn SH, Park SH, Wang SY, Bae G-U, Seo D-W, et al. Apicidin, a histone deacetylase inhibitor, inhibits proliferation of tumor cells via induction of p21WAF1/Cip1 and gelsolin. Cancer research. 2000;60(21):6068-74.
185. Ahn M-Y, Ahn S-G, Yoon J-H. Apicidin, a histone deaceylase inhibitor, induces both apoptosis and autophagy in human oral squamous carcinoma cells. Oral oncology. 2011;47(11):1032-8.
186. Bauden M, Tassidis H, Ansari D. In vitro cytotoxicity evaluation of HDAC inhibitor Apicidin in pancreatic carcinoma cells subsequent time and dose dependent treatment. Toxicology Letters. 2015;236(1):8-15.
187. Ueda T, Takai N, Nishida M, Nasu K, Narahara H. Apicidin, a novel histone deacetylase inhibitor, has profound anti-growth activity in human endometrial and ovarian cancer cells. Int J Mol Med. 2007;19(2):301-8.
188. Skrobek A, Shah FA, Butt TM. Destruxin production by the entomogenous fungus Metarhizium anisopliae in insects and factors influencing their degradation. BioControl. 2008;53:361-73.
189. Krasnoff SB, Gibson DM, Belofsky GN, Gloer KB, Gloer JB. New destruxins from the entomopathogenic fungus Aschersonia sp. Journal of Natural Products. 1996;59(5):485-9.
190. Liu B-L, Tzeng Y-M. Development and applications of destruxins: A review. Biotechnology advances. 2012;30(6):1242-54.
191. Steiner JR, Barnes CL. Crystal and molecular structure of Destruxin B. International Journal of Peptide and Protein Research. 1988;31(2):212-9.
192. Dong C, Yu J, Zhu Y, Dong C. Inhibition of hepatitis B virus gene expression & replication by crude destruxins from Metarhizium anisopliae var. dcjhyium. Indian Journal of Medical Research. 2013;138(6):969-76.
193. Chen H-C, Chou C-K, Sun C-M, Yeh SF. Suppressive effects of destruxin B on hepatitis B virus surface antigen gene expression in human hepatoma cells. Antiviral research. 1997;34(3):137-44.
194. Chao P-Z, Chin Y-P, Hsu IU, Liu C-M, Yu Y-C, Leung T-K, et al. Apoptotic toxicity of destruxin B in human non-Hodgkin lymphoma cells. Toxicology in Vitro. 2013;27(6):1870-6.
195. Muroi M, Shiragami N, Takatsuki A. Destruxin B, a specific and readily reversible inhibitor of vacuolar-type H+-translocating ATPase. Biochemical and biophysical research communications. 1994;205(2):1358-65.
196. Maragos CM, Probyn C, Proctor RH, Sieve KK. Cyclopiazonic acid in soft-ripened and blue cheeses marketed in the USA. Food Addit Contam Part B Surveill. 2023;16(1):14-23.
197. Kure CF, Skaar I. The fungal problem in cheese industry. Current Opinion in Food Science. 2019;29:14-9.

USC UNIVERSIDADE DE SANTIAGO DE COMPOSTELA

198. Balachandran C, Parthasarathy KR. Occurrence of cyclopiazonic acid in feeds and feedstuffs in Tamil Nadu, India. Mycopathologia. 1996;133(3):159-62.
199. Heperkan D, Somuncuoglu S, Karbancioglu-Güler F, Mecik N. Natural contamination of cyclopiazonic acid in dried figs and co-occurrence of aflatoxin. Food Control. 2012;23(1):82-6.
200. Holzapfel CW. The isolation and structure of cyclopiazonic acid, a toxic metabolite of Penicillium cyclopium Westling. Tetrahedron. 1968;24(5):2101-19.
201. Keblys M, Bernhoft A, Höfer CC, Morrison E, Larsen HJ, Flåøyen A. The effects of the Penicillium mycotoxins citrinin, cyclopiazonic acid, ochratoxin A, patulin, penicillic acid, and roquefortine C on in vitro proliferation of porcine lymphocytes. Mycopathologia. 2004;158(3):317-24.
202. Uka V, Moore GG, Arroyo-Manzanares N, Nebija D, De Saeger S, Diana Di Mavungu J. Unravelling the Diversity of the Cyclopiazonic Acid Family of Mycotoxins in Aspergillus flavus by UHPLC Triple-TOF HRMS. Toxins (Basel). 2017;9(1).
203. Casquete R, Benito MJ, Aranda E, Martín A, Hernández A, Córdoba MG. Cyclopiazonic acid gene expression as strategy to minimizing mycotoxin contamination in cheese. Fungal Biol. 2021;125(2):160-5.
204. Alsaidi ZZ, Humaish HH, Alasadi A. Toxic effects of cyclophosphamide on hepatic and kidney tissues in albino mice model. Research Journal of Pharmacy and Technology. 2022;15(10):4655-9.
205. Fliszár-Nyúl E, Faisal Z, Skaper R, Lemli B, Bayartsetseg B, Hetényi C, et al. Interaction of the Emerging Mycotoxins Beauvericin, Cyclopiazonic Acid, and Sterigmatocystin with Human Serum Albumin. Biomolecules. 2022;12(8).
206. Chang PK, Ehrlich KC, Fujii I. Cyclopiazonic acid biosynthesis of Aspergillus flavus and Aspergillus oryzae. Toxins (Basel). 2009;1(2):74-99.
207. Burdock GA, Flamm WG. Safety assessment of the mycotoxin cyclopiazonic acid. International Journal of Toxicology. 2000;19(3):195-218.
208. Gil-Serna J, Vázquez C, González-Jaén MT, Patiño B. Mycotoxins| Toxicology. 2014.
209. Ishii Y, Kawai T, Watanabe M. Inhibitory effects of cyclopiazonic acid on the spike after-hyperpolarization in rat sympathetic neurons. The Japanese Journal of Pharmacology. 1992;58(4):451-6.
210. Porter JK, Norred WP, Cole RJ, Dorner JW. Neurochemical effects of cyclopiazonic acid in chickens. Proceedings of the Society for Experimental Biology and Medicine. 1988;187(3):335-40.
211. European Food Safety A, Alvarez F, Arena M, Auteri D, Binaglia M, Castoldi AF, et al. Peer review of the pesticide risk assessment of the active substance Aspergillus flavus strain MUCL54911. EFSA Journal. 2022;20(3):e07202.
212. García-Estrada C, Ullán Ricardo V, Albillos Silvia M, Fernández-Bodega María Á, Durek P, von Döhren H, et al. A Single Cluster of Coregulated Genes Encodes the Biosynthesis of the Mycotoxins Roquefortine C and Meleagrin in Penicillium chrysogenum. Chemistry & Biology. 2011;18(11):1499-512.
213. Scott PM, Kennedy BPC. Analysis of blue cheese for roquefortine and other alkaloids from Penicillium roqueforti. Journal of Agricultural and Food Chemistry. 1976;24(4):865-8.
214. Finoli C, Vecchio A, Galli A, Dragoni I. Roquefortine C Occurrence in Blue Cheese. Journal of Food Protection. 2001;64(2):246-51.
215. Tiwary AK, Puschner B, Poppenga RH. Using roquefortine C as a biomarker for penitrem A intoxication. J Vet Diagn Invest. 2009;21(2):237-9.

USC UNIVERSIDADE DE SANTIAGO DE COMPOSTELA

216. Hymery N, Mounier J, Coton E. Effect of Penicillium roqueforti mycotoxins on Caco-2 cells: Acute and chronic exposure. Toxicol In Vitro. 2018;48:188-94.
217. Eriksen GS, Jäderlund KH, Moldes-Anaya A, Schönheit J, Bernhoft A, Jæger G, et al. Poisoning of dogs with tremorgenic Penicillium toxins. Medical Mycology. 2010;48(1):188-96.
218. Massarolo KC, Kupski L, Furlong EB, Drunkler DA. Distribution of mycotoxins during manufacture and storage of cheeses–A review. International Journal of Dairy Technology. 2024.
219. Aninat C, Hayashi Y, André F, Delaforge M. Molecular Requirements for Inhibition of Cytochrome P450 Activities by Roquefortine. Chemical Research in Toxicology. 2001;14(9):1259-65.
220. Arroyo-Manzanares N, Rodríguez-Estévez V, Arenas-Fernández P, García-Campaña AM, Gámiz-Gracia L. Occurrence of Mycotoxins in Swine Feeding from Spain. Toxins (Basel). 2019;11(6).
221. Dagnac T, Latorre A, Fernández Lorenzo B, Llompart M. Validation and application of a liquid chromatography-tandem mass spectrometry based method for the assessment of the co-occurrence of mycotoxins in maize silages from dairy farms in NW Spain. Food Additives & Contaminants: Part A. 2016;33(12):1850-63.
222. Schatzmayr G, Streit E. Global occurrence of mycotoxins in the food and feed chain: facts and figures. World Mycotoxin Journal. 2013;6(3):213-22.
223. Perrone G, Susca A. Penicillium Species and Their Associated Mycotoxins. Methods Mol Biol. 2017;1542:107-19.
224. Agahi F, Font G, Juan C, Juan-García A. Individual and Combined Effect of Zearalenone Derivates and Beauvericin Mycotoxins on SH-SY5Y Cells. Toxins (Basel). 2020;12(4).
225. Jia R, Liu W, Zhao L, Cao L, Shen Z. Low doses of individual and combined deoxynivalenol and zearalenone in naturally moldy diets impair intestinal functions via inducing inflammation and disrupting epithelial barrier in the intestine of piglets. Toxicol Lett. 2020;333:159-69.
226. Juan-García A, Carbone S, Ben-Mahmoud M, Sagratini G, Mañes J. Beauvericin and ochratoxin A mycotoxins individually and combined in HepG2 cells alter lipid peroxidation, levels of reactive oxygen species and glutathione. Food Chem Toxicol. 2020;139:111247.
227. Ma X, Ye Y, Sun J, Ji J, Wang J-S, Sun X. Coexposure of cyclopiazonic acid with aflatoxin B1 involved in disrupting amino acid metabolism and redox homeostasis causing synergistic toxic effects in hepatocyte spheroids. Journal of Agricultural and Food Chemistry. 2022;70(16):5166-76.
228. Lu H, Fernández-Franzón M, Font G, Ruiz MJ. Toxicity evaluation of individual and mixed enniatins using an in vitro method with CHO-K1 cells. Toxicol In Vitro. 2013;27(2):672-80.
229. Prosperini A, Font G, Ruiz MJ. Interaction effects of Fusarium enniatins (A, A1, B and B1) combinations on in vitro cytotoxicity of Caco-2 cells. Toxicol In Vitro. 2014;28(1):88-94.
230. Kouadio JH, Dano SD, Moukha S, Mobio TA, Creppy EE. Effects of combinations of Fusarium mycotoxins on the inhibition of macromolecular synthesis, malondialdehyde levels, DNA methylation and fragmentation, and viability in Caco-2 cells. Toxicon. 2007;49(3):306-17.
231. Klarić MS, Rumora L, Ljubanović D, Pepeljnjak S. Cytotoxicity and apoptosis induced by fumonisin B(1), beauvericin and ochratoxin A in porcine kidney PK15 cells: effects of individual and combined treatment. Arch Toxicol. 2008;82(4):247-55.

USC DE COMPOSTELA

232. Sideman S. Preface: The Cellular Communications Maze. Annals of the New York Academy of Sciences. 2005;1047(1):xi-xxiv.
233. Silverthorn DU. Human Physiology: An Integrated Approach, Global Edition: Pearson; 2018.
234. Le Duc D, Schöneberg T. 44Cellular Signalling Systems. 2019 [cited 6/26/2024]. In: Oxford Handbook of Evolutionary Medicine [Internet]. Oxford University Press, [cited 6/26/2024]; [0]. Available from: https://doi.org/10.1093/oxfordhb/9780198789666.013.2.
235. Uings IJ, Farrow SN. Cell receptors and cell signalling. Mol Pathol. 2000;53(6):295-9.
236. Miller EJ, Lappin SL. Physiology, cellular receptor. 2020.
237. Bootman MD. Calcium signaling. Cold Spring Harb Perspect Biol. 2012;4(7):a011171.
238. Clapham DE. Calcium signaling. Cell. 2007;131(6):1047-58.
239. Bootman MD, Bultynck G. Fundamentals of Cellular Calcium Signaling: A Primer. Cold Spring Harb Perspect Biol. 2020;12(1).
240. Daverkausen-Fischer L, Pröls F. Regulation of calcium homeostasis and flux between the endoplasmic reticulum and the cytosol. Journal of Biological Chemistry. 2022;298(7).
241. Zajac M, Modi S, Krishnan Y. The evolution of organellar calcium mapping technologies. Cell Calcium. 2022;108:102658.
242. Ahumada-Castro U, Puebla-Huerta A, Cuevas-Espinoza V, Lovy A, Cardenas JC. Keeping zombies alive: The ER-mitochondria Ca(2+) transfer in cellular senescence. Biochim Biophys Acta Mol Cell Res. 2021;1868(11):119099.
243. Lanner JT, Georgiou DK, Joshi AD, Hamilton SL. Ryanodine receptors: structure, expression, molecular details, and function in calcium release. Cold Spring Harb Perspect Biol. 2010;2(11):a003996.
244. Wang WA, Agellon LB, Michalak M. Organellar Calcium Handling in the Cellular Reticular Network. Cold Spring Harb Perspect Biol. 2019;11(12).
245. De Nicolo B, Cataldi-Stagetti E, Diquigiovanni C, Bonora E. Calcium and Reactive Oxygen Species Signaling Interplays in Cardiac Physiology and Pathologies. Antioxidants (Basel). 2023;12(2).
246. de Ridder I, Kerkhofs M, Lemos FO, Loncke J, Bultynck G, Parys JB. The ER-mitochondria interface, where Ca(2+) and cell death meet. Cell Calcium. 2023;112:102743.
247. Bonora M, Giorgi C, Pinton P. Molecular mechanisms and consequences of mitochondrial permeability transition. Nat Rev Mol Cell Biol. 2022;23(4):266-85.
248. Bauer TM, Murphy E. Role of Mitochondrial Calcium and the Permeability Transition Pore in Regulating Cell Death. Circ Res. 2020;126(2):280-93.
249. Endlicher R, Drahota Z, Štefková K, Červinková Z, Kučera O. The Mitochondrial Permeability Transition Pore-Current Knowledge of Its Structure, Function, and Regulation, and Optimized Methods for Evaluating Its Functional State. Cells. 2023;12(9).
250. Galione A, Muallem S. Preface. Endolysosomal calcium signalling. Cell Calcium. 2023;110:102696.
251. Rosencrans WM, Rajendran M, Bezrukov SM, Rostovtseva TK. VDAC regulation of mitochondrial calcium flux: From channel biophysics to disease. Cell Calcium. 2021;94:102356.
252. Yang Z, Kirton HM, MacDougall DA, Boyle JP, Deuchars J, Frater B, et al. The Golgi apparatus is a functionally distinct Ca2+ store regulated by the PKA and Epac branches of the β1-adrenergic signaling pathway. Sci Signal. 2015;8(398):ra101.
253. Maklad A, Sharma A, Azimi I. Calcium Signaling in Brain Cancers: Roles and Therapeutic Targeting. Cancers [Internet]. 2019; 11(2).

USC UNIVERSIDADE DE SANTIAGO DE COMPOSTELA

254. Prakriya M, Lewis RS. Store-Operated Calcium Channels. Physiol Rev. 2015;95(4):1383-436.
255. Zhang I, Hu H. Store-operated calcium channels in physiological and pathological states of the nervous system. Frontiers in cellular neuroscience. 2020;14:600758.
256. Catterall WA. Voltage-gated calcium channels. Cold Spring Harb Perspect Biol. 2011;3(8):a003947.
257. Zhang M, Ma Y, Ye X, Zhang N, Pan L, Wang B. TRP (transient receptor potential) ion channel family: structures, biological functions and therapeutic interventions for diseases. Signal Transduction and Targeted Therapy. 2023;8(1):261.
258. Zheng J. Molecular mechanism of TRP channels. Compr Physiol. 2013;3(1):221-42.
259. Vangeel L, Voets T. Transient receptor potential channels and calcium signaling. Cold Spring Harbor perspectives in biology. 2019;11(6):a035048.
260. Gees M, Colsoul B, Nilius B. The role of transient receptor potential cation channels in Ca2+ signaling. Cold Spring Harbor perspectives in biology. 2010;2(10):a003962.
261. Hattori M, Gouaux E. Molecular mechanism of ATP binding and ion channel activation in P2X receptors. Nature. 2012;485(7397):207-12.
262. Xu X, Liu S, Liu H, Ru K, Jia Y, Wu Z, et al. Piezo Channels: Awesome Mechanosensitive Structures in Cellular Mechanotransduction and Their Role in Bone. Int J Mol Sci. 2021;22(12).
263. Feletou M. Calcium signaling in vascular cells and cell-to-cell communications. Part. 2011;1:19-43.
264. D'Arcy MS. Cell death: a review of the major forms of apoptosis, necrosis and autophagy. Cell Biol Int. 2019;43(6):582-92.
265. Zhivotovsky B, Orrenius S. Calcium and cell death mechanisms: a perspective from the cell death community. Cell Calcium. 2011;50(3):211-21.
266. Walkon LL, Strubbe-Rivera JO, Bazil JN. Calcium Overload and Mitochondrial Metabolism. Biomolecules. 2022;12(12).
267. Kuo C-L, Ponneri Babuharisankar A, Lin Y-C, Lien H-W, Lo YK, Chou H-Y, et al. Mitochondrial oxidative stress in the tumor microenvironment and cancer immunoescape: foe or friend? Journal of Biomedical Science. 2022;29(1):74.
268. Vitale I, Pietrocola F, Guilbaud E, Aaronson SA, Abrams JM, Adam D, et al. Apoptotic cell death in disease—Current understanding of the NCCD 2023. Cell Death & Differentiation. 2023;30(5):1097-154.
269. Elmore S. Apoptosis: a review of programmed cell death. Toxicol Pathol. 2007;35(4):495-516.
270. Fotakis G, Timbrell JA. In vitro cytotoxicity assays: comparison of LDH, neutral red, MTT and protein assay in hepatoma cell lines following exposure to cadmium chloride. Toxicol Lett. 2006;160(2):171-7.
271. Lemasters JJ, Ramshesh VK. Imaging of mitochondrial polarization and depolarization with cationic fluorophores. Methods in cell biology. 2007;80:283-95.
272. Lakshmanan I, Batra SK. Protocol for Apoptosis Assay by Flow Cytometry Using Annexin V Staining Method. Bio Protoc. 2013;3(6).
273. Crowley LC, Marfell BJ, Scott AP, Waterhouse NJ. Quantitation of Apoptosis and Necrosis by Annexin V Binding, Propidium Iodide Uptake, and Flow Cytometry. Cold Spring Harb Protoc. 2016;2016(11).
274. Alvariño R, Alonso E, Bornancin L, Bonnard I, Inguimbert N, Banaigs B, et al. Biological Activities of Cyclic and Acyclic B-Type Laxaphycins in SH-SY5Y Human Neuroblastoma Cells. Mar Drugs. 2020;18(7).

USC DE COMPOSTELA

275. Yin Y, Shen H. Common methods in mitochondrial research. International Journal of Molecular Medicine. 2022;50(4):1-29.
276. Bonora M, Morganti C, Morciano G, Giorgi C, Wieckowski MR, Pinton P. Comprehensive analysis of mitochondrial permeability transition pore activity in living cells using fluorescence-imaging-based techniques. Nature protocols. 2016;11(6):1067-80.
277. Darzynkiewicz Z, Juan G. DNA content measurement for DNA ploidy and cell cycle analysis. Current protocols in cytometry. 1997(1):7-5.
278. Martínez M, Martínez NA, Silva WI. Measurement of the Intracellular Calcium Concentration with Fura-2 AM Using a Fluorescence Plate Reader. Bio Protoc. 2017;7(14):e2411.
279. Begum H, Murugesan P, Tangutur AD. Western blotting: a powerful staple in scientific and biomedical research. Biotechniques. 2022;73(1):58-69.
280. Gegunde Mosquera S. Modulación farmacológica de enfermedades con base inflamatoria con compuestos de origen marino. 2021.
281. Chou T-C, Talalay P. Analysis of combined drug effects: a new look at a very old problem. Trends in Pharmacological Sciences. 1983;4:450-4.
282. Awuchi CG, Ondari EN, Nwozo S, Odongo GA, Eseoghene IJ, Twinomuhwezi H, et al. Mycotoxins' Toxicological Mechanisms Involving Humans, Livestock and Their Associated Health Concerns: A Review. Toxins (Basel). 2022;14(3).
283. Marin S, Ramos AJ, Cano-Sancho G, Sanchis V. Mycotoxins: occurrence, toxicology, and exposure assessment. Food Chem Toxicol. 2013;60:218-37.
284. Bonnet MS, Roux J, Mounien L, Dallaporta M, Troadec JD. Advances in deoxynivalenol toxicity mechanisms: the brain as a target. Toxins (Basel). 2012;4(11):1120-38.
285. Brera C, Caputi R, Miraglia M, Iavicoli I, Salerno A, Carelli G. Exposure assessment to mycotoxins in workplaces: aflatoxins and ochratoxin A occurrence in airborne dusts and human sera. Microchemical Journal. 2002;73(1-2):167-73.
286. Brasel TL, Martin JM, Carriker CG, Wilson SC, Straus DC. Detection of airborne Stachybotrys chartarum macrocyclic trichothecene mycotoxins in the indoor environment. Applied and environmental microbiology. 2005;71(11):7376-88.
287. Flannigan B. Mycotoxins in the air. International biodeterioration. 1987;23(2):73-8.
288. Huttunen K, Korkalainen M. Microbial secondary metabolites and knowledge on inhalation effects. Exposure to microbiological agents in indoor and occupational environments. 2017:213-34.
289. Viegas S, Viegas C, Oppliger A. Occupational exposure to mycotoxins: Current knowledge and prospects. Annals of work exposures and health. 2018;62(8):923-41.
290. Straumfors A, Uhlig S, Eriksen GS, Heldal KK, Eduard W, Krska R, et al. Mycotoxins and other fungal metabolites in grain dust from Norwegian grain elevators and compound feed mills. World Mycotoxin Journal. 2015;8(3):361-73.
291. Straumfors A, Mundra S, Foss OAH, Mollerup SK, Kauserud H. The airborne mycobiome and associations with mycotoxins and inflammatory markers in the Norwegian grain industry. Scientific reports. 2021;11(1):9357.
292. Ndaw S, Jargot D, Antoine G, Denis F, Melin S, Robert A. Investigating multi-mycotoxin exposure in occupational settings: A biomonitoring and airborne measurement approach. Toxins. 2021;13(1):54.
293. Agriopoulou S, Stamatelopoulou E, Varzakas T. Advances in occurrence, importance, and mycotoxin control strategies: Prevention and detoxification in foods. Foods. 2020;9(2):137.

USC UNIVERSIDADE DE SANTIAGO DE COMPOSTELA

294. Dvorackova I. Aflatoxin inhalation and alveolar cell carcinoma. British medical journal. 1976;1(6011):691.
295. Dvoráčková I, Pichova V. Pulmonary interstitial fibrosis with evidence of aflatoxin B1 in lung tissue. 1986.
296. Georggiett OC, Muino JC, Montrull H, Brizuela N, Avalos S, Gomez RM. Relationship between lung cancer and aflatoxin B1. Revista de la Facultad de Ciencias Medicas (Cordoba, Argentina). 2000;57(1):95-107.
297. Hayes RB, Van Nieuwenhuize JP, Raatgever JW, Ten Kate FJW. Aflatoxin exposures in the industrial setting: an epidemiological study of mortality. Food and Chemical Toxicology. 1984;22(1):39-43.
298. EFSA. Scientific Opinion on the risks to human and animal health related to the presence of beauvericin and enniatins in food and feed. EFSA Journal. 2014;12(8):3802.
299. Zhang J, You L, Wu W, Wang X, Chrienova Z, Nepovimova E, et al. The neurotoxicity of trichothecenes T-2 toxin and deoxynivalenol (DON): Current status and future perspectives. Food and Chemical Toxicology. 2020:111676.
300. Huang D, Cui L, Dai M, Wang X, Wu Q, Hussain HI, et al. Mitochondrion: A new molecular target and potential treatment strategies against trichothecenes. Trends in Food Science & Technology. 2019;88:33-45.
301. Osuchowski MF, Sharma RP. Fumonisin B1 induces necrotic cell death in BV-2 cells and murine cultured astrocytes and is antiproliferative in BV-2 cells while N2A cells and primary cortical neurons are resistant. Neurotoxicology. 2005;26(6):981-92.
302. Osuchowski MF, Edwards GL, Sharma RP. Fumonisin B1-induced neurodegeneration in mice after intracerebroventricular infusion is concurrent with disruption of sphingolipid metabolism and activation of proinflammatory signaling. Neurotoxicology. 2005;26(2):211-21.
303. Venkataramana M, Chandra Nayaka S, Anand T, Rajesh R, Aiyaz M, Divakara ST, et al. Zearalenone induced toxicity in SHSY-5Y cells: The role of oxidative stress evidenced by N-acetyl cysteine. Food Chem Toxicol. 2014;65:335-42.
304. Meca G, Ruiz MJ, Soriano JM, Ritieni A, Moretti A, Font G, et al. Isolation and purification of enniatins A, A(1), B, B(1), produced by Fusarium tricinctum in solid culture, and cytotoxicity effects on Caco-2 cells. Toxicon. 2010;56(3):418-24.
305. Meca G, Font G, Ruiz MJ. Comparative cytotoxicity study of enniatins A, A_1, A_2, B, B_1, B_4 and J_3 on Caco-2 cells, Hep-G_2 and HT-29. Food Chem Toxicol. 2011;49(9):2464-9.
306. Gammelsrud A, Solhaug A, Dendelé B, Sandberg WJ, Ivanova L, Kocbach Bølling A, et al. Enniatin B-induced cell death and inflammatory responses in RAW 267.4 murine macrophages. Toxicol Appl Pharmacol. 2012;261(1):74-87.
307. Park KS, Jo I, Pak K, Bae SW, Rhim H, Suh SH, et al. FCCP depolarizes plasma membrane potential by activating proton and Na+ currents in bovine aortic endothelial cells. Pflugers Arch. 2002;443(3):344-52.
308. Yin F, Boveris A, Cadenas E. Mitochondrial energy metabolism and redox signaling in brain aging and neurodegeneration. Antioxid Redox Signal. 2014;20(2):353-71.
309. Tarafdar A, Pula G. The Role of NADPH Oxidases and Oxidative Stress in Neurodegenerative Disorders. Int J Mol Sci. 2018;19(12).
310. Juan C, de Simone G, Sagratini G, Caprioli G, Mañes J, Juan-García A. Reducing the effect of beauvericin on neuroblastoma SH-SY5Y cell line by natural products. Toxicon. 2020;188:164-71.
311. Montesano D, Juan-García A, Mañes J, Juan C. Chemoprotective effect of carotenoids from Lycium barbarum L. on SH-SY5Y neuroblastoma cells treated with beauvericin. Food Chem Toxicol. 2020;141:111414.

USC DE COMPOSTELA

312. Agahi F, Álvarez-Ortega N, Font G, Juan-García A, Juan C. Oxidative stress, glutathione, and gene expression as key indicators in SH-SY5Y cells exposed to zearalenone metabolites and beauvericin. Toxicol Lett. 2020;334:44-52.
313. Hymery N, Masson F, Barbier G, Coton E. Cytotoxicity and immunotoxicity of cyclopiazonic acid on human cells. Toxicology in Vitro. 2014;28(5):940-7.
314. Metin B. Penicillium roqueforti Secondary Metabolites: Biosynthetic Pathways, Gene Clusters, and Bioactivities. Fermentation [Internet]. 2023; 9(9).
315. Zhao M, Ma J, Li M, Zhang Y, Jiang B, Zhao X, et al. Cytochrome P450 Enzymes and Drug Metabolism in Humans. Int J Mol Sci. 2021;22(23).
316. Wu Y, Zhao D, Zhuang J, Zhang F, Xu C. Caspase-8 and Caspase-9 Functioned Differently at Different Stages of the Cyclic Stretch-Induced Apoptosis in Human Periodontal Ligament Cells. PLoS One. 2016;11(12):e0168268.
317. Suzuki S, Saito S, Narushima Y, Kodani S, Kagaya N, Suenaga H, et al. Notch activator cyclopiazonic acid induces apoptosis in HL-60 cells through calcineurin activation. J Antibiot (Tokyo). 2024;77(1):30-8.
318. Bonyadi F, Hasanzadeh S, Malekinejad H. Cyclopiazonic acid induced p53-dependent apoptosis in the testis of mice: Another male related risk factor of infertility. Environ Toxicol. 2021;36(5):903-13.
319. Miani M, Barthson J, Colli ML, Brozzi F, Cnop M, Eizirik DL. Endoplasmic reticulum stress sensitizes pancreatic beta cells to interleukin-1β-induced apoptosis via Bim/A1 imbalance. Cell Death Dis. 2013;4(7):e701.
320. Streit E, Schatzmayr G, Tassis P, Tzika E, Marin D, Taranu I, et al. Current situation of mycotoxin contamination and co-occurrence in animal feed--focus on Europe. Toxins (Basel). 2012;4(10):788-809.
321. Alassane-Kpembi I, Schatzmayr G, Taranu I, Marin D, Puel O, Oswald IP. Mycotoxins co-contamination: Methodological aspects and biological relevance of combined toxicity studies. Critical Reviews in Food Science and Nutrition. 2017;57(16):3489-507.
322. Fernández-Blanco C, Font G, Ruiz MJ. Interaction effects of enniatin B, deoxinivalenol and alternariol in Caco-2 cells. Toxicol Lett. 2016;241:38-48.
323. Vejdovszky K, Warth B, Sulyok M, Marko D. Non-synergistic cytotoxic effects of Fusarium and Alternaria toxin combinations in Caco-2 cells. Toxicol Lett. 2016;241:1-8.
324. de la Unión Europea DO. Reglamento (CE) No 1881/2006 de la comisión de 19 de diciembre de 2006 por el que se fija el contenido máximo de determinados contaminantes en los productos alimenticios. Comisión de las Comunidades Europeas. 2006.
325. Ivanova L, Skjerve E, Eriksen GS, Uhlig S. Cytotoxicity of enniatins A, A1, B, B1, B2 and B3 from Fusarium avenaceum. Toxicon. 2006;47(8):868-76.
326. Chalyy ZA, Kiseleva MG, Sedova IB, Minaeva LP, Sheveleva SA, Tutelyan VA. [Dried fruits marketed in Russia: multi-mycotoxin contamination]. Vopr Pitan. 2021;90(1):33-9.
327. Olleik H, Nicoletti C, Lafond M, Courvoisier-Dezord E, Xue P, Hijazi A, et al. Comparative Structure-Activity Analysis of the Antimicrobial Activity, Cytotoxicity, and Mechanism of Action of the Fungal Cyclohexadepsipeptides Enniatins and Beauvericin. Toxins (Basel). 2019;11(9).
328. Fraeyman S, Croubels S, Devreese M, Antonissen G. Emerging Fusarium and Alternaria Mycotoxins: Occurrence, Toxicity and Toxicokinetics. Toxins (Basel). 2017;9(7).
329. Pier AC, Belden EL, Ellis JA, Nelson EW, Maki LR. Effects of cyclopiazonic acid and aflatoxin singly and in combination on selected clinical, pathological and immunological responses of guinea pigs. Mycopathologia. 1989;105(3):135-42.

USC UNIVERSIDADE DE SANTIAGO DE COMPOSTELA

330. Chou TC. Drug combination studies and their synergy quantification using the Chou-Talalay method. Cancer Res. 2010;70(2):440-6.
331. Carreras-Sureda A, Pihán P, Hetz C. Calcium signaling at the endoplasmic reticulum: fine-tuning stress responses. Cell Calcium. 2018;70:24-31.
332. Audoin C, Sánchez JA, Genta-Jouve G, Alfonso A, Rios L, Vale C, et al. Autumnalamide, a prenylated cyclic peptide from the cyanobacterium Phormidium autumnale, acts on SH-SY5Y cells at the mitochondrial level. J Nat Prod. 2014;77(10):2196-205.
333. Sánchez JA, Alfonso A, Leirós M, Alonso E, Rateb ME, Jaspars M, et al. Spongionella Secondary Metabolites Regulate Store Operated Calcium Entry Modulating Mitochondrial Functioning in SH-SY5Y Neuroblastoma Cells. Cell Physiol Biochem. 2015;37(2):779-92.
334. Pagliaro L, Marchesini M, Roti G. Targeting oncogenic Notch signaling with SERCA inhibitors. J Hematol Oncol. 2021;14(1):8.
335. Luciani DS, Gwiazda KS, Yang TL, Kalynyak TB, Bychkivska Y, Frey MH, et al. Roles of IP3R and RyR Ca2+ channels in endoplasmic reticulum stress and beta-cell death. Diabetes. 2009;58(2):422-32.
336. Jilani K, Qadri SM, Lang E, Zelenak C, Rotte A, Bobbala D, et al. Stimulation of erythrocyte phospholipid scrambling by enniatin A. Mol Nutr Food Res. 2011;55 Suppl 2:S294-302.
337. Benz R, McLaughlin S. The molecular mechanism of action of the proton ionophore FCCP (carbonylcyanide p-trifluoromethoxyphenylhydrazone). Biophys J. 1983;41(3):381-98.
338. Alonso-Garrido M, Escrivá L, Manyes L, Font G. Enniatin B induces expression changes in the electron transport chain pathway related genes in lymphoblastic T-cell line. Food and Chemical Toxicology. 2018;121:437-43.
339. Horng T. Calcium signaling and mitochondrial destabilization in the triggering of the NLRP3 inflammasome. Trends Immunol. 2014;35(6):253-61.
340. Obejero-Paz CA, Gray IP, Jones SW. Ni2+ block of CaV3.1 (alpha1G) T-type calcium channels. J Gen Physiol. 2008;132(2):239-50.
341. Hernández-Morales M, Sobradillo D, Valero RA, Muñoz E, Ubierna D, Moyer MP, et al. Mitochondria sustain store-operated currents in colon cancer cells but not in normal colonic cells: reversal by non-steroidal anti-inflammatory drugs. Oncotarget. 2017;8(33):55332-52.
342. Demine S, Renard P, Arnould T. Mitochondrial Uncoupling: A Key Controller of Biological Processes in Physiology and Diseases. Cells. 2019;8(8).
343. Glitsch MD, Bakowski D, Parekh AB. Store-operated Ca2+ entry depends on mitochondrial Ca2+ uptake. Embo j. 2002;21(24):6744-54.
344. Liu X, Song S, Wang Q, Yuan T, He J. A mutation in β-amyloid precursor protein renders SH-SY5Y cells vulnerable to isoflurane toxicity: The role of inositol 1,4,5-trisphosphate receptors. Mol Med Rep. 2016;14(6):5435-42.
345. Stanzione R, Forte M, Cotugno M, Bianchi F, Marchitti S, Rubattu S. Relevance of stromal interaction molecule 1 (STIM1) in experimental and human stroke. Pflugers Arch. 2022;474(1):141-53.
346. Juan-García A, Ruiz MJ, Font G, Manyes L. Enniatin A1, enniatin B1 and beauvericin on HepG2: Evaluation of toxic effects. Food Chem Toxicol. 2015;84:188-96.
347. Oliveira CAF, Ivanova L, Solhaug A, Fæste CK. Enniatin B(1)-induced lysosomal membrane permeabilization in mouse embryonic fibroblasts. Mycotoxin Res. 2020;36(1):23-30.
348. Levy D, Bluzat A, Seigneuret M, Rigaud JL. Alkali cation transport through liposomes by the antimicrobial fusafungine and its constitutive enniatins. Biochem Pharmacol. 1995;50(12):2105-7.

USC DE COMPOSTELA

349. Habauzit D, Lemée P, Botana LM, Fessard V. Toxicity Predictions for Mycotoxins: A Combined In Silico Approach on Enniatin-Like Cluster. Exposure and Health. 2023;15(2):315-31.
350. Taibon J, Sturm S, Seger C, Strasser H, Stuppner H. Quantitative Assessment of Destruxins from Strawberry and Maize in the Lower Parts per Billion Range: Combination of a QuEChERS-Based Extraction Protocol with a Fast and Selective UHPLC-QTOF-MS Assay. Journal of Agricultural and Food Chemistry. 2015;63(23):5707-13.
351. Rocchetti G, Ghilardelli F, Masoero F, Gallo A. Screening of Regulated and Emerging Mycotoxins in Bulk Milk Samples by High-Resolution Mass Spectrometry. Foods [Internet]. 2021; 10(9).
352. Garcia-Cela E, Kiaitsi E, Medina A, Sulyok M, Krska R, Magan N. Interacting Environmental Stress Factors Affects Targeted Metabolomic Profiles in Stored Natural Wheat and That Inoculated with F. graminearum. Toxins [Internet]. 2018; 10(2).
353. Kanehisa M, Goto S. KEGG: Kyoto Encyclopedia of Genes and Genomes. Nucleic Acids Research. 2000;28(1):27-30.
354. Lu CL, Lin HI, Chen BF, Jow GM. Beauvericin-induced cell apoptosis through the mitogen-activated protein kinase pathway in human nonsmall cell lung cancer A549 cells. J Toxicol Sci. 2016;41(3):429-37.
355. Ahn MY. HDAC inhibitor apicidin suppresses murine oral squamous cell carcinoma cell growth in vitro and in vivo via inhibiting HDAC8 expression. Oncology letters. 2018;16(5):6552-60.
356. Park H, Im JY, Kim J, Choi WS, Kim HS. Effects of apicidin, a histone deacetylase inhibitor, on the regulation of apoptosis in H-ras-transformed breast epithelial cells. International journal of molecular medicine. 2008;21(3):325-33.
357. Wu CC, Chen TH, Liu BL, Wu LC, Chen YC, Tzeng YM, et al. Destruxin B Isolated from Entomopathogenic Fungus Metarhizium anisopliae Induces Apoptosis via a Bcl-2 Family-Dependent Mitochondrial Pathway in Human Nonsmall Cell Lung Cancer Cells. Evid Based Complement Alternat Med. 2013;2013:548929.
358. Huang Liu R, Chen S-P, Lu T-M, Tsai W-Y, Tsai C-H, Yang C-C, et al. Selective apoptotic cell death effects of oral cancer cells treated with destruxin B. BMC complementary and alternative medicine. 2014;14:1-10.

USC UNIVERSIDADE DE SANTIAGO DE COMPOSTELA

USC
UNIVERSIDADE
DE SANTIAGO
DE COMPOSTELA

CAMPUS
TERRA

En la presente tesis se ha profundizado en el estudio del mecanismo de acción de las micotoxinas emergentes más frecuentes en alimentos, las eniatinas, definiendo por primera vez que los análogos A, A1, B y B1 no son ionóforos de calcio, pero actúan modulando la homeostasis del ion. También se ha evaluado la toxicidad de estos compuestos y de otras micotoxinas reguladas y emergentes, tanto individualmente como en combinación. Se ha observado que las micotoxinas emergentes producen una mayor toxicidad, con una potenciación de sus efectos cuando se mezclan. Dado su elevada prevalencia, los resultados obtenidos sugieren que estos compuestos pueden suponer un riesgo para la salud pública.